Development and evaluation of new analytical concepts for the determination of ^{89}Sr and ^{90}Sr in a variety of applications to sample matrices with a high calcium content

Dissertation

Zur Erlangung des Doktorgrades der Naturwissenschaften (Dr. rer. nat.)

an der Fakultät für Chemie und Pharmazie

der Universität Regensburg

vorgelegt von

Alina Scheklaukov

aus Temirtau, Kasachstan

im März 2023

This dissertation was performed between November 2019 and March 2023 under the supervision of Dr. Robert Schupfner at the Institute of Analytical Chemistry, Chemo- and Biosensors, Department of Radiochemistry URA/ZRN, University of Regensburg.

Promotionsgesuch eingereicht am: 24.01.2020
Die Arbeit wurde angeleitet von: Dr. Robert Schupfner
Prüfungsausschuss:
Vorsitzender: Prof. Dr. Oliver Tepner
Erstgutachterin: Prof. Dr. Antje Bäumner
Zweitgutachter: Prof. Dr. Axel Dürkop
Drittprüfer: Prof. Dr. Werner Kunz

Abstract

The subject of this work was the improvement, validation and increase of the efficiency of the established Hot Column Chromatography separation method for the detection of ^{90}Sr.

The focus was to determine the ^{90}Sr activity through its daughter nuclide ^{90}Y. The two nuclides are in radioactive equilibrium with each other and have an activity ratio of 1:1. The advantages of ^{90}Y as an analyte are its narrow elution region, faster elution compared to Sr and the good separation between Y and Cs. To test the separation of Y in the Hot Column Chromatography, elution curves of it as well as of the interfering elements K and Ca were recorded. A significant overlap was found, and it was tried to counteract it with a slower elution in the elution region of Y, K and Ca. But this increased the overlap instead of decreasing it. The final goal was a direct Cherenkov measurement of the Y fraction without post treatment. For this, it was tried to find an optimal sampling fraction, which could not exceed 20 mL and should contain as much of the Y and as little K and Ca as possible. Then complete analyses were performed with the Hot Column separation immediately followed by a direct Cherenkov measurement and another after two weeks, for background determination. This is due to the short 64-hour half-life of ^{90}Y. The results were satisfactory, with almost all the added tracer activity found in the samples and a complete separation from potassium. But they also showed the susceptibility of this method to slight fluctuations of the elution, due to the narrow elution region of Y.

The established separation method was also tested for different sample types, to find out whether the sample material has a significant effect on the calcium content of the sample ash and on the separation of the ions in the column. The Ca-content showed variations, but it was in the same range for all sample types. The elution experiments also showed comparable results for different sample matrices. The elution region of Y was always quite narrow. The salad sample was the only one that showed a significant overlap between the elution regions of Y and Cs. The overlap between the elution regions of Sr and Cs was a lot less significant for the samples apart from milk.

During the project, the column material Dowex®50WX8 200-400 (H) was no longer available from the original provider Serva. It was purchased from the alternative providers Alfa Aesar and Sigma Aldrich, which unfortunately caused a broadening and shift of the Sr elution region to higher eluent volumes. This would make the analysis even longer and more laborious. To counteract this effect, it was tried to accelerate the elution by changing the eluent from ammonium-lactate to 6 M HCl, as soon as Sr was separated from the interfering substances. The acceleration was successful, but the low pH of the new eluent disrupted the further sample processing, especially the filtration step, so it could not be applied in routine analytics. Then it was tried to accelerate the Sr elution by slightly lowering the pH of the eluent ammonium-lactate from 7 to 6. This method was successful in accelerating the elution and did not interfere with the sample processing. It was tested for environmental samples, ivory age determination and in a ring analysis. Even though it achieved smaller Sr yields than the established method, it was sufficient to reach the necessary levels of detection.

Also, several potential quick separation techniques of Y from Ca and K were tried. It was hoped that these could be implemented as additional separations, either before or after the Hot Column Chromatography. But neither of the tried methods were successful.

Zusammenfassung

Gegenstand dieser Arbeit war die Verbesserung, Validierung und Erhöhung der Effizienz der etablierten Hot Column Chromatographie Auftrennungsmethode zur Bestimmung von ^{90}Sr.

Der Hauptfokus war die Bestimmung der Aktivität von ^{90}Sr über sein Tochternuklid ^{90}Y. Die beiden Nuklide liegen im radioaktiven Gleichgewicht vor und haben ein Aktivitätsverhältnis von 1:1. Die Vorteile von ^{90}Y als Analyt sind sein schmaler Elutionsbereich, die schnellere Elution im Vergleich zu Sr und die gute Auftrennung zwischen Y und Cs. Um die Abtrennung von Y in der Hot Column Chromatographie zu testen, wurden Elutionskurven davon aufgenommen, genauso wie von den Störelementen K und Ca. Eine signifikante Überlappung der Elutionskurven wurde festgestellt und es wurde versucht dem durch eine Verlangsamung der Elution in den Elutionsbereichen von Y, K und Ca entgegenzuwirken. Aber dies verstärkte die Überlappung nur. Das Endziel war eine direkte Cherenkov Messung der Y Fraktion ohne Nachbehandlung. Dafür wurde versucht einen optimalen Probenahmebereich zu finden, der 20 mL nicht überschreitet und so viel Y und so wenig K und Ca enthält wie möglich. Dann wurden Komplettanalysen durchgeführt, die Abtrennung über Hot Column Chromatographie, eine Cherenkov Messung direkt im Anschluss und eine nach zwei Wochen, zur Untergrundbestimmung. Der Grund dafür war die 64 h kurze Halbwertszeit von ^{90}Y. Die Ergebnisse waren zufriedenstellend. Fast die gesamte zugegebene Tracer Aktivität wurde in den Proben wiedergefunden und eine komplette Abtrennung von K erreicht. Aber sie zeigten auch eine Anfälligkeit dieser Methode für kleine Schwankungen der Elution aufgrund des schmalen Elutionsbereiches von Y.
Die etablierte Auftrennungsmethode wurde auch für verschiedene Probenarten getestet, um herauszufinden, ob das Probenmaterial einen signifikanten Effekt auf den Ca-Gehalt der Probenasche und auf die Auftrennung in der Ionenchromatographie hat. Der Ca-Gehalt variierte, aber war in derselben Größenordnung für alle Probenarten. Die Elutionsexperimente zeigten auch vergleichbare Ergebnisse für alle Probenmatrices. Der Elutionsbereich von Y war immer schmal. Die Salatprobe war die einzige, die eine signifikante Überlappung zwischen den Elutionsbereichen von Y und Cs zeigte. Die Überlappung zwischen den Elutionsbereichen von Sr und Cs war für die anderen Proben viel weniger ausgeprägt als für die Milchprobe.
Während des Projekts war das Säulenmaterial Dowex®50WX8 200-400 (H) von Serva nicht mehr verfügbar. Das Material wurde von den alternativen Anbietern Alfa Aesar und Sigma Aldrich erworben. Unglücklicherweise verursachte das neue Material eine Verbreiterung und Verschiebung des Elutionsbereiches von Sr zu höheren Laufmittel-Volumina, was die Analyse noch länger und aufwändiger machen würde. Um dem entgegenzuwirken, wurde versucht die Elution zu beschleunigen. Dafür wurde der Laufmittelwechsel von Ammoniumlactat zu 6 M HCl, sobald das Sr von den Störsubstanzen abgetrennt ist, getestet. Die Beschleunigung war erfolgreich. Jedoch störte der geringe pH-Wert des neuen Laufmittels die weitere Probenaufarbeitung, insbesondere den Filtrationsschritt. Also konnte sie nicht in der Routineanalytik angewendet werden. Dann wurde versucht die Sr Elution zu beschleunigen, indem der pH des Laufmittels Ammoniumlactat leicht gesenkt wurde, von 7 auf 6. Das führte zu einer erfolgreichen Beschleunigung der Elution und hatte keinen negativen Einfluss auf die weitere Probenaufarbeitung. Diese Methode wurde anhand von Umweltproben, der Elfenbeinaltersbestimmung und in einem Ringversuch in der Praxis getestet. Obwohl dabei kleinere Sr Ausbeuten erzielt wurden als mit der etablierten Methode, reichten sie aus um die nötigen Nachweisgrenzen zu erreichen.
Außerdem wurden mehrere Schnellabtrennungsverfahren von Y von Ca und K getestet. Das Ziel war diese als Zusatzabtrennungen etablieren zu können, entweder vor oder nach der Hot Column Chromatographie. Aber keine der getesteten Methoden war erfolgreich.

Danksagung

Ich bedanke mich von Herzen bei Dr Robert Schupfner für die Bereitstellung des Themas, seine Betreuung während der Arbeit, stete Erreichbarkeit und die Bereitschaft die Arbeit auch in sehr spontanen Besprechungen durchzugehen und sein umfassendes Expertenwissen dazu beizutragen.

Mein Dank gilt auch Prof. Dr. Antje Bäumner für ihre Bereitschaft als meine Doktormutter zu fungieren und das Erstgutachten für diese Arbeit zu erstellen.

Ich danke auch Prof. Dr. Axel Dürkop für die Erstellung des Zweitgutachtens.

Herrn Prof. Dr. Kunz möchte ich für seine Bereitschaft als Drittprüfer die Arbeit zu begleiten danken.

Für die Übernahme des Vorsitzes danke ich Prof. Dr. Oliver Tepner.

Für die hervorragende Organisation im bürokratischen Bereich und die Verwaltung der URA/ZRN Gruppe bedanke ich mich ganz herzlich bei Sigrid Schwarzfischer. Ohne sie würde Chaos herrschen.

Helga Gammel gilt ein großer Dank für die Einführung in die Hot Column Chromatographie Analysemethode und die allgemeine Hilfsbereitschaft und Fachkompetenz im Labor.

Ich danke dem gesamten Laborteam: Helga Gammel, Erika Treml, Heidi Kastl, Gabriele Seibert, Marjo Schäfer und nicht zuletzt meinem Doktorandenkollegen Gerhard Gottinger für die gute Zusammenarbeit.

Bei den studentischen und wissenschaftlichen Hilfskräften bedanke ich mich ganz herzlich für die Kühlung der Gammadetektoren, die Arbeit im Strahlenschutz und die gute Stimmung, die ihr verbreitet.

Ich danke Vanessa Tomanek und Joachim Rewitzer für ihre umfassende Hilfe bei den ICP-OES- Messungen, von denen es sehr viele gab.

Ein großer Dank gilt dem Strahlenschutzbeauftragten der Gruppe, Gerald Haas, für seinen Einsatz für die Sicherheit bei der Arbeit mit radioaktiven Stoffen.

Bei Michael Hechtel bedanke ich mich für die Bereitstellung von ^{137}Cs Kalibrierkurven für die Gammamessgeräte GEM3 und GEM4 und sein fröhliches Gemüt.

Ich danke der Glasbläserei für die Spezialanfertigung und die Hilfe bei der Wartung der Säulen für die Hot Column Chromatographie.

Mein Dank geht auch an Dr. Stefanie Schmid für ihre Vorarbeit an dem Projekt Hot Column Chromatographie.

Ein großes Danke an meine Freunde und Doktorandenkollegen, die diese Monsterarbeit für mich korrekturgelesen und Verbesserungsvorschläge eingebracht haben: Alissa Wieberneit, Gerhard Gottinger, Andreas Schreiber und Alexander Moreno.

Allgemein bedanke ich mich bei allen meinen Freunden, die mich während der Promotion moralisch unterstützt haben und das Leben heller und lebenswerter machen. Allen voran danke ich dafür meinem Partner Mario Marinovic.

Der größte Dank gilt nicht zuletzt meiner Familie, vor allem meiner Mutter Elena Weigel und meinen Großeltern Lydia Rapsch und Alexej Rapsch, die mich immer geliebt, unterstützt, gefördert und an mich geglaubt haben, auch wenn ich das selbst nicht konnte.

Abbreviations

CCD: Semiconductor detector

CITES: Convention on International Trade in Endangered Species of Wild Fauna

DC: Direct Current

DOWEX: Dowex®50WX8 200-400 (H) resin, column material

EOP: Setup of a system with axial plasma observation

FEP: Full energy peak

Hot Chroma: Hot Column Chromatography separation

HP-Ge: High purity germanium crystal

ICP-OES: Inductively coupled plasma-optical emission spectrometry

LSC: Liquid Scintillation Counting (LSC)

RC circuit: Circuit consisting of a resistor and a capacitor

ROI: Region of interest

SQPE: Spectral Quench Parameter of the External standard

Symbols

α: Alpha radiation

β: Beta radiation

γ: Gamma radiation

Δm_{Ca}: Uncertainty of the calculated calcium mass

Δt: Time difference between the reference time and the current time

η_{chem}: Chemical efficiency of a method

η_{phys}: Physical efficiency of a method

λ: Decay constant

µSv: Micro-Sievert

σ: Curve width

A: Radioactivity

A_0: Radioactivity at the start time

a: Specific activity, radioactivity divided by mass

Bq: Becquerel, SI unit for activity, one decay per second

Ca: Calcium

CHN: Channel number, represents the emission energy

CHNO: Channel number at the count maximum of the emission curve

Cs: Cesium

cm: Centimeter

CO_2: Carbon dioxide

cpm: Counts per minute

cps: Counts per second

K: Potassium

keV: Kilo electron volt

km: Kilometer

m: Mass

m: Meter

M: Molar mass

MeV: Mega electron volt

n: Amount of substance in mol ($6.022 \cdot 10^{23}$)

N: Number of measurements

N: Number of radionuclides

N_0: Number of radionuclides at the start time

R: Net count rate

s: Second

S: Standard deviation of the measured values

Sr: Strontium

StrlSchV: Strahlenschutzverordnung

t: Table value of the Student distribution (t-distribution) with an α value of 0.05 and therefore a level of confidence of 95 %

t: Time

$t_{1/2}$: Half-life of a nuclide

Y: Yttrium

Y: Transition probability

Y_0: Maximum count number

Chemicals

Acids and bases

Chemical	Characterization	Supplier	Purity
HCl	Hydrochloric Acid Code: H/1200/PB17 Lot: 2042637 MW: 36.46 UN: 1789	Fisher Chemical	approx. 37 % analytical reagent grade
HNO_3	Nitric Acid Code: N/2185/PB17 Lot: 2215305 MW: 63.01 UN: 2031	Fisher Chemical	65 % analytical reagent grade
H_2SO_4	Sulfuric Acid Code: S/9240/PB17 Lot: 2042306 MW: 98.07 UN: 1830	Fisher Scientific	≥ 95 % analytical reagent grade
H_2O_2	Hydrogen Peroxide solution Code: 102270478 Lot: STBJ7639 MW: 34.01 g/mol d:1.130 g/cm^3	Sigma Aldrich	34.5-36.5 %
Lactic acid	DL-Lactic acid (T) 2-Hydroxypropionic acid $C_3H_6O_3$ MW: 90.08 g/mol d: 1.209 g/cm^3	Sigma Aldrich	approx. 90 %
NaOH pellets	Sodium Hydroxide pellets Code: S/4920/60 Lot: 2038017 MW: 40.00 UN: 1823	Fisher Chemical	analytical reagent grade
NH_3	Ammonia solution K51944632943 1.05432.2500	Merck	25 % for analysis

Diluted acids, bases and mixtures

Chemical	Preparation
6 M HCl	591.24 g HCl (37 %) filled up to 1 L with bidistilled water
1 M HCl	98.54 g HCl (37 %) filled up to 1 L with bidistilled water
0.025 M HCl	2.46 g HCl (37 %) filled up to 1 L with bidistilled water
SO_4^{2-} water	approx. 3 mL H_2SO_4 (96 % p.a) filled up to 250 mL with bidistilled water
1.5 M lactic acid	150.04 g lactic acid (approx. 90 %) filled up to 250 mL with bidistilled water
6 M HCl: 1.5 M lactic acid (1:1)	Prepared from a 1:1 mixture of 6 M HCl and 1.5 M lactic acid
Ammonium-lactate at pH 7 or 6	203.04 g NH_3 (25 % p.a) and 300.08 g lactic acid (90 %) mixed, pH adjusted with pH-meter and HCl (37 %), filled up to 2 L with bidistilled water

Salts

Chemical	Characterization	Supplier	Purity
YCl_3	Yttrium (III) chloride hexahydrate trace metals basis Lot: #0000070562 Y·6 H_2O MW: 303.36 g/mol mp.: 100°C d: 2.18 g/mL at 25°C form: crystals and lumps	Sigma Aldrich	99.9 %
K_2SO_4	Kalium sulfate 1.05153.0500 M: 174.27 g/mol	Merck	p.a
KCl	Potassium chloride 1.04936.1000 EMSURE Charge/lot: K40610636013 MW: 74.55 g/mol	Merck	p.a
$SrCl_2$·6 H_2O	Strontium chloride-hexahydrate 1.07865.0250 MW: 266.62 g/mol		p.a

Tracers

Chemical	Characterization/ Preparation	Supplier	Purity
Y-tracer (10 mg/mL)	3.412 g YCl_3·6 H_2O filled up to 100 mL with bidistilled water		
Y-Standard	Multi-Element Calibration Standard 2 CAS#: HNO_3 [7697-37-2] Lot#: CL5-175MKBY1 PE#: N9300232 5% HNO_3 10 µg/mL: Ce, Dy, Er, Eu, Gd, Ho, La, Lu, Nd, Pr, Sc, Sm, Tb, Th, Tm, Y, Yb	Perkin Elmer Pure Plus	10 µg/mL
Sr-tracer (50 mg/mL)	7.609 g $SrCl_2$·6H_2O filled up to 50 mL with bidistilled water		
ICP standard K	ICP-Standard Potassium KNO_3 in nitric acid 0.5 mol/L 03773.0000 Charge-Nr.: 20045795 UN3264 LQ	Bernd Kraft	1.000 g K/L
ICP standard Ca	ICP-Standard Calcium $CaCO_3$ in nitric acid 0.5 mol/L 03832.0000 Charge-Nr.: 20043116 UN3264 LQ	Bernd Kraft	1.000 g Ca/L
ICP standard Y	ICP-Standard Yttrium Y_2O_3 in nitric acid 0.5 mol/L 03794.0000 Charge-Nr.: 19022131 UN3264 LQ	Bernd Kraft	1.000 g Y/L
ICP standard Sr	ICP-Standard Strontium $SrCO_3$ in nitric acid 0.5 mol/L 03937.0000 Charge-Nr: 20042660 UN3264 LQ	Bernd Kraft	1.000 g Sr/L
^{137}Cs- tracer	2_Cs-137 tracer 14.88 Bq/mL preparation date: 01.01.1989 ($t_{1/2}$ 30.08 years)		
^{90}Sr tracer	Sr-90 tracer, 20000 Bq/1006 g preparation date: 2.12.2004 ($t_{1/2}$ 28.5 years)		
^{229}Th-tracer	Ac-227 (5_Ac227) tracer 0.0279 Bq/mL in 7.2 M HNO_3, 23.06.96		

Multi nuclide tracer

Supplier	Characterization
Eckert & Ziegler	calibration mark: D-K-15203-01-00 calibration standard: Ng1-202 type: QCYB410 serial no: AN-7723 batch: 20/2 form: open m: (100.721 ± 0.001) g V: approx. 100 mL d: 1.008 g/cm^3 reference date: 01.04.2020 12:00 UTC impurities: Rb-84 < 1 Bq Nuclides as chlorides in 0.5 M HCl solution, 20 µg/mL solution per element prepared through weighing of calibration standards, tested with gamma-measurements storing conditions: temperature: 21°C ± 5, humidity: 45% rF ± 20% rF

radioactivity data of the contained nuclides:

nuclide	photon-energy [keV]	activity [Bq]	photon-emission rate [s^{-1}]	relative measurement uncertainty of the activity [%]
Barium-133	81	6250	2290	2
Cobalt-57	122	6010	5140	2
Cerium-139	166	6000	4800	2
Barium-133	356	6250	3880	2
Strontium-85	514	29900	2950	2
Cesium-137	662	11700	9960	2
Manganese-54	835	12000	12000	2
Yttrium-88	898	29800	28000	2
Zinc-65	1116	30000	15100	2
Yttrium-88	1836	29800	29600	2

Ion exchanger column material

Ion exchanger material	Characterization	Supplier
DOWEX® 50 WX8 (200-400 mesh)	Order number: 41630.02 pract. Lot#: 150482 storing condition: +15-+30° counter ion: H^+ Capacity (eq/L): 2.1 loss on drying (%): 53.9	Serva
DOWEX® 50 WX8 (200-400 mesh)	Order number: L13922.30 Lot#: 1029089 CAS: 11119-67-8	Alfa Aesar
DOWEX® 50 WX8 (200-400 mesh)	Order number: 44519-100G counter ion: H^+, strongly acidic PCode: 102452001 Source: BCCH1036	Sigma Aldrich- Merk
CHELEX 100 Resin	Cat.#: 142-2832 100-200 mesh, sodium form, Control: 64442725 MFG lot: 64415846	Bio-Rad Laboratories

Remaining chemicals

Chemical	Characterization	Supplier	Purity
QSA Scintillation cocktail	Quicksafe A Liquid Scintillation Cocktail (Lot#200301) contains 4-Nonylphenol, branched, ethoxylated, Bis(isopropyl)naphthalene	Zinser Analytic	
Acetone	Lot# STBJ9578 32201-1L-M CAS:67-64-1 UN1090 C_3H_6O MW: 58.08 g/mol mp:-94°C bp: 56°C Flp:-17°C d: 0.7910 g/L	Sigma Aldrich	p.a. ≥ 99.5 %
Atmospheric Spectroscopy Standard wash solution	CAS #: HNO_3[7697-37-2]	Perkin Elmer	1 % HNO_3
ICALisation solution	20 mL/L HCl and 20 mL/L HNO_3 and the following atom concentrations with a deviation of at most 0.5 % Ca 1 mg/L, Be 2 mg/L, Li 2 mg/L, Sr 2 mg/L, Mn 5 mg/L, Mo 5 mg/L, Na 5 mg/L, Sc 5 mg/L, Ce 10 mg/L, Cu 10 mg/L, Fe 10 mg/L, Eu 10 mg/L, In 10 mg/L, K 10 mg/L, Ni 10 mg/L, P 10 mg/L, Si 10 mg/L, Ti 10 mg/L, V 10 mg/L, Y 10 mg/L, Zr 10 mg/L, S 50 mg/L		

Not contaminated sample matrix

Sample matrix	Characterization
Whole milk Berchtesgadener Land	Berchtesgadener Land haltbare Bergbauernmilch 3.5% Milchwerke Berchtesgadener Land Chiemgau eG D-83451 Piding DE BY 13110 EG contents: per 100 mL 275 kJ/ 66 kcal Fat: 3.6 g of that 2.4 g saturated fatty acids carbohydrates: 5.0 g of that 5.0 g sugar protein: 3.3 g salt: 0.11 g calcium: 124 mg

Devices

Measurement devices

Device	Model name	Supplier
UV-Vis measurement device	Spectroquant	NovaGO (Merck)
pH meter	Lab 855 pH-meter	SI Analytics aχylem brand
ICP-OES	Spectroblue FMX36	Metek Materials Analysis Devision
Gamma detector	GEM3, GEM 4, GEM 40	
LSC and Cherenkov detector	1220 Quantulus Liquid Scintillation Counter	Perkin Elmer
α and β detector	Berthold LB 770-2: 10 Channel Low-Level Counter	Berthold München GmbH

Sample preparation devices

Device	Characterization
Oven	Nabertherm More than heat 30-3000 muffle furnace with switchgear and control plant additional model by Heraeus
Stirring and heating plates	
Thermometer	
Theromostate	three different models: HAAKE F3+ HAAKE M thermomix_1480 b. Braun Messungen AG HAAKE D8
Scale and analytical scale	
Centrifuge	HERMLE 2300
Sand bath	
Ultrasonic bath	BRANSON 2200

Laboratory materials

Glass materials	Remaining materials
Volumetric flasks (different sizes)	Agitators
Quartz bowls	Pipettes
Big glass columns with reservoirs	Eppendorf-pipettes
Glass column with 2 cm diameter and a frit with the pore size GO	Pipette tips
Beakers (different sizes)	LSC-vials 20 mL by Zinser Analytic
Watch glasses (different sizes)	Centrifuge tubes
Crystallizing dishes	Whatman-42 filters
Dropping funnel	Buckets
Satorius suction unit	Troughs

Table of contents

1 Introduction and motivation

Nuclear power production is a stable energy source with low CO_2 emissions [1], but also poses problems and risks. Nuclear catastrophes are a major risk. Chernobyl and Fukushima are tragic examples. Such disasters can be caused by human error, a technical malfunction, an accident, a natural disaster or possibly even a targeted attack. As the previous accidents have shown, such an event can lead to the long-term contamination of huge regions and endanger a large amount of people [2]. Remaining ^{137}Cs from the Chernobyl catastrophe is still found on many external surfaces today [3]. But even if a nuclear power plant works according to plan, a significant amount of nuclear waste is produced [4]. Thus, the German parliament resolved the shut-down of all nuclear power plants in the federal territory over the next years [5]. However, this process could be delayed due to the unstable gas supply because of the international sanctions imposed on Russia as a reaction to its attack on Ukraine [6]. But even if all nuclear power plants were ordered to shut down immediately, the shut off and dismantling of the reactors is a long and complicated process. In addition, nuclear waste remains active for several generations after it has been used to generate nuclear energy, posing a threat to the public and the environment. Where this waste should be put is also a very complicated technical and political decision [4]. The question of the location of a final nuclear depository is regularly all around the media [7,8]. There is significant resistance from the population against a final depository near them, for fear of contamination and negative effects on their health or surrounding. Another risk associated with radioactivity is the threat of atomic bombs. In addition to their immediate devastating destruction, they cause a similar contamination in the surrounding as a collapsed nuclear power plant [9]. ^{90}Sr, stemming from the nuclear weapon tests performed in the mid of the century, can still be found in the environment and incorporated into the tusks of elephants through their diet [10].

This shows that, even when it has been fortunately a long while since the last nuclear attack and more and more nuclear power plants, at least in Germany, are shut down, the monitoring of radionuclides and radioactive contamination is still relevant and will stay relevant in the future [10]. On the one hand, quick and reliable analysis methods are needed in case of a nuclear emergency. On the other hand, routine measurements of the activity surrounding nuclear power plants are crucial, to ensure that no contamination has leaked out.

One of the main radionuclides in environmental monitoring is ^{90}Sr [3]. For the separation of Sr from the sample matrix, Milton et al. [11] developed the Hot Chromatography separation method. It makes the separate measurement of Sr nuclides without the interference of other radionuclides possible. This method was the focus of many research projects in this group, with the aim to improve, validate and adapt it to different sample matrices. Even though this is a reliable method, that is routinely applied and delivers low levels of detection and a good yield, it is still very laborious and time, energy and chemicals consuming.

The aim of this work was to further improve this established method and make it more efficient. The focus was to separate the decay product of ^{90}Sr, ^{90}Y, from the matrix and measure it instead. From the results of the ^{90}Y measurement, the activity of ^{90}Sr could be determined. Additionally, it was tried to pre-separate the confounding nuclide ^{40}K from the matrix. It was also tested whether different sample matrices influence the separation of Sr and Y. Finally, a new column material batch was validated and the separation conditions adjusted for an optimal separation.

2 Theoretical foundation

In the following section the background knowledge, necessary for the understanding of the research approach and results presented in this work, is summarized. First, the basics of radioactivity are presented, then the term "radioactive equilibrium" is explained. After that, the analytes and interfering elements and nuclides are elaborated on. Finally, the kinds of samples relevant for this work are introduced.

2.1 Radioactivity fundamentals

Radionuclides are unstable isotopes, which decay into other nuclides and emit ionizing radiation during this process. This behavior is called radioactivity. The radioactive decay is a statistical process, which is represented with the following equations.

$$-\frac{dN}{dt} = \lambda N \tag{2.1}$$

$$-\frac{dN}{dt} = \lambda N = A \tag{2.2}$$

$$\lambda = \frac{ln2}{t_{1/2}} \tag{2.3}$$

N is the number of the radionuclides. -dN/dt is the decay rate and represents the decreasing number of the decaying radionuclides with time, which is defined as activity A. The SI unit for the activity is Becquerel (Bq), with 1 Bq representing one decay per second. Equation 2.2 shows that the number of nuclides N and their activity A are proportional to each other. λ is the decay constant, which is indirectly proportional to the half-life $t_{1/2}$ of the nuclide, the time needed for half of the present nuclides of one kind to decay [10].

As equation 2.1 presents the speed of a reaction of the first order, from its integration from N_0 to N and from 0 to t, equation 2.4 is obtained [10]. In this equation N_0 is the number of radionuclides at the start time, N is the number of nuclides at the reference time, and t is the time difference between the start time and the reference time.

$$N = N_0 \cdot e^{-\lambda t} \tag{2.4}$$

With this equation, the number of radionuclides after a certain decay-time can be calculated, if the number of radionuclides at the beginning, as well as their half-life, is known. Because the number of nuclides and their activity are proportional, this equation can also be applied to the activity.

$$A = A_0 \cdot e^{-\lambda t} \tag{2.5}$$

From this, also the activity of a sample can be calculated after a certain decay time, if the half-life of the nuclide and the activity at the start are known.

The specific activity is the activity of a sample divided by its mass.

$$a = \frac{A}{m} \tag{2.6}$$

Kinds of radiation

Radiation is an umbrella term for different kinds of radiation, produced through radioactive decay. The different kinds of ionizing radiation differ in their nature, their energy and their danger for the human health and are explained more precisely in the following section.

α-radiation

Alpha-radiation is emitted in form of Helium He^{2+} cores, consisting of two protons and two neutrons, by the α-active radionuclide during its decay. Thus, alpha radiation is a form of particle radiation and is only emitted by radionuclides with a high mass. Through emitting an alpha particle, the mass number of the radionuclide decreases by four and the valency number by two units. The α-particles leave the nucleus of the radionuclide with a speed of 10,000-20,000 km/s, which corresponds to a kinetic energy of several MeV. The energy of the decay is transferred in form of kinetic energy to the daughter nuclide and the α-particle in a reverse relation to their mass [12]. Therefore, the energy of the alpha particles is clearly defined and can be used to identify its emitting radionuclide. α particles have a quite small depth of penetration of matter because of their relatively large size and their charge. It can be easily shielded from by several centimeters of air as distance or a piece of paper. But α-radiation can be very dangerous if incorporated into the body, where it can damage cells through its high energy [13].

β-radiation

Beta-radiation is a form of ionizing particle radiation emitted due to the β-decay of a radionuclide. β radiation consists of electrons, in the case of the more common β^- decay, or of positrons, in the case of the rarer β^+ decay. During the β^- decay, a neutron turns into a proton, an electron and an electron-antineutrino in a nucleus with excess neutrons. The electron and the antineutrino leave the nucleus, increasing the atomic number by one while the mass number stays the same This process is visualized in the equations 2.7 and 2.8 [14].

$$ {}^{1}_{0}n \rightarrow {}^{1}_{1}p + {}^{0}_{-1}e + {}^{0}_{0}\nu_e \tag{2.7}$$

$$ {}^{A}_{Z}X \rightarrow {}^{A}_{Z+1}Y + {}^{0}_{-1}e \tag{2.8}$$

The emitted electrons have a continuous energy distribution, with a value between 0 an E_{max}, the maximal β energy, due to the distribution of E_{max} between the electron and the electron-antineutrino. This was originally also the reason for the postulation of the electron-antineutrino [14].

If a β-particle enters a material, energy is transferred and ionization takes place through the impacts of the electrons with the material. The β particles are deflected and slowed down in the surface layer of the material. The interaction of β-radiation with skin can damage its outer layers, cause burn injuries and in the long-term lead to skin cancer. If incorporated into the

body, β-particles can cause radiation damage to the surrounding tissue, but not as severe as α-particles, as they have a lower energy. In the long term they can also cause cancer. β-radiation can be shielded with a one cm thick plexiglass disc or a shield from a material with relatively light atoms, like aluminum, to protect the shield from the x-ray bremsstrahlung, that can be a side product of the interaction of β-particles with the material [15].

γ-radiation

Gamma-radiation is a type of electromagnetic radiation in form of uncharged photons or quants and not a particle radiation like β- and α-radiation. It is comparable to X-rays, but with a higher energy of over 200 keV, whereas the energy of X-rays is between 0.1-250 keV. The radiation emitted by γ-active radionuclides has a characteristic energy, which can be used to identify its source nuclide. γ-decay is often preceded by other decay modes. A nucleus in an excited state after a previous decay can emit γ quanta of a certain energy and fall back to a lower energy state. The energy of the nucleus changes but the atomic number and the mass number stay the same. Because of its nature as electromagnetic radiation, γ radiation has the biggest penetration depth of all the presented kinds of radiation. The energy of gamma radiation sinks exponentially with the penetration depth. Mostly lead is used as shielding material against γ-radiation, because of its high density. If γ-radiation interacts with tissue, it is absorbed and can cause ionization and secondary radiation like x-rays and released electrons. Through this, cells are damaged during cell division, which can cause mutations. This can harm the production of quickly produced and replaced cells like blood cells, cause cancer and genetic damage to the offspring of the exposed people or animals [16].

2.2 Radioactive equilibrium

A very important term in radiochemistry is the radioactive equilibrium. If a radionuclide decays into another radionuclide, the first one is referred to as parent radionuclide and the second as daughter nuclide. The radioactive equilibrium is achieved in a decay series when the activity ratio between the parent radionuclide and the daughter products is constant. This happens when the half-life of the parent nuclide $t_{1/2}$ (1) is much longer than the half-life of the daughter nuclide $t_{1/2}$(2). In this case the equilibrium is secular. If the nuclides are separated from each other at the time 0, the number of the daughter nuclides is represented by equation 2.9. With N_1 being the number of the parent nuclides and N_2 being the number of the daughter nuclides. This means that all the daughter nuclides present are generated through the decay of the parent nuclides [10].

$$N_2 = N_1 \frac{t_{1/2}\,(1)}{t_{1/2}\,(2)} \left(1 - e^{-\frac{\ln(2)}{t_{1/2}\,(2)} t}\right) \tag{2.9}$$

After ten half-lives of the daughter nuclide have passed, the radioactive equilibrium can be considered as established and equations 2.10 and 2.11 are applicable [10].

$$\frac{N_2}{N_1} = \frac{t_{1/2}\,(1)}{t_{1/2}\,(2)} \tag{2.10}$$

$$N_1 t_{1/2}\,(1) = N_2 t_{1/2}\,(2) \tag{2.11}$$

$$A_1 = A_2 \tag{2.12}$$

In radioactive equilibrium, each daughter nuclide decays as fast as it is produced by the decay of the parent nuclide, due to their short half-life. Therefore, the activity ratios between the radionuclides stay constant. In a secular radioactive equilibrium, the activities of both nuclides are the same, as the activity of the parent nuclide is the limiting factor for the activity of the daughter nuclide [10].

As a summary, a radioactive equilibrium can only be achieved if the following requirements are met. The half-life of the parent nuclide must be significantly longer than that of all the daughter nuclides in the decay series. Enough time must pass for the equilibrium to establish. No interferences can be present, like the external addition of daughter nuclides, which could influence the radio nuclides in the decay series [10].

2.3 Analytes

Many radioactive nuclides are known, as can be seen in the Karlsruhe nuclide chart. Not all of them are analysed separately in laboratories or are part of environmental monitoring, as only very few of them are produced by nuclear fission. In the following, the main analytes of this work are presented and it is explained why such a focus is placed on them, why a laborious analysis is performed to detect them and why these research efforts to improve said analysis are justified.

2.3.1 Strontium-90 and Strontium-89

The main analyte of this research project is Strontium, more precisely two of its β-active isotopes ^{89}Sr and ^{90}Sr. They are both created as fission products in nuclear reactors and two of the main radionuclides in environmental monitoring. This classification was decided because Sr accumulates in calcium rich matrices, like milk and bones, due to the chemical similarity of these elements. This means potentially radioactive strontium form the food is deposited in the activity sensitive bone marrow and causes high internal radiation exposure. From there it is only excreted with an effective biological half-live of 50 years and therefore can cause radiation damage over a long time. This is especially dangerous for children, due to their calcium rich diet [17].

As ^{89}Sr and ^{90}Sr are pure beta-emitters, a quite complex and time-consuming analysis process is necessary to separate them sufficiently from the sample matrix, to achieve a satisfactory limit of detection and to prevent false positive results.

Because of its short half-live of 50.5 days [18], ^{89}Sr is only present during the active operation of nuclear power plants or directly after an atomic bomb attack. By approximation, radioactive waste is considered mostly subsided and no longer a risk if 10 half-lives of the radionuclide have passed. So, one and a half years after the ^{89}Sr source was deactivated, the nuclide is basically completely decayed. As more and more of the German nuclear power plants are shut

down and all of them will be deactivated in the near future [5], ^{89}Sr will become mostly irrelevant in German environmental monitoring. Because of this, the focus of this work will be on the detection and quantification of ^{90}Sr.

This nuclide has a half-life of 28.9 years [18] and will therefore be still active over 200 years after the shut- down of all nuclear power plants. ^{90}Sr is formed in nuclear reactors with a splitting yield of 5.8 % [19]. After the atmospheric nuclear tests during the cold war, the deposition density, which means the activity per unit area deposited on the ground, of ^{90}Sr was 2140 Bq/m^2 in the northern hemisphere and about one fourth of that value in the southern hemisphere [20]. The dose coefficient for the effective dose for a singular ingestion through inhalation is 0.0077 µSv/Bq for ^{90}Sr in radioactive equilibrium with ^{90}Y, considering the whole body. For the critical organ bone marrow, it is 0.63 µSv/Bq for ^{90}Sr [17]. These values are applicable for adults of the general public.

All in all, the presented information on ^{90}Sr, from its origins and its accumulation in bone marrow, to its long half-life, shows that ^{90}Sr analysis will stay relevant in the future.

2.3.2 Yttrium-90

^{90}Y is the short-lived decay product of ^{90}Sr [21, 22], that decays to the stable nuclide ^{90}Zr. ^{90}Y has a half-life of 64 hours [18, 23]. It is also a pure beta-emitter, which makes a separation of the nuclide from the matrix before measurement necessary. After an adjustment phase, a radioactive equilibrium between ^{90}Y and ^{90}Sr is maintained, as the half-life of ^{90}Sr is much longer than the half-life of ^{90}Y. In the radioactive equilibrium, their activity ratios are constant and, in this case, almost 1:1. This makes is possible to determine the activity of ^{90}Sr through the analysis of its daughter nuclide ^{90}Y.

With such a short half-life, working with ^{90}Y makes the waste disposal process easier, compared to the long lived ^{90}Sr. But the short half-life also means that after the separation of ^{90}Y from the sample matrix, the measurement process must begin as soon as possible, to prevent a significant yield loss.

2.4 Interfering elements and nuclides

Sample preparation is necessary to detect α or β activity in a sample and correctly attribute it to the nuclide that is causing it. During this process the analyte nuclide is separated from the interfering nuclides and elements. This is necessary, because the energy resolution for α and β measurements is either not present at all, or not good enough to attribute the measured activity to a certain nuclide and correct for overlap. In the best case, only one radionuclide is present in the final measurement preparation of the sample, so all the measured activity can be traced back to it. The sample preparation is usually the most laborious and time-consuming aspect of the analysis. The most interfering nuclides and elements have to be identified and their removal planed. In the following, the identified interfering nuclides and elements for the ^{90}Sr and ^{90}Y analysis are presented and it is explained in which way they would disturb the analysis, if not separated properly.

2.4.1 Calcium

Calcium is present in high amounts in many environmental and food samples like ivory, bones, milk, fruits, vegetables and different kinds of grain. The high calcium amount in the samples can lead to precipitation during the Hot Chromatography separation. This would disrupt the whole sample separation process, by clogging the separation device, and possibly damaging the column and the resin. Because of their chemical similarity, the precipitation of calcium would also lead to a coprecipitation of strontium and cause a significant yield loss. To prevent precipitation, the separation of Sr from the sample matrix takes place at 87°C, so calcium stays in solution as Ca^{2+}-ions. The high calcium content of the samples is one reason, why an elaborate and time-consuming separation process, preceding the analysis, is necessary.

2.4.2 Potassium-40

A confounding nuclide for the ^{90}Sr and ^{90}Y analysis is ^{40}K, a naturally occurring radioactive isotope of potassium. It makes up 0.012 % (120 ppm) of the total amount of potassium found in nature [24]. ^{40}K is a primordial radio nuclide, which means the ^{40}K found on earth was created through stellar processes even before the planet was formed and not through radioactive decay or through human intervention, which has not significantly changed the amount of ^{40}K present [25]. With its very long half-life of 1.251 billion years, it is the largest source of radioactivity in animals, including humans. Its long half-life also makes it relatively harmless, as it decays very slowly and therefore emits only little radiation. ^{40}K is a β- emitter, that can undergo both kinds of β-decay. In 89.28 % of cases ^{40}K decays to ^{40}Ca by emitting a β- particle or electron and an antineutrino. In 10.72 % of cases ^{40}K decays to ^{40}Ar by emitting a neutrino and then a γ-quant at 1460 keV. In the rare case of 0.001 % of all decays, ^{40}K forms ^{40}Ar by emitting a β^+ particle, or positron [26, 27, 28, 29, 30]. Because ^{90}Sr and ^{90}Y are also β-emitters, the background radiation of ^{40}K could lead to a false positive ^{90}Sr or ^{90}Y signal. So, the proper separation of the analyte nuclide from the ever-present ^{40}K is one of the main aims of the sample preparation.

2.4.3 Cesium-137

Another very important interfering nuclide is ^{137}Cs. Like ^{90}Sr it is a fission product in nuclear reactors, where it is formed with a slightly higher splitting yield of 6.2 % than ^{90}Sr. It is apart form ^{90}Sr the most relevant long lasting fission product. They also have quite similar half-lives with the half-life of ^{137}Cs being 30.05 years [31, 17]. ^{137}Cs is also a β emitter. In 94.6 % of cases, it decays to the metastable ^{137m}Ba. In the remaining cases, ^{137}Cs decays to the stable ^{137}Ba in the ground state. The metastable ^{137}mBa has a half-life of 153 seconds and decays to the stable ^{137}Ba by emitting gamma rays with the energy of 661.7 keV [32]. This happens in 85.1 % of all ^{137m}Ba decays [33]. The decay of the short lived ^{137m}Ba is responsible for the γ-activity of ^{137}Cs [32].

The deposition density of ^{137}Cs after the atmospheric nuclear tests during the cold war was 1.6 times higher the that of ^{90}Sr. Despite their similar origin, these two radionuclides have a

completely different radiological hazard potential for living organisms. If ingested, ^{137}Cs is distributed almost homogeneously in the tissues of vertebrates and therefore humans. And it is excreted with an effective half-life of four months. This is very fast in comparison with ^{90}Sr. Because of this, the dose coefficient for the effective dose for a singular ingestion through inhalation is 11 times higher for ^{90}Sr considering the whole body than it is for ^{137}Cs. For the critical organ bone marrow, it is even 63 times higher for ^{90}Sr than for ^{137}Cs [17].

This shows that ^{137}Cs is less radiologically dangerous for the population than ^{90}Sr, even though they share a lot of similarities. At the same time ^{137}Cs is more present in our surrounding and emits the same radiation as ^{90}Sr and ^{90}Y during its decay. This means, a sufficient separation of these nuclides, as well as ^{90}Y from ^{137}Cs, is necessary to prevent a false positive result and the overestimation of the present danger.

2.5 Sample types

The Hot Chroma separation method is used to separate strontium from calcium rich matrices, to be able to measure the activity of the Sr-radionuclides, especially ^{90}Sr, without interferences. It can also be used to separate ^{90}Y from the sample matrix, to determine the ^{90}Sr contend through the activity of its daughter nuclide. The samples, for which this separation is necessary, contain a big amount of calcium. In this laboratory, this method is mostly used for the determination of ^{90}Sr in agricultural food products and in ivory. For which purposes these analyses are performed is explained in the following paragraphs.

Agricultural samples

The URA laboratory regularly analyses agricultural food samples from farms surrounding several nuclear power plants. The analysis of ^{90}Sr is part of this analytical program. It is performed to ensure the safety of the food produced on these farms for the consumer. Additionally, the measurements show whether there were some undocumented leaks of radionuclides form the nuclear power plants into their surroundings. All in all, these measurements are part of the monitoring of the areas surrounding nuclear power plants. The tested agricultural products are diverse: grains, mostly wheat but also spelt and barley, corn, apples, sugar beets, salad and milk. The plant-based products are tested yearly and are mostly sent to the laboratory directly after the harvest. The milk samples, which make up most of the samples, are tested semi-annually. Because of their high calcium content, they are especially prone to be contaminated with ^{90}Sr. The nuclide would be transferred from the large amounts of grass or hay, that the producing cow ate, into the calcium rich milk, because of the chemical similarity between calcium and strontium. As the milk is then even further concentrated to produce several dairy products, the ^{90}Sr content would rise even more. Because of this special focus on the milk samples, this matrix was chosen for most of the experiments performed in this work.

Ivory samples

Elephants are one of the most endangered animal species. A main cause for the decline in population is the hunting and poaching of elephants for their ivory, which is considered very valuable [34]. In 1989, elephants were included in the Convention on International Trade in Endangered Species of Wild Fauna (CITES). Asian- and most populations of the African elephants are considered directly threatened with extinction. Because of this, they receive the highest level of protection and the trade with parts from elephants, especially ivory, is strictly regulated [35, 36]. Trade of ivory newer than 1990 is prohibited without exception and the export of unprocessed tusks is illegal. Trade of ivory extracted between 1976 and 1990 is legal within Europe, but the reexport is prohibited. For the trade and re-export of ivory extracted between 1947 and 1976, an age certificate and a license are required. An exception poses processed ivory objects, if they were verifiably produced before June 1947, as they are considered antiques [37, 38, 39].

To decide which regulation applies to a certain ivory tusk or object, and whether its possession and trade is legal, a reliable and unambiguous age determination is necessary. One well known method to achieve this is radiocarbon dating. The content of ^{14}C can be determined precisely consuming only low amounts of material. But the dating is ambiguous in the period between 1950 and 1990, due to the "bomb curve" shape fundamental to this analysis, caused by the high amounts of emitted radionuclides through the atom bomb tests in the middle of the last century (see figure 1) [40]. To close this blind spot the radiocarbon dating is complemented by the determination of the ^{90}Sr content and the $^{228/232}Th$ ratio in the ivory sample [10, 41]. ^{90}Sr is produced through nuclear fission and was distributed during the global nuclear fallout in the 1960s [3]. As alkaline earth element ^{90}Sr behaves very similarly to calcium and is therefore transferred to calcium containing tissues like ivory, after being incorporated through the food chain. Due to its long half-life of 28.5 years, ^{90}Sr from the fallout can be detected even now. Remarkably, the specific activity of $^{90}Sr/Ca$ is much higher in ivory compared to other calcium rich matrices like human bone tissue, which makes ivory a suitable matrix for this analysis [10]. As ^{90}Sr was emitted through nuclear bomb tests, the temporal evolvement of the $^{90}Sr/Ca$ values also shows a bomb curve (see figure 2), similar in shape to the $^{14}C/C$ bomb curve. If the ratio of $^{90}Sr/Ca$ is lower than 0.003 Bq/g Ca, the death occurred before 1958. Given values of, for example 0.4 Bq/g Ca, the time of death can be assumed to be 1960 or 1970. If the interpretation is ambiguous, an additional thorium analysis is necessary. The activity ratio of the naturally occurring thorium isotopes ^{228}Th and ^{232}Th is time dependent and can be determined very sensitively. With an increasing time-difference between death and analysis, the activity ratio of $^{228}Th/\ ^{232}Th$ decreases from about 40 to about 1 if death occurred before 1968 [37].

Previous analyses of ivory samples of known age resulted in "bomb" curve graphs. These enable us to determine the age of a suspicious ivory sample through its ratios of $^{14}C/C$ and $^{90}Sr/Ca$.

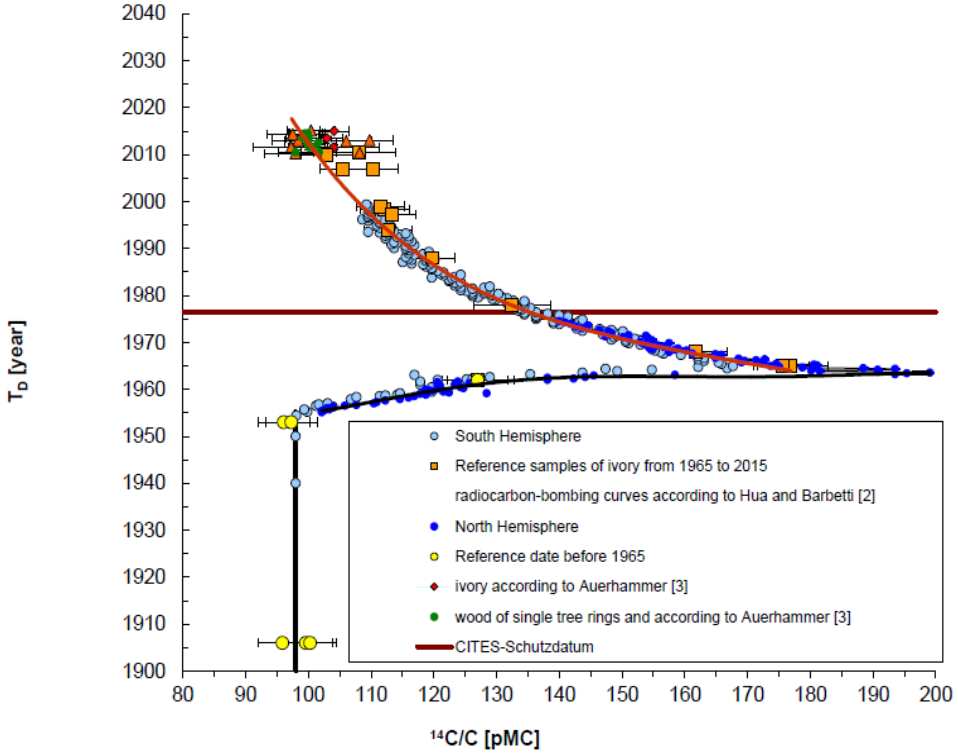

Figure 1: ^{14}C bomb curves [37, 42, 43, 44]

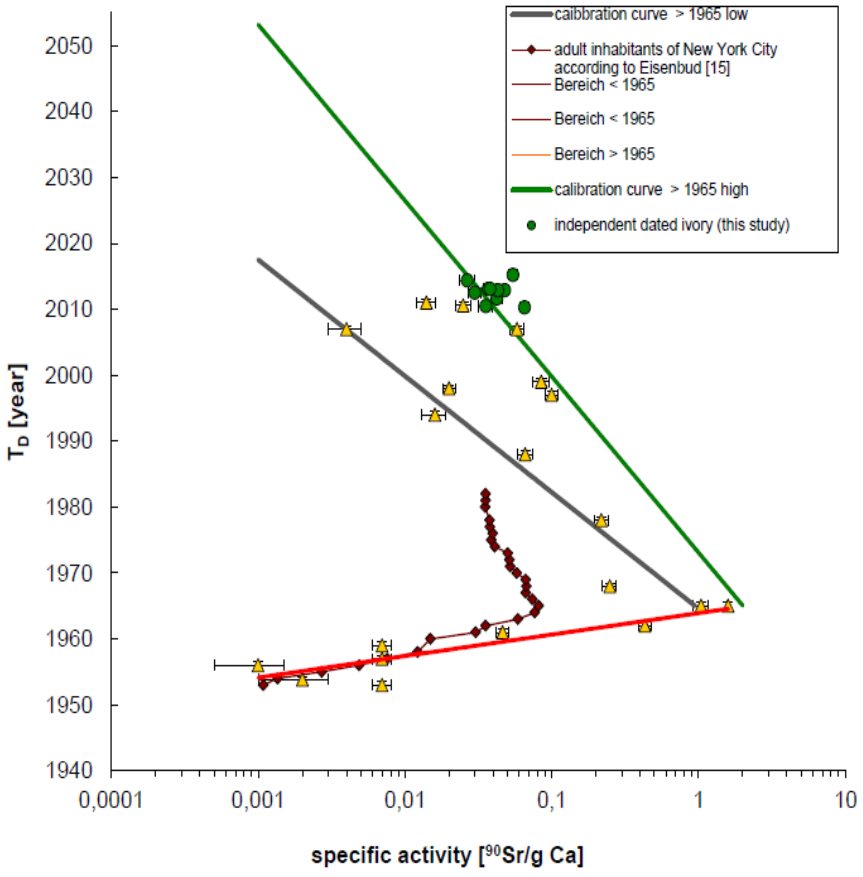

Figure 2: ^{90}Sr bomb curves [10, 40, 45, 46]

The separation of Sr from the ivory matrix and determination of the ^{90}Sr activity needed for this age determination is performed with the Hot Chroma method [47], which is the subject of this work. Modifications of this method have at least in part been tested with ivory samples in a validation process, to make sure the modified method is still applicable for the age determination of ivory.

3 Research approach

The aim of this research work was to further improve, validate and increase the efficiency of the Hot Column Chromatography separation method. This method was developed by Milton et al. [11] for the separation of Sr from a sample matrix and over the years was more and more adjusted and improved by several researchers in this group. It is an established method used in routine analyses and provides low levels of detection and a good yield, but is very laborious, time consuming, elaborate and cost intensive.

A first step of the research was to test this separation method for different sample types, that it already is applied for, to find out whether the sample material has a significant effect on the separation of the ions in the column. The tested sample matrices were milk, wheat, salad and corn ashes. For this, the calcium contents of the samples were determined and elution curves for the different matrices recorded. As tracer a mixed-nuclide solution was used, which contained a variety of gamma-active nuclides, among them ^{88}Y and ^{85}Sr, which behave chemically like the analyte isotopes ^{90}Y and ^{90}Sr, and ^{137}Cs, one of the main confounding nuclides. The determined elution curves showed the elution ranges of the different nuclides, that were separated by the column material. These could be compared among the different sample materials and determined whether the sample-matrix has a significant effect on the separation of the target analytes or not.

Another project incorporated in this work was the validation of the use of a new batch of column material, the Dowex®50WX8 200-400 (H) resin. The resin had to be bought from a new provider, as the established provider Serva, that it was usually purchased from, did not offer it anymore. The offered Dowex®50WX8 200-400 (H) resins by Alfa Aesar and Sigma Aldrich were tested for their suitability for the Hot Column Chromatography separation method. The new batches of column material were expected to behave the same as the old one, as they have the same trade name. But as a resin is a complex product and the analyses rely on knowing the exact elution regions of the analytes, it had to be made sure the properties of the new resin were suitable for the analysis aim. So, the following questions for the validation were asked and tried to be answered through elution experiments: Is the new column material suitable for the separation of Y and Sr from each other and from the confounding elements or nuclides? Do the elution parameters have to be modified for the new column material? If yes, which parameters have to be modified? And finally, how do these parameters have to be modified?

The main task of this work was to make the separation and analysis more efficient, to save time and costs during it and make it more suitable for analyses in the case of a nuclear emergency. One way to do this was by shifting the focus from the analyte ^{90}Sr to its daughter nuclide ^{90}Y. The two nuclides are in radioactive equilibrium with each other and the ^{90}Sr activity can also be determined by the analysis of ^{90}Y in the sample, as they have an activity ratio of 1:1. For this, elution curves of yttrium had to be recorded and the separation of yttrium from the interfering nuclides and elements evaluated. The advantages of ^{90}Y as an analyte would be its narrow range of elution, faster elution compared to Sr and the good separation between Y and Cs. The final goal was a direct Cherenkov measurement of the Y fraction without post treatment. As ^{90}Y has a half-life of only about 64 hours, the measurement has to be performed immediately after the separation. But an advantage of this short half-life is the easier waste management of ^{90}Y, as it decays so fast, and the possibility to directly measure the background of the sample after the ^{90}Y analyte has decayed.

Additionally, it was tried to pre-separate potassium from the sample, as ^{40}K is the main confounding nuclide for the ^{90}Y analysis. This is caused by their similar elution regions and the fact that they are both β-emitters. A pre-separation of yttrium through hydroxide precipitation was explored. As another option, the separation of yttrium from potassium and eventually calcium in a CHELEX 100 column was examined.

4 Methods

To obtain the research results in this work, many different analysis and measurement methods were used, which are presented and explained in the following section. Ion exchange chromatography and inductively coupled plasma-optical emission spectrometry (ICP-OES) are commonly used analytical techniques that were part of this work. Detection methods, specialised for the detection of radionuclides, were gamma-spectrometry for γ-emitters and Liquid Scintillation Counting (LSC), Cherenkov Counting and Low level α and β counting for β-emitters. α-emitters were not investigated in this work.

4.1 Ion exchange chromatography

Chromatography is a separation and analysis method for mixtures of multiple components into the individual substances. The analytes are solved in the mobile phase and moved across the stationary phase. Due to interactions between them, the analytes are separated, in most cases in a chromatography column. Analytes that interact stronger with the stationary phase are retained longer, while analytes with weaker interactions are transported faster with the mobile phase. The analytes are detected after they leave the column. The visualization of the detector signal as a function of the elution time or elution volume is called a chromatogram, a schematic example is shown in figure 3. The first peak represents the mobile phase and t the time it takes the eluent to pass the column. A and B are two separated analytes, causing peaks in the chromatogram with the retention times t_r^A and t_r^B and the base widths w_A and w_B. Δt is the difference between the retention times of the analytes [48].

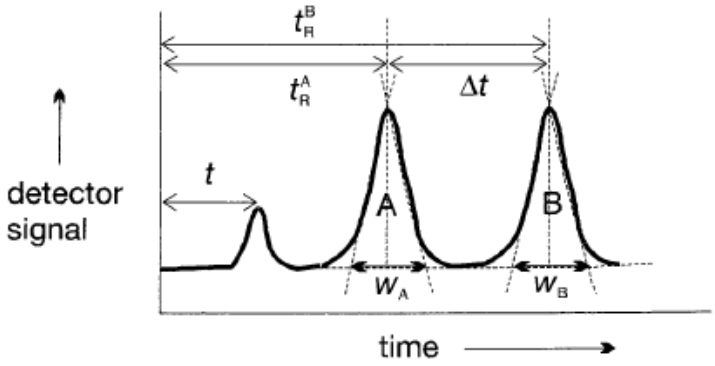

Figure 3: Schematic representation of a chromatogram with the characteristic values visualized [48]

The distribution of an analyte between the stationary phase and the mobile phase is determined by the partition equilibrium. It is represented by the partition coefficient K, the concentration of the analyte in the stationary phase divided by the concentration of the analyte in the mobile phase, as shown in equation 4.1 [48].

$$K = \frac{c_S}{c_M} \text{ [48]} \tag{4.1}$$

Another important characterizing quantity for a chromatographic separation is the retention factor k, expanding the partition coefficient by the quotient of the analyte volume in the stationary phase and in the mobile phase, as shown in equation 4.2 [48].

$$k = K \cdot \frac{V_s}{V_M} = \frac{t_R - t}{t} \text{ [48]} \quad (4.2)$$

It can be also calculated by the difference between the retention time of the analyte in the column t_R and the time needed for the mobile phase to pass the column without retention t, divided by t, as shown in equation 4.2. The optimum for the retention factor is between 1 and 5. If it is too small, the analytes are eluted too fast and the separation is insufficient. If it is too big, unnecessarily long elution times are needed [48].

The velocity of the analyte elution υ is calculated according to equation 4.3 [48].

$$\upsilon = \frac{L}{t_R} = \frac{L}{t} \cdot \frac{1}{1+k} \text{ [48]} \quad (4.3)$$

L represents the length of the packed column material, t_R the retention time of the analyte in the column and t the time needed for the mobile phase to pass the column without retention. k is the retention factor [48].

The quality of the separation between the peaks of two analytes in a chromatogram is quantified by the selectivity factor, also called separation factor α. It is calculated according to equation 4.4 with A and B representing two different analytes separated chromatographically [48].

$$\alpha = \frac{K_B}{K_A} = \frac{k_B}{k_A} \cdot \frac{t_R^B - t}{t_R^A - t} \text{ [48]} \quad (4.4)$$

The peak broadening in a column is a direct measure for its separation efficiency. This connection is illustrated in the classical theory of chromatography, according to which several distinct partition steps take place in a column during the elution. The column is assumed to be divided in theoretical plates. According to the theory, on each of these theoretical plates an equilibrium of the separation of the analyte between the stationary and the mobile phase is established. So, when the analyte passes the column, it wanders from one separation equilibrium to the next [48].

$$N = \frac{L}{H} = 16 \cdot \left(\frac{t_R}{w}\right)^2 = 5.54 \cdot \left(\frac{t_R}{w_H}\right)^2 \text{ [48]} \quad (4.5)$$

The number of theoretical plates in a column N can be calculated by dividing the column length L by the height equivalent of a theoretical plate H, as shown in equation 3.5. In practice it can be calculated from the chromatogram with the retention time of the analyte t_R and the base width w or the half width of its peak w_H. The higher the number of theoretical plates and the lower consequently the plate height, the higher is the column resolution and efficiency. It is therefore useful for the characterization of the separation. However, the plate theory is only an approximation of the reality in the column and multiple equilibria cannot be completely established while the mobile phase is in motion [48].

The peak broadening is caused by a kinetic effect, encompassing the finite rate at which the mass transfer between the phases can occur while the analyte passes the column. This effect depends on the length of the different possible passages between the mobile phase and the stationary phase. It is therefore directly proportional to the flow rate of the mobile phase. To describe it, the dependence between the flow rate of the mobile phase u and the plate height H had to be determined. It is approximated by the Van Deemter equation 4.6 [48], which is visualized in figure 4.

$$H = A + \frac{B}{u} + C \cdot u \text{ [48]} \quad (4.6)$$

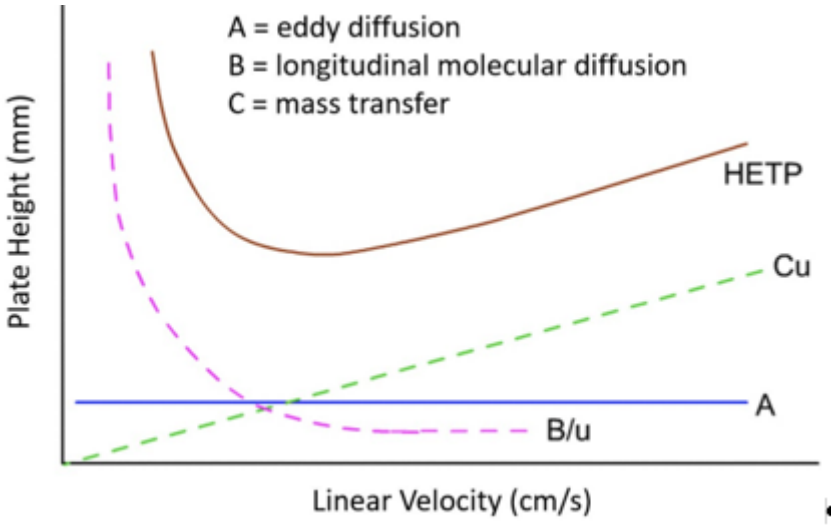

Figure 4: Visualization of the Van Deemter equation and its approximation to the relation between the plate height H and the flow rate of the mobile phase [49]

A represents the eddy diffusion, B the longitudinal diffusion and C the mass transfer between the mobile phase and the stationary phase. The eddy diffusion, analogue to a turbulent flow, is caused by the inhomogeneity of pathways and flow velocities through the stationary phase. The narrower the stationary phase, the smaller the eddy diffusion. The longitudinal diffusion represents the diffusion of analyte particles away from the peak center, as it is directly proportional to the diffusion coefficients of said particles in the mobile phase. It increases with decreasing relative molar mass. This term is only slightly relevant in liquid chromatography but is important in gas chromatography. During an elution, a constant mass transfer of the analytes between the mobile and the stationary phases takes place. For this to happen, the interface between the phases has to be reached by the analytes through diffusion in the mobile phase. The time for this varies for the particles, depending on their position in the column. This variation is accounted for in the mass transfer term. It is directly dependent on the column diameter and the particle diameter of the resin and inversely proportional to the diffusion coefficient in the mobile phase. The mass transfer constant also depends on the adsorption and desorption rates of the analytes in the stationary phase. Based on this information, the following optimizations can be performed to obtain a lower plate height H and therefore a better resolution of the separation. The particle size of the stationary phase can be decreased and a narrow size distribution ensured. The stationary phase can be packed more homogeneously and a smaller column diameter can be chosen [48].

The resolution R_S is another measure for the separation quality in a chromatogram. Contrary to the separation factor α, it also takes the peak width into account and not just the peak position. Its calculation is presented in equation 4.7 [48].

$$R_S = \frac{t_R^B - t_R^A}{\left(\frac{w_A - w_B}{2}\right)} = \frac{t_R^B - t_R^A}{t_R^B} \cdot \frac{\sqrt{N}}{4} = \frac{k_R^B - k_R^A}{1 + k_R^B} \cdot \frac{\sqrt{N}}{4} = \frac{\sqrt{N}}{4} \cdot \left(\frac{\alpha - 1}{\alpha}\right) \cdot \frac{k_R^B}{1 + k_R^B} \text{ [48]} \qquad (4.7)$$

The resolution R_s is dependent on the retention times of the analytes A and B $t_R{}^A$ and $t_R{}^B$ and their base widths w_A and w_B. It can also be presented as dependent on the retention factors k, the number of theoretical plates N and the separation factor α. In case of symmetric peaks of equal intensity, $R_S = 1$ is sufficient for baseline separation. If the peaks do not fulfil these conditions, higher resolutions are necessary for peak separation [48].

The asymmetry of a peak in a chromatogram is presented in figure 5 [50].

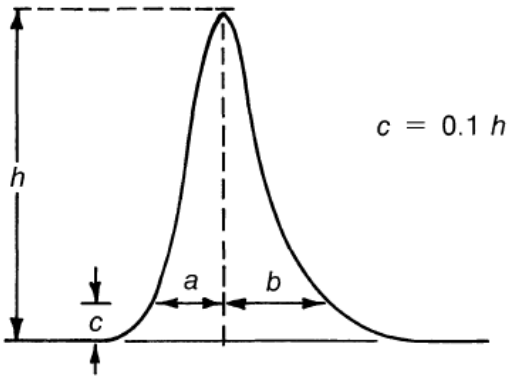

Figure 5: Visualization of peak asymmetry in a chromatogram and the parameters necessary for the asymmetry calculation [50]

The asymmetry of a peak A_S is calculated according to equation 4.8 with the quotient of half the widths of the peak at 10 % of the maximal height a and b.

$$A_S = \frac{b}{a} \text{ [50]} \tag{4.8}$$

If the A_S value is bigger than one, peak tailing is present, a fast signal increase and slow decrease. This is caused by adsorption processes in the column. If the A_S value is smaller than one, peak leading or fronting is present, a slow signal increase and fast decrease. This is due to a shortage of suitable adsorption sites in the stationary phase for the analyte, which causes some particles to pass the peak center [50].

The peak capacity is another important characterization of a separation system and is a measure for the number of peaks that can be resolved in one chromatogram and therefore the number of analytes that can be separated in one chromatographic process. It can be approximately calculated with equation 4.9 [48].

$$n = 1 + \frac{\sqrt{N}}{4} \cdot ln \frac{V_R^n}{V_R^1} \text{ [48]} \tag{4.9}$$

N is the number of theoretical plates, V_R^1 is the retention volume of the fastest analyte and V_R^n is the retention volume of the slowest analyte. The higher the number of theoretical plates N, the higher the peak capacity of a column [48].

The ion exchange chromatography is an analysis and separation technique based on the distribution equilibria of the analytes between a solid stationary phase and a liquid mobile phase. As stationary phase a porous ion exchange resin is used. Depending on whether it is a cation-exchanger or an-anion exchanger, the resin is either negatively or positively charged. For cation exchange, the SO_3^- or the COO^- groups are most commonly present. If the resin is coated with SO_3^- groups, it is considered a strong acid exchanger and if it is coated with COO^- groups, it is considered a weak acid exchanger. For anion exchange the NH_3^+ or NR_3^+ groups are most common. The capacity of the resin depends on the number of these bound groups. The mobile phase usually consists of aqueous eluents containing ions of the same charge as the analytes. They compete with the analyte for the binding spots to the stationary phase and ultimately replace them, eluting the analyte ions from the column. The distribution of the analytes between the phases is caused by the formation of heteropolar bonds between the ions bound to the solid ion exchange material in the column and the mobile counterions. The

separation is achieved through the adsorption-desorption process between the analyte ions and the ionic functional group of the resin [48].

$$\text{Resin-}SO_3^- H^+ + M^+A^- \rightleftharpoons \text{Resin-}SO_3^- M^+ + H^+A^- \text{ [50]}$$

Different analyte ions electrostatically interact to a varied degree with the charged ions of the column material and therefore are retained in the column for different times. Through a constant eluent flow, the ions are removed from the column. The stronger the ions interact with the column material, the slower they are eluted. This enables the full or partial separation of the ions from each other, as they have different elution regions, meaning the amount of eluent that passed through the column, in which the analyte ion is found. Generally, multivalent ions show stronger interactions with the column material as monovalent ions. In the case of ions with the same charge, the bigger ones are retained more strongly, as they have a smaller hydrate shell [51]. The most significant parameters for the separation are the kind of resin used as stationary phase and the ion strength and pH of the eluent [48].

The advantage of the classic ion chromatography in comparison to the modern HPLC and GC techniques is its higher capacity, which is needed for the separation in this work. Its disadvantage is the slow elution process, compared to these methods [48].

In this work the DOWEX® 50 WX8 200-400 (H) resin was used as column material for the Hot Column Chromatography separation. It is a strongly acidic cation-exchange-resin, a styrene-divinylbenzene-copolymer with sulphonic acid groups as anchor groups [52]. Its structure is shown in figure 6.

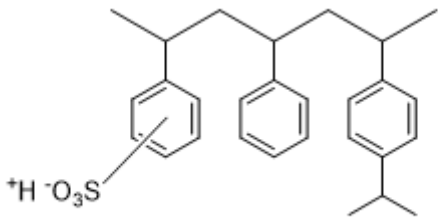

Figure 6: DOWEX® 50 WX8 200-400 (H) resin structure,
styrene-divinylbenzene-copolymer with sulphonic acid groups as anchor groups [53]

Styrene-divinylbenzene-copolymers are highly pH stable, which enables the use of strong acids and bases as eluents and for rinsing the column. They have only a limited stability against organic solvents but a low sensitivity towards complex matrices. This makes them suitable for the analysis of food, wastewater or body fluid samples [50]. The styrene-divinylbenzene-copolymers are the most common materials for the synthesis of cation exchangers. The copolymerization of polystyrene with divinylbenzene is necessary to achieve the required stability of the resin. The two functional groups of divinylbenzene crosslink two polystyrene chains with each other. The amount of divinylbenzene determines the amount of crosslinking. If the material is crosslinked too much, ion exclusion for larger ions occurs in addition to a limitation of the mass transfer, that leads to a lower column efficiency. If the material is not crosslinked enough, it becomes mechanically unstable [50]. The DOWEX® 50 WX8 200-400 (H) is a microporous resin. It is prepared by bead polymerization in polar solvents. The inert solvent is added to the monomer suspension. The monomers are soluble in the solvent, but not the resulting polymer. After the polymerization, the solvent inclusions in the resulting polymer

are washed out. As alternative to the liquid solvent, a finely ground inorganic salt, like calcium carbonate, can be used as inert polymerization solvent. The resulting polymer particles are spherical with a large surface area of 25-800 m^2/g, depending on the polymer. The microporous particles have a high degree of crosslinking and are therefore mechanically stable and the swelling and shrinkage of the material is suppressed [50]. To function as a cation exchanger, the surface of the styrene-divinylbenzene-copolymer is sulfonated. This is done with concentrated sulfuric acid. The exchange capacity of the resin is determined by its degree of sulfonation, which can be controlled by the reaction time and temperature during the reaction. The typical degrees of sulfonation are between 0.005-0.1 mequiv/g. Due to the hydrophobicity of the interior of the stationary phase, fully dissociated ions like Na^+, K^+ and Mg^{2+}do not diffuse inside. This ensures shorter diffusion pathways and therefore higher chromatographic efficiency [50].

The DOWEX 50WX8 200-400 (H) in combination with the eluent ammonium-lactate at pH7 are used to separate the strontium and yttrium analyte ions from confounding ions and the sample matrix, as they would disrupt the measurement. Therefore, in this work the ion chromatography is used as a separation method as part of the sample preparation and not directly as an analysis method. The different fractions eluted from the chromatography column are subsequently measured with other analysis techniques, presented in this chapter, to determine the kind and quantity of the analytes in the fractions. Other methods for strontium separation are not applicable in case of such high calcium concentrations, as present in many environmental and ivory samples. The special aspect of the Hot Column Chromatography separation is the high temperature of 87 °C, at which it is performed. This is necessary because of the high calcium content of the samples. The high temperature keeps the calcium from precipitating and the sample solution liquid and suitable for ion chromatographic separation [10]. Additionally, the separation is performed on a big scale, with a large column, big amounts of stationary and mobile phase and long separation times that are needed for a successful separation. The Hot Column Chromatography is presented in detail in section 5.1.

4.2 Inductively coupled plasma-optical emission spectrometry (ICP-OES)

Model

In this work the ICP-OES device with the designation SPECTROBLUE FMX36, model FMX 36 of the type 76004563, produced by SPECTRO AMETEK materials analysis division was used.

Operating principle

This model is an automatic optical emission spectrometer. It consists of inductively coupled plasma, for the excitation of the sample, and a semiconductor-based system, for the detection of the optical analyte signal. With this model, simultaneous measurements are possible for the quantitative and semi-quantitative analysis of liquid samples [54].

First the liquid sample is nebulized. Then the resulting aerosol is fed into the plasma. After that the sample evaporates in the plasma, due to its high temperature of 6000-8000 K, and the analyte molecules dissociate further into their atoms. Those atoms are excited and partly ionized by the high energy of the plasma. Then the excited atoms and ions emit radiation at an element specific wavelength. This radiation is then fed into an optical system by transfer optics. There it is diffracted into its spectral components and its intensity is measured with semiconductor detectors (CCD). The signal is then processed in the instrument. The further evaluation of the intensities of the measured element signal is performed by the Smart Analyzer software [54].

Before the measurement, a method is set up tailored to the specific analysis question. Methods contain calibration functions for each element of interest in the sample. To obtain those calibration functions, several calibration samples with a known and varying concentration of the analyte element must be measured. From the resulting ratio of concentration to signal the calibration functions are calculated. Those are in turn used to calculate the concentrations from the measured intensities emitted by the analyte samples [54].

The measured concentrations of the analyte atoms are displayed on the computer screen, saved in a database and printed on a printer [54].

Device structure

Number	Component
1	Air filter
2	UV Plus Purifier
3	Generator exhaust
4	Torch box exhaust
5	PC
6	Window to observe plasma
7	Torch box housing
8	Sample introduction chamber
9	Plasma off
10	Peristaltic pump (sample transport)
11	Connections
12	Main switch

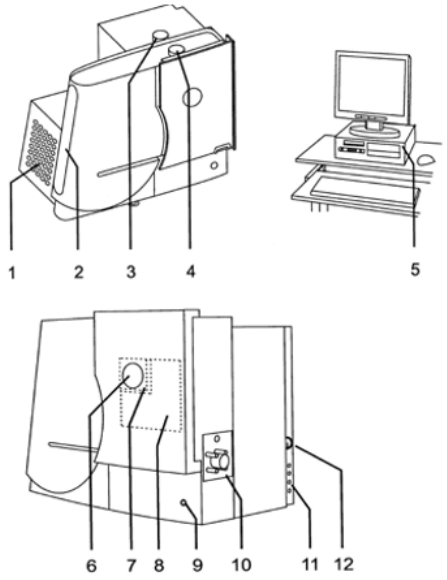

Figure 7: SPECTROBLUE FMX36 ICP-OES device structure, as it is visible from the outside [54]

Figure 7 shows the SPECTROBLUE FMX36 device, as it is visible from the outside. Interactive components, as the main switch (12) for the whole device, the plasma off (9) for the plasma emergency shut off and the connections (11) for the supply of electricity, gas and the connection to the computer (5) are visibly located on the outside of the device. The peristaltic pump (10) is located on the right-hand side, from where the sample is pumped inside the sample introduction chamber (8). There it is nebulized and enters the torch box housing (7), where the plasma is located and is visible through an observation window (6). The UV Plus Purifier is a part of the optical system, which is also visible from outside. The unit cover also contains openings for the inlet or outlet of air, for the ventilation of the system: air filter (1), generator exhaust (3) and torch box exhaust (4) [54].

Number	Component
1	Main switch
2	External port for plasma signal
3	PC connection
4	Oxygen or additional gas connection
5	Argon connection
6	Power cable
7	Extractable transport handle

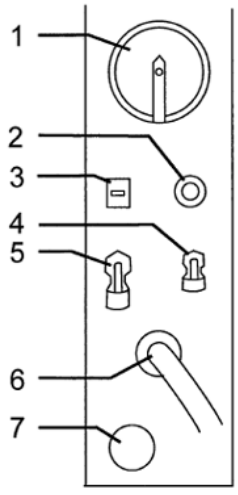

Figure 8: Close-up of the connections of the SPECTROBLUE FMX36 ICP-OES device [54]

Figure 8 shows, additionally to the main switch (1) and the extractable transport handle (7), where each part of the setup is connected to the main device. 2 shows the external port for the plasma signal, 6 the power cable and 3 where the computer is connected to the spectrometer. 4 and 5 show the two gas inlets, 5 for argon to create the plasma and 4 the additional optional inlet, for example for oxygen [54].

Number	Component
1	Lead through to sample introduction chamber
2	Peristaltic pump

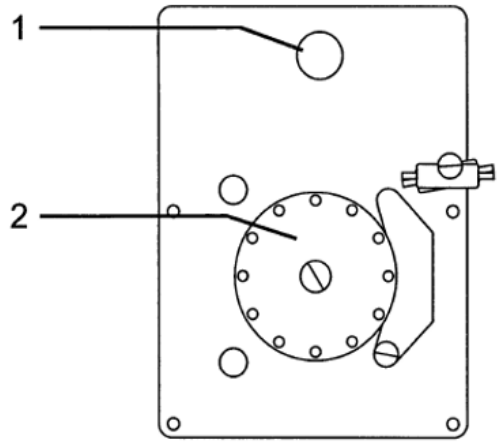

Figure 9: Close-up of the peristaltic pump of the SPECTROBLUE FMX36 ICP-OES device [54]

Figure 9 shows the peristaltic pump (2), which pumps the liquid sample through a tube by rotating. The tube starts in the liquid, for example the washing solution or the sample, goes into the pump and from there into the lead through to the sample introduction chamber (1), where it transports the liquid sample [54].

The following figures show schematically the setup of a system with axial plasma observation (EOP), as is present in our laboratory, in which the plasma torch in the torch box housing is built in horizontally.

Number	Component
1	Plasma torch
2	Clamp
3	Nebulizer
4	Argon connection
5	Sample introduction connection (from peristaltic pump)
6	Spray chamber outlet
7	Spray chamber

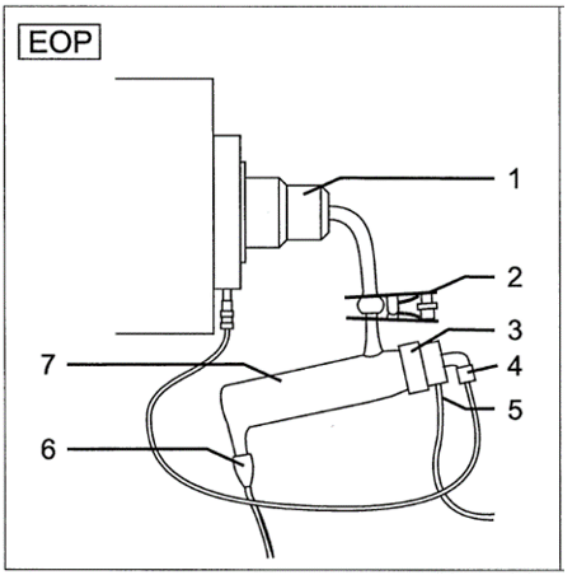

Figure 10: Close-up of the sample introduction system of the SPECTROBLUE FMX36 ICP-OES device [54]

Figure 10 shows the sample introduction system. The sample introduction connection (5) brings the liquid sample from the peristaltic pump to the nebulizer (3), where the liquid sample is nebulized into an aerosol and mixed with argon, which is provided through the argon

connection (4). From there the mixture is transported into the spray chamber (7) where it is excited by the plasma. The plasma is induced by the plasma torch box (1), which is connected to the spray chamber (7) through a clamp (2). After the process, the remaining sample is emitted through the spray chamber outlet (6) into a waste canister [54].

Number	Component
1	Exhaust
2	Plasma torch bracket
3	Plasma torch
4	Connection to sample introduction system
5	Clamp
6	Nebulizer gas connection
7	Load coil
8	Plasma interface
9	Twin interface

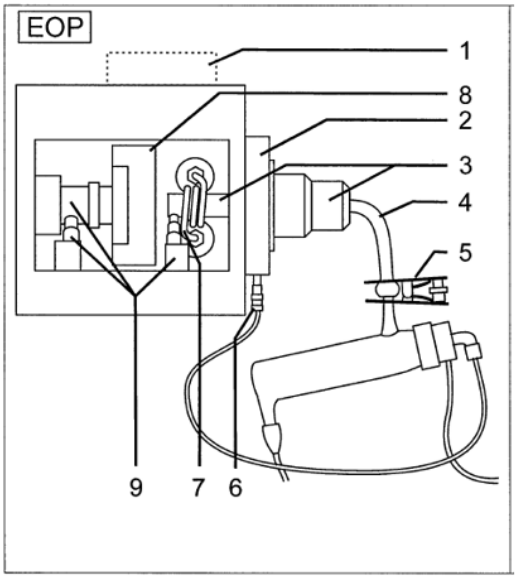

Figure 11: Close-up of the plasma torch box of the SPECTROBLUE FMX36 ICP-OES device [54]

Figure 11 shows the detailed setup of the plasma torch box. The plasma torch (3) is connected to the sample introduction system via a tube (4), held in place by a clamp (5), and to the nebulizer by a gas connection (6) and situated in the torch bracket (2). Inside the box, the plasma torch is connected to the load coil (7), which provides it with electrical current to induce the plasma. The load coil is in contact with the twin interface (9), which is also in contact with the plasma interface (8). Above the plasma torch box is an exhaust (1) for ventilation [54].

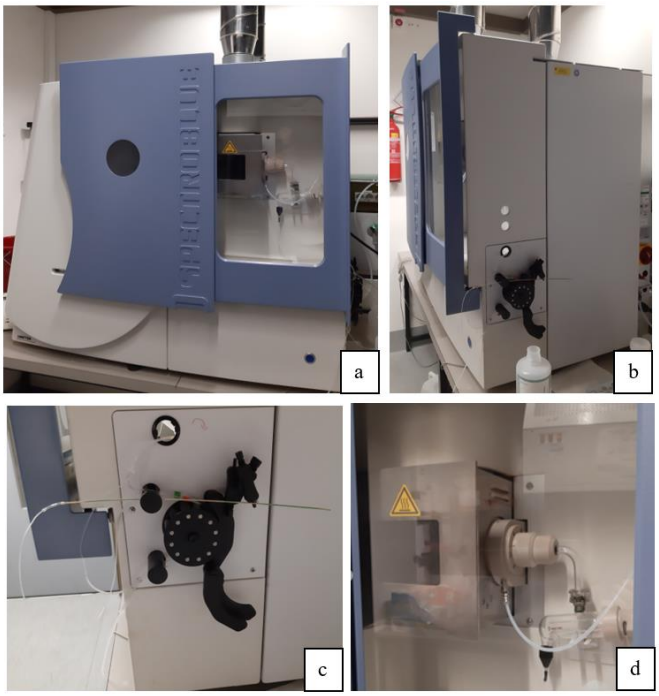

Figure 12: Real depiction of the SPECTROBLUE FMX36 ICP-OES device
a) device from the front b) device from the side
c) close-up of the peristaltic pump d) close-up of the plasma torch box and the sample introduction system

Figure 12 shows the real SPECTROBLUE FMX36 ICP-OES device. In part a) it is seen from the front, with the focus on the torch box housing, which is visible from an observation window. A close-up of it is shown in part d), where the sample introduction system and the plasma torch box are presented in the EOP setup. Part b) shows the device from the side with the focus on the peristaltic pump. A close-up of it is depicted in part c). The functions and setups of the peristaltic pump, the sample introduction system and the plasma torch box were explained in detail in the previous sections, in combination with schematic depictions of these parts.

Operation conditions

Table 1: Operation conditions for the SPECTROBLUE FMX36 ICP-OES device, optimum and acceptable conditions [54]

Variable	Value
Storage ambient temperature	2°C -40°C
Operation ambient temperature	15°C -35°C
Argon gas purity	≥ 99.996 %
Argon gas pressure	6-8 bar, 7 bar optimum
Air humidity	< 80 %
Power supply	230 V ± 5 % AC 50/60 Hz
Dust load	< 36 Mio particles/m^3

Table 1 shows the conditions necessary for a smooth and unobstructed operation of the SPECTROBLUE FMX36 spectrometer. The operating temperature of 15°C-35°C is in the range of the normal room temperature and can be upheld without problems throughout the year. The storage temperature allows an even wider temperature range of 2°C-40°C, without the risk of damage for the device. The requirement for the humidity to be lower than 80 % can be easily

met inside the laboratory. The required dust load, of lower than 36 Mio particles/ m^3, is ensured, if the laboratory is cleaned regularly. The dust load of a normal, regularly cleaned, office is 18-36 Mio particles/ m^3. In total, the ambient requirements for the operation are met in a normal laboratory. Higher quality criteria must be met by the argon gas, with a purity of at least 99.996 % necessary to ensure interference free measurements. The gas pressure also has to be adjusted precisely between 6 and 8 bar with an optimum at 7 bar. Finally, an AC 50/60 Hz power supply of 230 V with an acceptable variation of 5 % is needed for the operation of the SPECTROBLUE FMX36 spectrometer [54].

Operation instruction

The operation was always supervised by Joachim Rewitzer or Vanessa Tomanek. Before the measurement, the name of the operator and the analytes have to be entered in the operation list. Then the supply of argon gas must be checked. The gas pressure at the gas cylinder must be at least 50 bar. Per hour of measurement 10-20 bar of argon gas are used. After that, the computer can be switched on and the Smart Analyzer software started. Then the tubes for the sample transport and the washing steps are controlled for damage and adjusted in the pump. After that, the plasma can be started in the software with the command "Plasma on". Ten seconds after that the pump can be started in the software with the command "Pump on". When the plasma starts to glow, the sample tube can be inserted in the washing solution. The tube system must be washed and the measurement system heated for 15 min before the measurement starts. As washing solution, the atmospheric Spectroscopy Standard wash solution with 1 % HNO_3 by Perkin Elmer is used (CAS #: HNO_3[7697-37-2]) [54, 55].

In the following situations an ICALisation is necessary: in case of a wavelength drift (indicated by a software message), after the spectrometer has been switched on as soon as the temperature has stabilized, if a new method is set up and before high-precision measurements. For the ICALisation of the system, the tubes are inserted into the ICAListaion solution. Then the section "System" is selected, the function "ICALisation" chosen and the question in the next tab answered with "yes". After the measurement, the button "ok" is pressed and the tube is put back into the washing solution. The ICALisation solution contains 20 mL/L HCl, 20 mL/L HNO_3 and the atom concentrations shown in table 2 with a deviation of at most 0.5 % [54].

Table 2: Elements in the ICALisation solution and their concentrations

Element	Concentration [mg/L]	Element	Concentration [mg/L]
Ca	1	Eu	10
Be	2	In	10
Li	2	K	10
Sr	2	Ni	10
Mn	5	P	10
Mo	5	Si	10
Na	5	Ti	10
Sc	5	V	10
Ce	10	Y	10
Cu	10	Zr	10
Fe	10	S	50

To create a new calibration method, the section “method” is opened and the function “new method” selected. Then one goes through the shown bullet points of the method generation protocol and selects the relevant elements for one’s analysis. The pump speed and argon flow can be kept at the preselected values, the measurement time can be adjusted. Then in the standard measurement file all calibration concentrations are entered and the calibration solutions measured. Starting with the lowest concentration, in most cases the blank solution, and ending with the highest concentration. For the standardization, the highest and the lowest concentrations of calibration solutions are used. After the measurement, the regression is calculated by choosing the commands “regression” and then “calculate all”. After that, the line definition is activated by pressing the corresponding command and the measured standards are loaded. Then the measured spectra are processed by choosing the relevant peaks for one`s analytes. The background right and left from the peak is chosen and the peaks modeled with the Polynome 1 function command. Then the peak position is selected by aiming for the center of the peak. This process is repeated for all relevant peaks of the chosen analyte atoms. After that, the method is saved and can be applied [54,55].

For the measurement of the samples, the relevant method is selected, which can be found in the “method” section. To make sure, that the spectrometer is still measuring at the same quality as when the method was implemented, control measurements are performed. For this, the section “analysis” is opened and then again “analysis”. The section “method measurement” is opened and there the relevant method is chosen. Then the sample tube is put in the blank solution and the measurement is started with the command “measure”. After the measurement, the command “finish sample” is activated. Then the calibration solution with the highest concentration is measured by putting the sample tube inside it and entering “ok”. After the measurement, the tube is put back in the washing solution and the commands “finish sample” and “calculate” are activated. In the section “method” the command “standardization” is activated and an orange calibration curve is shown. If it is congruent or almost congruent with the one originally recorded, one can proceed with the measurements [54,55].

To start the measurements, the section “analysis” is opened and the double arrow button, which represents multiple measurements, is pressed. The sample name is entered in the pop-up box, the tube is put in the sample and the “start measurement” command is pressed. After the measurement, the command “finish sample” is pressed. To start the next measurement, the

double arrow button is pressed again. This process is repeated for all samples, which are measured with the same method. To see the recorded spectra, the section “spectra” is opened and the command “open” pressed. Then the according sample spectrum is selected and loaded. There one can inspect the spectra and all the occurring peaks [54,55].

Before the pump and plasma are shut off, the spectrometer is run and rinsed with washing solution for another 30 minutes. The sample tube is then removed from the washing solution and the device dried, as the pump makes a clacking noise. Then the plasma is turned off and when the notice pops up that the program is ready, it is also turned off, as well as the computer [54,55].

4.3 Gamma-spectrometry

Model

For this work the gamma spectrometers GEM3, GEM4 and GEM 40 were used.

Operating principle

Gamma spectrometry is used for the detection and identification of γ-decaying radio nuclides. The radiation of each γ-emitting decay has a characteristic energy, that can be used to identify its source nuclide. Gamma-radiation is comparable to X-rays, as they are both forms of electromagnetic radiation and have a similar energy. Gamma-decay is often preceded by other decay modes. A nucleus in an excited state, after a previous decay, can emit γ-quanta of a certain energy and fall back to a lower energy state. The energy of the nucleus changes but the atomic number and the mass number stay the same. Gamma-radiation can be detected by pure germanium detectors. Those allow a simultaneous detection of multiple different γ-emitters. The γ-quanta cause electron-hole pairs in the germanium semiconductor, which must be always cooled electrically or by liquid nitrogen. This is done to prevent defects by preventing electrons from crossing the narrow bandgap of the semiconductor. The electron hole pairs are collected by a high voltage and the signal is amplified. The obtained data can be represented as a pulse height spectrum. The count rates of the impulses, representing the activity of the sample, are plotted on the y-axis against the energy, for the identification of the emitting nuclide, on the x-axis [25, 56, 57, 58, 59].

The electron-hole pairs caused by the interaction of γ-quants with germanium are only a secondary effect of this interaction. Before the electron-hole pairs are formed, the following primary energy transfers can occur [25, 56, 57, 58, 59].

In case of a photo-effect, a γ-quant or a primary electron transforms their complete energy to one or more secondary electrons. This effect is seen as a local maximum in the spectrum, called the photopeak or FEP (full energy peak), that is used for the qualitative and quantitative characterization of the emitting nuclide [25, 56, 57, 58, 59].

The Compton effect occurs at higher energies. It describes how the γ-quants or primary electrons only transfer a part of their energy through collision with secondary electrons. How much energy is transferred depends on the collision angle and leads to a characteristic distribution of impulse heights for each γ impulse energy. This is known as the Compton continuum, which looks like background noise in the spectrum. The continuum shows a sharp edge, which represents the collision between photon and electron at 180°, the collision angle for the maximum energy transfer [25, 56, 57, 58, 59].

The pairing effect occurs if the energy of the incoming γ-quant is over 1022 keV and therefore so high, that it is enough to generate an electron and a positron with a rest energy of about 511 keV near a germanium nucleus. Through the annihilation of positron and electron two gamma quants are formed with opposite directions and the energy of 511 keV each This generates the annihilation peak at 511 keV [25, 56, 57, 58, 59].

Gamma spectrometry has a very good energy resolution and is quite selective. But it is not very sensitive and long measurement times are needed, especially for low level samples.

Device structure

A HP-Ge detector, the acronym for high purity germanium crystal, is the main element of the used gamma spectrometers. As a semiconductor with a high atomic number, germanium enables a low level of detection and a high physical efficiency of the measurement. This semiconductor functions as a diode, that lets the current pass in one direction and blocks it in the other direction. DC is applied on the crystal in blocking direction through electrodes. This means that normally there is no current. But if γ-quants hit the detector material and interact with the electron shells of the germanium atoms in the crystal, electron-hole pairs are generated. This interaction is quite weak. For example, only one in one hundred γ-quants with the energy of 662 keV interacts with the germanium atoms. This is the reason for the low physical efficiency of this method and the necessity of long measurement times. These electron-hole pairs move towards the electrodes of a RC circuit in the electrical field, caused by the applied high voltage of +2,000 to +3,000 V and are detectable as current pulses. This signal is amplified through a current sensitive amplifier and fed into a multichannel analyzer, which assigns it to the corresponding channel, depending on its energy. The maximal height of a current pulse, abbreviated as pulse height, is proportional to the energy of the γ-quant that caused it. The energy of the γ-quant produced at the decay of a nucleus can therefore be determined and is shown on the x-axis of a pulse height spectrum in form of channel numbers, with each channel attributed to a certain energy range. The number of pulses at a certain energy is represented on the y-axis of said spectrum [25, 56, 57, 58, 59].

The HP-Ge crystal has to be cooled to 77 K. It would have a big leakage current, due to the applied high voltage necessary for operation, at room temperature, and it would destroy the detector [25, 56, 57, 58, 59]. The used detectors are continuously cooled with liquid nitrogen filled in dewars. Around the detector a lead shield is built to minimize background noise, still leaving enough room for the samples.

Figure 13 shows the gamma-spectrometer GEM4. The HP-Ge detector itself is not visible, as it is surrounded by the lead shielding, which is the main focus of the picture. The shielding can be opened at the top and the sample placed inside, for which the ladder, visible on the right side, is used. Below the shielded detector, a dewar, filled with liquid nitrogen, is placed for its cooling. The bright red round object in the picture is the centering ring for samples in LSC vials.

Figure 13: Real depiction of the gamma-spectrometer GEM4

Operation conditions

The germanium detector crystal has to be cooled at all times, no matter if a measurement is performed at that moment or not. In this laboratory, it is done with liquid nitrogen, but electrical cooling is also possible. If the cold chain is interrupted, defects can be formed in the germanium crystal and the efficiency of the measurement is decreased.

The germanium crystal has also to be protected from contamination. All liquid samples are checked for leakage and all sample containers for contamination on the outside, before they are placed into the detector. Additionally, a sheet of tissue paper is placed between the sample and the detector to prevent contamination.

Operation instruction

Before a gamma measurement is started, it is important to make sure that no other measurement takes place at the chosen detector at that time. If this is not the case, one can proceed to fill out a form about the sample, which can be found in the main drawer in the desk, where the computer for the control of the gamma spectrometers is placed. The form is called “Aktivitästbestimmung radioaktiver Stoffe”. The name of the operating person, the date and time of the start of the measurement, the sample number and or description, the material of the sample, the origin of the sample, its weight, density and condition: dry, in solution, moist or ash, have to be entered in the form. Additionally, the measurement geometry has to be entered: 1 L ring tray, 2 L ring tray, 100 mL in 500 mL Kautex tray, 200 mL in 500 mL Kautex tray, 5.5 cm filter, 20 mL LSC-vial or other. With this information a documentation about what sample was measured when is provided and the information is more easily accessible for the interpretation of the measured data.

After the sample is checked for outward contamination, the lead shield can be opened or removed (depending on the kind of shielding) and the sample can be placed on the detector with a piece of tissue paper in between them. The detector looks like a thick protruding pole inside the lead shield. If the sample is filled into an LSC-vial, a centering ring is first placed on the detector and then the sample inside it, to make sure that the sample is exactly in the center of the detector. Then the lead shield is closed again and the measurement can be started. For that the program "Gamma Vision" is opened on the computer. The right detector is selected in the command bar and the measurement can be started with the green "go" button. Then the measurement has to be labeled. For this the "services" section is opened and the command "sample description" is selected. For an easily assignable description, the used detector, the sample name, number, weight and other relevant details, the measurement date and the operator's name are entered. If everything is entered correctly, the "OK" button is pressed.

Then the spectrum is formed with time from bottom to top and not from left to right, as seen with many other measurement systems, where for example different wavelength are scanned through. The formed spectrum is a pulse height spectrum. The decays are registered as impulses and sorted into a channel that corresponds to their energy. If one impulse at a certain energy is registered, a count is added to the corresponding channel and the bar in the spectrum rises by one. As the gamma spectrometers have quite small physical efficiencies, long measurement times are needed. The shortest measurement times in this work, except for premeasurements, were 900 s or 15 min. More usual measurement times were one hour, half a day, over-night, over a whole day or over the weekend. If the measurement time should be limited to a certain value, this can be done. With a right click, a section is opened and there the "MCB properties" are chosen. There, the section "presets" is selected and a time limit for the real time or the live time is entered. The live time is the dead time corrected measurement time used for data processing. After the set time has passed, the measurement stops automatically. If no measurement time was preset, the measurement has to be stopped manually by pressing the red "stop" button after enough counts, in most cases 10,000, have been detected. Then the real time and live time of the measurement have to be noted on the sample form. After that, the measurement has to be saved under the section "file" with the command "save as" in the folder of one´s choice. To find the measurement data more easily, it is mostly saved under the section "Data", there the "lokaler Datenträger (D:)" is selected, then the folder for the used detector, then the folder for measurements and then the folder with one`s name or project. The data can be processed while measuring or in the buffer window, where one can open saved spectra. To find out which nuclides are in the sample, peaks can be selected per hand, or one can let the program lead one through with the left and right buttons near the "peak" function, on the right side of the program. If the curser is on a peak, the marker number or channel number, the energy in keV and the count number for this peak are shown on the bottom of the screen. The energy can be compared to the printed-out table next to the computer or to a reliable online data source, like NuDat 3, to find out which nuclide caused the peak, as the energy is characteristic for the nuclide it was emitted by. Then the whole peak can be marked by going to the section ROI (region of interest), switching the setting to "mark" and using the arrow keys of the keyboard to move the cursor left and right. This way, the whole peak and five to ten channels left and right of the peak are marked. The marked background is important, so the program can calculate the background noise from the counts in these channels. The marking should be as symmetrical as possible. If one then clicks on the marking, the gross area, meaning the number of counts in the marked channels, and the net area, meaning the number of counts with the background counts subtracted, can be seen in the bottom of the screen. If the marking is finished, the function can be shut off by going to the "ROI" section and selecting the setting "off". If accidentally too many channels or a wrong channel were marked, the "ROI" section is opened and the setting "unmark" selected. By then moving over the faulty marked channel with the

arrow keys, the mark can be removed. If a whole peak-mark has to be removed, one can click right on it and select “clear ROI”. In the same pop up window, opening after the right click, the zoom in or zoom out in the spectrum can be selected, which can also be achieved by pressing the “+” or “-“ keys on the keyboard. In that pop-up window, the function to “stop” the measurement, to “clear” or delete the measurement, to “copy the file to buffer” and to access the “MCB properties” can be found. If the section “peak info” in this pop up window is opened, the following information is shown: the “peak” channel and the corresponding energy in keV, the half-width of the peak ”FWHM” and the base width “FW”, which are both indicators for the resolution of the spectrum, the narrower the widths the better the resolution, the “gross area” with error, the “net area” with error, which are both a measure of the activity of the specific nuclide which emits this gamma-line and finally the relation of the gross count rate/ net count rate in cps. This information also becomes visible with a double click on the marked peak.

To detect all the gamma emitting nuclides in the sample, one moves through the entire spectrum and marks the peaks as described above, for which the arrow buttons in the peak section on the right side of the screen are used to jump from peak top to peak top. Or certain peaks are selected at the corresponding energies to prove the presence or absence of selected relevant analytes. Some nuclides can cause several peaks at several energies, as they decay in different kinds of ways, emitting γ-rays. The peak at 511 keV is the decay peak and is caused by higher energetic γ-quants decaying into an electron and a positron. It is quite characteristic and present in almost every spectrum with higher energetic analytes but cannot be attributed to one specific γ-decay. As one can move from peak to peak with the arrow keys next to “peak”, one can move through the marked ROIs with the arrow keys next to ROI.

When all relevant peaks are marked, the ROI-report can be printed out. As the spectrum cannot be easily opened in most programs, the information of the spectrum is saved and printed in form of an ROI report for further data processing. It contains all the relevant information on the marked peaks: the marked channels, their corresponding energy, the gross area, the net area, the live time and the real time are most relevant for the determination of the activity of the sample. To generate the ROI report, the section “analyze” is opened and the “ROI report” selected. After the right printer has been selected and the format set to “paragraph”, the button “OK” is pressed and the ROI report is printed. From the net area, the activity of a nuclide can be calculated with the radioanalytical basic equation.

$$A = \frac{R}{\eta_{phys} * \eta_{chem} * Y} \tag{4.10}$$

A represents the searched for activity and R the net count rate. The net count rate is the net area, all recorded counts minus the background counts, divided through the live time, the death time corrected measurement time. Y is the transition probability. For a nuclide with only one decay mode, it is one. If there are more decay modes, it is less than one and the exact values can be found tables, for example in NuDat 3. The η_{chem} and η_{phys} are the chemical and physical efficiencies of the method. Because of the penetrability of γ-radiation, normally no complex radiochemical separation or sample preparation is needed. The sample is placed in a fitting tray and measured as it is. Therefore, no sample parts are lost due to chemical processing and η_{chem} can be considered 1. η_{phys} varies for different measurement geometries and thorough the spectrum. The higher the energy, the lower is η_{phys}. And the higher the activity, the lower is η_{phys}, as the more impulses are present, the smaller is the percentage that can be detected by the germanium crystal. The bigger the volume of the sample, the lower is η_{phys}, because of the shielding and self-absorption properties of the material. One recent calibration experiment for the GEM4 was performed by Michael Hechtel for his final thesis, in which he determined the

η_{phys} for ^{137}Cs samples in LSC-Vials at different filling volumes with a standard ^{137}Cs solution of a known activity [60]. A similar experiment is performed in a student laboratory course [25]. For this calibration ^{152}Eu is used, as it is producing gamma radiation of various energies at a similar rate and therefore generates many peaks in the spectrum. The activity is known and is the same for all peaks, as a known ^{152}Eu standard is used. The transition probabilities for the peaks are given in a table and the net count rates are measured in the experiment. From this information, the η_{phys} can be calculated for all the peaks using equation 4.10. The values can then be plotted against the energies of the selected ^{152}Eu peaks and a mathematical formula can be formulated to calculate the η_{phys} for a certain energy of a peak, provided that the same measurement geometry is used.

The gamma detectors are tested regularly by measuring a standard ^{137}Cs specimen for 100 seconds, which causes a distinct peak at 661.7 keV with a certain count number that decreases with time. The net area with error is recorded, which shows the measurement efficiency, as well as the half-width of the peak" FWHM" and the base width "FW", which are both indicators for the resolution. The energy of the peak centrum, or the peak position, as well as the death time, are also recorded and compared to the target value, as seen in the table below. The data is paired with the measurement date and signed for correctness by the operator. This measurement is optimally performed weekly, to make sure that the detectors work precisely.

Table 3: Target values for the quality control of gamma-spectrometers with a ^{137}Cs specimen

Evaluated property	**Target value**
net area	41578-43424 counts (end of 2021)
half width FWHM	1.36-1.45 keV
base width FW	2.52-2.70 keV
peak position	661.2-662.2 keV
dead time	10.59 %

4.4 Liquid Scintillation Counting (LSC) and Cherenkov Counting

Model

For this work the 1220 QUANTULUS liquid scintillation counter by LKB Wallac was used. The maintenance is performed by PerkinElmer. The measurement site number is 2200026.

Operating principle

LSC- Liquid Scintillation Counting

One of the most important analysis methods for α and β radiation is Liquid Scintillation Counting (LSC). Its main principle is energy transfer and light detection. The sample is mixed as homogeneously as possible with a LSC cocktail, that can cause flashes of light as a result of its interaction with the ionizing radiation of the sample. The LSC cocktail contains, in most cases, fluorescing molecules with an extended π-system in an organic solvent. The energy of the radioactive decays in the sample is transferred to the scintillator molecules. Or it is transferred to the organic solvent molecules by collisions, which then transfer it to the organic fluorophores in the solvent. This leads, in both cases, to their stimulation into the excited state. By falling back to the ground state, the fluorophores emit photons. The photons are collected by photomultipliers. This signal is further enhanced, registered, electronically processed into an electrical signal and registered by the computer. The results can be represented as a pulse height spectrum. The count rate of the impulses, representing quantity, plotted against the energy, for the identification of the emitting nuclides. A significant advantage of LSC are the high physical efficiencies for α- and β- emitters, even for β emitters which emit only low energies. LSC also enables low levels of detection with relatively short measurement times. The light is emitted isotopically with this technique, which allows for an energy resolution and therefore an attribution of the peaks in the spectrum to the nuclides they originated from. This makes a simultaneous detection of several nuclides possible, event though not to the same extent as with γ-spectrometry, as LSC has a significantly lower energy resolution [25].

Cherenkov Counting

Another important method is Cherenkov counting. Cherenkov radiation is visible in form of blue light, which appears if electrons move faster in a medium than the light in this medium and is typically associated with nuclear fuel elements. The electrons then have such a high energy, that it suffices for the polarization of a suitable detector material, like water with the dipole moments in its molecules, that change with time. This produces light with such a short wavelength, that it can exit the detector material. For this, the electrons must be fast enough and the speed of light slow enough in the detector material. As the speed of light in a transparent medium depends on its refraction index, the refraction has to be as strong as possible. The refraction index of water is 1.33, and as it is polarizable, due to its dipole moments, and already the standard medium of many samples, it is in most cases the medium of choice for Cherenkov counting. From the refraction index of the solvent, a concrete threshold energy for the formation

of Cherenkov-light can be calculated. For water this threshold is 270 keV. But as for many β-emitting nuclides the ratio between energy maximum and medium energy is 3:1, only β-nuclides with a maximum energy of over 800 keV can be efficiently detected with Cherenkov-counting. This makes this method only applicable for high energy β-radiators. An additional disadvantage is that the Cherenkov-light is not emitted isotopically, but along the electron track. This means an energy resolution, and therefore a peak attribution to the origin nuclide, is not possible and only the total radiation of the sample can be determined. Cherenkov radiation can be detected by the photomultiplier tubes in the same device used for LSC. An advantage of this method is that Cherenkov is simpler in sample preparation than LSC: no reducing to a small quantity, no precipitation, no ashing is necessary. Also, no organic scintillation cocktail is needed, saving costs and making waste management easier, as the cocktails are in most cases toxic and have to be disposed of as organic waste [25].

Device structure

The 1220 QUANTULUS is a low-level detector for α- and β-radiation in form of LSC and Cherenkov counting. It provides high physical measurement efficiencies and a low background. For example, for ^{3}H its efficiency is ≥ 65 %, if unquenched, and the background is only 0.4-1.2 cpm. For ^{14}C its efficiency is ≥ 95 %, if unquenched, with a background of < 0.3 cpm. Generally, for alpha radiation its efficiency is > 9 % and the background < 0.1 cpm. The QUANTULUS is a large device with a width of 101 cm, a height of 156 cm and a depth of 92 cm. It stands on four feet, 90 cm apart from each other and each with a base area of 28 cm^2. The device weighs 1,000 kg [61].

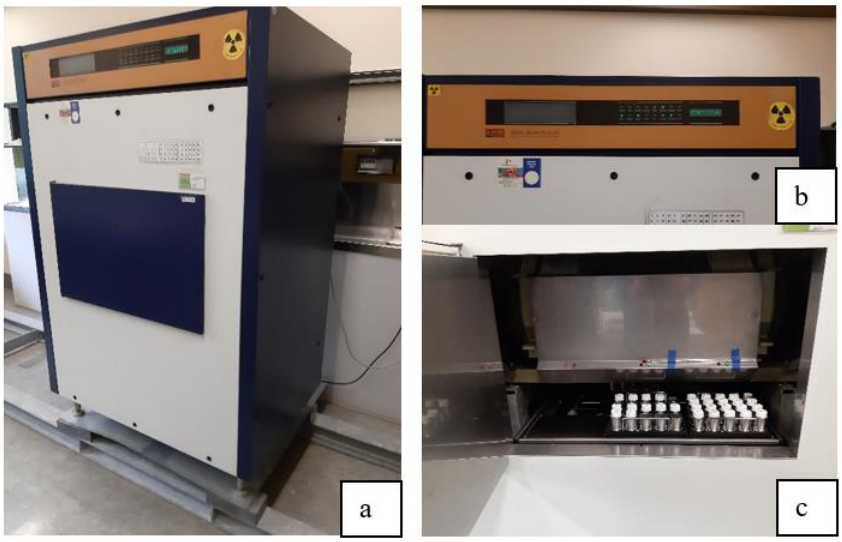

Figure 14: Real depiction of the 1220 QUANTULUS
a) complete device b) close-up of the device display c) close-up of the sample trays

Figure 14 shows the 1220 QUANTULUS. In part a) the complete device is depicted. It had to be placed on rails to distribute its weight more evenly and prevent damage of the flooring. In part b) the display of the device is seen. It shows the state, in which the QUANTULUS is, and during a running measurement the pulse height spectrum of the sample. Part c) depicts the cooled inside of the device, with a focus on the sample trays and the automated sample changing system.

The 1220 QUANTULUS contains a sample detector assembly, consisting of two low noise and low background photomultiplier tubes for signal counting. A light-emitting diode is also included in the assembly for the automatic spectrum stabilization. The guard and sample detectors are optically isolated from each other and the sample chamber is fully enclosed in the guard detector. An automatic continuous spectrum stabilizer that uses green Gap LEDs as a reference light source is used to check the performance of the photomultiplier tubes 62 times per second. The signal output is also kept constant through the automatically adjusted high voltage. The device is equipped with active and passive shielding, stopping most gamma radiation and all cosmic radiation, using an anticoincidence guard detector and a lead radiation shield. For the radiation shielding low radioactivity lead was used, surrounding the detector with a varying thickness. The shielding has a thickness of 200 mm on top of the detector, which constitutes the maximum thickness. The thickness of the side walls is 100 mm and of the shielding below the detector 150 mm. A part of the passive shielding is the head of the piston, which is made from copper. An asymmetric guard counter with a length of 350 mm and a width of 160, filled with scintillation liquid, is installed as an active shield against environmental gamma radiation and cosmic particles. Its copper container provides additional passive attenuation against environmental radiation. Two 2 `` photomultipliers in summed coincidence are used to monitor the guard. It operates in anticoincidence with the sample detector and they are optically isolated from each other. The operation of the guard is sample independent. A static eliminator, a high bias threshold, a RF suppression and a pulse amplitude comparator are used to additionally reduce the background. An ionizer unit is included for the elimination of static electricity, created by the rack movement on the conveyor lane and sample preparation. The static is additionally minimized by the metal material of the conveyor base and the vial holders. An antenna, operating in anticoincidence with the sample detector, is used to eliminate electromagnetic noise interference from radiofrequency sources and power lines [61].

The sample conveyer of the device consists of three racks, that hold in total 60 samples, 20 samples each. A random-access sampling enables auto sampling. This means no manual sample changes are needed, which allows for more efficient measurement plans and a higher sample throughput. The samples can be measured in a preprogrammed order or at random. The first sample change time is 45 s. For samples in the same rack, it is then reduced to 20 seconds. The sample and rack positions, as well as movements, are controlled with electro-optical sensors. Light leaks are prevented by a special shutter seal of the vial holders. A wide range of vial types can be used with this device, the standard being 20 mL glass and plastic vials. Additionally, special copper-teflon vials in the sizes of 20, 15, 7 and 3 mL may be used, as long as the maximum vial diameter of 28 mm and the maximum vial length of 62 mm are not exceeded. For other sizes 20 mL adapters are necessary [61].

Four Peltier elements are used for the cooling system, to maintain the set temperature inside the instrument and especially the sample chamber within 12°C from the ambient temperature. A water inlet is installed in the cooling unit fins, to increase the cooling. The lead shielding additionally functions as a temperature isolation, preventing the temperature from increasing significantly, even during a multi hour power failure. For spectral analysis, two dual programmable multichannel analyzers are installed. With this component, up to four spectra for samples under different conditions and an additional external standard spectrum for the sample can be recorded simultaneously. The full spectral information is stored on the computer and can be transferred to mobile data storage. Lost counts of high activity samples are compensated for by built-in dead time correction. The program allows for default configurations, as well as a multitude of tailored ones and up to 8 pre-programable counting windows. Background signals caused by optical crosstalk in liquid scintillation counting can be reduced by user adjustable pulse amplitude comparison levels. In case of mixed radiation samples, a simultaneous

acquisition and sensitive discrimination between pure alpha and beta spectra is achieved with pulse shape analysis. The according circuit is combined with the detector guards and allows for the effective measurement of alpha emitters, even with a 100,000-fold excess of beta radiation. Additionally, the alpha backgrounds are strongly reduced. This leads to a great sensitivity, especially in the LSC measurements, of alpha emitters. The pulse shape analysis is user adjustable, to allow for optimal settings for the analytes in question [61].

The software for the operation of the QUANTULUS is the program WinQ, which offers a multi-user set-up for the sorting of parameter groups and protocols, of which an unlimited number can be generated. A live view of the measured spectra is also possible [61].

To prevent damage or data loss from power failure, a stand-by power supply is provided with battery support. It can cover a blackout for a maximum of 50 hours for RAM memory and provides an automatic restart of the measurement program after the power is back on. The EEPROM memory ensures indefinite parameter group data storage. Additional electronic hardware components are microprocessor-controlled counting and data reduction, memory configuration EEPROM 16 k, RAM 642 k and ROM 128 k and a logarithmic A/D converter for the beta energy range of 1-2000 keV. Quench evaluation and correction are ensured with a SQP(E) quench monitor. ^{152}Eu is used as external standard with a low activity of 37 kBq and a high energy. It is stored in a sealed stainless-steel capsule. The internal quench curve validity for samples is checked by a sample quality monitor when counting in DPM mode. Random coincidences are detected by a chemiluminescence monitor, based on delayed coincidence [61].

Operating conditions

For the optimal operation of the 1220 QUANTULUS, the temperature in the room should be between +15 and +35°C and the humidity maximum should not exceed 75 %. For the power supply, the voltages of 100, 115, 120, 220, and 240 V are suitable, with an acceptable variation of ± 10 % and a frequency of 50/60 Hz. The device consumes 200 VA and the cooling system additionally consumes 200 VA [61].

Operating instruction

For a measurement of a sample with LSC or Cherenkov counting, the sample has to be filled in a 20 mL LSC vial and labeled on the lid with the sample number, the (assumed) nuclides inside and the date. The label is placed on the lid and not on the body of the vial, because an inscription would prevent a part of the emitted light from leaving the vial and being detected, reducing the efficiency of the measurement. For a Cherenkov measurement, the whole vial is filled with the aqueous sample. For LSC, the analyte is either extracted with a hydrophobic scintillation cocktail, like the Opti-Fluor ®O by Perkin Elmer. Or 10 mL of the aqueous sample are mixed with 10 mL of a hydrophilic scintillation cocktail, like QSA Quicksafe A by Zinsser Analytic, that forms a gel when mixed with water, which enables a more homogeneous distribution of the analyte in the vial. Color, dirt or clouding in the sample could stop a part of the emitted light or cause self-absorption, leading to a lower efficiency of the measurement. It is therefore important to prepare the sample in an as clear and colorless condition as possible and filtrate or centrifugate it beforehand, if necessary. When the samples are ready, they can be positioned into the QUANTULUS. The door of the device is opened and the sample vials are placed into the cooled trays, each in an empty position, and cooled before the measurement. Multiple samples can be programmed for the measurement at once. The positions of the samples can be

read from a table on the device and are noted. Then the samples are entered into a protocol book with the following information: the name of the operator, the date of the measurement start, the time of the measurement start, the total measurement time in minutes, the folder, in which the measurement data is saved, the positions of the samples, the project, the samples belong to, the isotope(s) in the samples, the labels of the vials and if necessary a comment.

Then the WinQ-Counter 1 program on the operating computer is opened. In the window "Counters" in the section "View" the spectrum, that is recorded in the moment, is shown. In case of a LSC measurement, there is an energy resolution and the different peaks can be traced back to the nuclides, that cause them. In case of a Cherenkov measurement, there is no energy resolution and the measurement shows only the total activity of the sample. Those measurement methods are not differentiated operatively but only through sample preparation. In the users section, the measurement can be programmed. There, the operator selects one's name and the according measurement protocol for the nuclides in the samples. If there is no protocol for this sample type, a new one can be created by copying an existing protocol and modifying it. For this, the protocol of choice is marked and the copy button is pressed. After that, a user folder is selected, where the protocol should be saved, a name for the new protocol is entered and the "ok" button pressed. Then the program can be opened and the "general parameters" section pops up, where the path, under which the data is saved, can be modified. In most cases the path follows this direction: D:\SCHE\SA220922 with D: being the data carrier, SCHE one's user folder, SA one's initials and 220922 the starting date of the measurement. The number of cycles can also be modified but is in most cases left at one. The checkbox for parameter listing normally also stays active. The settings under the "MCA Window Setting" also stay mostly the same and are not modified much. Under the section "Sample Parameters" the measurement is programmed and the sample information entered. The measurement time and position of the sample in the QUANTULUS are entered here as measurement instructions for the device. The sample names and information are entered here, which is important to later be able to connect the measurement results to the sample. Following information for each sample is entered in the table from left to right: under ORD the consecutive number of the order, then the position number of the sample, then the number or name of the sample and the measurement time in minutes (mostly 60-1000 min). The rest of the table entries are as following and are normally not changed.

Table 4: Constant table entries under the section "Sample Parameters" for the programming of a sample measurement in the 1220 QUANTULUS

Counts	Counts	MCW	Rep	Y	STMS	STIME
No Limit	No Limit	2	1	St	1/10	0:15

One of the advantages of the QUANTULUS is that multiple samples can be programmed at the same time and through auto sampling, they are measured one after the other. This increases efficiency, as samples do not have to be changed manually, and makes measurement programs over night and over the weekend possible. New samples can be added to the programmed list with the "+ New" button or by copying and pasting existing sample entries. If an entry is superfluous, it can be deleted with the corresponding button. In the bottom line of the section, the number of samples and the cumulative counting time of the measurement can be seen. After the program is ready, the "OK" button can be pressed. The protocol is marked and the "Queue" button is pressed, so the measurement can directly start, as soon as the previously queued programs are finished. When a measurement is about to be started, the according tray is pulled back and the sample is pushed up with a stamp into the measurement chamber. The digital display then shows a miniature version of the detected spectrum.

The measured data can be found under start, then workplace and then local data carrier D, where the respective user folders are saved. Under the right user folder, the measurement data is in a folder named after the operators initials and the date of the measurement start. There, the data file for each sample and the registry text file are found. The measurement parameters are documented in the registry text file. The most important parameters for data processing are the measurement names and the SQP(E) values. The measurement names have a form like Q011401N.001, the second and third digits being the order number of the sample and the fourth and fifth digits being the position of the sample in the QUANTULUS. The rest is constant. These measurement names are also the names of the measurement data files and are important to connect the files to the samples. The SQP(E) values of the measurements show their efficiencies and are influenced by the color, cloudiness and dirt in the sample. The higher the SQP(E) value, the better the measurement efficiency.

To implement the measured data into EXCEL, the program is opened, the main button pressed and then the “open” command chosen. There one selects one´s measurement document, sometimes “all data types” have to be selected, to be able to view the files. In the pop-up menu “separated” as data format is selected and one moves to the next slide. Then “blank space” is selected as separating character. In the next slide “standard” is selected and the “complete” command activated. After that, the EXCEL document with the measurement data is opened.

4.5 Low-level α and β counter

Model

For this work a PC-controlled 10 channel α-β-measuring station LB 770-2 Win-PC by Berthold GmbH & Co. KG was used.

Operating principle

The LB 770-2 Win-PC device was constructed for the monitoring of radioactivity in the environment and in the medical and pharmacological sphere. With its structure, the measuring station provides low levels of detection for α and β emitting nuclides and a high sample throughput, because it allows simultaneous measurements for at most 10 samples and the detection of α- and β emitters at the same time. The beta-background for a sample trey with the diameter of 60 mm is lower than 1 cpm. The radioactivity is measured with 10 flow meter pipes, one for each measuring channel, which are highly sensitive for alpha and beta particles. Simultaneously, the background, partly caused by cosmic radiation, is suppressed through the following measures. Firstly, the background radiation is reduced, using materials low in internal activity and a strong lead shielding of the device. Secondly, an additional overarching flow meter, which is connected in anticoincidence with the ten individual flow meter pipes for the measuring sites, allows for the influences of cosmic radiation to be largely eliminated. The overarching flow meter detects mostly cosmic radiation, but not the sample radiation, because it is shielded from it by thick electrolyte-copper walls. So, measuring events simultaneously detected by an individual flow meter and the overarching flow meter are recognized and eliminated as cosmic radiation. The remaining background radiation can be identified by background measurements and automatically subtracted from the measurement results [62].

The measurement of radioactivity with flow meters, also called proportional counter pipes, is based on the principle of the multiplication of electrical charge in close proximity to a thin counting wire, which is connected to positive high voltage and is surrounded by special counting gas. The radiation, emitted by the sample, ionizes the atoms of the counting gas, in our case P-10 gas, along its trajectory. The electrons, which were released this way, move with an increasing speed towards the anode wire, also called counting wire, and gain more energy the closer they get, until they form new ion pairs. Near the wire, the number of ion pairs increases massively. Through this multiplication process, the electrical charge reaches a measurable level. The charge generated through this process is proportional to the energy loss of the radiation used for the primary ionization. With this principle, almost every α or β particle that enters the measurement counter causes a counting pulse. The additional overarching flow meter is based on the same principle but specialized for cosmic radiation [62].

For a simultaneous measurement of α and β emitters, the radiation types have to be differentiable. This is possible through the vastly different ionization they cause in the counting gas. The α particles cause an ion avalanche, or specific ionization, near the counting wire, that is by some orders of magnitude lager than the one caused by β particles, and therefore cause a much stronger analog signal in the amplifier. This is due to the double positive charge of the α particles and their rest mass, that is 8,000 times larger than the rest mass of β particles. The separation of the α and β signals takes place in the amplifier channels, the alpha-channel and

the Beta-channel. The entrance of the alpha-channel consists of a passive differentiating level and a subsequent attenuator. This excludes most β-impulses from overcoming the discriminator threshold in the alpha-channel because of their small amplitude. In the beta-channel, the weak β signals are first accelerated 20 times, before they arrive at the discriminator threshold. But the entering α signals are also accelerated this way and have to be separated later. This is achieved by the alpha channel having two discriminator thresholds, one with a low threshold and one with a significantly higher threshold. If an α-pulse, which can enter the alpha- and the beta-channel, passes the lower threshold in the Alpha-channel, this causes a veto in the Beta-channel and no pulse will be detected at the exit of the channel. This does not completely exclude α pulses from the Beta-channel, as they also show a variation in pulse amplitudes, due to pre-absorption in air and the detector foil. Because of this, smaller α amplitudes are in the range of β amplitudes and cannot be differentiated. The lower discriminator threshold is therefore chosen at a value that is high enough to separate most α pulses and low enough to register most β pulses. The high discriminator threshold in the alpha-channel helps to provide a correct α count rate. It is adjusted to let as many α pulses pass as possible, but no β pulses [62].

Device structure

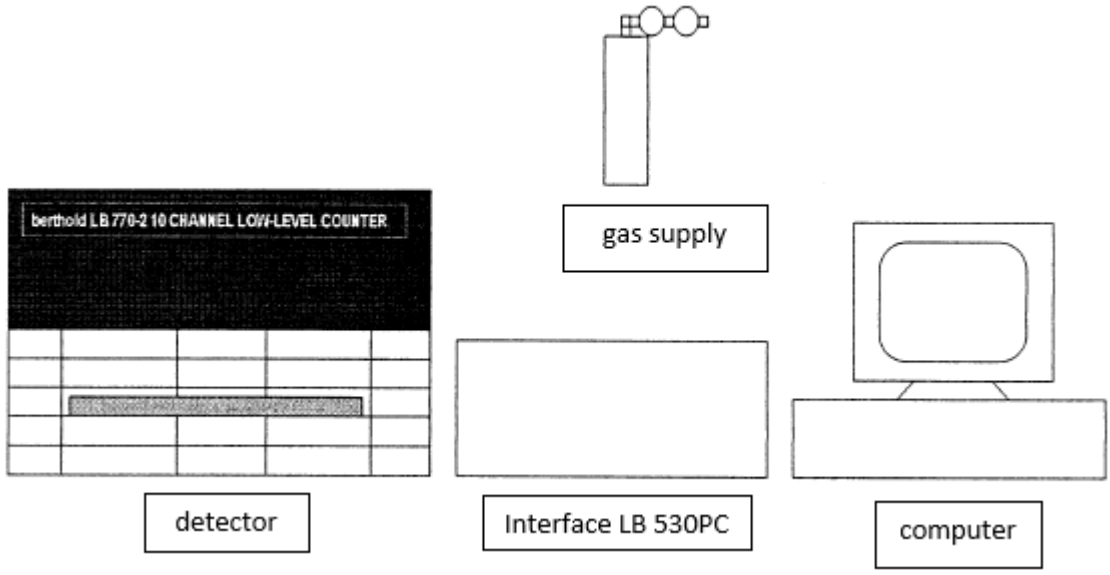

Figure 15: Device structure of a LB 770-2Win-PC 10-channel measuring station [62]

The measurement system of a LB 770-2 Win-PC 10 channel measuring station consists of a detector, a preamplifier, an interface, a gas providing system, and a computer with the according control and analysis program, as is depicted in figure 15.

The detector contains 10 low-level α and β measurement sites with one flow meter for each measurement site and one overarching flow meter to detect cosmic radiation. The measurement trays are positioned in an extendable slide made from copper in two rows of five. The 10 ultra-shallow flow meters have a diameter of 60 mm and a height of 8 mm, are situated directly over the trays and are protected from contamination by a thin hostafan foil (0.5 mg/cm^2) with aluminum deposited on one side through vaporization. Each flow meter contains two counting wires made from tungsten with a diameter of 50 µm. The wires of all flow meters are hung

isolated by a teflon base and are all supplied by a joint high voltage. The ten flow meters are covered by a 2 mm thin copper plate, over which an overarching flow meter is situated. The negative charges, that are generated near the counting wire, are guided to a charge sensitive preamplifier through a high-voltage capacitor. The whole device is surrounded by a lead shielding consisting of normed lead bricks with a thickness of 10 cm and a total weight of 650 kg [62].

Outside the lead shielding, the 20-fold preamplifiers for the α- and β-measurement channels and the overarching flow meter with its anticoincident connection are installed. In total, there are 21 preamplifiers. For each measurement site one for the alpha-channel and one for the beta-channel, directly connected to the flow meters, and one for the overarching flow meter. All preamplifiers direct the signal towards the interface [62].

For the charge multiplication process in the flow meters, a special gas mixture is used, that consists of 95.5 % argon and 4.5 % methane, also called P10. To ensure the desired gas flow, a double pressure reducer is needed, that is either installed at the gas cylinder or at the central gas distribution system. The gas must flow unhindered through all flow meters. The detector has to be pre flushed with gas for at least 60 min at 100 cm^3/min to ensure reliable measurement results [62].

As interface, the model LB 530 PC is used. It provides the high voltage for all the flow meters in the detector through two separate high voltage entities. The interface provides the data acquisition and control function for the detector hardware and regulates the communication between detector and computer through a defined data protocol. The interface functions as an autonomous data acquisition system, which fulfills real time measurement tasks and relieves the computer from time-sensitive data processing tasks. As soon as the measurement is started, the interface executes the active measurement (or the active cycle of a multicycle measurement) until the pre-entered measurement time runs out, even if the computer is separated from the interface in that time. Because of the battery powered storage, parameters stay saved for at least 6 weeks, even when the interface is shut off. The interface also communicates data to the computer or fulfills orders entered into the computer program. Further interface functions are the accumulation of measured data, the correction of the background, the half-life and the spillover, the calculation of statistical errors, the setting of the high voltage and the control of the detector function [62].

A computer is used to control the measurement process and to calculate and analyze the measured data. As software, the Windows program UMS for LB770 is used [62].

Figure 16 shows a real depiction of a LB 770-2 Win-PC 10 channel measuring station. Part a) shows an overview of the complete set-up with the detector, the gas supply, the interface and the computer, similar to figure 11. Part b) depicts the extendable copper slide for the 10 measurement trays, where the samples are positioned for the measurement. Part c) shows the flow-meter set-up, that is normally installed over the measurement sites inside the device, and their power supply.

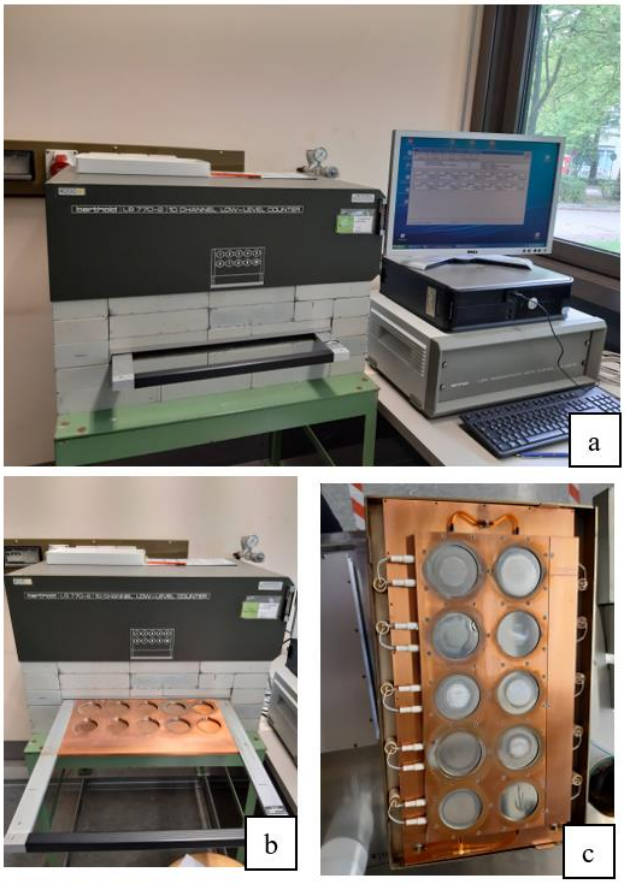

Figure 16: Real depiction of the LB 770-2Win-PC 10 channel measuring station
a) complete device with detector, interface, gas supply and computer
b) an extendable slide for the 10 measurement trays
c) flow-meter set-up installed over the measurement sites

Operation conditions

The LB 770-PC measurement system should be operated in a normally tempered room with low dust levels and a low and stable background-radiation.

Operation instruction

Before measurements can be performed, a user protocol has to be set up, which contains the degree of efficiency, the background values and the high voltage work point for the measurement. To create it, plateau-measurements have to be performed with selected and defined radiation sources, to find out the optimal high voltage for the measurements. After the work point was selected, the background is measured, which is repeated regularly for quality management. Then, reference radiation sources with a known activity are measured, to calculate the degree of efficiency of the measurements. As a predefinition for the acceptable statistical error, 1 Sigma was selected with a confidence interval of 68.3 % [62].

These pretests had to be performed for all ten measurement sites to obtain the relevant system parameters and pre-settings for the sample measurements.

For the β measurements relevant in this work, the following user protocol has been used: the system modus of “just alpha” is used and ips is selected as measuring unit, no normalization

factor is implemented and for both the alpha and beta working points the high voltage of 1,700 V is set. No alpha background is pre-entered and the efficiency is set to 1 for all 10 measurement sites, as it is measured and processed through separate measurements. For the count thresholds, 0.0 ips is selected as the lowest threshold, infinite as the highest. This is done because the measurement time is selected beforehand and not determined by the activity of the sample and a selected maximum count cut-off point. As measurement time, 1000 minutes are selected for routine β measurements and only one cycle is measured. As error 1.0 % is assumed.

The measurements are always started in the afternoon, earliest at 3 pm, to make sure that the measurement is finished the next morning, when staff has already arrived in the laboratory and can switch of the gas to prevent waste. The gas-flow of the P10 gas must be started at least one hour before the measurement start, to flood the measurement device. The main ventil on the gas cylinder is opened first, then the safety gas switch next to the door of the operating measurement laboratory and then the gas ventil connected to the device itself. A display shows the present gas pressure, which has to be at 10 in this display for an optimal measurement. Then the interface can be switched on with a toggle switch on the backside of the device. When this is done, the information sheet on the keyboard is removed, to show colleagues that the device is on. After one hour, the measurement can be started.

Before the samples are measured, their measurement positions, the measurement date and the operator are entered into an overview EXCEL sheet. Then the samples can be positioned in the according trays. Normally the outer positions 1,5, 6 and 10 are not used, because they have a higher background noise than the inner measurement positions. Then the UMS program is opened and further the “sample” section. A pop-up window appears, informing one that a regular repeat inspection has not yet been performed that day and asks if it should be performed. This is answered with “no”. After this the sample description file appears. First the “protocol” sheet is opened and the measurement time adjusted, which is in most cases 1,000 min. The modus file is opened and the high voltage entered. If α and β radiation have to be measured simultaneously, 750 V is entered for the alpha working point and 1,700 V for the β working point. If only β has to be measured, 1,700 V is entered for both working points. The rest can normally remain unchanged and the “ok” button is pressed. After that one comes back to the sample description file. As user protocol “sample-measurement” is normally already entered. Next to user, the operator`s name is entered, as data file the initials of the operator and the current date (for example AS08092022). This entry is the most important one, as this will be the name of the file under which the results can be found and are identifiable by. In the comment field, every information can be entered freely, that can help identify the samples and the measurement. In most cases it is stated whether it is an alpha and beta or only a beta measurement, which nuclides are measured, the sample names and their positions in the detector, the date and the name of the operating person. Then, under the section “samples”, it is entered which sample is measured at which measurement site (number 1 to 10). This is important for the pairing of the samples and the measurement results afterwards. Then the measurement is started with pressing “start”. A pop-up window opens, asking if a background-measurement should be performed, which is answered with “no”. Then one is asked to position the sample. If this is already done, the “ok” button is pressed. The measurement is started after some seconds and the screen shows 10 windows, one for each measurement site, with a live view of how the count rate changes with the measurement time.

After the measurement is finished, the button “stop” is pressed. To save the measurement file, the section “file” is opened and the command “print” is activated. The pdf creator opens and

the file is saved with the according command. Then the pdf version of the measurement report opens and is saved under the section “file” with the command “save under” first choosing DATA then URA and then the folder with the current year and either α or β measurement. There the file is saved under the same name as entered in “data file”.

Then the interface is shut off and the information sheet placed back on the keyboard, stating that the device is off. The gas-supply is shut off, first at the device itself, then next to the door to the laboratory and finally at the gas cylinder.

5 Experiments and Results

In the following section, the experiments are presented, which were performed to answer the questions, that have arisen in context of the research objective. The results of said experiments are also presented, visualized and interpreted in the following section, to gain a full insight in the research project and the individual subprojects.

5.1 Experimental foundations

The foundation of this work is the “Hot Column Chromatography”. All the experiments in the experimental section were performed to validate this method and aimed to improve it and increase its efficiency. The “Hot Column Chromatography” was first developed by Milton et al. [11] for the separation of strontium from a sample matrix and was subject of many research projects in this group. This method is now used in routine analytics. In the following fundamentals section, it is explained how this method works, from sample preparation to yield determination.

5.1.1 Sample preparation

The aim of the sample preparation is to remove organic sample constituents. This reduces the sample mass to an applicable amount and prevents disturbances. The whole sample preparation process can take one to two weeks.

First, the samples are placed in labelled quartz bowls and weighed, after the tara of the bowls was determined. The fruit and vegetable samples like apples, salad and sugar beets are chopped beforehand, to maximize their surface and fit more sample in the bowl. Then the samples are dried in an oven to remove as much water as possible. Liquid samples like milk are evaporated on the sand bath. Grain samples like corn and wheat are already dry enough and do not have to be pre-dried. Then the samples are incinerated overnight in a muffle furnace at 650°C ± 20°C. After the sample is cooled down to room temperature, enough 65 % concentrated nitric acid (HNO_3) is added to coat the ash and 60 to 80 mL are added in excess, depending on how much sample ash remains. The sample nitric acid mix is heated in the sand bath, until the liquid is completely evaporated and the sample is dry. During this process, bright orange nitro gases are emitted from the sample. This step is used to bind organic sample constituents and remove them via the formation of said nitro gases [52, 63].

In the next step, that sample is incinerated overnight in the muffle furnace again at 650°C ±20°C and cooled down to room temperature. After that, enough 32 % concentrated hydrochloric acid (HCl) is added, to coat the ash, and 60 to 80 mL are added in excess, depending on how much sample ash remains. The sample hydrochloric acid mix is heated in the sand bath until the liquid is completely evaporated and the sample is dry. During this process, intense gas emission occurs and the sample and hydrochloric acid take on a yellow colour. This step is used to remove remaining nitrates, which would disturb the column material [52, 63].

Finally, the sample is incinerated one last time overnight in a muffle furnace at 650°C ± 20°C. After the sample has cooled down, the quartz bowl is weighed again. The remaining, now white, ash is removed from the quarts bowl, grinded in a mortar and weighed [52, 63].

Then the sample ash is ready for the “Hot Column Chromatography” analysis. This whole process can take one to two weeks, depending on the sample.

5.1.2 Eluent preparation

As eluent for the “Hot Column Chromatography”, ammonium-lactate at pH7 is used. This solution is prepared in the laboratory, as big volumes of it are needed for the analysis and this process is more economically sensible then acquiring a ready-made solution.

The solution is mixed from ammonia and lactic acid. For two litres of ammonium-lactate, about one litre of bidistilled water is filled in a 5 L beaker. Then 300.08 g lactic acid (approx. 90 %) and 203.04 g ammonia (25 %) are added to the water in the fume cupboard, as those are highly concentrated acids and a mixture with water causes gas emission and heat production. The accuracy of the added quantities is ensured with a scale. Then the beaker is placed in an ice-bath, still in the fume cupboard, to cool the mixture back down to room temperature while stirring. The temperature is controlled with a thermometer. As soon as the mixture is at room temperature, the pH is adjusted to 7 by adding approximately 47 mL of hydrochloric acid (37 %) while stirring. The pH is controlled by a pH-meter. After the pH is adjusted, the solution is filled in a 2 L volumetric flask and the flask is filled up to the calibration mark. Finally, the solution is mixed thoroughly in the flask.

After this process, the ammonium-lactate solution at pH7 can be used as an eluent.

5.1.3 Hot Column Chromatography parameters and column preparation

The basis for this method is a large double-walled glass column, as presented in figure 17. The used columns are custom-built by the in-house glassblower workshop. A column has a total length of about 70 cm, a big reservoir and an outlet. Its double walled structure allows for thermostatic control through a heating water circuit, that is connected to a thermostat. This is necessary to maintain the operating temperature of 87°C, to prevent the precipitation of Calcium. As column material, the ion exchange resin DOWEX® 50 WX8 (H^+) of the size 200-400 mesh by Serva is used. Each column is filled with 150 g of the resin. One advantage of this resin is, that one column filling can last for at least 11 separations. The resin is suspended in 6 molar hydrochloric acid, filled in the column and washed with 6 molar hydrochloric acid, until the passing liquid is colorless. Before the separation, the pH of the column is adjusted by conditioning with 250 mL of 1.5 molar lactic acid. After the separation, the column is regenerated with 500 mL of 6 molar hydrochloric acid [10, 52, 63].

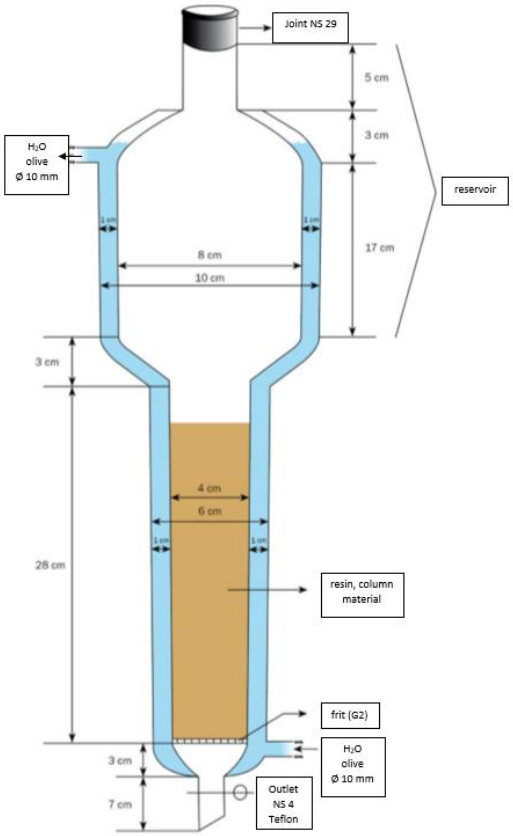

Figure 17: Schematic depiction of the Hot Column [10]

5.1.4 Routine strontium separation and analysis with the Hot Column Chromatography

Before the sample is applied to the column, a stable strontium-tracer containing 50 mg Sr and 80 mL of a 1:1 mix of 6 molar hydrochloric acid and 1.5 molar lactic acid are added to10 g of the prepared ash sample. The mixture is heated while stirring, until the ash is almost completely dissolved. Then the sample is centrifuged. The supernatant is applied to the column and run in at the velocity of 2.5 mL per minute. The velocity is controlled with a scale, measuring how much eluent has left the column, and a stopwatch, measuring how much time has passed [10, 52, 63].

As eluent, 800 mL of 1.5 molar ammonium-lactate solution at pH 7 is used. A constant velocity of 2.5 mL/min is important for the reproducibility of this process and a good separation. This has to be controlled and eventually adapted manually. This step is the focus of the optimization. The flow rate is not automatically constant. Different elution fractions have different flow rates. The velocity is additionally influenced by the mass of eluent in the column reservoir. The separation takes about four hours. The region of 460 g to 600 g eluent contains the ^{90}Sr fraction without ^{137}Cs. This elution region is separated for further analysis [10, 52, 63].

After the separation, the ^{90}Sr fraction is concentrated to a volume of about 200 mL by evaporation in the sand bath. After cooling down, the strontium is precipitated as $SrSO_4$ (strontium sulphate). This is done by slowly adding concentrated sulfuric acid (97 %), while stirring and in an ice bath, to compensate the produced heat. The precipitation is completed

during at least half an hour in an ice cooled ultrasonic bath. Then the precipitate is filtered through a Satorius filter cubicle with a paper filter (Whatman 42) and washed with 10 mL sulphate containing water and 10 mL acetone (p.a.) [10, 52, 63].

If the sample is measured in the low level β counter Berthold, the filter is labelled on the rim and placed in a round little steel tray with a diameter of 55 mm and measured as described in the section 4.5.

If the activity is measured via liquid scintillation counting in the QUANTULUS, the filter is incinerated at 600°C ± 20°C for 30 minutes in the muffle furnace in a weighed porcelain bowl. After the resulted ashes are cooled in an exicator in the absence of air, the resulting ashes are weighed in an analytical balance. The ash is mixed with 7 mL bidistilled water and 13 mL of the scintillation cocktail Quicksafe A by Zinsser Analytic in a LSC vial through strong shaking. The sample is measured with liquid scintillation counting (LSC) as described in the according section [10, 52, 63].

The chemical yield for the strontium separation can be determined with two methods.

The first method is gravimetric and based on the weight of the remaining ashes after the burning of the filter for the LSC measurement. From this weight, the chemical yield of the strontium separation can be calculated, as the filter is completely burned and only the filtered $SrSO_4$ (strontium sulphate) remains. As 50 mg strontium were added as tracer in the beginning, this equates to 0.00057 mol, as the molecular weight of strontium is 87.62 g/mol. For $SrSO_4$ (strontium sulphate) 0.00057 mol equates to 0.1048 g, as its molecular weight is 183.68 g/mol. If the measured weight of the filtered $SrSO_4$ (strontium sulphate) is divided by 0.1048 g and multiplied by 100 %, the strontium yield in % is obtained, as shown in equation 5.1, with y being the measured $SrSO_4$ ash weight in g [10, 52, 63].

$$\eta_{chem} = \frac{y}{0.1048g} \cdot 100\% \tag{5.1}$$

$$\Delta\eta_{chem} = \eta_{chem} \cdot \sqrt{\left(\frac{\Delta y}{y}\right)^2 + \left(\frac{\Delta m_{sr}}{m_{sr}}\right)^2} \tag{5.2}$$

The uncertainty of the chemical yield can be calculated with the chemical yield η_{chem}, the measured $SrSO_4$ ash weight y, its uncertainty Δy, the mass of the strontium in the added tracer m_{Sr} and its uncertainty Δm_{Sr}, as seen in equation 5.2 [10, 52, 63].

The other method for the determination of the chemical yield is titrimetric. The filter with the precipitate is not burned but placed in a 150 mL beaker and 10 mL 0.1 molar EDTA solution is added. Then 4 mL concentrated ammonia is added and the precipitate is solved through light heating of the sample. After that, 1 mL ammonium-chloride (NH_4Cl) is added and it is checked whether the pH of the solution is above 10 with pH-paper. If this is not the case, it can be adjusted with concentrated ammonia. Then a little bit of the pH indicator Eriochrome black T is added and the solution is titrated with 0.1 molar zinc sulphate ($ZnSO_4$) solution until its color changes from bule to violet. The added EDTA complexes the strontium ions in the solution. The remaining EDTA reacts with the added zinc sulphate ($ZnSO_4$) solution. As soon as all EDTA molecules have complexed either Sr or Zn, the color changes when a surplus of zinc

sulphate solution is added. The chemical yield is calculated from the volume of zinc sulphate ($ZnSO_4$) solution needed for the color change. The less is needed, the more EDTA has already reacted with strontium, the more strontium is present in the solution and the higher the chemical yield [64].

$$\eta_{chem} = (V(EDTA) - V(ZnSO_4)_{used}) \cdot \frac{8.763 \frac{mg}{mL}}{m(Sr - tracer)} \cdot 100\% \tag{5.3}$$

Equation 5.3 shows the calculation of the chemical yield for the tirtrimetric method. V(EDTA) is the added volume of the 0.1 molar EDTA solution, which is 10 mL. $V(ZnSO_4)_{used}$ is the volume of $ZnSO_4$ needed for the color change and m(Sr-tracer) is the mass of strontium added in the beginning of the analysis, which is 50 mg [64].

In case of a LSC measurement, normally a gravimetric yield determination is chosen, as the filter has to be burned anyway for the sample preparation. In case of a low level β measurement with the Berthold, both methods are applicable and the preferred one can be chosen by the operator.

5.2 Comparison of the elution curves of different sample matrices

The same procedure and parameters for the analysis and determination of ^{89}Sr and ^{90}Sr is used for all the different food samples in context of environmental monitoring. But the Hot Column Chromatography method was mainly validated for milk and ivory samples [10, 52] and the results transferred to other food samples. In the following section, it is examined more precisely, if different sample types have significantly different calcium contents, which could influence the separation. Additionally, it was tested if a difference in sample type causes a shift in the elution regions of the analytes. For this, experiments with the different sample types, that are analyzed in environmental monitoring, were performed and the results compared and presented in the following sections.

5.2.1 Ca-content determination for different sample matrices

Food samples have a varying calcium content, depending on the food type. As calcium is such an important interfering element in the Hot Column Chromatography, the analysis method is optimized for a certain calcium load of 3 ± 0.5 g of calcium in the sample. Based on this value, the amount of sample used for the analysis is chosen, with the standard being 10 g of ash sample or all of the ash sample, if 10 g cannot be provided.

In the following section, the calcium content of the different food sample types was determined, to see if the chosen sample mass is suitable for all the samples or has to be adapted, based on the calcium content.

The determination of the calcium content was performed with the Spectroquant® calcium cell test by Merck KGaA [65]. This method is based on the reaction of calcium ions in neutral solution with phthalein purple. Through this reaction, a violet dye is formed, that is then determined photometrically. As the measuring range of this test is 10-250 mg/L Ca, because it is mostly intended for water samples, the sample ashes have first to be solved and then diluted [66].

1 g of sample ashes were solved in 80 mL of a 1:1 mixture of 6 molar hydrochloric acid and 1.5 molar lactic acid while heating and stirring. Then the pH of the solution had been adjusted to the value 3 with hydroxide pallets, as is required in the instruction for the calcium test [66]. After the solution cooled down, it was transferred into a 100 mL volumetric flask and filled up to 100 mL with bidistilled water. One mL of this solution was retrieved and again diluted 1:100 in a volumetric flask [66].

Then one mL of this solution was filled in a reaction cell from the calcium cell test kit, that was already filled with a kit solution. One mL of the reagent Ca-1K solution was added and the reagents mixed. The solution turned violet after mixing. The reaction cell was left for exactly 3 minutes of reaction time and then 0.5 mL of the yellow reagent Ca-2K was added. After the sample was mixed, it was measured in the Spectroquant® photometer with the suitable settings program for a calcium measurement [65]. The following results were obtained, as shown in table 5.

Table 5: Results of the determination of the calcium content of different sample types with a 1:10,000 dilution of the ash samples

sample	sample mass [g]	calcium concentration in solution [mg/L]
milk	1.00	12
sugar beets	1.00	15
salad	1.00	< 10 (8)
corn	1.00	< 10 (7)
spelt	1.00	11
barley	1.00	< 10 (7)
wheat	1.00	10

This experiment shows that the measured calcium concentrations in the prepared solutions are in the same range and vary only slightly between the samples. This implies, that a variation of the used sample mass should not be necessary. Milk and sugar beets had the highest concentrations and salad, corn and barley had the lowest concentrations. As the concentrations of salad, corn and barley were lower than the intended measuring range of 10 to 250 mg/L calcium of the test, the results were not exact and the measurement was repeated with a lower dilution.

From the original dilution of 1 g sample ash in 100 mL solution, 10 mL were retrieved and again diluted 1:10 in a volumetric flask. Then one mL of this solution was filled in a reaction cell from the calcium cell test kit, that was already filled with a kit solution. One mL of the reagent Ca-1K solution was added and the reagents mixed. The solution turned violet after mixing. The reaction cell was left for exactly 3 minutes of reaction time and then 0.5 mL of the yellow reagent Ca-2K were added. After the sample was mixed, it was measured in the Spectroquant® photometer with the suitable settings program for a calcium measurement. The following results were obtained, as shown in table 6.

Table 6: Results of the determination of the calcium content of different sample types with a 1:1,000 dilution of the ash samples

sample	sample mass [g]	calcium concentration in solution [mg/L]
milk	1.00	67
sugar beets	1.00	41
salad	1.00	22
corn	1.00	35
spelt	1.00	42
barley	1.00	43
wheat	1.00	54

With the lower dilution, more reliable results could be achieved. The concentrations for all samples were approximately in the same range. But milk had a significantly higher calcium concentration than the other samples. Wheat had the second highest calcium concentration, followed by barley, spelt and sugar beets, that had almost the same concentration. Corn had a slightly lower calcium concentration and salad had the lowest calcium content.

From the measured calcium concentrations in the solutions, the calcium concentrations in the sample ashes could be calculated [66]:

For the stronger dilution of 1:100 and again 1:100, in total 1:10,000:

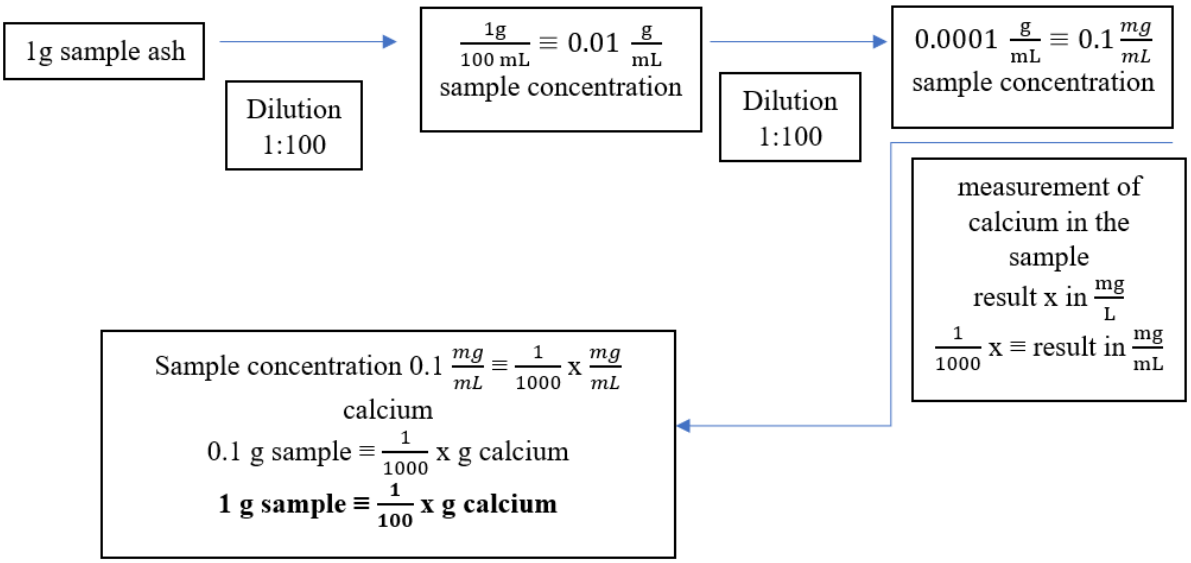

For the weaker dilution of 1:100 and again 1:10, in total 1:1,000:

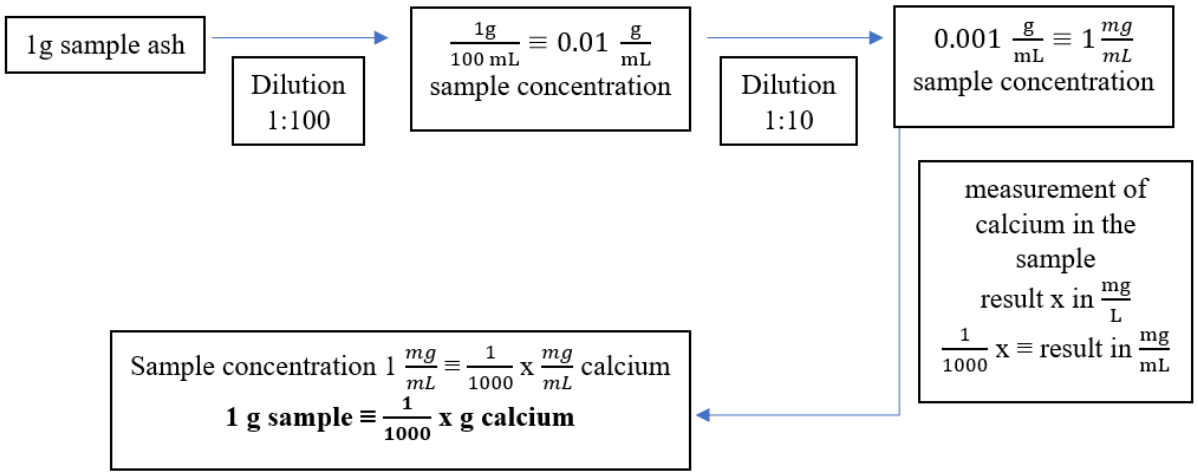

With this method, the following concentrations could be calculated from the measured results of the Spectroquant® photometric calcium cell test, as seen in table 7.

Table 7: Calcium concentration in different sample matrices, calculated from the measurements with 1:10,000 dilution and 1:1,000 dilution

sample	calcium concentration test diluted 1:10,000 [mg/L]	calcium content in sample ash [g/g ash]	calcium content in sample ash [g/10 g ash]	calcium concentration test diluted 1:1,000 [mg/L]	calcium content in sample ash [g/g ash]	calcium content in sample ash [g/10 g ash]
milk	12	0.12	1.2	67	0.067	0.67
sugar beets	15	0.15	1.5	41	0.041	0.41
salad	<10 (8)	0.08	0.8	22	0.022	0.22
corn	<10 (7)	0.07	0.7	35	0.035	0.35
spelt	11	0,11	1.1	42	0.042	0.42
barley	<10 (7)	0.07	0.7	43	0.043	0.43
wheat	10	0.1	1	54	0.054	0.54

These results show vastly different calcium concentrations in the ash samples, depending on whether they were calculated from the measurement of the 1:10,000 diluted sample or the 1:1,000 diluted sample. The results for the lower dilution were approximately half of the results of the higher dilution. On the one hand, the results of the lower dilution are more trustworthy, as the results of the higher dilution were out of the detection range or really close to the limit of the detection range of the test. But the results of the higher dilution show concentrations that are closer to the aim of 3 g calcium per 10 g sample, for which the column was optimized. The differences could be due to problems during the sample preparation, as some samples could not be solved completely or were not distributed homogeneously in the solution. Or they could be traced back to potential problems during the measurements in the photometer. Either way, all samples show a calcium content in approximately the same range. And for none of the samples a calcium content of 3 g per 10 g sample ash could be reached. As this circumstance did not lead to problems during the separation or to a lower Sr-yield in either sample type, the necessity to reach 3 g of calcium in the sample seems not to be essential for the analysis. The general recommendation to use 10 g of sample for each analysis, independent of the sample type, can be maintained.

5.2.2 Comparison of the elution curves for different sample matrices

The different food samples, that are analysed for environmental monitoring, are first processed, dehydrated and incinerated, as presented in the chapter above, until the water and all organic constituents are removed. The remaining ash consists only of the inorganic components of the samples and contains the analyte strontium, if it was present in the sample in the first place. As the composition of each sample type varies, so does the composition of their ashes. The question is, if this variation in ash composition influences the separation in the Hot Column Chromatography or if different sample types cause a shift in the elution regions of the analytes. To answer these questions, elution curves for the different sample-types were recorded with a standardized multi-nuclide tracer and gamma-spectrometry as detection method. The results of these experiments are presented in the following sections.

For the detection of the elution curves, approximately 10 g of each sample ash were used, as is described in the instruction.

As tracer a multi-nuclide tracer by Eckert & Ziegler was used. The gamma active nuclides were present as chloride salts in a 0.5 molar hydrochloric acid solution with 20 µg/mL of each element present. In total, 100 mL of the solution were available. This multi-nuclide solution was originally intended for the calibration of gamma detectors and contains an assortment of different nuclides with an exactly known activity, as presented in table 8. The reference date for the stated activities is april the first 2020, 12:00.

Table 8: Nuclides in the mixed-nuclide tracer and their photon energies, activities, photoemission rates and relative measurement uncertainties

nuclide	photon-energy [keV]	activity [Bq]	photon emission rate [s^{-1}]	relative measurement uncertainty of the activity [%]
Barium-133	81	6250	2290	2
Cobalt-57	122	6010	5140	2
Cerium-139	166	6000	4800	2
Barium-133	356	6250	3880	2
Strontium-85	514	29900	2950	2
Cesium-137	662	11700	9960	2
Manganese-54	835	12000	12000	2
Yttrium-88	898	29800	28000	2
Zinc-65	1116	30000	15100	2
Yttrium-88	1836	29800	29600	2

Table 8 shows the nuclides present in the multi-nuclide tracer and their radioactive parameters. The nuclides of special interest are ^{85}Sr and ^{88}Y, as they are isotopes of the same elements as the main analytes ^{90}Sr and ^{90}Y and behave chemically the same. But the nuclides in the tracer are gamma active and are therefore easier detectable with gamma-spectrometry, without the need of chemical pre-separation, as is the case for the main analytes. ^{137}Cs is one of the most relevant interfering nuclides and as it is beta active, it can interfere with the detection of ^{90}Sr and ^{90}Y, but as it is also indirectly gamma-active, it can be detected with gamma spectrometry in this experiment series. ^{133}Ba is another naturally occurring radionuclide, that could theoretically interfere with the detection of ^{90}Sr and ^{90}Y, but it has a vastly different elution region than the analytes and is removed from the column after the separation with 6 M hydrochloric acid.

Approximately 7.53 mL of this multi-nuclide solution were added to the sample ashes as tracer. This value was chosen to get enough counts during the gamma spectrometry in a sensible amount of measurement time, as for an elution curve many samples had to be measured, while handling as little activity as necessary, to ensure the safety of the operator and prevent unnecessary radioactive waste and contamination. The aim was to use enough tracer, to result in about 10,000 decay counts of the reference nuclide ^{137}Cs in a timeframe of 10 to 15 minutes.

Before the tracer was added to the sample, it was filled in a LSC vial and filled up to 10 g with 4 molar hydrochloric acid, to gain the same measurement geometry as for the elution curve samples later. Then the vial was measured in a gamma spectrometer for about 13000 s as 100 % sample. This was done to make a relative measurement possible. So, the measured decay rates for the different nuclides for the different samples could be expressed as % of the 100 % sample. This made the process easier, as the activities for each nuclide and each sample did not have to be calculated. For the calculation of the activity of a species of radionuclide in a sample the radiochemical core equation is needed:

$$R = A \cdot \eta_{phys} \cdot \eta_{chem} \cdot Y \tag{5.4}$$

$$A = \frac{R}{\eta_{phys} \cdot \eta_{chem} \cdot Y} \tag{5.5}$$

R is the decay rate, the measured counts in the energy region of a nuclide divided by the live time, the death time corrected measurement time. This value is obtained from the measurement. η_{chem} is the chemical yield, representing how much of the analyte is retained through the chemical sample preparation. As the 100 % sample and the eluent samples are measured directly, without chemical preparation, this value is in this case 1. Y is the transition probability, which represents with which probability a nuclide decays through the way that is observed with the measurement system, in this case the gamma decay at a certain energy.

This shows that additional values would be needed to calculate the activities of the nuclides in the samples from the decay rates. The Y values for the nuclides can be found in official tables, for example NucDat3 [18]. The physical efficiency depends on the emission energy of the nuclide and the sample geometry. To obtain a formula connecting the emission energy and the physical efficiency for a certain geometry, an additional calibration would have to be performed.

If the 100 % sample is measured at the same detector and in the same geometry as the samples for the elution curve, this is not necessary, as a relative distribution of the tracer during the elution process can be determined.

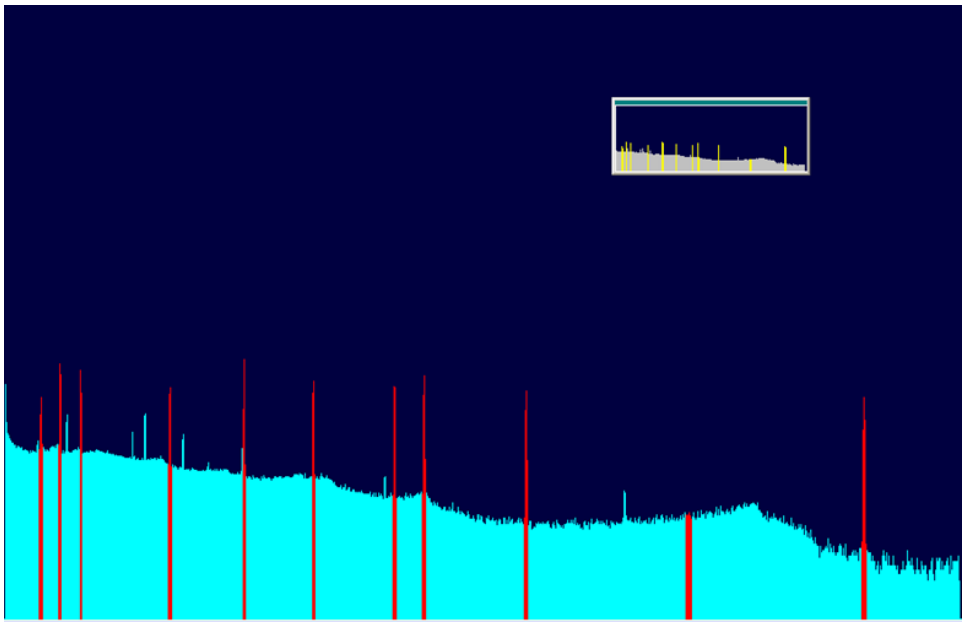

Figure 18: Logarithmic 100 % spectrum of 7.53 g of the mixed nuclide solution filled up to 10 g with 4 molar hydrochloric acid in a LSC vial, death time corrected measurement time 1,321.98 s, GEM40

Figure 18 shows the gamma spectrum of the 100 % measurement of 7.53 g of the mixed nuclide solution filled up to 10 g with 4 molar hydrochloric acid in a LSC vial. The death time corrected measurement time was 1,321.98 s. The spectrum is a pulse height spectrum with the x-axis representing the energies of the recorded decays in form of channels and therefore the kind of nuclides. The y-axis shows the number of decays recoded during the measurement time, which is representative for the activity. In the spectrum several peaks can be distinctly seen, which are caused by the radionuclides in the mixed-nuclide tracer. The count rates calculated from these peaks represent the maximum activity of a nuclide added to the sample.

After the 100 % measurement was finished, the ROIs (regions of interest) were marked in the spectrum, as described in the gamma spectrometry section. For this, the energies of the nuclides in the multi-nuclide tracer, shown in the table 8, were taken into consideration. As the 100 % sample has a relatively high activity, in each ROI a peak stood out from the background and could be used as a point of orientation. After that, the ROI file was saved, as it could later be transferred to the background spectrum and the sample spectra. So, the ROIs did not have to be marked manually each time. Then the net area and uncertainty of the net area of each ROI were noted and attributed to the corresponding nuclide in table 8. Through the division of the net area by the live time, the death time corrected measurement time, the count rate could be calculated for each nuclide. This is illustrated in table 9, showing the data processing of the 100 % measurement of the tracer for the milk analysis.

Table 9: Results of the gamma-spectrometric measurement of 7.53 g of the mixed nuclide solution filled up to 10 g with 4 molar hydrochloric acid in a LSC vial, as 100 % sample

Live time [s]	**Real time [s]**			
1,321.98	1,373.08			
Nuclide	**ROI [keV]**	**Net Area**	**Uncertainty Net Area**	**Count Rate [cps]**
Barium-133	75.15-81.27	10,025	209	7.583
Cobalt-57	117.17-122.01	39,456	244	29.846
Cerium-139	161.72-165.80	30,811	207	23.307
Barium-133	352.44-357.52	18,511	176	14.002
Strontium-85	510.59-516.68	58,923	289	44.572
Cesium-137	659.14-664.21	30,431	196	23.019
Manganese-54	831.51-838.33	27,405	185	20.730
Yttrium-88	894.71-901.79	42,507	227	32.154
Zinc-65	1,111.85-1,118.91	26,752	173	20.236
Yttrium-88	1,826.67-1,836.44	25,778	167	19.500

Additionally, the background was measured, to make sure that background radiation would not be mistaken for sample radiation. The background measurements have very long measurement times, at least over night or over several days, when the gamma-spectrometer is not otherwise used. This is necessary, as the background is quite low, to make sure that significantly interfering natural nuclides are found. A spectrum of a background measurement is shown in figure 19.

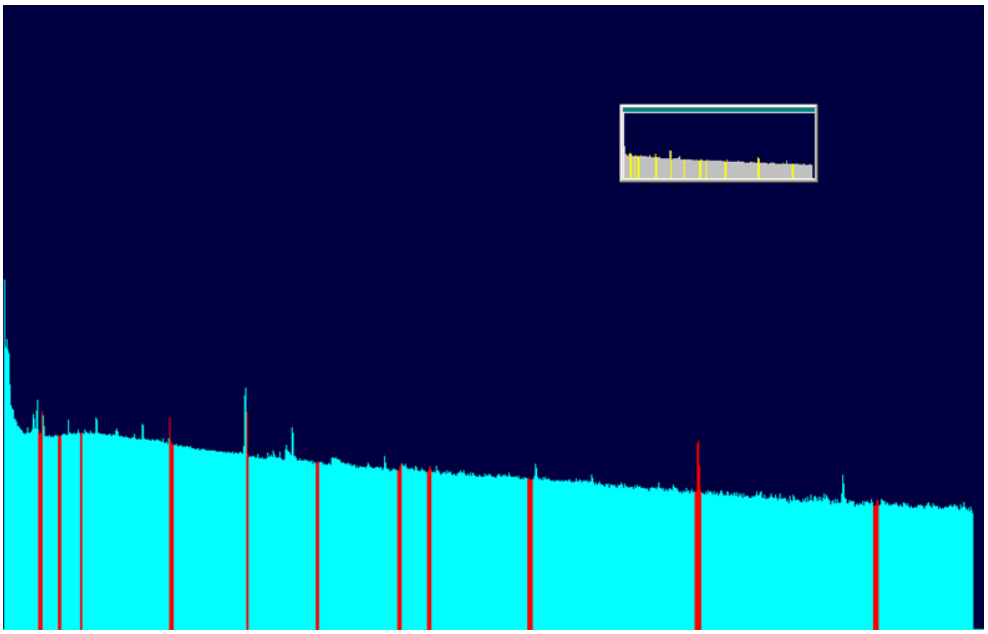

Figure 19: Background measurement of an empty gamma detector, death time corrected measurement time 2320,342 s, GEM40

Figure 19 shows a background gamma spectrum. The death time corrected measurement time was 2320,342 s. The spectrum is a pulse height spectrum with the x-axis representing the energies of the recorded decays in form of channels and therefore the kind of nuclides. The y-axis shows the number of decays recoded during the measurement time, which is representative for the activity. Despite the long measurement time, only few peaks can be found in the spectrum and those are quite small. The only peak worth mentioning is the ^{40}K peak at

1,460 keV. Usually, ^{40}K contributes significantly to the background radiation signal, as it is a naturally occurring radionuclide, that is significantly present in all potassium containing materials.

The ROI file of the 100 % measurement was transferred to the background measurement, to determine which background was present at the emission energies of the examined nuclides. This data was processed in a similar way as for the 100 % measurement. The net area and its uncertainty were noted, attributed to the corresponding nuclide and the count rate was calculated. This is illustrated in table 10, showing the data processing of one background measurement.

Table 10: Results of a gamma-spectrometric background measurement

Live time [s]	**Real time [s]**			
2320342	2320683			
Nuclide	**ROI [keV]**	**Net Area**	**Uncertainty Net Area**	**Count rate [cps]**
Barium-133	77.80-85.85	-2,054	291	0
Cobalt-57	119.44-124.24	-135	209	0
Cerium-139	163.61-167.65	41	174	0.000000431
Barium-133	352.91-357.96	-923	193	0
Strontium-85	512.93-515.21	-731	69	0
Cesium-137	658.06-663.11	136	135	0.0000586
Manganese-54	829.95-836.76	-107	172	0
Yttrium-88	893.05-900.12	422	170	0.000182
Zinc-65	1,103.05-1,111.88	114	183	0.000000431
Yttrium-88	1,827.94-1,837.79	-14	129	0

In some regions of interest with especially low count rates, negative values for the net area were found, which were caused by a background correction of the program. As this is a program error and negative decays do not exist, those values were corrected to zero. Additionally, in the cases where the net area was smaller than its error, the value was also corrected to 1/ (Live time) [67].

After the tracer was measured, it was added to the sample ash and the sample was prepared and applied to the column, according to the instruction in the section 5.1.4. A special column was selected for these experiments and only used for them, to prevent possible radioactive contamination of the samples for environmental monitoring. As eluent, ammonium-lactate at pH7 was used. The eluent, that left the column, was collected in 10 g fractions in labelled 20 mL LSC vials. The elution speed was regulated to a constant 2.5 mL per minute with a scale and a timer. The fraction weight was controlled with a scale. The complete eluent was collected, as soon as the sample inlet was started, and not just after the eluent has been applied to the column. All in all, 100 fractions à 10 mL, representing the whole elution process, were collected.

Each of these elution fractions was measured for at least 15 minutes with the gamma spectrometer. The fractions, in which the least activity was expected, were measured for a longer time, over the lunch break or overnight.

Then the ROI file of the 100 % measurement was transferred to each fraction measurement and corrected, in case of a slight energy shift. The measurement data was processed in a similar way as for the 100 % measurement. The net area and its uncertainty were noted, attributed to the

corresponding nuclide and the count rate was calculated. As an example for this process, the tables and figures below show the data processing for one elution fraction with a high activity and one elution fraction with a low activity, both recorded for the milk sample.

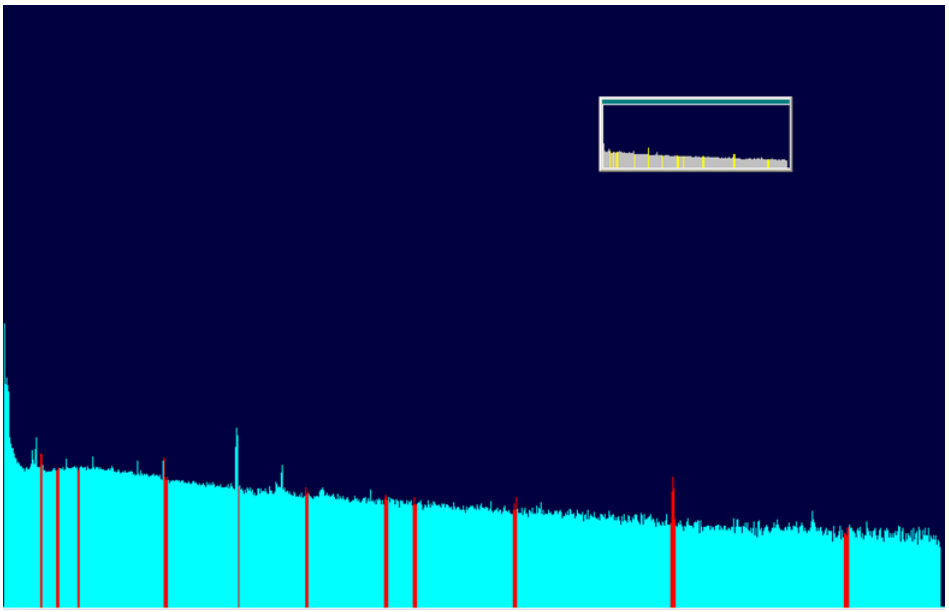

Figure 20: Measurement of fraction 1 of the milk elution curve, death time corrected measurement time 336,853.88 s, GEM40

Figure 20 shows the gamma spectrum of fraction one of the milk elution curve. The death time corrected measurement time was 336,853.88 s. The spectrum is a pulse height spectrum with the x-axis representing the energies of the recorded decays in form of channels and therefore the kind of nuclides. The y-axis shows the number of decays recoded during the measurement time, which is representative for the activity. Despite the long measurement time, only few peaks can be found in the spectrum and those are quite small. The spectrum looks very similar to the background spectrum depicted in figure 19. The only peak worth mentioning is the ^{40}K peak at 1,460 keV. The spectrum of fraction 1 represents a typical spectrum of an elution fraction, which contains very little to no radioactivity.

Table 11: Results of a gamma-spectrometric measurement of fraction 1, 0-10 g eluent, example of a fraction with a low total activity

Live time [s]	**Real time [s]**			
336,853.88	336,902.4			
Nuclide	**ROI**	**Net Area**	**Uncertainty Net Area**	**Count Rate [cps]**
Barium-133	80.25-83.56	529	60	0.00157
Cobalt-57	117.17-122.01	87	80	0.00026
Cerium-139	161.72-165.80	34	66	0,0000030
Barium-133	352.44-357.52	49	70	0,0000030
Strontium-85	512.88-514.91	-20	17	0
Cesium-137	659.14-664.21	-82	56	0
Manganese-54	831.51-838.33	-3	65	0
Yttrium-88	894.71-901.79	94	63	0.00028
Zinc-65	1,111.85-1,118.91	-126	63	0
Yttrium-88	1,826.67-1,836.44	-29	50	0

Table 11 shows the results of the gamma spectrometric measurement of fraction 1, as an example of an elution fraction with a low total activity. As described above for the background measurement, net area values, which were negative were corrected to zero. And if the error of a value was bigger than the value, it was corrected to 1/(Live time) [67].

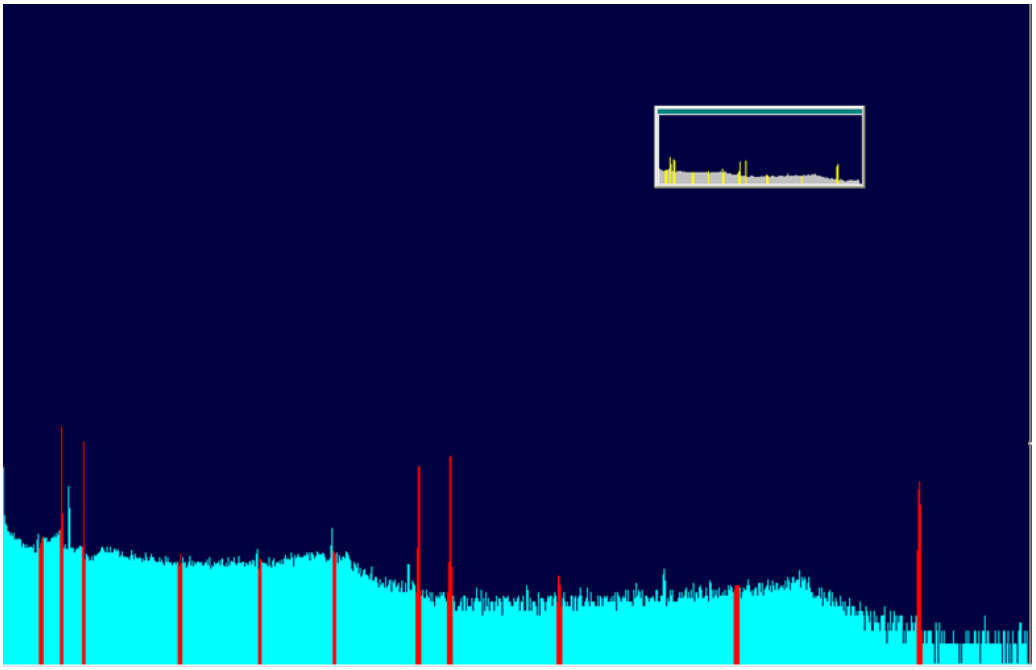

Figure 11: Measurement of fraction 33 of the milk elution curve, death time corrected measurement time 900 s, GEM40

Figure 21 shows the gamma spectrum of fraction 33 of the milk elution curve. The death time corrected measurement time was 900 s. The spectrum is a pulse height spectrum with the x-axis representing the energies of the recorded decays in form of channels and therefore the kind of nuclides. The y-axis shows the number of decays recoded during the measurement time, which is representative for the activity. In the spectrum several peaks can be distinctly seen, which are caused by the radionuclides from the mixed-nuclide tracer. The fraction contains significant amounts of ^{57}Co, ^{139}Cer, ^{54}Mn and ^{88}Y, which all have a similar elution region. It also contains a small amount of ^{65}Zn, that is mostly separated at this point of the elution. The spectrum of fraction 33 represents a spectrum of an elution fraction, which contains significant amounts of radioactivity.

Table 12: Results of a gamma-spectrometric measurement of fraction 33, 320-330 g eluent, example of a fraction with a high total activity

Live time [s]	**Real time [s]**			
900	906.56			
Nuclide	**ROI [keV]**	**Net Area**	**Uncertainty Net Area**	**Count rate [cps]**
Barium-133	75.15-81.27	-105	64	0
Cobalt-57	117.17-120.74	10,951	111	12.168
Cerium-139	160.70-164.78	7,112	90	7.902
Barium-133	352.44-357.52	65	33	0.072
Strontium-85	510.59-516.68	-2	42	0
Cesium-137	659.14-664.21	-44	40	0
Manganese-54	825.44-833.28	6,674	89	7.416
Yttrium-88	888.14-895.98	9,538	104	10.598
Zinc-65	1,104.78-1,113.61	124	32	0.138
Yttrium-88	1,814.40-1,823.67	5,817	80	6.463

Table 12 shows the results of the gamma spectrometric measurement of fraction 33 as an example of an elution fraction with a high total activity. As is evident from the values, the fraction was part of the main elution regions of ^{57}Co, ^{139}Cer, ^{54}Mn and ^{88}Y. It also contained some remaining ^{65}Zn. As described above for the background measurement, net area values, which were negative, were corrected to zero.

After all the fraction measurements were processed individually, the resulting count rate for each nuclide in each fraction was divided by the count rate of this nuclide for the 100 % sample and multiplied with 100 %. With this, the relative activity of a nuclide in the fraction, in reference to the 100 % sample, was calculated in %.

Then this value was decay corrected, as the analytes are radioactive nuclides and their concentration, and respective activity, decreases with time. Because the 100 % sample was measured before the fraction samples and they were measured over a longer time, as they were so many, this time difference, and therefore decay, had to be corrected for. The half-lives for each present nuclide are presented in table 13.

Table 13: Nuclides present in the mixed-nuclide tracer and their half-lives [18]

Nuklide	**$t_{1/2}$ [d]**
Barium-133	3,848
Cobalt-57	271.83
Cerium-139	137.66
Strontium-85	64.849
Cesium-137	11,000
Manganese-54	312.15
Yttrium-88	106.63
Zinc-65	243.94

^{85}Sr has the lowest half-life of all the nuclides, as can be read in table 13, and therefore, for this nuclide, the decay correction is the most necessary. For the decay correction, the time differences between the measurement of the 100 % sample and measurement of each fraction

sample were calculated. Form this, the A/A_0 ratio, the activity of the nuclide in the sample at the measurement time divided by the hypothetical activity at the measurement time of the 100 % sample, was calculated with equation 5.7. $t_{1/2}$ represents the half-life of the nuclide and Δt represents the time difference between the measurement of the respective fraction sample and the 100 % sample.

$$A = A_0 \cdot e^{-\frac{ln2}{t_{1/2}} \cdot \Delta t} \tag{5.6}$$

$$\frac{A}{A_0} = e^{-\frac{ln2}{t_{1/2}} \cdot \Delta t} \tag{5.7}$$

Through this ratio, the relative activity values of the nuclides in the fractions, representing A, were divided, to get the decay time corrected A_0 values. These values were visualized together with the eluent fraction in the elution curves for the different sample types, which are presented and discussed in the following section.

5.2.2.1 Elution curve with milk ash sample

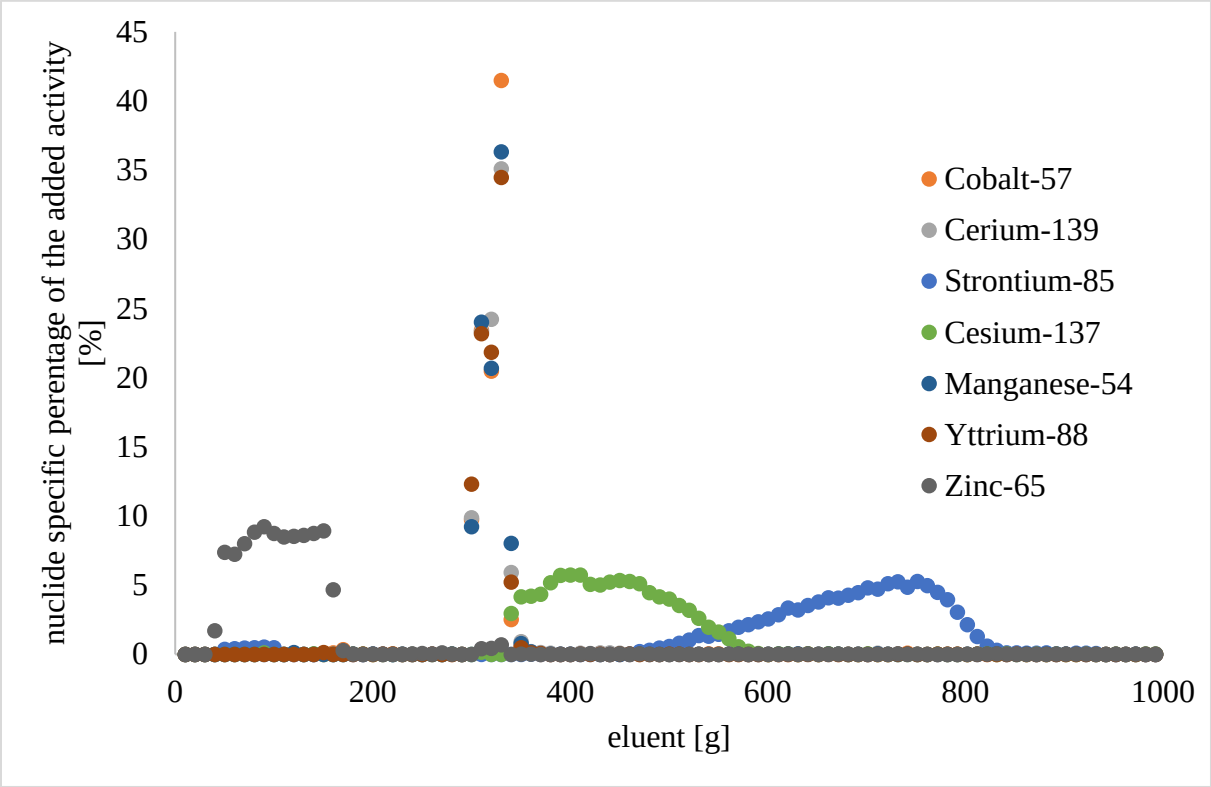

Figure 22: Elution curve with milk ash sample and multi-nuclide tracer, GEM40

Figure 22 shows the elution curve for a milk ash sample with added multi-nuclide tracer, containing Barium-133, Cobalt-57, Cerium-139, Strontium-85, Cesium-137, Manganese-54, Yttrium-88 and Zinc-65. The percentage of the activity of the added nuclides in each fraction was plotted against the eluent volume it represents. The different analytes were detected at different decay energies. The time difference between the measurement of the 100 % tracer and the measurements of the fractions was mathematically compensated for. The elution range of yttrium was originally determined through ICP-OES at 270-330 g and was shifted by 20 g in this elution curve to 290-350 g. This could partially be explained by the higher tracer and therefore sample volume. The nuclides ^{88}Y, ^{57}Co, ^{54}Mn and ^{139}Ce shared the narrow elution region between 290 and 350 g eluent. Almost no separation between these nuclides could be achieved and only a small overlap between this collective elution region and the ^{137}Cs elution region was present. ^{65}Zn, ^{137}Cs and ^{85}Sr were present in extensive elution regions. A significant overlap between the elution region of ^{85}Sr, between 480 and 820 g eluent, and the elution region of ^{137}Cs between 340 and 570 g eluent is noticeable. This overlap between 480 and 570 g eluent spanned 90 g eluent and was already detected in the previous work by Stefanie Schmied [52]. It has the effect, that this elution region cannot be used for the Sr-analysis, as it could lead to a contamination of the sample with the interfering nuclide ^{137}Cs. So, only a part of the elution region of Sr is used for the analysis, which leads to a lower chemical yield in exchange for an interference free measurement. The elution region of ^{65}Zn between 40 and 160 g eluent was eluted from the column right at the beginning and this analyte was completely separated from all the other nuclides in the sample. ^{133}Ba did not even appear in this graphic, because it was retained so strongly by the column material. It could only be completely removed by the regeneration of the column with 6 molar hydrochloric acid. As barium behaves chemically similar to radium, this can mean that also a complete separation of potentially present radium from the analytes would be achieved.

All in all, these results are comparable to the results Stefanie Schmied [52] achieved with a milk sample with added multi-nuclide tracer. The only significant difference is that in her work the elements manganese and cobalt were present in an additional elution region between 70 and 90 g eluent. As this elution region and these elements were not significant for the separation of the analytes yttrium and strontium, and therefore this work, this difference was not further investigated. All in all, the results were reproduced.

Most of the fractions stayed liquid and colorless after the separation and cooling down to room temperature. A slight yellow coloring was present in the elution region of 300 to 330 g, which overlapped with the elution region of ^{88}Y, ^{57}Co, ^{54}Mn and ^{139}Ce at 290 to 350 g eluent. This could be due to the many nuclides in this elution region. In the elution region of 320 to 440 g eluent the fractions became solid and waxy after cooling down, due to a high calcium content in this elution region.

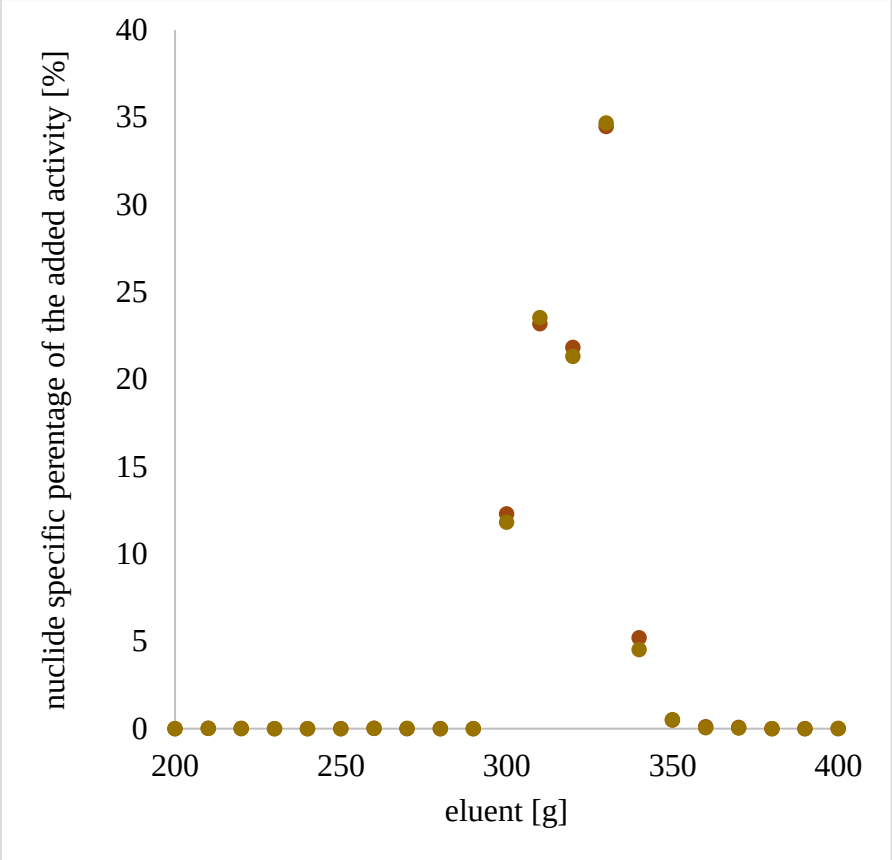

Figure 23: Elution curve of ^{88}Y in a milk ash sample with a multi-nuclide tracer, GEM40

Figure 23 shows a chromatogram of only ^{88}Y. As ^{88}Y has two γ-decay modes, it could be separately quantified at two different energies, 898 keV and 1,836 keV, the energies of these two decays. These quantifications are shown in the graphic as red and golden points. The almost congruent data sets show the precision of this quantification method.

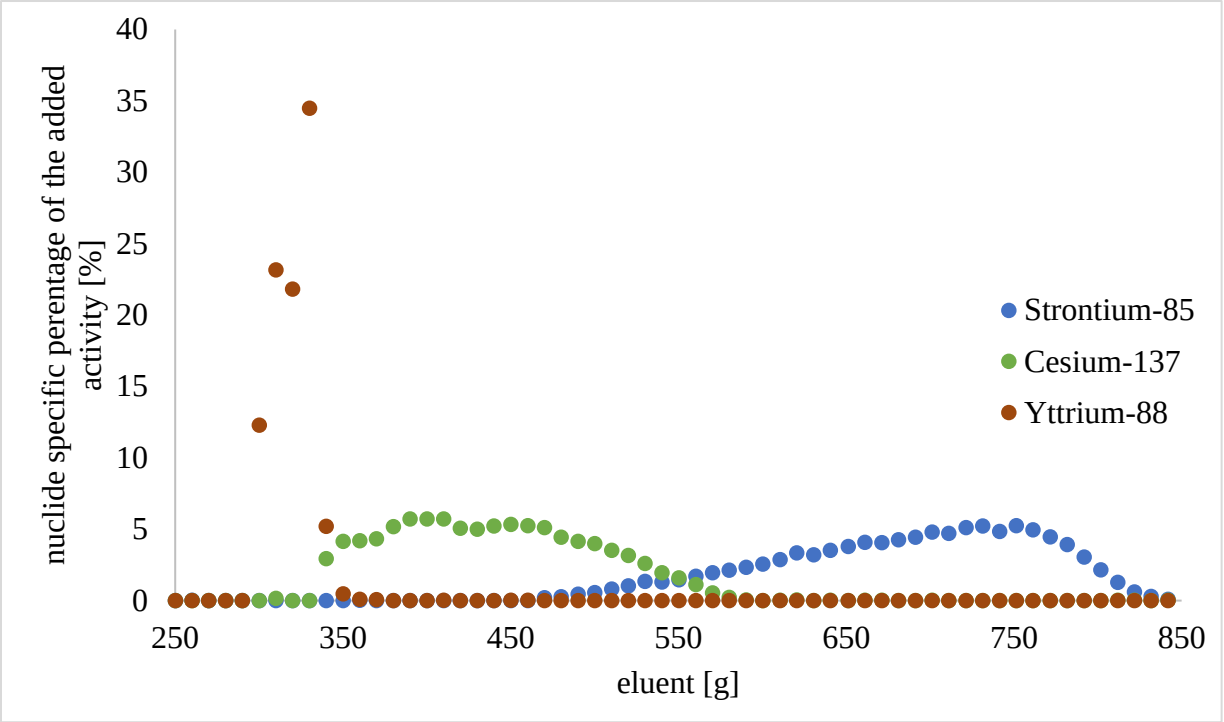

Figure 24: Elution curves of ^{88}Y, ^{137}Cs and ^{85}Sr in a milk ash sample with a multi-nuclide tracer, GEM40

Figure 24 shows the same elution curve as above, only reduced to the analytes yttrium and strontium and the most significant interfering nuclide ^{137}Cs. Only a small overlap of 20 g between the elution regions of yttrium and ^{137}Cs is visible between 330 and 350 g eluent. ^{137}Cs can be completely separated from yttrium without significant yield loss because the overlap is outside of the yttrium elution maximum. Therefore, ^{137}Cs has a smaller effect on the analysis region of yttrium as it has on the analysis region of strontium, due to the strong overlap of the elution regions of strontium and cesium. This overlap was already elaborated on in the previous paragraph and is especially evident in figure 24.

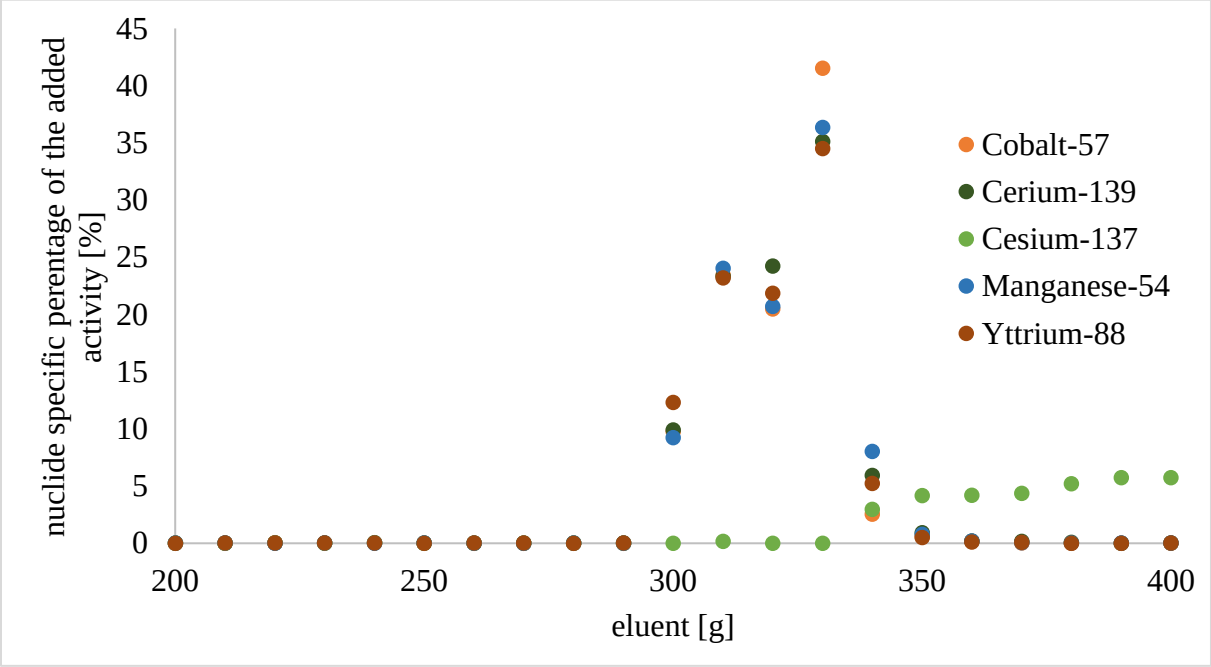

Figure 25: Elution curves of ^{88}Y, ^{57}Co, ^{54}Mn, ^{139}Ce and ^{137}Cs in a milk ash sample with a multi-nuclide tracer, GEM40

Figure 25 shows the same elution curve as above, only focused on the elution region of the analyte yttrium, in which the elements cobalt, manganese and cerium were also present. They were not separated from yttrium. But it is not expected of these elements to appear in food samples, especially in form of radionuclides, even in food samples contaminated through a leak in the system of a nuclear power plant. So, this overlap was not problematic for the further separation optimization process. The small overlap between the yttrium elution curve and the cesium elution curve is also highlighted in this graphic. A good separation of yttrium from strontium, zinc and barium was achieved.

Table 14: Recovery rates of the added nuclides for the milk elution curve

Nuclide	Recovery rate generous [%] (All activities considered)	Recovery rate conservative [%] (Only activities with an activity percentage of ≥ 0.2 % of the 100 % sample are considered)
Cobalt-57	99	98
Cerium-139	101	99
Strontium-85	106	100
Cesium-137	97	96
Manganese-54	100	99
Yttrium-88	98	98
Zinc-65	102	99
Yttrium-88	97	96

The recovery rates for all the tracer nuclides were calculated, as presented in table 14. After the separation process, a control was performed to investigate if some active species remained in the column, but none were found. The determination of recovery rates was not as easy as for other experiments, as sometimes recovery rates of over 100 % were calculated, which logically of course does not make sense. This could be due to a small amount of background radioactivity, which could have caused a significant noise during the gamma-measurement in comparison to the often very small analyte activities in the elution fractions. The measurement time per sample could not be chosen too long, to reduce the noise, due to the sheer number of samples. As a result, the signal to noise ratio, especially in samples with very low activity, was very low. This was especially relevant for the nuclide ^{88}Sr, as its emission energy is very close to the annihilation peak at 511 keV. It was very difficult to differentiate, which counts originated from this nuclide in the samples and which from the annihilation. Therefore, it was sometimes hard to assign the counted impulses to the actual activity from the measured fraction or just to noise, as in many cases the signal was barely above the background.

The generous recovery rate was calculated through adding up all the nuclide specific percentages of the added activities of all fractions for the respective nuclide, if their count numbers were positive and above the count error. The conservative recovery rate was calculated by adding up only the percentages of the added activities for the respective nuclide if they were higher than 0.2 % of the nuclide specific activity in the 100 % tracer. This was done to reduce the contribution of the background noise to the measured activity and eliminate false positives.

All in all, good recovery rates of the used nuclides were achieved and it can be assumed that they were completely eluted from the column during the process. A recovery rate for barium could not be calculated, as its elution region was outside of the investigated region. It is removed from the column during its reconditioning with 6 M hydrochloric acid.

Table 15: Rounded decontamination factors of the different nuclides during the elution of a milk ash sample in relation to the Y elution region

Nuclide	Decontamination factor in relation to the Y elution region
Cobalt-57	1.04
Cerium-139	1.05
Barium-133	194
Strontium-85	20057
Cesium-137	32
Manganese-54	1.03
Zinc-65	67

The decontamination factors of the other nuclides in relation to the analyte Y were calculated, which represent the quality of the separation of these potentially interfering elements from the analyte. The determined values are presented in table 15. For the calculation, the total activity of the nuclide in the 100 % sample was divided through the sum of the activities of this nuclide in the fractions in the elution region of yttrium (290-340 g).

The higher the decontamination factor, the better the separation. The results show a very good separation of yttrium from strontium, the other analyte, and Barium-133, a potential interfering nuclide. The separation from Cesium-137, another interfering nuclide, and Zinc-65 is also quite good. The separation from Cobalt-57, Cerium-139 and Manganese-54 was not successful, as they basically have the same elution region as yttrium. But this is not a problem for the analysis, as these nuclides are normally not present in the kind of samples that are analyzed with this method.

5.2.2.2 Elution curve with wheat ash sample

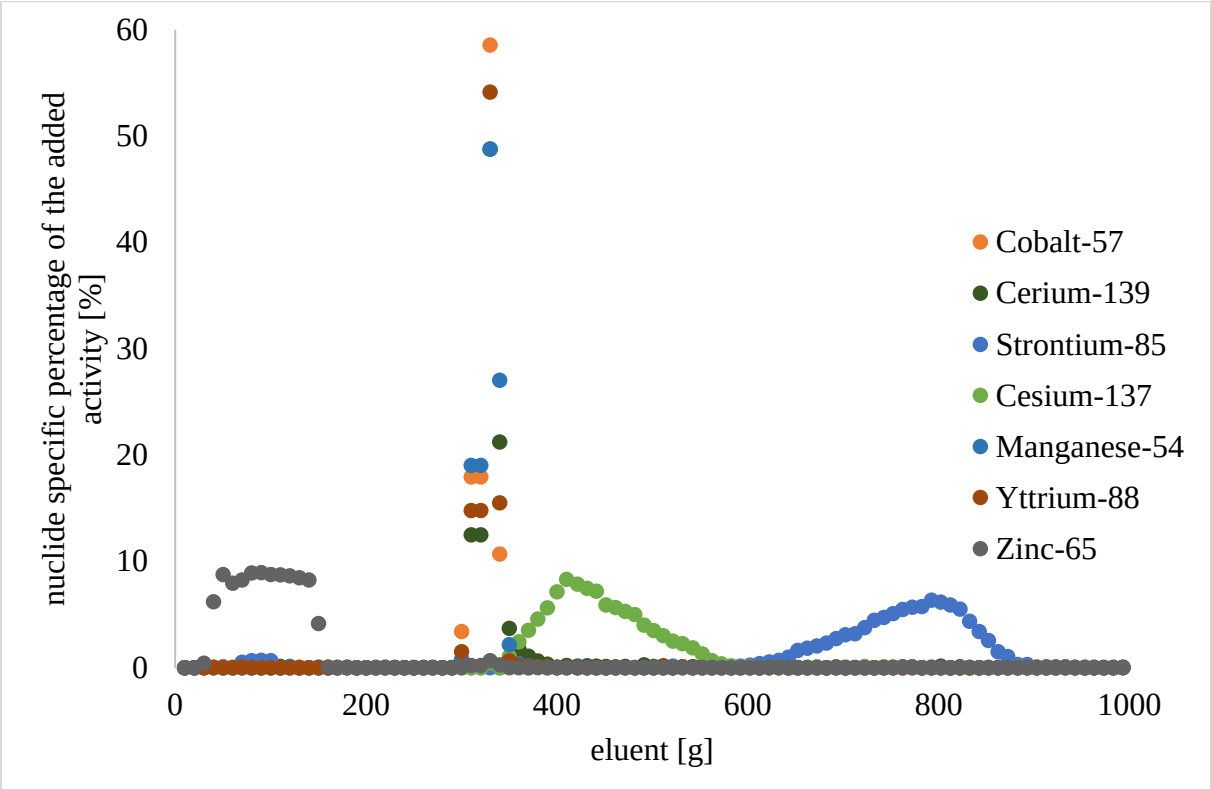

Figure 26: Elution curve with wheat ash sample and multi-nuclide tracer, GEM40

Figure 26 shows the elution curve for a wheat ash sample with added multi-nuclide tracer containing Barium-133, Cobalt-57, Cer-139, Strontium-85, Cesium-137, Manganese-54, Yttrium-88 and Zink-65. The percentage of the activity of the added nuclides in each fraction was plotted against the eluent volume it represents. The different analytes were detected at different decay energies. The time difference between the measurement of the 100 % tracer and the measurements of the fractions was mathematically compensated for. The elution range for yttrium was exactly as for the milk sample at 290 to 350 g eluent. The nuclides ^{57}Co, ^{54}Mn and ^{139}Ce shared this narrow elution region with yttrium. Almost no separation between these nuclides could be achieved and only a small overlap between this collective elution region and the ^{137}Cs elution region was present. The elution region of ^{139}Ce was prolonged until 380 g eluent, but only with low activity values. A good separation between the elution regions of ^{85}Sr between 610 and 870 g eluent and the elution region of ^{137}Cs between 350 and 560 g eluent was achieved. The elution region of ^{65}Zn between 40 and 150 g eluent was eluted from the column right at the beginning of the elution and this analyte was completely separated from all the other nuclides in the sample. ^{133}Ba does not even appear in this graphic, because it was retained so strongly by the column material. It can only be completely removed by the regeneration of the column with 6 M hydrochloric acid. As barium behaves chemically similar to radium, this can mean that also a complete separation of potentially present radium from the analytes would be achieved. All in all, the results for milk and wheat samples were consistent, the only difference was the shifted strontium elution region, which allows for a better separation from ^{137}Cs for the wheat sample. This means, in general the same elution parameters can be used for these two sample types, especially for the separation of yttrium.

Most of the fractions stayed liquid and colorless after the separation and cooling down to room temperature. A yellow coloring was present in the elution region of 300 to 370 g, which overlaps with the elution regions of ^{88}Y, ^{57}Co, ^{54}Mn and ^{139}Ce at 290 to 350 g eluent. The color was quite mute on the edges of the elution region between 300 to 370 g eluent and became more intense in the middle of this region. This could be due to the many nuclides in this elution region. In the elution region of 330 to 360 g eluent, the fractions formed precipitate after cooling down. In the region of 360-390 g eluent, they became solid and waxy after cooling down. This is due to a high calcium content in this elution region.

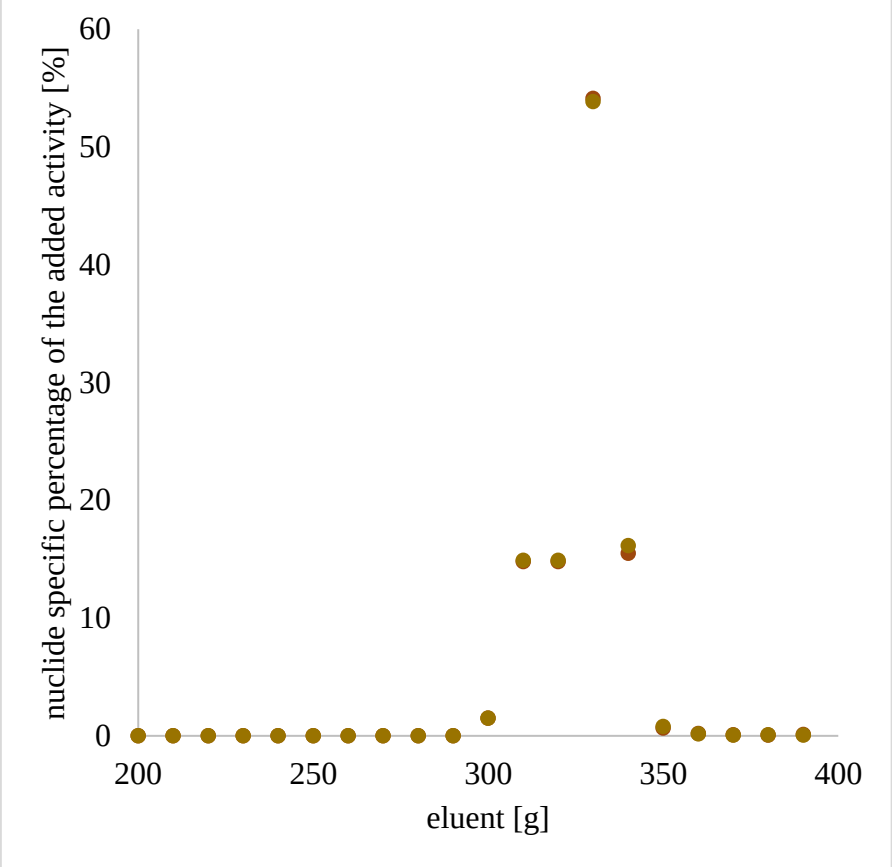

Figure 27: Elution curve of ^{88}Y in a wheat ash sample with a multi-nuclide tracer, GEM40

Figure 27 shows a chromatogram of only ^{88}Y. As ^{88}Y has two γ-decay modes, it could be separately quantified at two different energies, 898 keV and 1836 keV, the energies of these two decays. These quantifications are shown in the graphic as red and golden points. The almost congruent data sets show the precision of this quantification method.

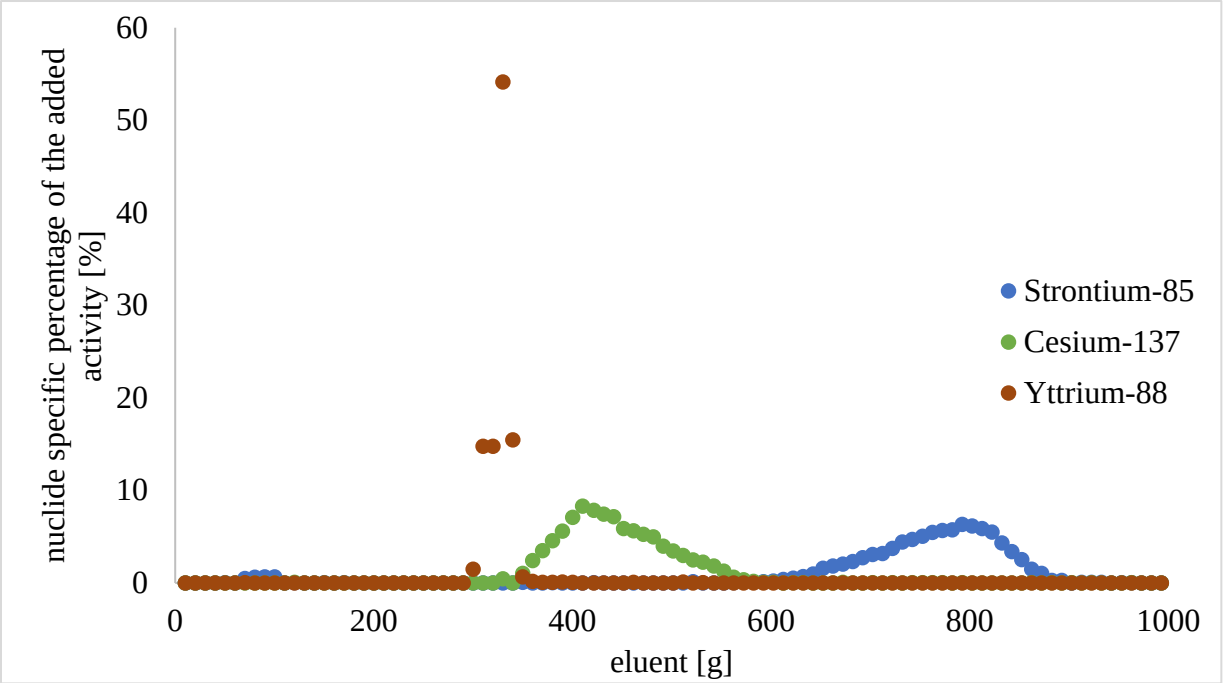

Figure 28: Elution curves of ^{88}Y, ^{137}Cs and ^{85}Sr in a wheat ash sample with a multi-nuclide tracer, GEM40

Figure 28 shows the same elution curve as above, only reduced to the analytes yttrium and strontium and the most significant interfering nuclide ^{137}Cs. Only a small overlap of 10 g between the elution regions of yttrium and ^{137}Cs is visible between 340 and 350 g eluent, where the activities of ^{88}Y and ^{137}C were both quite low. This means ^{137}Cs can be completely separated from yttrium without significant yield loss, because the overlap is outside of the yttrium elution maximum. Additionally, the good separation between strontium and cesium is shown, which would make the analysis of the complete strontium elution region possible and lead to a greater chemical yield of the analyte.

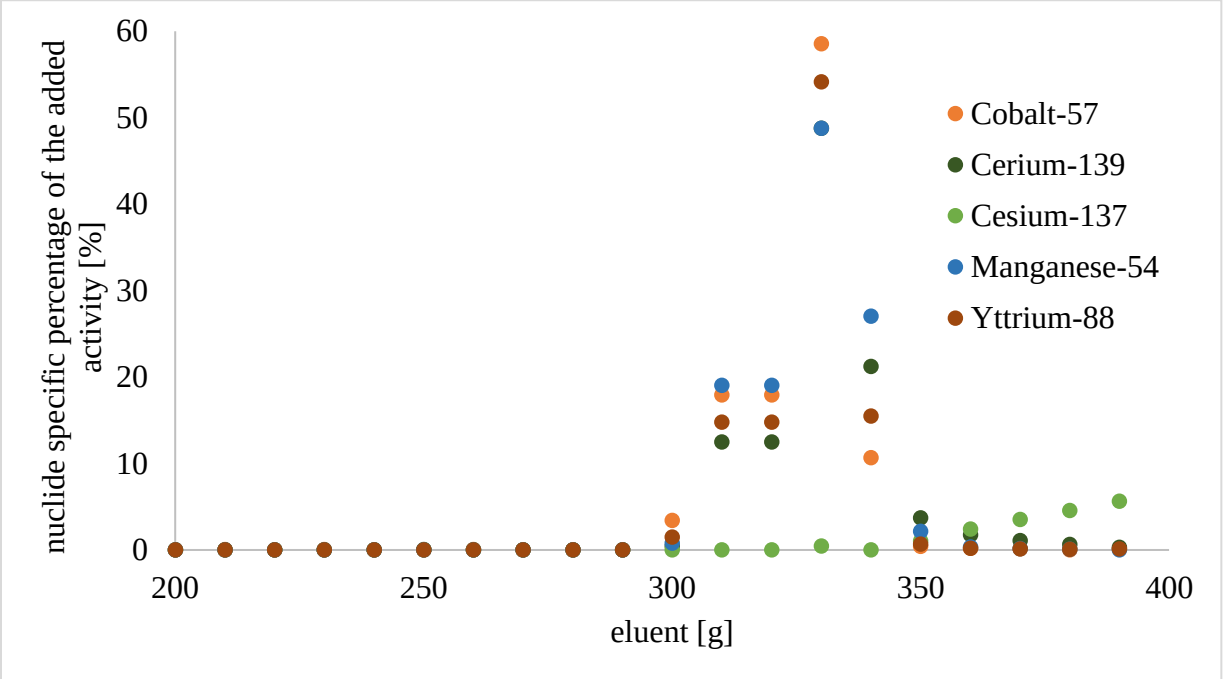

Figure 29: Elution curves of ^{88}Y, ^{57}Co, ^{54}Mn, ^{139}Ce and ^{137}Cs in a wheat ash sample with a multi-nuclide tracer, GEM40

Figure 29 shows the same elution curve as above, only focused on the elution region of the analyte yttrium, in which the elements cobalt, manganese and cerium were also present. They were not separated from yttrium. But it is not expected of these elements to appear in food samples, especially in form of radionuclides, even in food samples contaminated through a leak in the system of a nuclear power plant. So, this overlap was not problematic for the further separation optimization process. Figure 29 also shows that there is basically no overlap between the yttrium and the cesium elution regions and that a complete separation is possible.

Table 16: Recovery rates of the added nuclides for the wheat elution curve

Nuclide	Generous recovery rate (All activities considered)	Conservative recovery rate (Only activities with an activity percentage of ≥0.2 % of the 100 % sample are considered)
Cobalt-57	111	109
Cerium-139	106	103
Strontium-85	96	92
Cesium-137	98	96
Manganese-54	118	117
Yttrium-88	102	101
Zinc-65	98	96
Yttrium-88	103	102

The recovery rates for all the tracer nuclides were calculated, as presented in table 16. The determination of recovery rates was not as easy as for other experiments, as sometimes recovery rates of over 100 % were calculated, which logically of course does not make sense. This could be due to a small amount of background radioactivity, which could have caused a significant noise during the gamma-measurement in comparison to the often very small analyte activities in the elution fractions. The measurement time per sample could not be chosen too long, to reduce the noise, due to the sheer number of samples. As a result, the signal to noise ratio, especially in samples with very low activity, was very low. Therefore, it was sometimes hard to assign the counted impulses to the actual activity from the measured fraction or just to noise, as in many cases the signal was barely above the background. Another problem was a fluctuation of the voltage during the measurement of the tracer, which lead to an energy jump and an underestimation of the added 100 % activity.

The generous recovery rate was calculated through adding up all the nuclide specific percentages of the added activities of all fractions for the respective nuclides, if their counts were positive and above the count error. The conservative recovery rate was calculated by adding up only the percentages of the added activities for the respective nuclide if they were higher than 0.2 % of the nuclide specific activity in the 100 % tracer. This was done to reduce the contribution of the background noise to the measured activity and eliminate false positives.

All in all, good recovery rates for the used nuclides were achieved and it can be assumed that they were completely eluted from the column during the process. A recovery rate for barium could not be calculated, as its elution region was outside of the investigated region. It was removed from the column during its reconditioning with 6 M hydrochloric acid.

Table 17: Rounded decontamination factors of the different nuclides during the elution of a wheat ash sample in relation to the Y elution region

Nuclide	Decontamination factor in relation to the Y elution region
Cobalt-57	0.94
Cerium-139	1.08
Barium-133	5672
Strontium-85	12235
Cesium-137	215
Manganese-54	0.88
Zinc-65	75

The decontamination factors of the other nuclides in comparison to the analyte yttrium were calculated. They represent the quality of the separation of these potentially interfering elements from the analyte. The determined values are presented in table 17. For the calculation, the total activity of the nuclide in the 100 % sample was divided through the sum of the activities of this nuclide in the fractions in the elution region of yttrium (290-350 g).

The higher the decontamination factor, the better the separation. The results show a very good separation of yttrium from strontium, the other analyte and Barium-133, a potential interfering nuclide. The separation from Cesium-137, another interfering nuclide, and Zinc-65 was also quite good. The separation from Cobalt-57, Cerium-139 and Manganese-54 was not successful, as they basically have the same elution region as yttrium. But this is not a problem for the analysis, as these nuclides are normally not present in the kind of samples that are analysed with this method.

5.2.2.3 Elution curve with salad ash sample

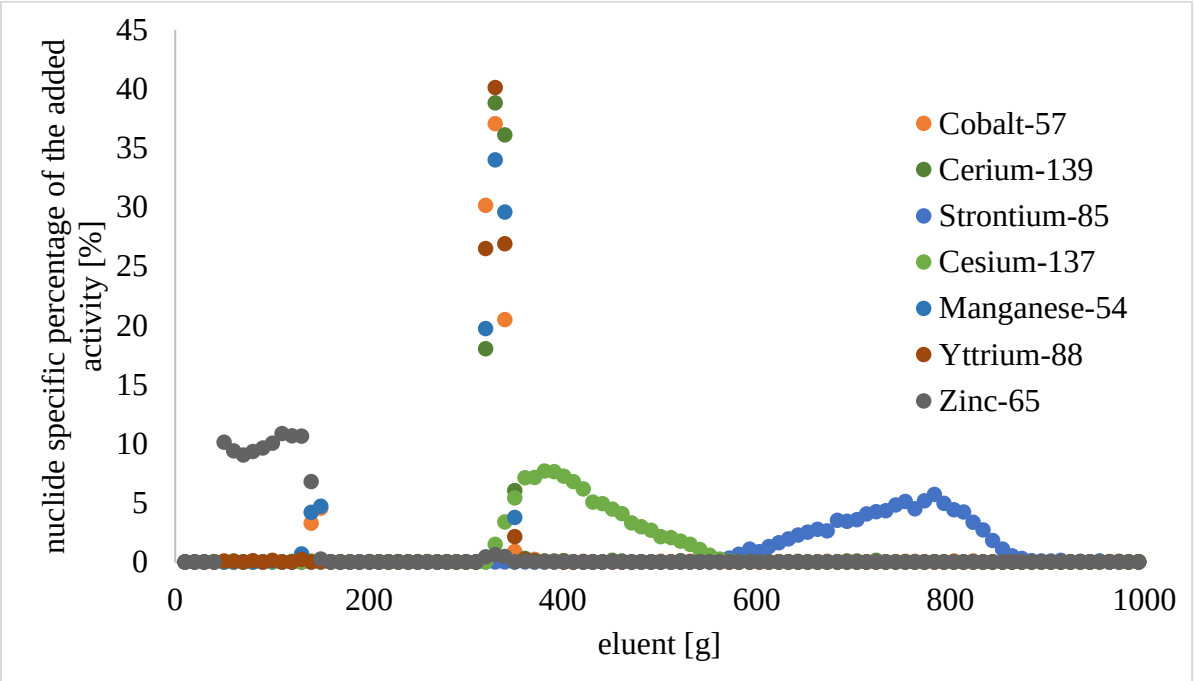

Figure 30: Elution curve with salad ash sample and multi-nuclide tracer, GEM40

Figure 30 shows the elution curve for a salad ash sample with added multi-nuclide tracer containing Barium-133, Cobalt-57, Cer-139, Strontium-85, Cesium-137, Manganese-54, Yttrium-88 and Zink-65. The percentage of the activity of the added nuclides in each fraction was plotted against the eluent volume it represents. The different analytes were detected at different decay energies. The time difference between the measurement of the 100 % tracer and the measurements of the fractions was mathematically compensated for. The elution range for yttrium was similar to the ones for the other matrices at 310-350 g eluent. The nuclides ^{57}Co, ^{54}Mn and ^{139}Ce shared this narrow elution region with yttrium. Almost no separation between these nuclides could be achieved. The separation between yttrium and cesium was not as good this time. There was a significant overlap of the elution regions. This shows, that with salad samples the separation has to be performed more carefully, to prevent a false positive result. An additional elution region for ^{54}Mn and ^{57}Co between 130 and 150 g eluent was found. This additional elution region reminds of the results of Stefanie Schmied [52] but was not present for the other sample types. ^{65}Zn, ^{137}Cs and ^{85}Sr were present in extensive elution regions. A good separation between the elution regions of ^{85}Sr between 580 and 860 g eluent and of ^{137}Cs between 330 and 550 g eluent was achieved. The elution region of ^{65}Zn between 50 and 140 g eluent was eluted from the column right at the beginning of the elution and this analyte was completely separated from all the other nuclides in the sample. ^{133}Ba does not even appear in this figure, because it was retained so strongly by the column material. It could only be completely removed by the regeneration of the column with 6 molar hydrochloric acid. As barium behaves chemically similar to radium, this can mean that also a complete separation of potentially present radium from the analytes would be achieved. All in all, the results for salad, milk and wheat samples are consistent. The only difference is the shifted strontium elution region, which allows for a better separation from ^{137}Cs for the wheat and salad sample. A disadvantage for the salad sample is the significantly stronger overlap between the yttrium and the cesium elution regions.

Most of the fractions stayed liquid and colorless after the separation and cooling down to room temperature. A yellow coloring was present in the elution region of 110 to 150 g eluent, which overlaps with the elution regions of ^{57}Co and ^{54}Mn, and 310 to 340 g eluent, which overlaps with the elution regions of ^{88}Y, ^{57}Co, ^{54}Mn and ^{139}Ce at 290 to 350 g eluent. The color was quite mute on the edges of the colored elution regions and became more intense in the middle of these regions. This could be due to the many nuclides in these elution regions. In the elution region of 330-370 g eluent, the fractions became solid and waxy after cooling down. This is due to the high calcium content in this elution region.

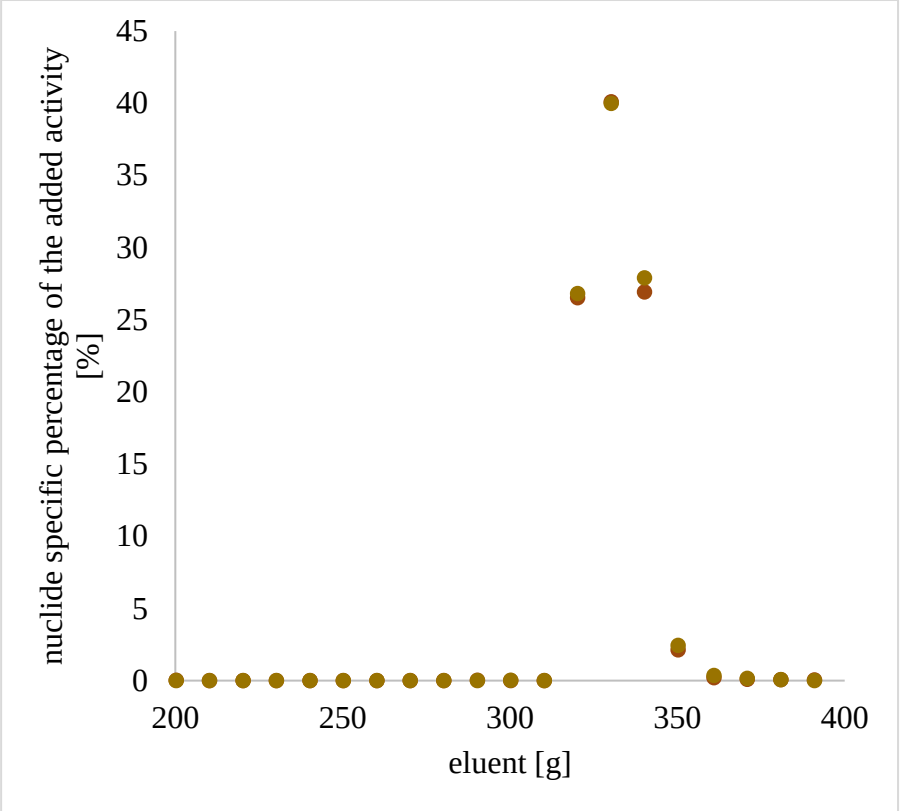

Figure 31: Elution curve of ^{88}Y in a salad ash sample with a multi-nuclide tracer, GEM40

Figure 31 shows a chromatogram of only ^{88}Y. As ^{88}Y has two γ-decay modes, it could be separately quantified at two different energies, 898 keV and 1836 keV, the energies of these two decays. These quantifications are shown in the graphic as red and golden points. The almost congruent data sets show the precision of this quantification method.

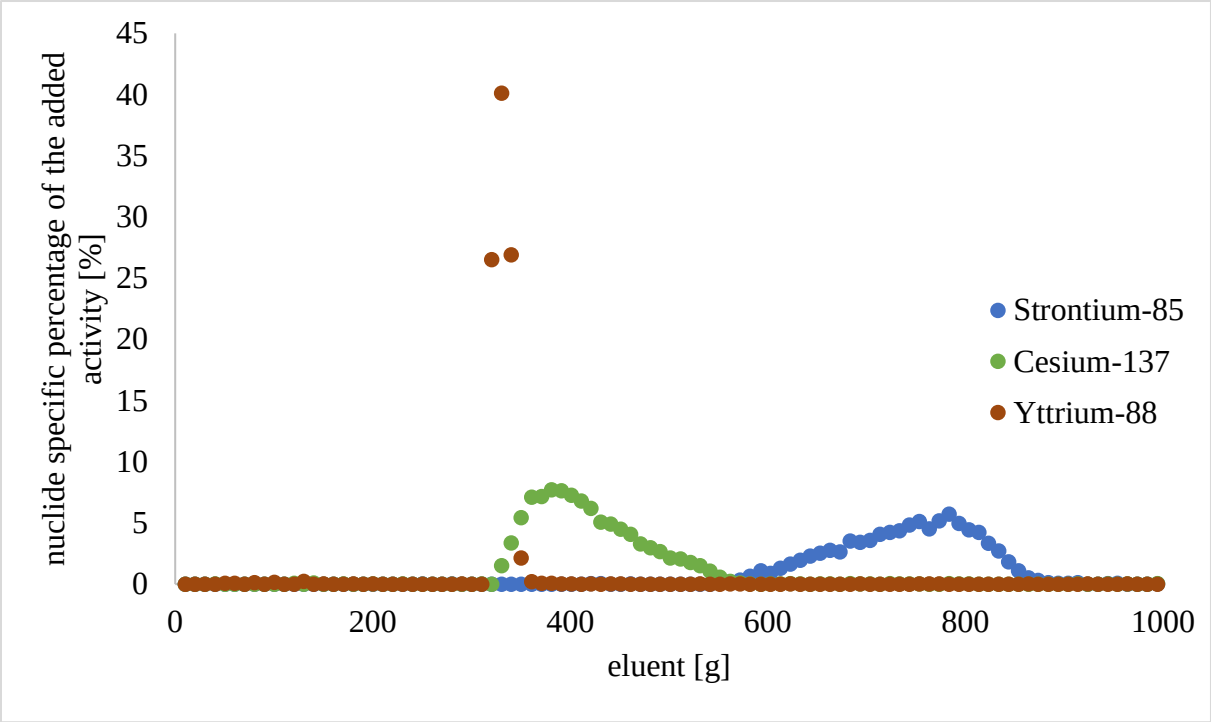

Figure 32: Elution curves of ^{88}Y, ^{137}Cs and ^{85}Sr in a salad ash sample with a multi-nuclide tracer, GEM40

Figure 32 shows the same elution curve as above, only reduced to the analytes yttrium and strontium and the most significant interfering nuclide ^{137}Cs. A strong overlap of 40 g between the elution regions of yttrium and ^{137}Cs is visible between 320 and 360 g eluent, encompassing the whole yttrium elution region. This means a complete separation between yttrium and cesium would be quite difficult, if possible at all. Additionally, the good separation between strontium and cesium is shown, which would make the analysis of the complete strontium elution region possible and lead to a greater chemical yield of the analyte.

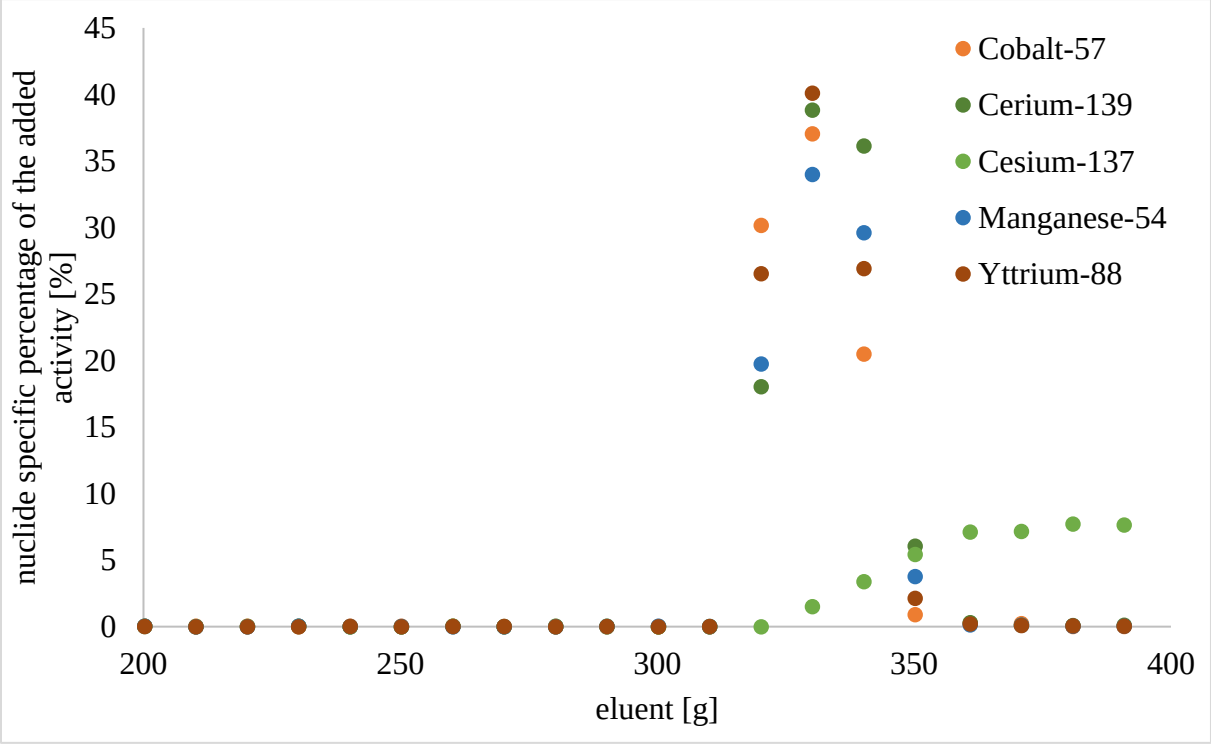

Figure 33: Elution curves of ^{88}Y, ^{57}Co, ^{54}Mn,^{139}Ce and ^{137}Cs in a salad ash sample with a multi-nuclide tracer, GEM40

Figure 33 shows the same elution curve as above, only focused on the elution region of the analyte yttrium, in which the elements cobalt, manganese and cerium were also present. They were not separated from yttrium. But it is not expected of these elements to appear in food samples, especially in form of radionuclides, even in food samples contaminated through a leak in the system of a nuclear power plant. Figure 33 also shows the strong overlap between the yttrium and the cesium elution regions, that makes a complete separation difficult.

Table 18: Recovery rates of the added nuclides for the salad elution curve

Nuclide	Recovery rate generous [%] (All activities considered)	Recovery rate conservative [%] (Only activities with an activity percentage of ≥ 0.2 % of the 100 % sample are considered)
Cobalt-57	99	97
Cerium-139	102	99
Strontium-85	91	90
Cesium-137	98	97
Manganese-54	98	97
Yttrium-88	97	96
Zinc-65	99	97
Yttrium-88	98	98

The recovery rates for all the tracer nuclides were calculated, as presented in table 18. For this separation, good recovery rates could be achieved. The determination of recovery rates was not as easy as for other experiments, as sometimes recovery rates of over 100 % were calculated, which logically of course does not make sense. This could be due to a small amount of background radioactivity, which could have caused a significant noise during the gamma-measurement in comparison to the often very small analyte activities in the elution fractions. The measurement time per sample could not be chosen too long, to reduce the noise, due to the sheer number of samples. As a result, the signal to noise ratio, especially in samples with very low activity, was very low. Therefore, it was sometimes hard to assign the counted impulses to the actual activity from the measured fraction or just to noise, as in many cases the signal was barely above the background.

The generous recovery rate was calculated through adding up all the nuclide specific percentages of the added activities of all fractions for the respective nuclide, if their counts were positive and above the count error. The conservative recovery rate was calculated by adding up only the percentages of the added activities for the respective nuclide if they were higher than 0.2 % of the nuclide specific activity in the 100 % tracer. This was done to reduce the contribution of the background noise to the measured activity and eliminate false positives.

All in all. good recovery rates of the used nuclides were achieved and it can be assumed that they were completely eluted from the column during the process. A recovery rate for barium could not be calculated, as its elution region was outside of the investigated region. It was removed from the column during its reconditioning with 6 M hydrochloric acid.

Table 19: Rounded decontamination factors of the different nuclides during the elution of a salad ash sample in relation to the Y elution region

Nuclide	Decontamination factor in relation to the Y elution region
Cobalt-57	1.14
Cerium-139	1.03
Barium-133	254
Strontium-85	21302
Cesium-137	10
Manganese-54	1.16
Zinc-65	65

The decontamination factors of the other nuclides in comparison to the analyte yttrium were calculated, which represent the quality of the separation of these potentially interfering elements from the analyte. The determined values are presented in table 19. For the calculation, the total activity of the nuclide in the 100 % sample was divided through the sum of the activities of this nuclide in the fractions in the elution region of yttrium (310-350 g).

The higher the decontamination factor, the better the separation. The results show a very good separation of yttrium from strontium, the other analyte, and Barium-133, a potential interfering nuclide. The separation from Zinc-65 is also quite good. The separation from Cesium-137 is significantly worse than for the other sample types. The separation from Cobalt-57, Cerium-139 and Manganese-54 was not successful, as they basically have the same elution region as yttrium. But this is not a problem for the analysis, as these nuclides are normally not present in the kind of samples that are analyzed with this method.

5.2.2.4 Elution curve with corn ash sample

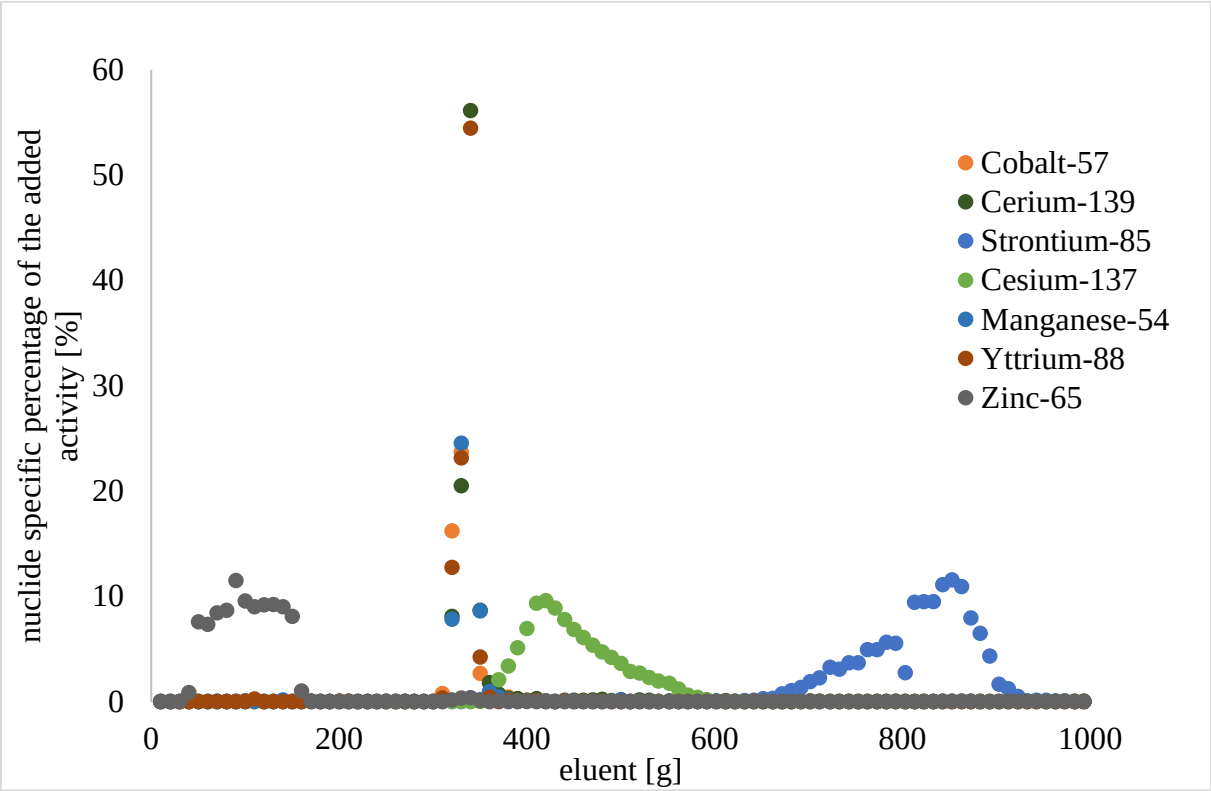

Figure 34: Elution curve with corn ash sample and multi-nuclide tracer, GEM40

Figure 34 shows the elution curve for a corn ash sample with added multi-nuclide tracer containing Barium-133, Cobalt-57, Cer-139, Strontium-85, Cesium-137, Manganese-54, Yttrium-88 and Zink-65. The percentage of the activity of the added nuclides in each fraction was plotted against the eluent volume it represents. The different analytes were detected at different decay energies. The time difference between the measurement of the 100 % tracer and the measurements of the fractions was mathematically compensated for. The nuclides ^{88}Y, ^{57}Co, ^{54}Mn and ^{139}Ce shared the narrow elution region between 310 and 370 g eluent. Almost no separation between these nuclides could be achieved and only a small overlap between this collective elution region and the ^{137}Cs elution region was present. ^{65}Zn, ^{137}Cs and ^{85}Sr were present in extensive elution regions. A good separation between the elution regions of ^{85}Sr between 640 and 920 g eluent and ^{137}Cs between 360 and 580 g eluent was achieved. The elution region of ^{65}Zn between 40 and 160 g eluent was eluted from the column right at the beginning of the elution and this analyte was completely separated from all the other nuclides in the sample. ^{133}Ba does not even appear in this graphic, because it was retained so strongly by the column material. It could only be completely removed by the regeneration of the column with 6 molar hydrochloric acid. As barium behaves chemically similar to radium, this can mean that also a complete separation of potentially present radium from the analytes would be achieved. Most elution regions are shifted by 10 to 30 g eluent to higher eluent volumes compared to the other sample matrices. This could be due to an interruption of the separation at 260 g eluent because of a fire alarm. But all in all, the results are consistent with the milk and wheat matrices. This means, almost the same elution parameters can be used for these sample types.

Most of the fractions stayed liquid and colourless after the separation and cooling down to room temperature. A yellow colouring was present in the elution region of 320 to 360 g eluent, which overlaps with the elution regions of ^{88}Y, ^{57}Co, ^{54}Mn and ^{139}Ce at 310 to 360 g eluent. The yellow colour was intense in the elution region of 320-340 g eluent, had a medium intensity in the elution region of 340-350 g eluent and was quite mute in the elution region of 350-360 g eluent. This could be due to the many nuclides in this elution region. In the elution region of 330-380 g eluent the fractions became solid and waxy after cooling down. This is due to a high calcium content in this elution region.

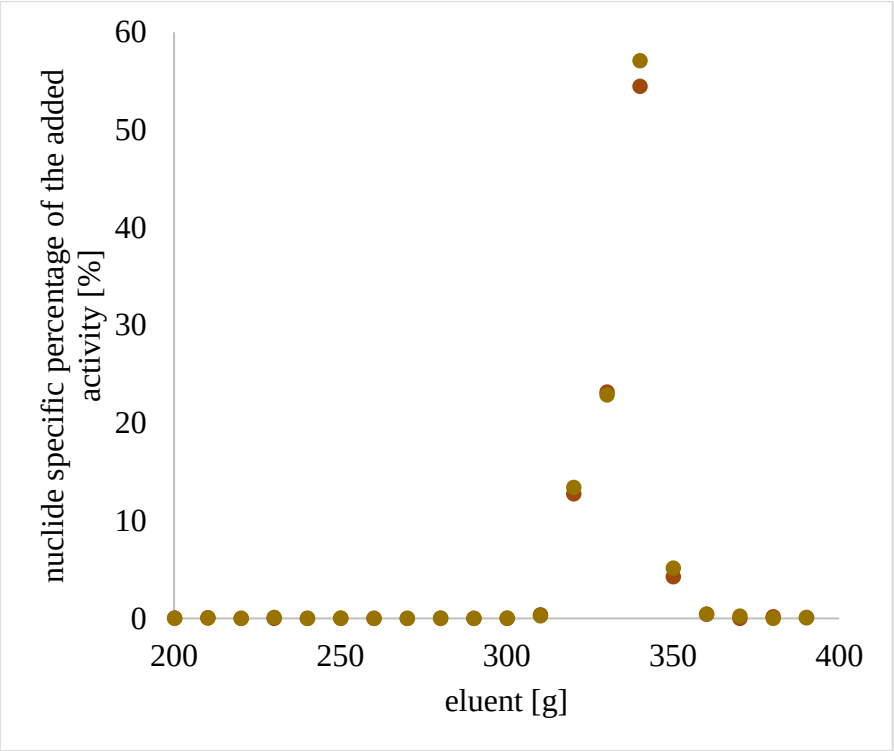

Figure 35: Elution curve of ^{88}Y in a corn ash sample with a multi-nuclide tracer, GEM40

Figure 35 shows a chromatogram of only ^{88}Y. As ^{88}Y has two γ-decay modes, it could be separately quantified at two different energies, 898 keV and 1836 keV, the energies of these two decays. These quantifications are shown in the graphic as red and golden points. The almost congruent data sets show the precision of this quantification method.

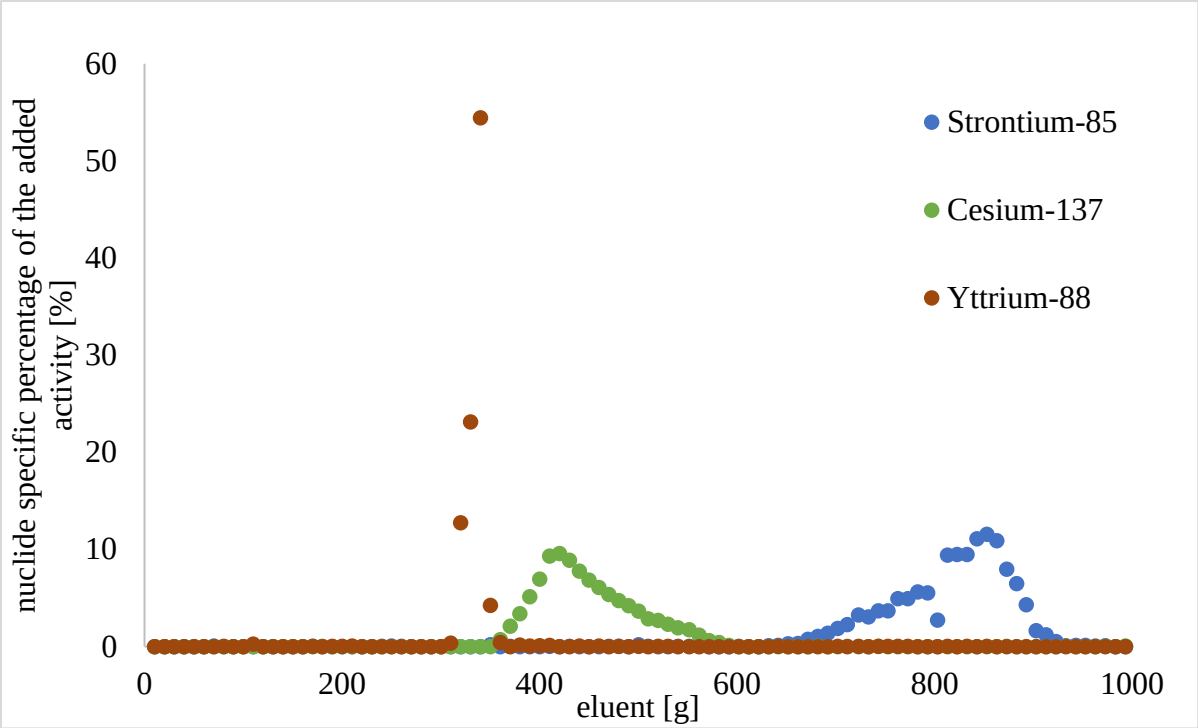

Figure 36: Elution curves of ^{88}Y, ^{137}Cs and ^{85}Sr in a corn ash sample with a multi-nuclide tracer, GEM40

Figure 36 shows the same elution curve as above, only reduced to the analytes yttrium and strontium and the most significant interfering nuclide ^{137}Cs. Only a small overlap of 10 g between the elution regions of yttrium and ^{137}Cs is visible between 360 and 370 g eluent, where the activities of ^{88}Y and ^{137}C were both quite low. This means ^{137}Cs can be completely separated from yttrium without significant yield loss. Additionally, the good separation between strontium and cesium is shown, which would make the analysis of the complete strontium elution region possible and lead to a greater chemical yield of the analyte.

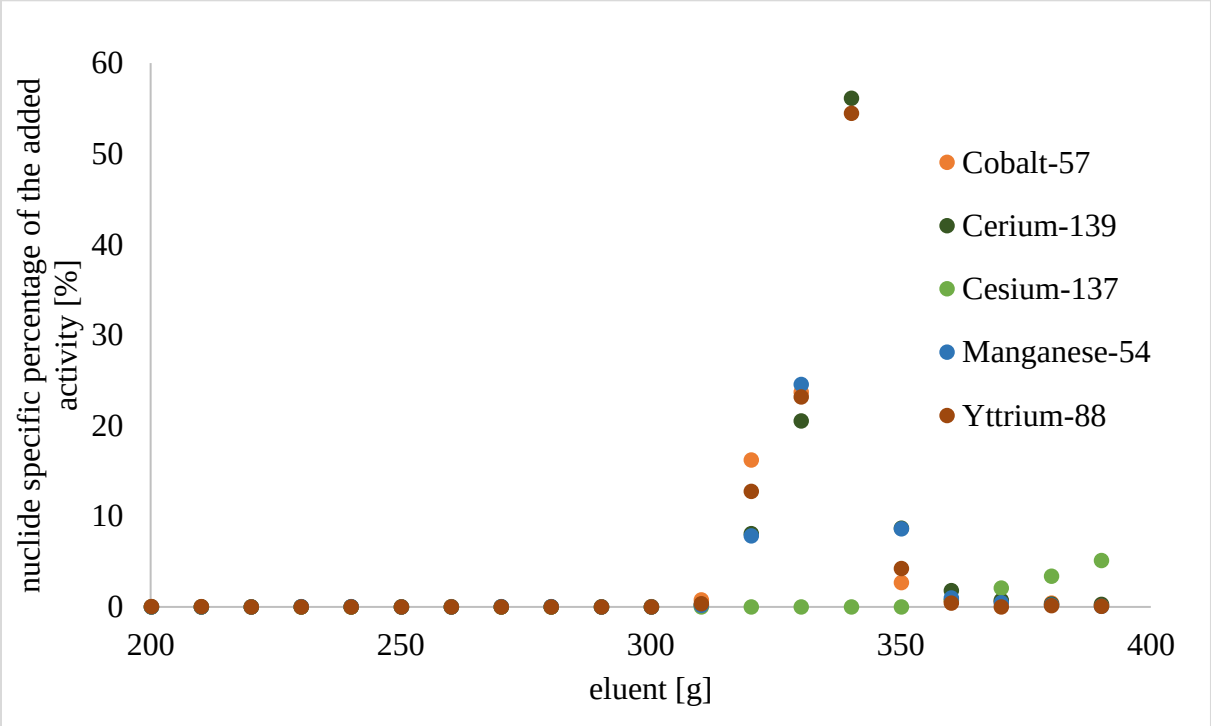

Figure 37: Elution curves of ^{88}Y, ^{57}Co, ^{54}Mn, ^{139}Ce and ^{137}Cs in a corn ash sample with a multi-nuclide tracer, GEM40

Figure 37 shows the same elution curve as above, only focused on the elution region of the analyte yttrium, in which the elements cobalt, manganese and cerium were also present. They were not separated from yttrium. But it is not expected of these elements to appear in food samples, especially in form of radionuclides, even in food samples contaminated through a leak in the system of a nuclear power plant. Figure 37 also shows that there is basically no overlap between the yttrium and the cesium elution regions and that a complete separation is possible.

Table 20: Recovery rates of the added nuclides for the corn elution curve

Nuclide	Generous recovery rate (All activities considered)	Conservative recovery rate (Only activities with an activity percentage of ≥ 0.2 % of the 100 % sample are considered)
Cobalt-57	114	113
Cerium-139	100	97
Strontium-85	131	130
Cesium-137	99	99
Manganese-54	109	107
Yttrium-88	97	95
Zinc-65	101	99
Yttrium-88	100	99

The recovery rates for all the tracer nuclides were calculated, as presented in table 20.

The determination of recovery rates was not as easy as for other experiments, as sometimes recovery rates of over 100 % were calculated, which logically of course does not make sense. This could be due to a small amount of background radioactivity, which could have caused a significant noise during the gamma-measurement in comparison to the often very small analyte activities in the elution fractions. The measurement time per sample could not be chosen too long, to reduce the noise, due to the sheer number of samples. As a result, the signal to noise ratio, especially in samples with very low activity, was very low. This was especially relevant for the nuclide ^{88}Sr, as its emission energy is very close to the annihilation peak at 511 keV. It was very difficult to differentiate which counts originated from the nuclides in the samples and which from the annihilation. Therefore, it was sometimes hard to assign the counted impulses to the actual activity from the measured fraction or just to noise, as in many cases the signal was barely above the background.

The generous recovery rate was calculated by adding up all the nuclide specific percentages of the added activities of all fractions for the respective nuclide if their counts were positive and above the count error. The conservative recovery rate was calculated by adding up only the percentages of the added activities for the respective nuclide if they were higher than 0.2 % of the nuclide specific activity in the 100 % tracer. This was done to reduce the contribution of the background noise to the measured activity and eliminate false positives.

All in all, good recovery rates of the used nuclides were achieved and it can be assumed that they were completely eluted from the column during the process. A recovery rate for barium could not be calculated, as its elution region was outside of the investigated region. It was removed from the column during its reconditioning with 6 molar hydrochloric acid.

Table 21: Rounded decontamination factors of the different nuclides during the elution of a corn ash sample in relation to the Y elution region

Nuclide	Decontamination factor in relation to the Y elution region
Cobalt-57	0.91
Cerium-139	1.08
Barium-133	849
Strontium-85	565
Cesium-137	134
Manganese-54	1.04
Zinc-65	114

The decontamination factors of the other nuclides in comparison to the analyte yttrium were calculated, which represent the quality of the separation of these potentially interfering elements from the analyte. The determined values are presented in table 21. For the calculation, the total activity of the nuclide in the 100 % sample was divided through the sum of the activities of this nuclide in the fractions in the elution region of yttrium (300-370 g).

The higher the decontamination factor, the better the separation. The results show a very good separation of yttrium from strontium, the other analyte and Barium-133, a potential interfering nuclide. The separation from Cesium-137, another interfering nuclide, and Zinc-65 is also very good. The separation from Cobalt-57, Cerium-139 and Manganese-54 was not successful, as they basically have the same elution region as yttrium. But this is not a problem for the analysis, as these nuclides are normally not present in the kind of samples that are analysed with this method.

After the fractions for the elution curve of corn ash were collected, the washing fraction of 500 mL 6 molar hydrochloric acid for the regeneration of the column and removal of remaining nuclides from it was also collected in a 500 mL kautex container. Then it was measured with a gamma detector for an extensive period of time. This was done to investigate whether the hypothesis was right, that barium is retained in the column and removed during column regeneration, and if other nuclides were also retained in the column.

Then the ROI file of the 100 % measurement was transferred to the washing fraction measurement and corrected, in case of a slight energy shift. The measurement data was processed in a similar way as for the 100 % measurement. The net area and its uncertainty were noted, attributed to the corresponding nuclide and the count rate was calculated. In the end, the resulting count rates were compared to the values of the 100 % sample. The results of the data processing can be seen in table 22.

Table 22: Results of the gamma-spectrometric measurement of the washing fraction of 500 mL 6 M hydrochloric acid in comparison to the 100 % sample (7.53 g of the mixed nuclide solution filled up to 10 g with 4 molar hydrochloric acid in a LSC vial), GEM40

Live time [s]	**Real time [s]**				
248604.04	248825.9	**Washing fraction**			**100% sample**
Nuclide	**ROI [keV]**	**Net area [counts]**	**Error net area [counts]**	**Count rate [cps]**	**Count rate [cps]**
Barium-133	78.50-83.05	325,753	734	1.310	7.447
Cobalt-57	119.95-123.99	176	295	0	21.793
Cerium-139	163.43-168.23	-118	406	0	12.683
Barium-133	353.00-359.07	751,961	896	3.025	14.147
Strontium-85	512.50-517.31	4,237	123	0.017	8.161
Cesium-137	655.82-665.18	272	65	0.001	23.272
Manganese-54	831.25-838.58	45	61	0	16.053
Yttrium-88	894.95-901.77	81	54	0	14.442
Zinc-65	1,110.81-1,119.91	-187	71	0	14.401
Yttrium-88	1,830.96-1,839.55	-19	36	0	8.549
K-40	1,454.33-1,465.45	876	65	0.004	0.045

As described above for the background measurement, net area values, which were negative were corrected to zero. And if the error of a value was bigger than the value, it was corrected to 1/(Live time) [67]. This resulted in the only significant nuclide finding to be ^{133}Ba, as expected. The other nuclides were almost completely recovered during the elution. As barium ions are retained quite strongly in the column, they are only released during the regeneration of the column and can be found in the washing solution, as is proved with this experiment. The count rates between the washing solution and the 100 % solution for ^{133}Ba vary significantly, as can be seen from the numbers in table 22. This is due to the different geometries of the samples: the 100 % sample was measured in a 20 mL LSC vial and the washing solution in a 500 mL Kautex container. This has a strong effect on the physical efficiency of the measuring device, which increases for smaller geometries and decreases for bigger ones. But as the activity ratios between the ^{133}Ba gamma line at 81 keV and at 356 keV are nearly the same for the washing solution and the 100 % sample, the measurement result is confirmed as trustworthy. So, the retention of barium in the column could be proven qualitatively, but its complete recovery from the column could not be proven quantitatively, due to the different measurement geometries.

Overview

Several challenges were met during these experiments. One of them was recovery rates over 100 %, due to high background noise. Another one was, that according to the work of Stefanie Schmied [52], yttrium and potassium seem to have almost the same elution range. As both are β-emitting radio nuclides and potassium a significant interfering element, this could lead to a false positive result. An additional problem were the overlapping elution regions of yttrium and calcium. The precipitation of calcium salts in the samples, when cooled down to room temperature, lead to an almost complete solidification of the samples. This would increase the level of detection. In addition to that, the yttrium containing fractions so far showed a significant yellow coloring. This is also unfavorable, as it could increase the level of detection.

Table 23: Comparison of the elution region of the main analytes for different sample matrices

sample	Y elution range [g eluent]	Cs elution range [g eluent]	Sr elution range [g eluent]
milk	290-350	340-570	480-820
wheat	290-350	350-560	610-870
salad	310-350	330-550	580-860
corn	310-370	360-580	640-920

Table 24: Rounded decontamination factors of the different nuclides during the elution of different sample types in relation to the Y elution region

	Decontamination factor in relation to the Y elution region			
Nuclide	**Milk**	**Wheat**	**Salad**	**Corn**
Cobalt-57	1.04	0.94	1.14	0.91
Cerium-139	1.05	1.08	1.03	1.08
Barium-133	194	5672	254	849
Strontium-85	20057	12235	21302	565
Cesium-137	32	215	10	134
Manganese-54	1.03	0.88	1.16	1.04
Zinc-65	67	75	65	114

On the positive note, the experiment showed that the elution curves for the different sample types looked very similar and were comparable. The elution regions of the analytes varied sometimes less and sometimes more as shown in table 23, which could be taken into consideration for future analyses. But the elution region of yttrium was always quite narrow, did not vary much and in most cases only a verry small overlap with the elution region of cesium was present. Table 24 shows the comparison of the decontamination factors in relation to the yttrium elution region for the different sample types. The low decontamination factors for cobalt, cerium and manganese were quite consistent for all sample types and indicate no separation from yttrium. The high decontamination factors for barium and strontium and middle decontamination factors for zinc and cesium vary significantly due to a variation in the measured background but indicate a sufficient separation for almost all sample types. The only exception was the salad sample, which showed a significant overlap between the elution regions of yttrium and cesium. Also, the overlap between the elution regions of strontium and cesium was a lot more significant for the milk sample than for the other samples (table 23). Therefore, a complete separation without a significant strontium yield loss could be possible for these sample types.

5.3 Validation of new batches of DOWEX® 50 WX8 (200-400 mesh) by different provides

The cause for this experiment series was that the DOWEX®50WX8 200-400 (H) resin was no longer offered by the original provider Serva. Without it the separation could not be performed, as this is the column material for the Hot Column Chromatography separation technique. The DOWEX®50WX8 200-400 (H) resin is also offered by other providers and was purchased from Alfa Aesar, taking into consideration the price and the delivery period. As the new column material was presented as the same material that was used before, it was expected that the separation results would be approximately the same for both materials. But a first test run showed that the elution region of strontium was significantly shifted to higher elution regions with the new DOWEX. This made clear that, even though the new product was still a DOWEX®50WX8 200-400 (H) resin, this is a complex product, which can have varying properties, depending on the provider, among other variables. As the performed analyses rely on knowing the exact elution regions of the analytes, it had to be ensured that the properties of this resin are suitable for the analysis aim. This initiated a validation process for the new DOWEX®50WX8 200-400 (H) resin from the provider Alfa Aesar and another provider Sigma Aldrich. For this process, the following questions were asked:

1) Is the new column material suitable for the separation of yttrium and strontium from each other and from the interfering elements and nuclides?

2) Have elution parameters to be modified for the new column material?

3) If yes, which parameters must be modified?

4) How do these parameters have to be modified?

These questions are explored and answered in the following sections, detailing the validation experiments.

For the experiments, a suitable glass column, specifically crafted by the glassblower workshop for the Hot Column Chromatography, was used. It was securely positioned and connected to a thermostat through rubber tubes, which contained flow control components and were secured with cable ties. After it was made sure that the set-up is leakproof and the thermostat had a strong enough pump system to fill the column, it could be filled. For this the standard mass of 151.5 g DOWEX®50WX8 200-400 (H) resin, which was optimized in previous works [52], was suspended in 500 mL 6 molar hydrochloric acid and filled in the column. The column material was then washed with 6 molar hydrochloric acid until the exiting elution liquid was clear.

5.3.1 DOWEX® 50 WX8 (200-400 mesh) by Alfa Aesar for the determination of K, Ca, Y and Sr in milk ash

The first experiment with the new DOWEX®50WX8 200-400 (H) resin by Alfa Aesar was the determination of the elution regions of yttrium, strontium, potassium and calcium. Because different isotopes of the same element behave chemically the same, and therefore their ions are separated in the same way in the Hot Column Chromatography, the elution regions could be determined using the stable forms of the elements as tracers. This eradicates the problem of radioactive decay and time dependent concentrations and activities and prevents unnecessary radioactive contamination and exposure of the operator. As detection method for the quantification of these elements in the different fractions ICP-OES was used.

As standard sample matrix, 10 g not contaminated milk ash, prepared from commercially available whole long-life milk by the brand Berchtesgadener Land, was used. It was solved in the usual 1:1 mixture of 6 M hydrochloric acid and 1.5 M lactic acid. Additionally, 1 mL of the stable yttrium tracer, containing 10 mg Y, and 2 mL of the stable strontium tracer, containing in total 100 mg Sr, were added. Potassium and calcium were naturally present in the sample matrix in significant amounts, according to the milk packaging 124 mg calcium per 100 mL. After the sample was solved and applied to the column, the Hot Column Chromatography was performed at the elution speed of 2.5 mL/min. During this, 100 elution fractions à 10 mL were collected. For the ICP-OES measurement, the fraction samples were diluted 1:250. Per ICP-OES sample 40 µL of the fractions were used and 2 mL concentrated nitric acid was added for pH adjusting. The samples were filled up to a volume of 10 mL with bidistilled water.

To reliably measure the analyte content in the samples, a calibration curve had to be calculated and prepared for all analytes. For this, the expected concentration range in the elution curve had to be estimated and divided by 250, the selected dilution. This is done because the ICP-OES is optimized for lower concentrations and ideally narrow concentration ranges. For calcium and potassium, the basis for the calibration concentrations was the information from the milk packaging and previous measurements. For yttrium, the added tracer concentration and the distribution of yttrium during the elution, known from previous experiments, were used to estimate an optimal concentration range. For strontium, the tracer volume was increased, because it was known from previous experiments, that its elution region is wide. This means the strontium is distributed over more individual fractions, which contain smaller concentrations. So, to be able to reliably measure strontium in those fractions, the concentration had to be increased.

Table 25: Calibration for the measurement of yttrium, strontium, potassium and calcium in the elution fractions with ICP-OES

sample	c(Y) [µg/kg]	c(Sr) [µg/kg]	c(K) [µg/kg]	c(Ca) [µg/kg]
C0	0	0	0	0
C1	10	20	400	400
C2	50	200	2,000	2,000
C3	100	500	4,000	4,000
C4	500	1,000	20,000	20,000
C5	1,000	1,500	40,000	40,000
C6	2,000	2,000	80,000	80,000
C7	0	3,000	100,000	100,000

Finally, the concentrations in the calibration curve were optimized to encompass as large of a concentration range as possible and sensible, as is seen in the table 25. The aim was to be able to quantify the concentration maximum of the elution curve and at the same time to still be able to detect 1 % of the concentration maximum in the different fractions. Another aim was to be able to prepare one set of calibration solutions for all the analytes and samples. As analyte sources for the preparation of the calibration, the ICP standards by Bernd Kraft were used, which had a standard concentration of 1 g/L and in some cases were prediluted to obtain volumes that were easier to handle with Eppendorf pipettes.

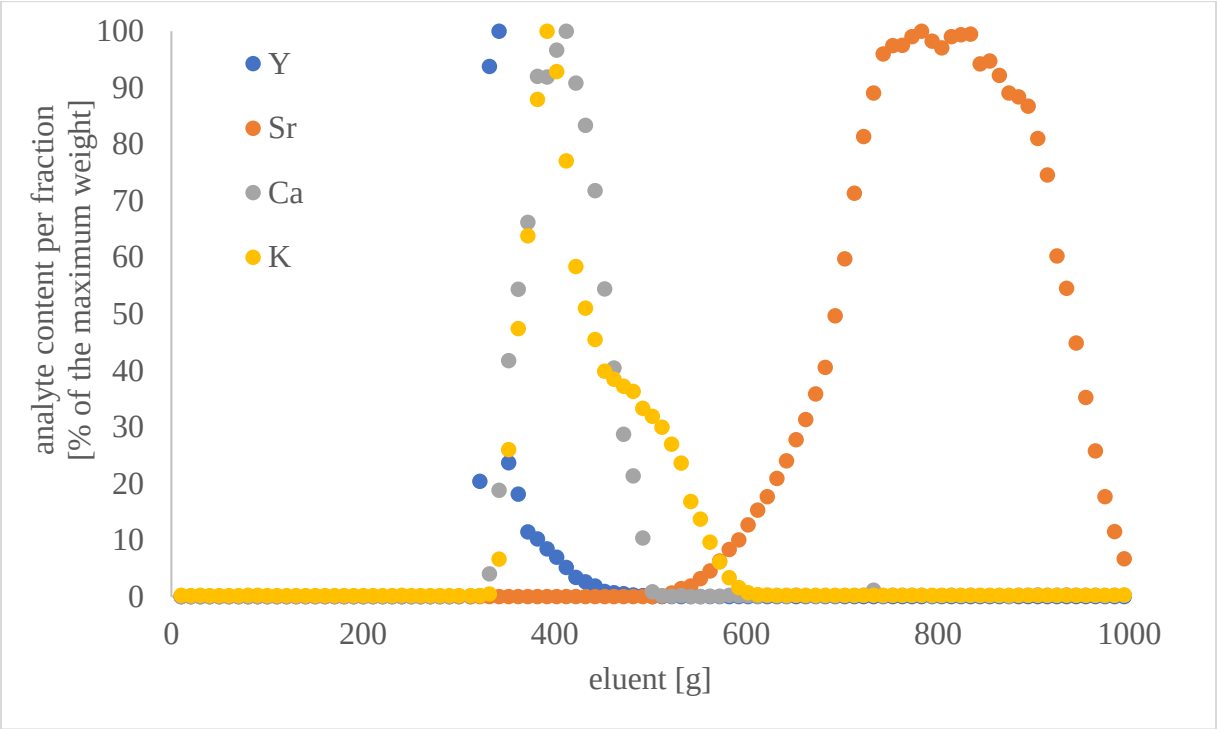

Figure 38: Relative elution curve for the determination of K, Ca, Y and Sr in milk ash with the DOWEX® 50 WX8 (200-400 mesh) by Alfa Aesar and sample measurement with ICP-OES

The resulting elution curve for the determination of K, Ca, Y and Sr in milk ash with the DOWEX® 50 WX8 (200-400 mesh) by Alfa Aesar and sample measurement with ICP-OES is shown above. This is the relative elution curve, with the concentration maximum normed to 100 % and the rest of the concentrations presented relative to the maximum of the concentration of the analyte during the elution. This presentation form has the advantage, that the distribution of the individual analytes is better visible this way. The disadvantage of this presentation form is that the concentration differences between the different analytes and the effect of these differences in the sample is not visible, and therefore is neglected.

A very good separation between yttrium and strontium, a good separation between calcium and strontium and an acceptable separation between potassium and strontium were achieved. The separation between yttrium, calcium and potassium was only mediocre. But at least the relative content of potassium and calcium was quite small in the maximum range of yttrium. The reason for this could also be, that fraction 34, which is the fraction with the highest yttrium content, contained solid precipitate, that could not be resolved through heating after the sample cooled down. This precipitate is likely calcium, but could also contain potassium, and subsequently was not accounted for during the ICP-OES measurement.

Table 26: Elution regions and the concentration maxima of the analytes K, Ca, Y and Sr in milk ash recorded with the DOWEX® 50 WX8 (200-400 mesh) by Alfa Aesar and sample measurement with ICP-OES

element	elution region [g]	concentration maximum [g]
yttrium	310-480	330-340
strontium	510-1,000	770-780
calcium	320-510	400-410
potassium	330-600	380-390

Table 26 shows the elution regions of the analytes and their concentration maxima for a direct comparison and numerical visualization of the overlap of their elution regions.

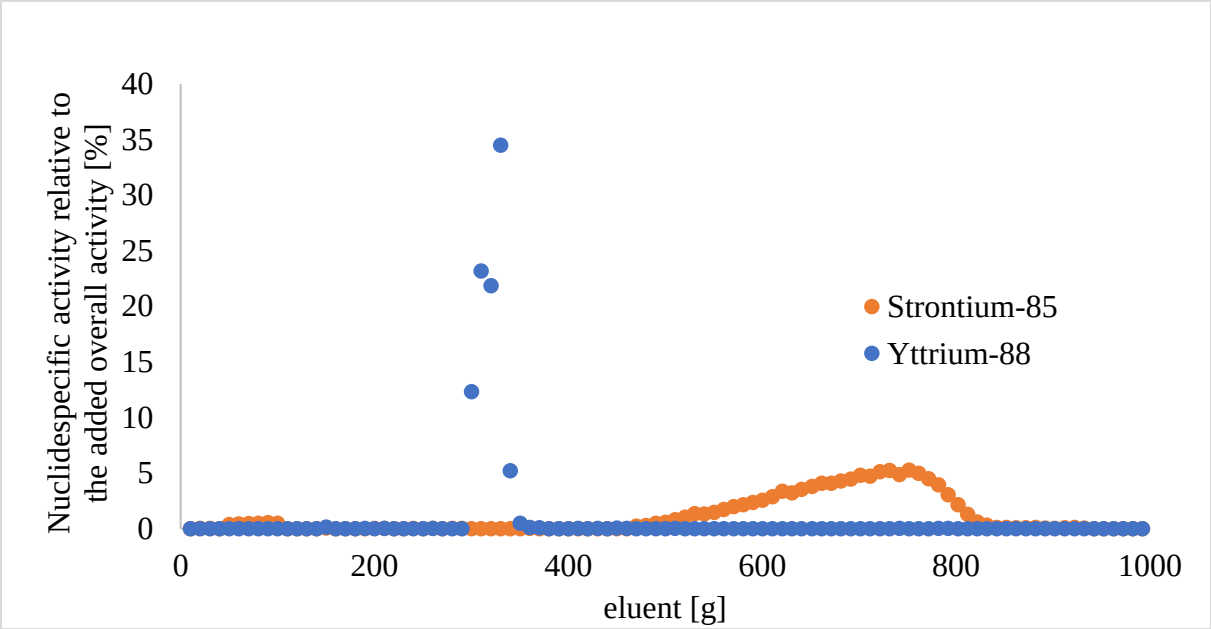

Figure 39: Elution regions of Y and Sr in milk as recorded with the established DOWEX®50WX8 200-400 (H) resin by Serva

Figure 39 shows an older recording of the elution regions of yttrium and strontium achieved with the established DOWEX®50WX8 200-400 (H) resin by Serva, to compare these results with the new results. The distribution was determined with a different method (5.2.2), a gamma active multi-nuclide tracer was used and the activities relative to the 100 % tracer were measured with gamma spectrometry. As the tracer did not contain calcium or potassium isotopes, their elution region could not be determined with this method. Because of the different methods, the absolute quantities of analytes in the individual samples cannot be compared, but the distribution of the analytes, alias the elution regions, are comparable, as the Hot Chroma separations were performed in an almost identical way.

Table 27: Comparison between the DOWEX® 50 WX8 (200-400 mesh) by Serva and by Alfa Aesar Elution regions and the concentration maxima of the analytes Y and Sr in milk ash

element	DOWEX®50WX8 200-400 (H) Serva		DOWEX®50WX8 200-400 (H) Alfa Aesar	
	elution region [g]	maximum [g]	elution region [g]	maximum [g]
yttrium	270-440	300-310	310-480	330-340
strontium	470-840	730-740	510-1,000	770-780

Figure 39 and table 27 show that the elution regions are at smaller eluent volumes for the older measurement. The shift of the yttrium elution region is quite small, only about 10 g eluent, which is relatively negligible for the comparison with the new resin. But the shift of the strontium elution region to higher eluent volumes of about 40 g with the new column material is striking. Additionally, the elution region was broadened significantly, so the strontium elution region extends to at least 1,000 g eluent with the new column material. This makes the separation of the strontium elution region more time consuming and increases the amount of necessary chemicals per sample with the new resin by Alfa Aesar.

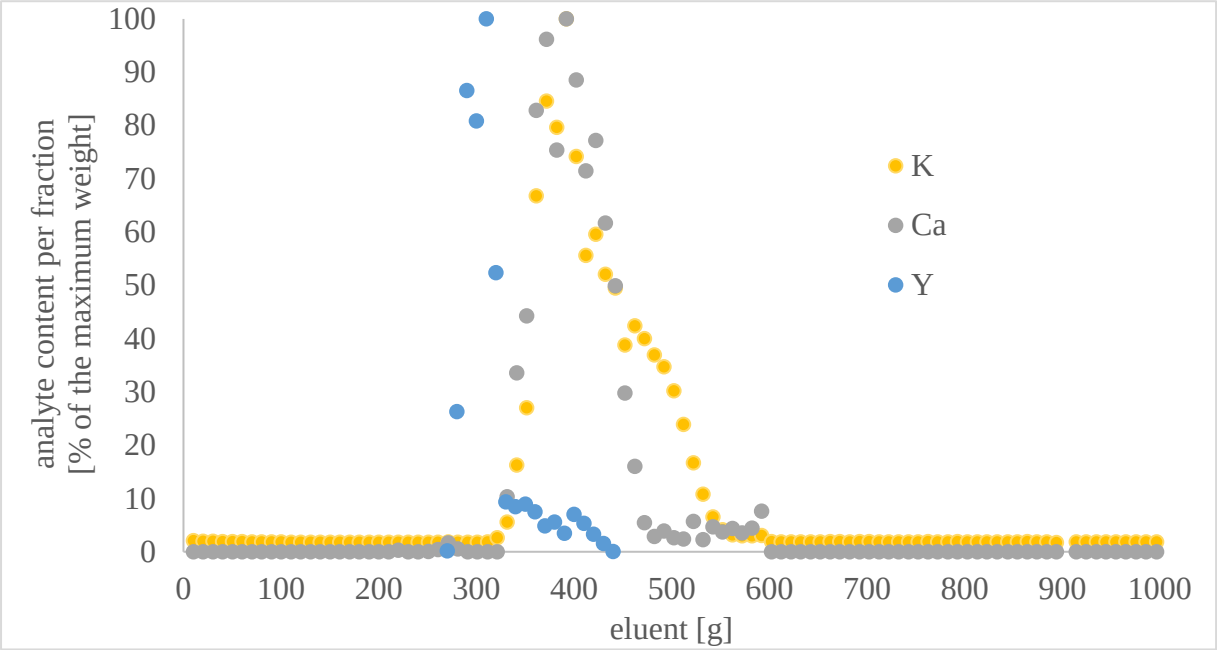

Figure 40: Elution regions of Y, Ca and K recorded with the established Dowex®50WX8 200-400 (H) resin by Serva

Figure 40 shows an older recording of the elution regions of yttrium, calcium and potassium, achieved with the established DOWEX®50WX8 200-400 (H) resin by Serva, to compare these results with the new results. These elution curves were also recorded with ICP-OES measurements, using stable tracers.

The older elution curve is not as exact as the newer one. This is because, instead of a professional standard, a self-made salt solution was used for the preparation of the ICP-OES calibration curve. Additionally, the yttrium curve was recorded separately from the calcium and potassium elution curves and there could be differences in the separations during the Hot Column Chromatography. Therefore, the edges of the elution regions for this older elution curves are less precise and tailing is present at their ends.

Table 28: Comparison between the DOWEX® 50 WX8 (200-400 mesh) by Serva and by Alfa Aesar elution regions and the concentration maxima of the analytes Y, Ca and K in milk ash

element	**Dowex®50WX8 200-400 (H) Serva**		**Dowex®50WX8 200-400 (H) Alfa Aesar**	
	elution region [g]	**maximum [g]**	**elution region [g]**	**maximum [g]**
yttrium	270-440	300-310	310-480	330-340
calcium	320-480	380-390	320-510	400-410
potassium	320-560	380-390	330-600	380-390

As is evident from table 28 and figure 40, the elution curves recorded with the DOWEX by Alfa Aesar show a shift of the elution regions to a higher eluent volume, compared to the older recording, which would make longer elution times necessary. The yttrium elution curves were shifted 30 to 40 g eluent to higher eluent volumes with the new DOWEX by Alfa Aesar. The elution regions of calcium and potassium were shifted by 10 to 20 g to higher eluent volumes and were broadened with the new DOWEX by Alfa Aesar. This resulted in a worse separation between yttrium and the interfering elements calcium and potassium than with the established column material by Serva, but it was still to an acceptable extent.

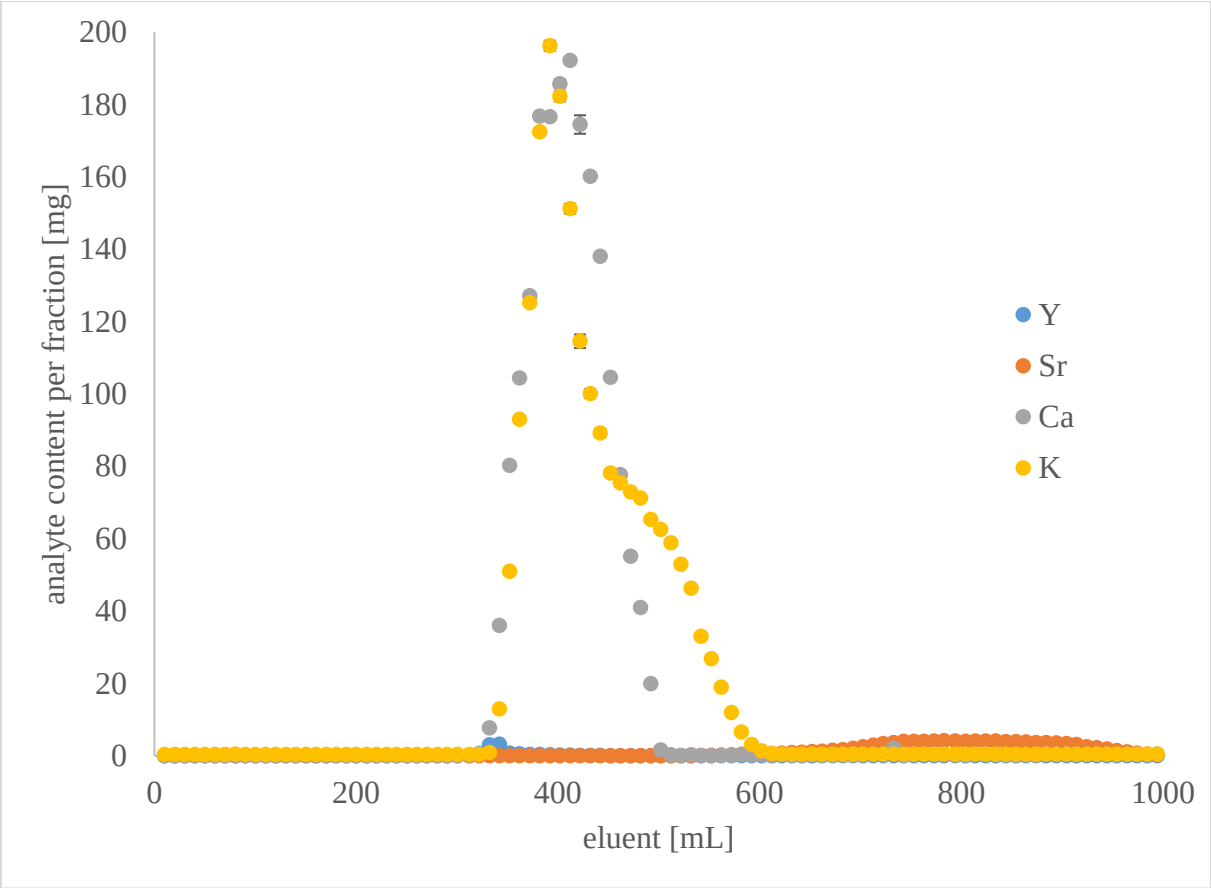

Figure 41: Absolute elution curve for the determination of K, Ca, Y and Sr in milk ash with the DOWEX® 50 WX8 (200-400 mesh) by Alfa Aesar and sample measurement with ICP-OES

For comparison, figure 41 shows the absolute results of the distribution of the different analytes during the elution process. The interfering elements calcium and potassium are present in much higher concentrations in the sample matrix than the expected amounts of the analytes yttrium and strontium, if they were present. Additionally, a significant potassium background was measured for all fractions. This could be because of the use of glassware, which contains potassium, or because of the insufficient separation performance of the column for potassium.

As a summary of the results, it was found that the new column material led to a shift of the elution regions to higher eluent volumes. The yttrium elution region was only shifted by 10 g to higher eluent volumes, but the strontium elution region was shifted by whole 40 g to higher eluent volumes and was significantly broadened. This would make longer elution times necessary.

5.3.2 DOWEX® 50 WX8 (200-400 mesh) by Alfa Aesar for the determination of ^{137}Cs in milk ash

In the following section, the determination of the elution region of ^{137}Cs, a very important interfering nuclide, with the new DOWEX® 50WX8 (200-400 mesh) by Alfa Aesar is presented. As cesium is not suitable for the measurement with ICP-OES, its elution region was determined separately with an active ^{137}Cs solution as tracer via liquid scintillation counting and gamma spectrometry.

For this process, 10 g of not contaminated milk ash was used as sample matrix and 49.98 Bq, equivalent to 9.1066 g of ^{137}Cs tracer was added. This activity was chosen as a compromise of work safety and acceptable measurement times. Then a Hot Column Chromatography was performed with ammonium-lactate at pH 7 as eluent and 100 elution fractions à 10 mL were collected. The fractions 33-43 became solid and waxy after they cooled down to room temperature, due to their high calcium content. To get rid of the precipitate, the elution fractions were heated in a water bath. But even after heating, the fractions 33 and 34 still contained solid residue. Additionally, fraction 33 showed a strong yellow coloring, which would reduce the efficiency of the measurement. As preparation for the LSC measurement, the sample solutions were mixed with 10 mL QSA scintillation cocktail and cooled. The LSC measurement was chosen for this experiment, because ^{137}Cs is a β-emitter and can be detected with this method. Additionally, the LSC measurement device QUANTULUS provides automated sample changing, which allows for a high sample throughput. The measurement could be started in the afternoon and in the morning all the samples were measured. Another advantage is the simple sample preparation for this method. Each of the 100 samples was measured for approximately 100 minutes.

The results of the LSC measurements showed, that there was a problem with overlapping emission regions between ^{137}Cs and ^{40}K, as they are both β-emitters and the energy resolution of LSC measurements is not that good. Because of the high amount of potassium in the milk sample, there was also a high amount of ^{40}K present, which caused this false positive effect. In the following, the LSC spectra of the used eluent ammonium-lactate (figure 42), a pure ^{137}Cs sample in the eluent (figure 43) and of a pure KCl sample in the eluent (figure 44) are shown. Those are pulse height spectra with the x-axis representing the energies of the recorded decays in form of channels and therefore the kind of nuclides. The y-axis shows the number of decays recoded during the measurement time, which is representative for the activity. From the spectra it is evident that ^{40}K and ^{137}Cs occupy almost the same emission region regarding the energy. The pure ^{137}Cs shows a second, significantly smaller peak, that is caused by the gamma transition of ^{137m}Ba, a short-lived decay product of ^{137}Cs, to the stable ^{137}Ba. Therefore, the presence of a second peak at this channel number indicates the presence of ^{137}Cs in the measured sample. In the pre-experiments, the count rate of ^{137}Cs was 1.18 cps/Bq and of ^{40}K was 55.55 cps/Bq.

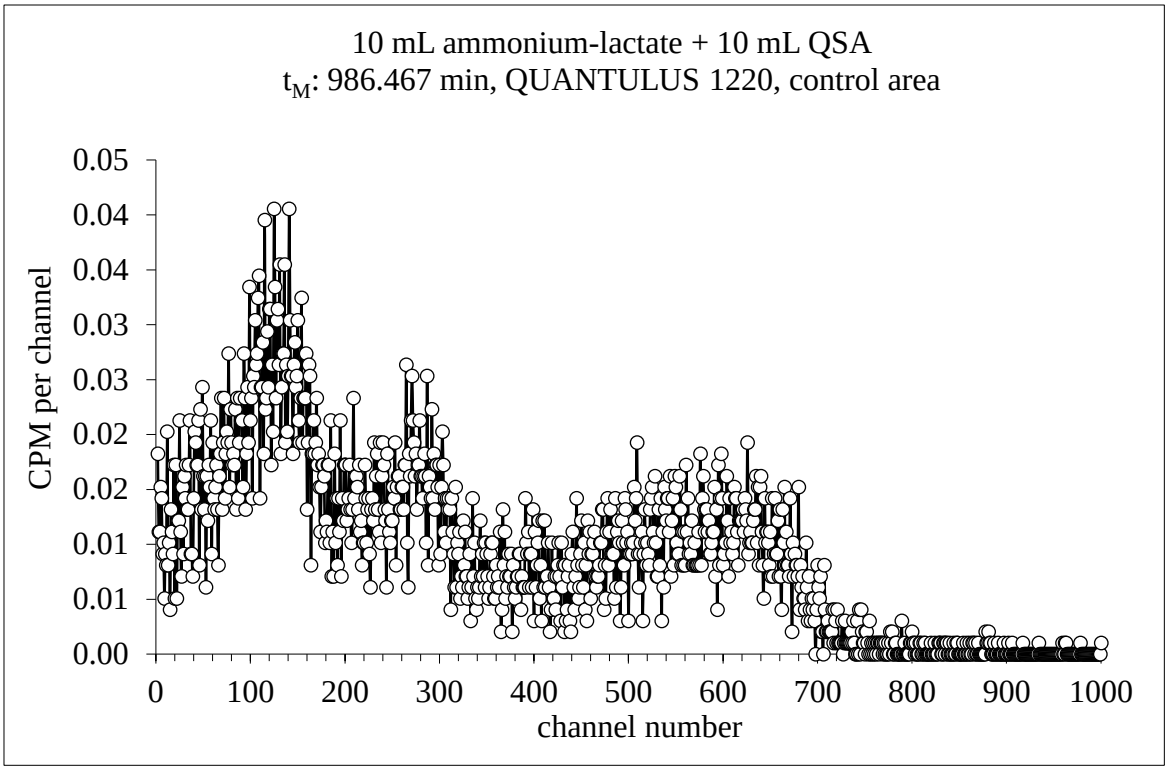

Figure 42: Background spectrum of the eluent ammonium-lactate, 10 mL + 10 mL QSA scintillation-cocktail, measurement time: 986.467 min, measured at the QUANTULUS in the control area

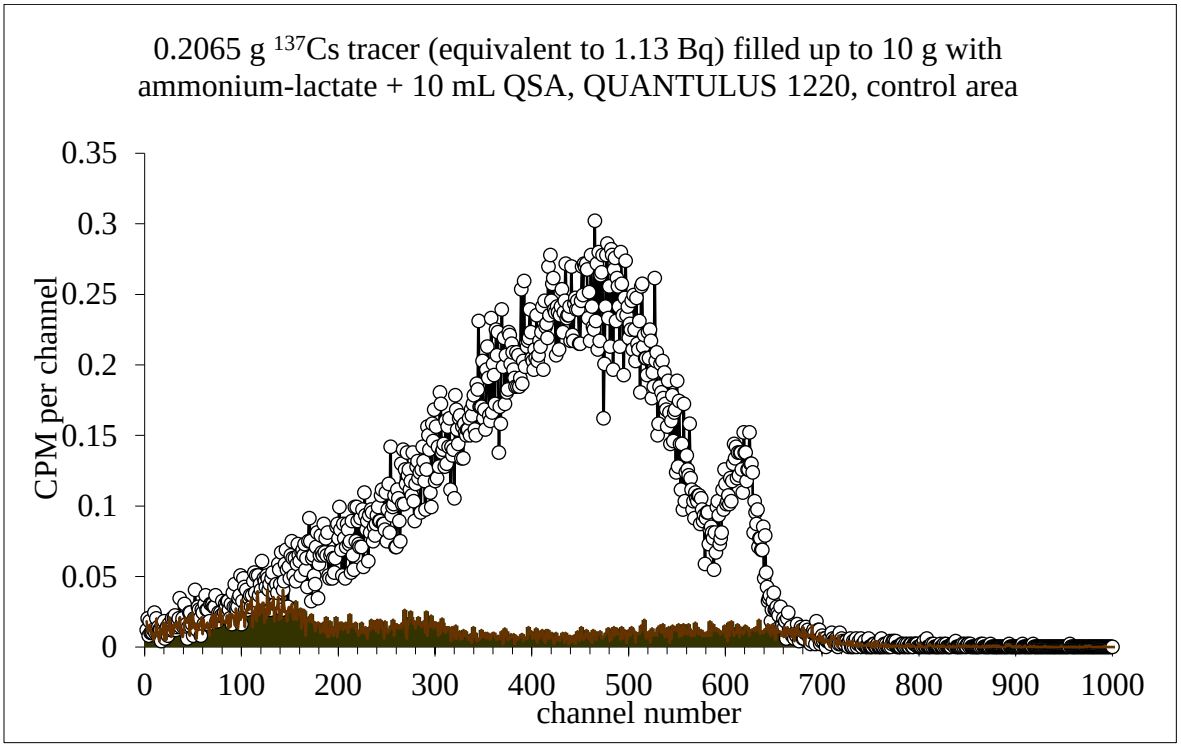

Figure 43: LSC-spectrum of the ^{137}Cs tracer, 0.2065 g ^{137}Cs- tracer (equivalent to 1.13 Bq) filled up to 10 g with the eluent ammonium lactate + 10 mL QSA scintillation-cocktail, measurement time: 493.204 min, measured at the QUANTULUS in the control area

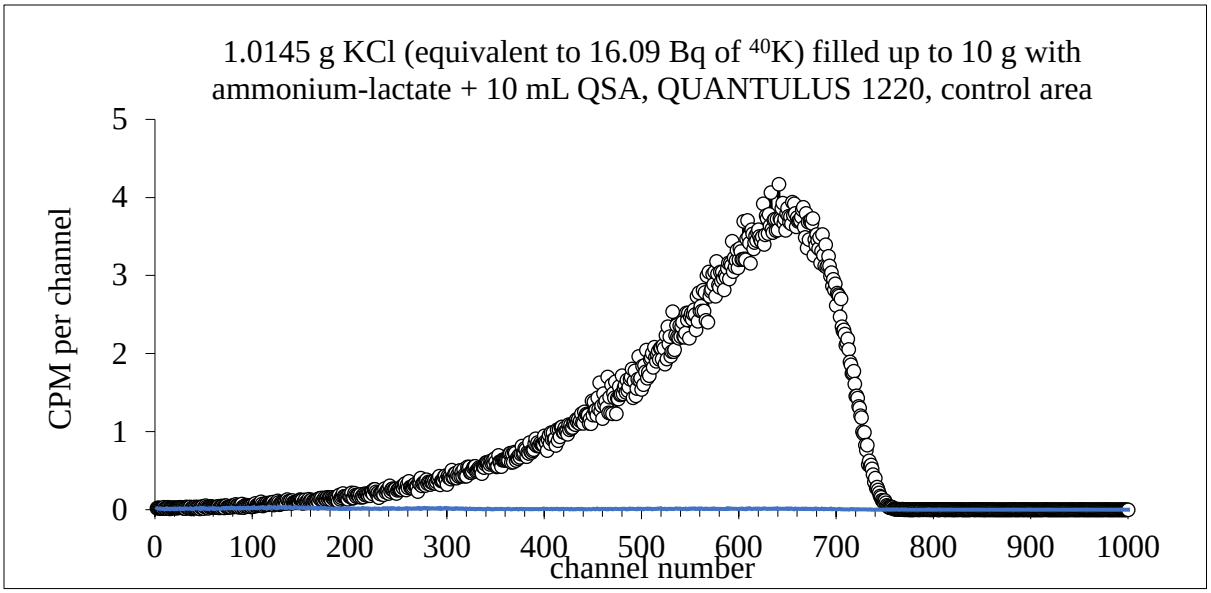

Figure 44: LSC-spectrum of potassium-chloride, 1.0145 g KCl (equivalent to 16.09 Bq) filled up to 10 g with ammonium-lactate + 10 mL QSA scintillation-cocktail, measurement time: 493.134 min, measured at the QUANTULUS in the control area

This overlap of the LSC signals of ^{40}K and ^{137}Cs led to the situation, that it could only qualitatively be differentiated if β radiation was present in the sample or not, but not whether it was emitted by ^{137}Cs or ^{40}K. From the pre-experiments, the sum count rate of ^{137}Cs and ^{40}K was determined as 56.73 cps/ Bq. The fractions 33-59 showed LSC signals, that were significantly higher than the background. Therefore, ^{137}Cs could be present in these fractions. Additionally, the second peak visible in fractions 45-56 and adumbrated in fractions 40-44 indicates the presence of ^{137}Cs in these fractions, as it is likely caused by its decay product ^{137m}Ba. All the other fractions showed signals, that were comparable to the background. In these, the presence of significant ^{137}Cs amounts could be ruled out. One example for this is the fraction 1, shown in the following figure.

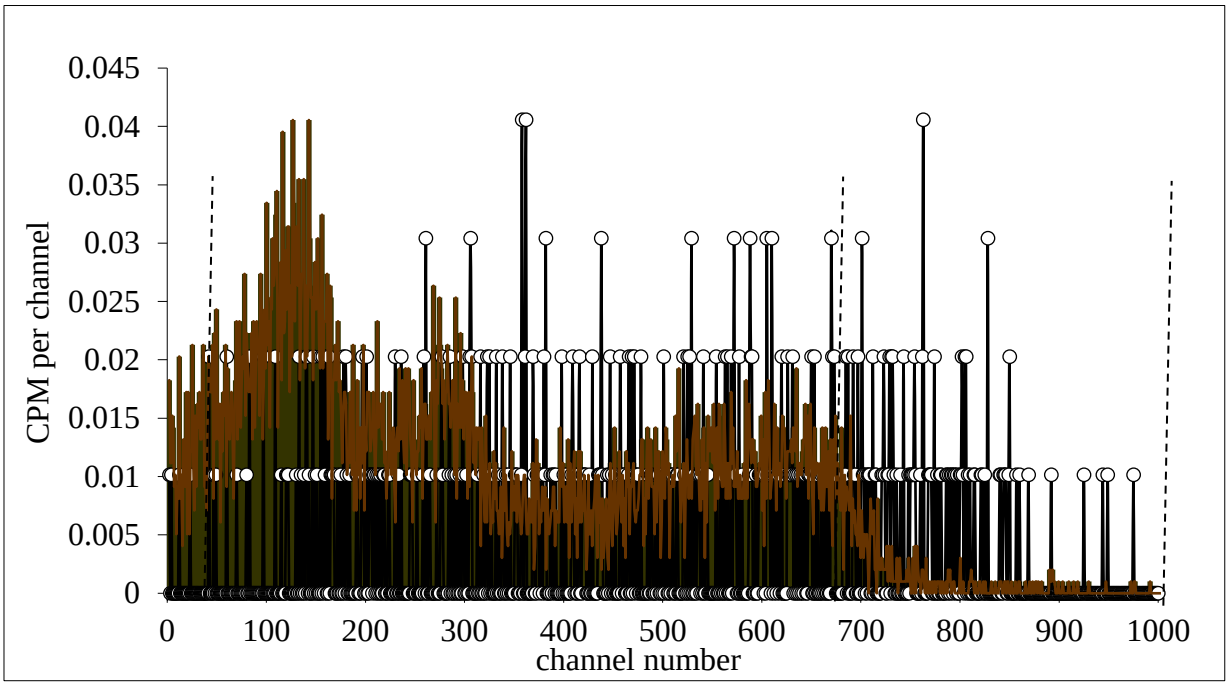

Figure 45: LSC-spectrum of fraction 1 (10 mL ammonium-lactate eluent + 10 mL QSA) in comparison to the background spectrum (see figure 42), measurement time: 98.650 min, measured at the QUANTULUS 1220 in the control area

In the following section, the LSC spectra of the fractions 33-59 are presented, for which the measured radioactivity values were significantly higher than the background. Technical problems occurred during the measurement of fraction 55 and therefore no reliable LSC spectrum is available for this fraction.

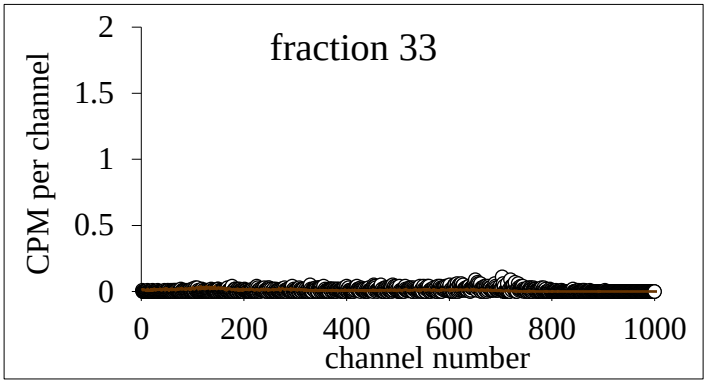

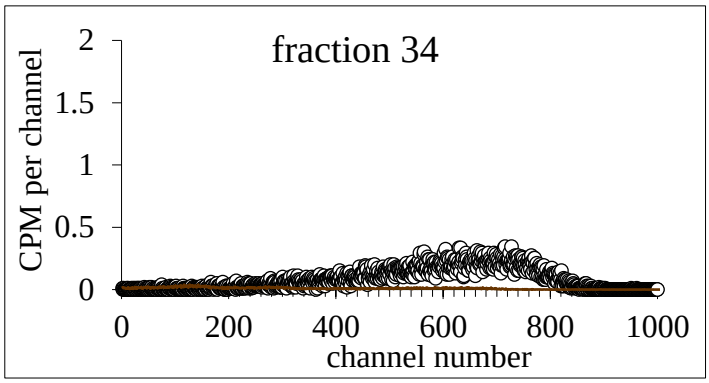

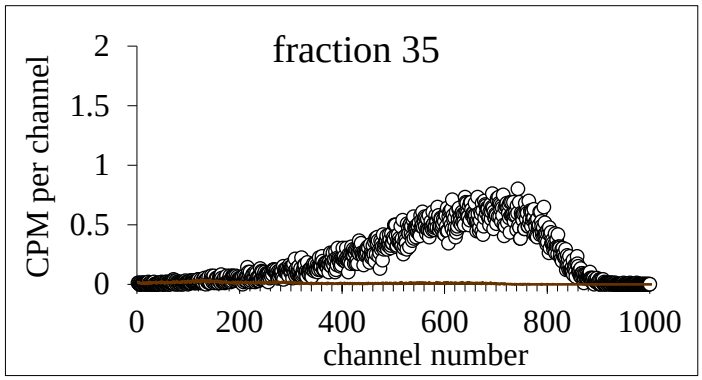

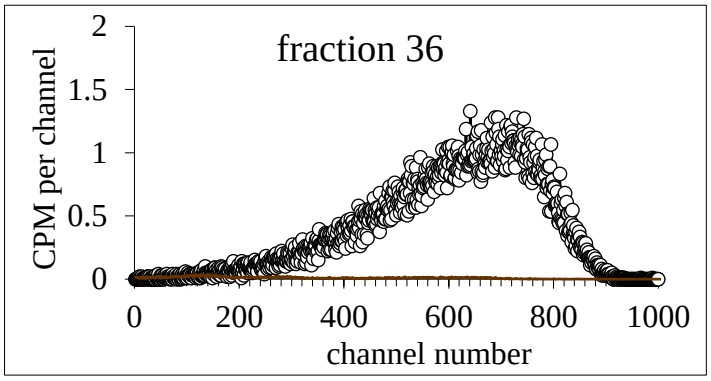

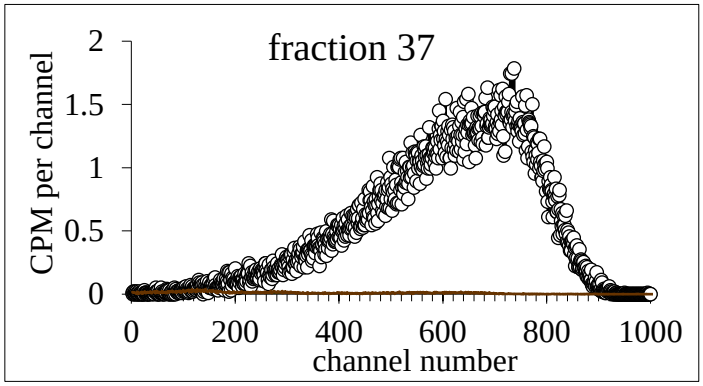

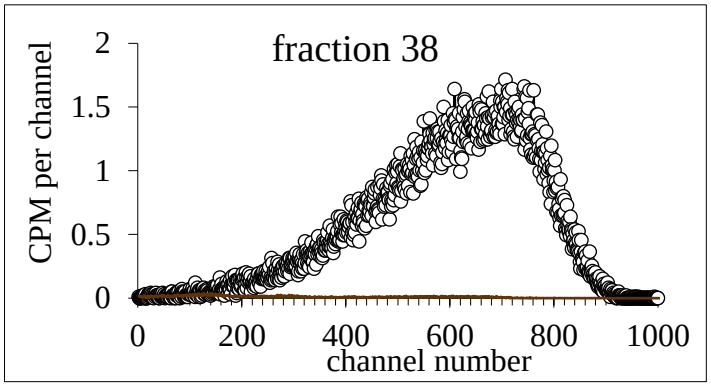

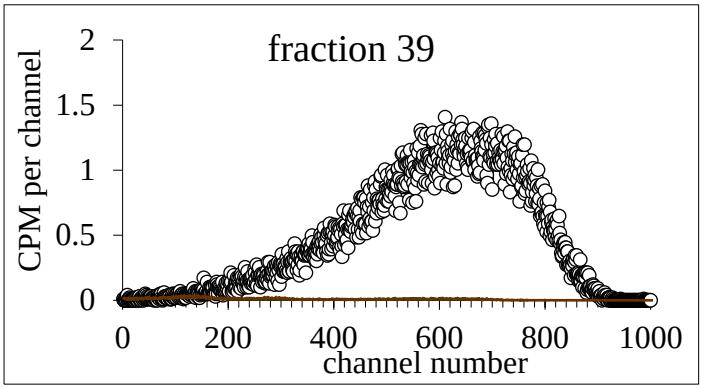

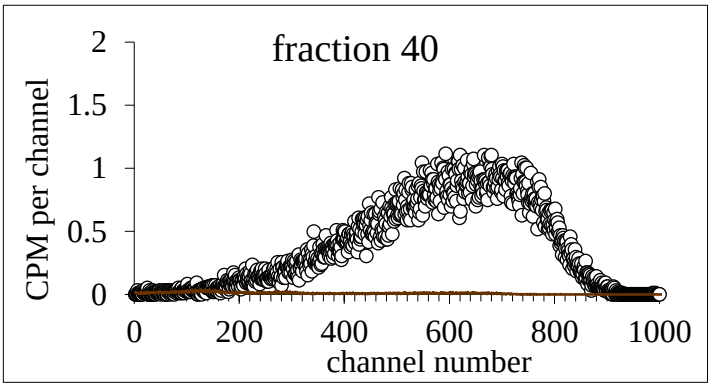

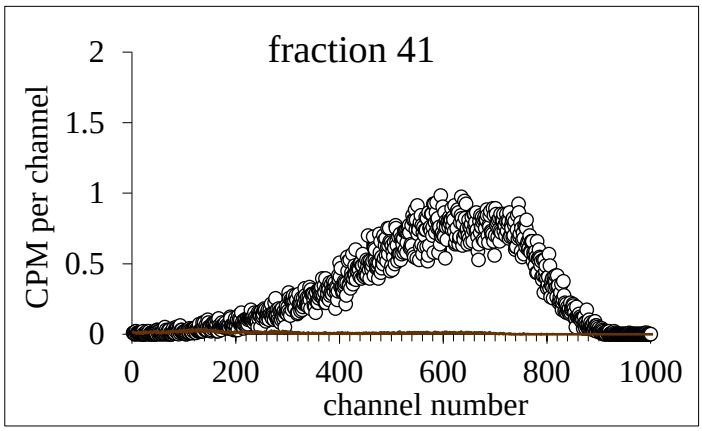
fraction 41
CPM per channel
channel number
0
0.5
1
1.5
2
0
200
400
600
800
1000

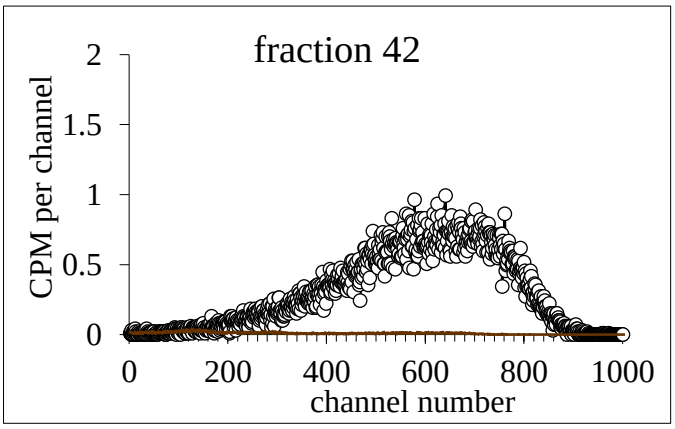
fraction 42
CPM per channel
channel number
0
0.5
1
1.5
2
0
200
400
600
800
1000

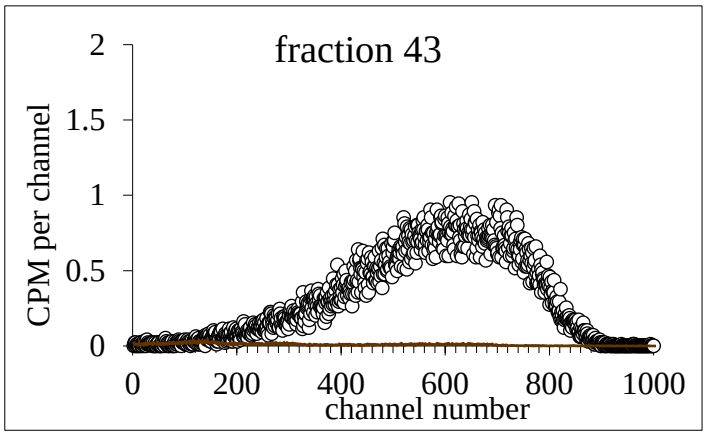
fraction 43
CPM per channel
channel number
0
0.5
1
1.5
2
0
200
400
600
800
1000

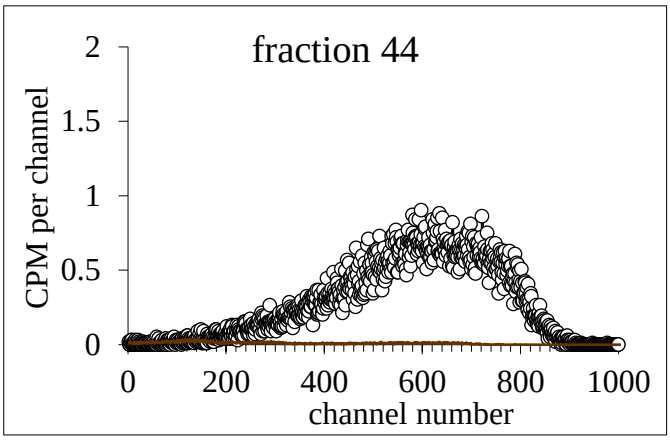
fraction 44
CPM per channel
channel number
0
0.5
1
1.5
2
0
200
400
600
800
1000

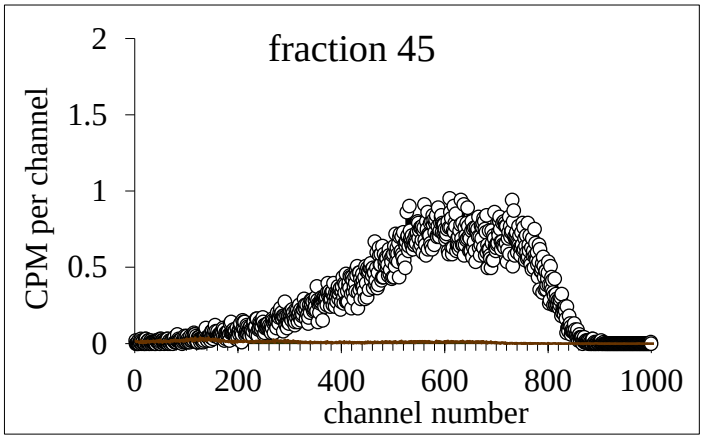
fraction 45
CPM per channel
channel number
0
0.5
1
1.5
2
0
200
400
600
800
1000

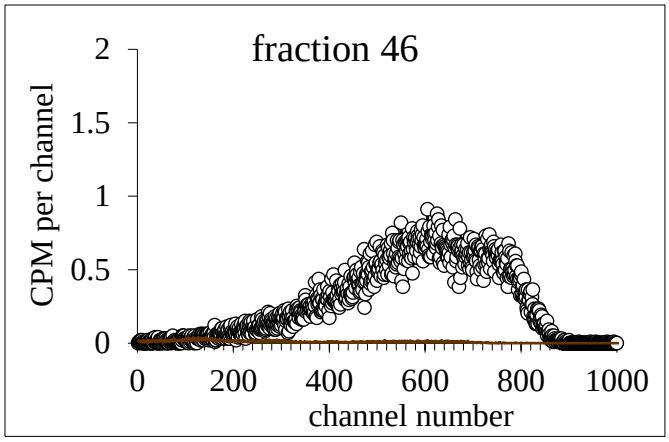
fraction 46
CPM per channel
channel number
0
0.5
1
1.5
2
0
200
400
600
800
1000

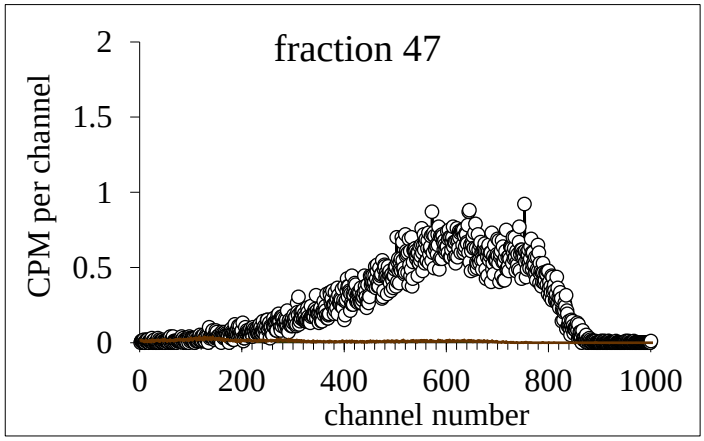
fraction 47
CPM per channel
channel number
0
0.5
1
1.5
2
0
200
400
600
800
1000

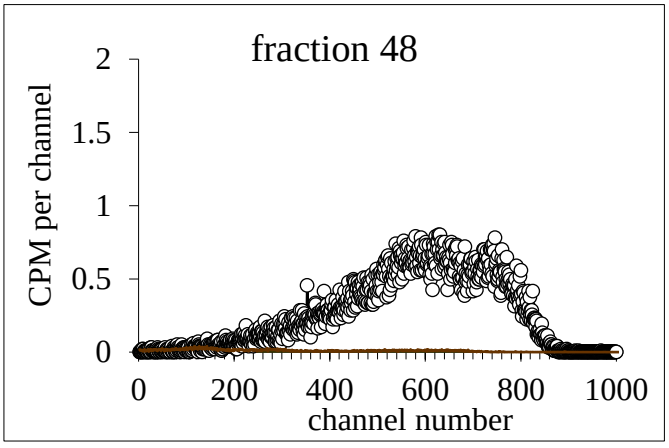
fraction 48
CPM per channel
channel number
0
0.5
1
1.5
2
0
200
400
600
800
1000

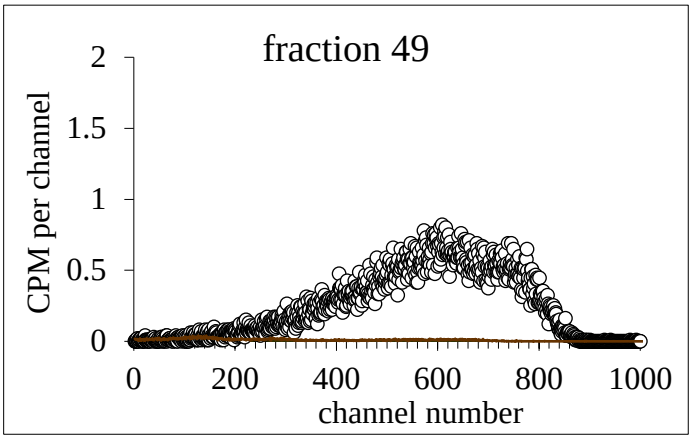
fraction 49
CPM per channel
channel number
0
0.5
1
1.5
2
0
200
400
600
800
1000

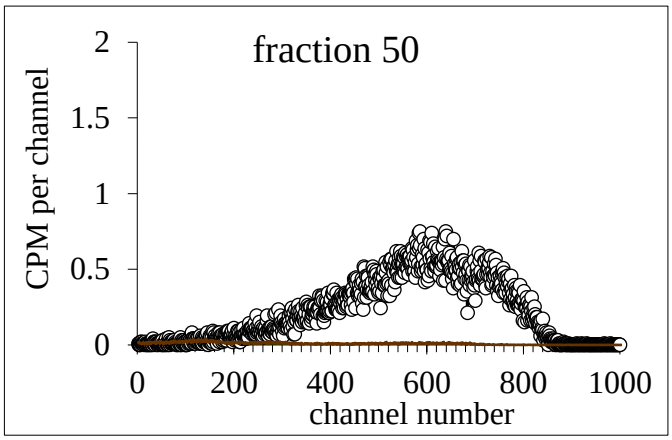
fraction 50
CPM per channel
channel number
0
0.5
1
1.5
2
0
200
400
600
800
1000

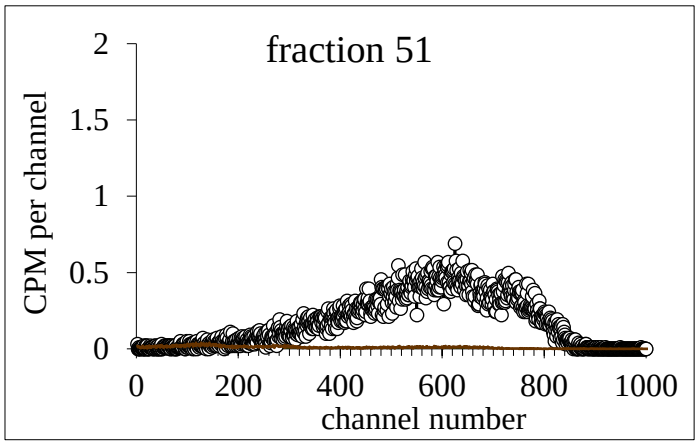
fraction 51
CPM per channel
channel number
0
0.5
1
1.5
2
0
200
400
600
800
1000

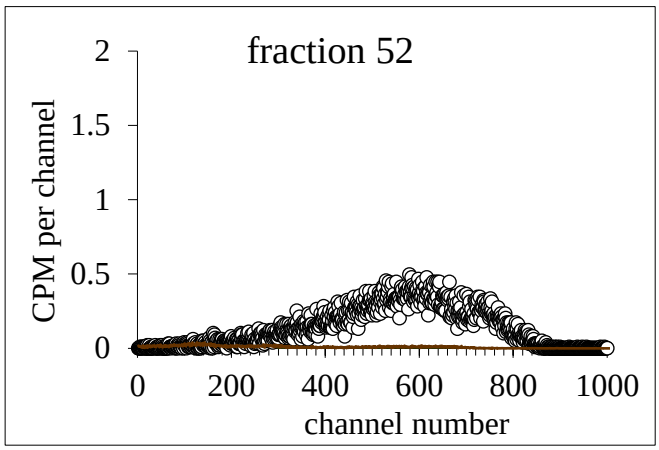
fraction 52
CPM per channel
channel number
0
0.5
1
1.5
2
0
200
400
600
800
1000

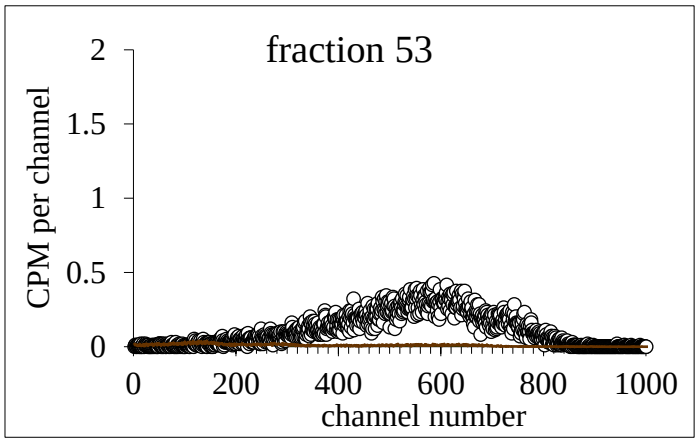
fraction 53
CPM per channel
channel number
0
0.5
1
1.5
2
0
200
400
600
800
1000

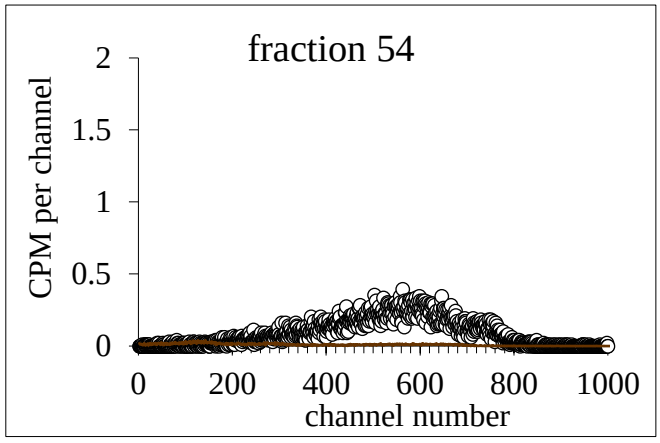
fraction 54
CPM per channel
channel number
0
0.5
1
1.5
2
0
200
400
600
800
1000

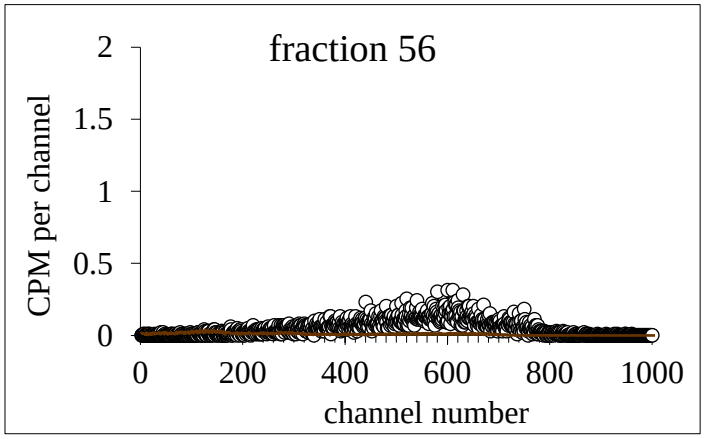
fraction 56
CPM per channel
channel number
0
0.5
1
1.5
2
0
200
400
600
800
1000

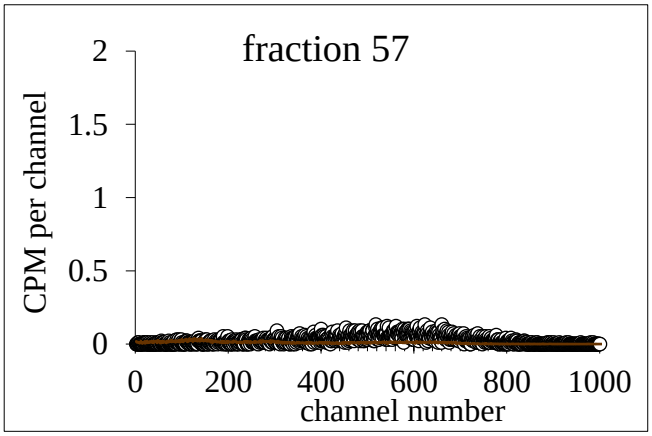
fraction 57
CPM per channel
channel number
0
0.5
1
1.5
2
0
200
400
600
800
1000

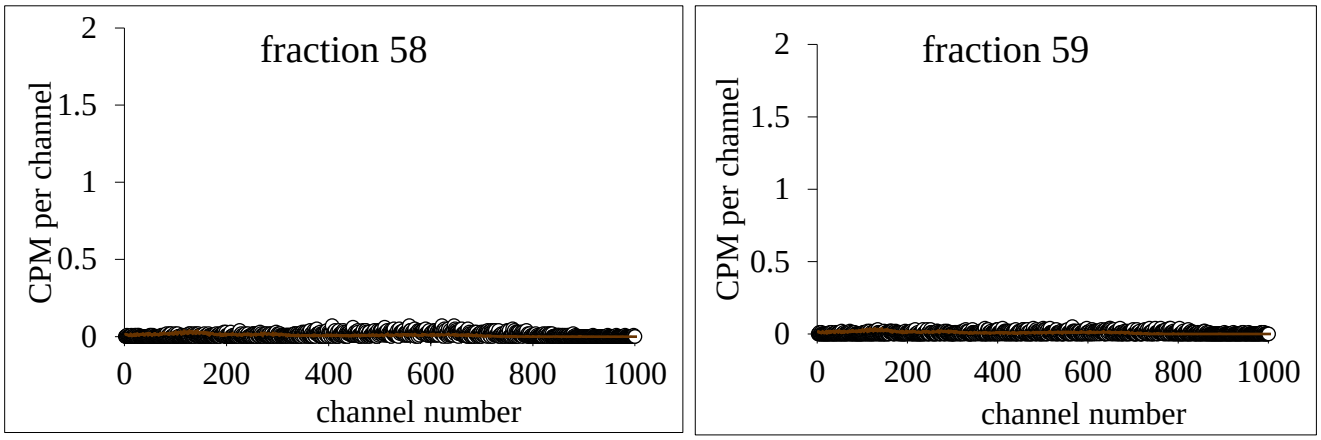

Figure 46: LSC-spectra of fractions 33-59 (10 mL ammonium-lactate eluent + 10 mL QSA) in comparison to the background spectrum (see Figure 42), measurement time: 98.6 min, measured at the QUANTULUS 1220 in the control area

The ^{137}Cs and ^{40}K emission curves in the LSC-spectra of the measured elution fractions overlapped. Because of this, it was only possible to determine whether β-radiation was present in the samples, but not, if it stemmed from ^{137}Cs or ^{40}K. To estimate the ^{137}Cs content in the elution fractions, the background values were subtracted from the measurement values, to obtain a net count rate in the region of interest.

After that, it was tried to determine the ^{137}Cs content in the elution fractions by subtracting the ^{40}K background from the measurement values. For this, the knowledge from pre-experiments (figure 43 and 44) was used, that the ^{137}Cs signal was present in the channels 50-680 and the ^{40}K signal was present in the wider channel range of 50-760. Therefore, all the counts above the background in channels higher than 680, which were measured in the elution fractions, could be attributed to ^{40}K. Based on the LSC pre-measurement, which was performed only with KCl solved in the eluent ammonium-lactate (figure 44), the ratio of the ^{40}K count rate in the cannels 50-680 to the ^{40}K count rate above channel 680 was calculated. With this ratio, the sum of the count rates in the channels above 680, which was caused exclusively by background radiation and ^{40}K radiation, was multiplied for each elution fraction. The aim of this was to determine the count rate in the ROI of channels 50-680, which could be traced back to ^{40}K. This count rate would be subtracted from the total count rate to determine the ^{137}Cs count rate in the sample. When it was tried to practically apply this method, the calculated ^{40}K count rate in the ROI of channels 50-680 was in all cases higher than the total count rate in this ROI. The subtraction would lead to negative ^{137}Cs count rates, which would not make sense. The reason for this might be, that the calculations were performed with count rates and not just with counts. But this was necessary, as the measurement time of the KCl pre-measurement was much longer than the measurement times for each individual fraction sample. Therefore, the recorded counts were not comparable. Additionally, it is not known if the shape of the emission spectrum of ^{40}K or its count distribution are stable or representative enough, to make conclusions about spectra of other samples based on this data. Especially in this case, when the samples contained a completely different amount of ^{40}K than the pre-sample. They also contained an additional radioactive nuclide, ^{137}Cs with an overlapping emission region with ^{40}K, which could have influenced the shape of the emission spectrum of ^{40}K.

Another attempt to fit the ^{40}K emission spectrum, to predict the ^{40}K background of a measurement, was with a Gaussfit.

$$fit\ value = Y_0 \cdot e^{\frac{-(CHN-CHN0)^2}{\sigma^2}} \tag{5.8}$$

The fit value depends on the channel number CHN, which represents the emission energy. It is also influenced by the parameters CHNO, which represents the channel number at the count maximum of the emission curve, Y_0, representing the maximum count number, and σ, representing the curve width. These parameters were manually selected and optimized by the operator, based on a measured emission curve, which was to be fitted.

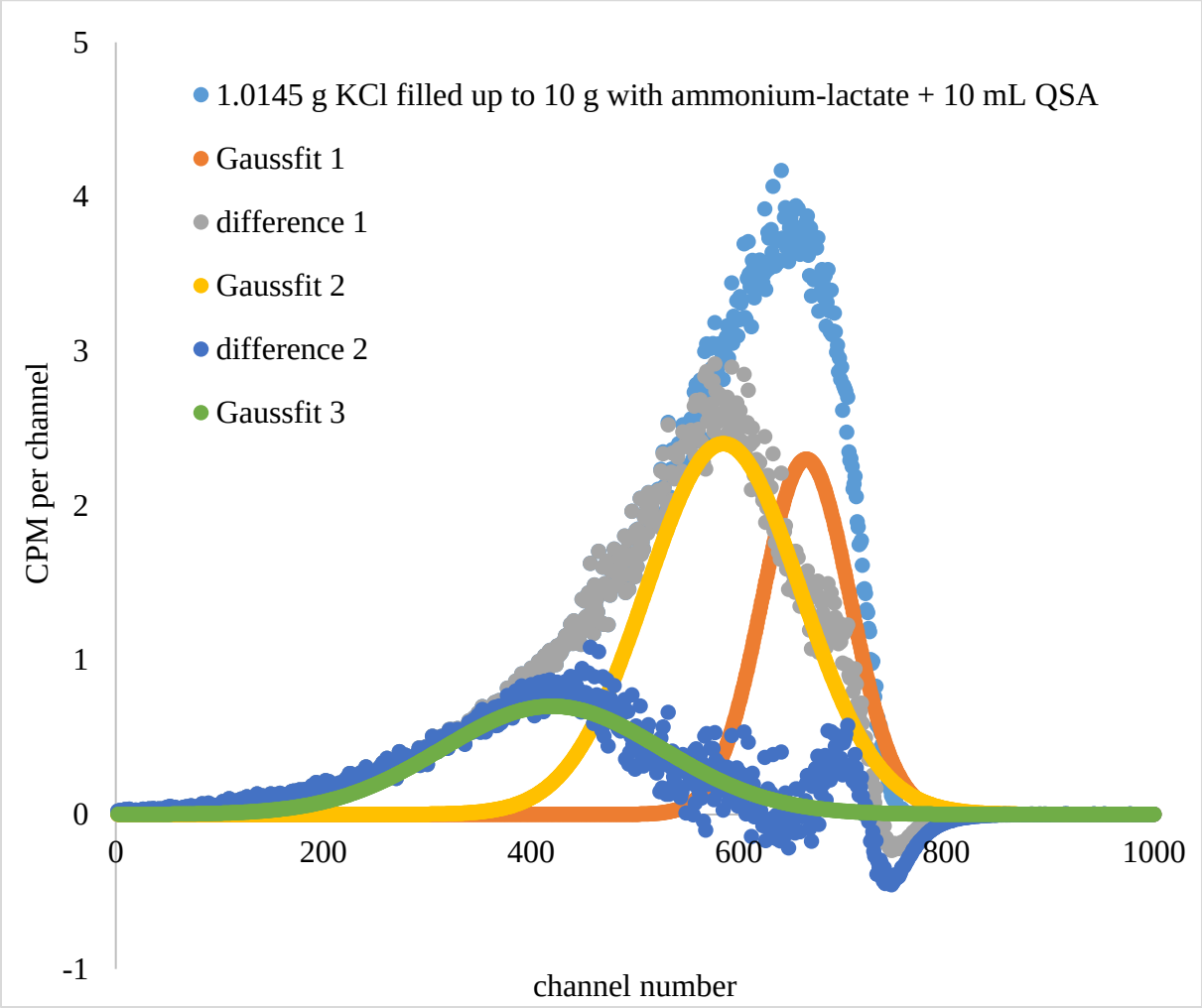

Figure 47: ^{40}K emission curve and its fit based on three Gauss curves and the respective differences between fit and real measured values

The LSC-spectrum of ^{40}K was fitted with three Gauss curves, as depicted in figure 47. Three Gauss fits were necessary, due to the asymmetrical form of the ^{40}K emission curve. First the emission curve made up of real measured data was fitted with a Gauss curve. For the fit, the value of the channel number at the count maximum was entered for the parameter CHNO, the count maximum of the emission curve was entered for the parameter Y_0 and the curve width was entered for the parameter σ. With these parameters, it was possible to calculate one Gauss value for each channel number, and therefore emission energy, to approximate the ^{40}K count rate. After the Gauss curve was calculated, the difference between the real emission curve and

the fitted Gauss curve was calculated. This difference curve was in turn fitted with a Gauss curve, based on the same principle as for the emission curve. Of this first difference curve and its fit, another difference curve was calculated. This second difference curve was again fitted with a Gauss curve (see figure 47). The values of these three Gauss curves were added to each other and resulted in a total fit curve for the ^{40}K LSC emission curve. Then the parameters of the three Gauss curves were adjusted and optimized in a way, that would make the difference between the real measured values for the ^{40}K emission curve and its total Gaussfit as small as possible. The optimized parameters are presented in table 29. The final result of the fit procedure is presented in figure 48.

Table 29: Parameter values for the Gaussfits for the approximation of the ^{40}K LSC spectrum

	CHN0	**Y_0**	**σ**
Gaussfit 1	665	2.3	60
Gaussfit 2	585	2.4	105
Gaussfit 3	420	0.7	150

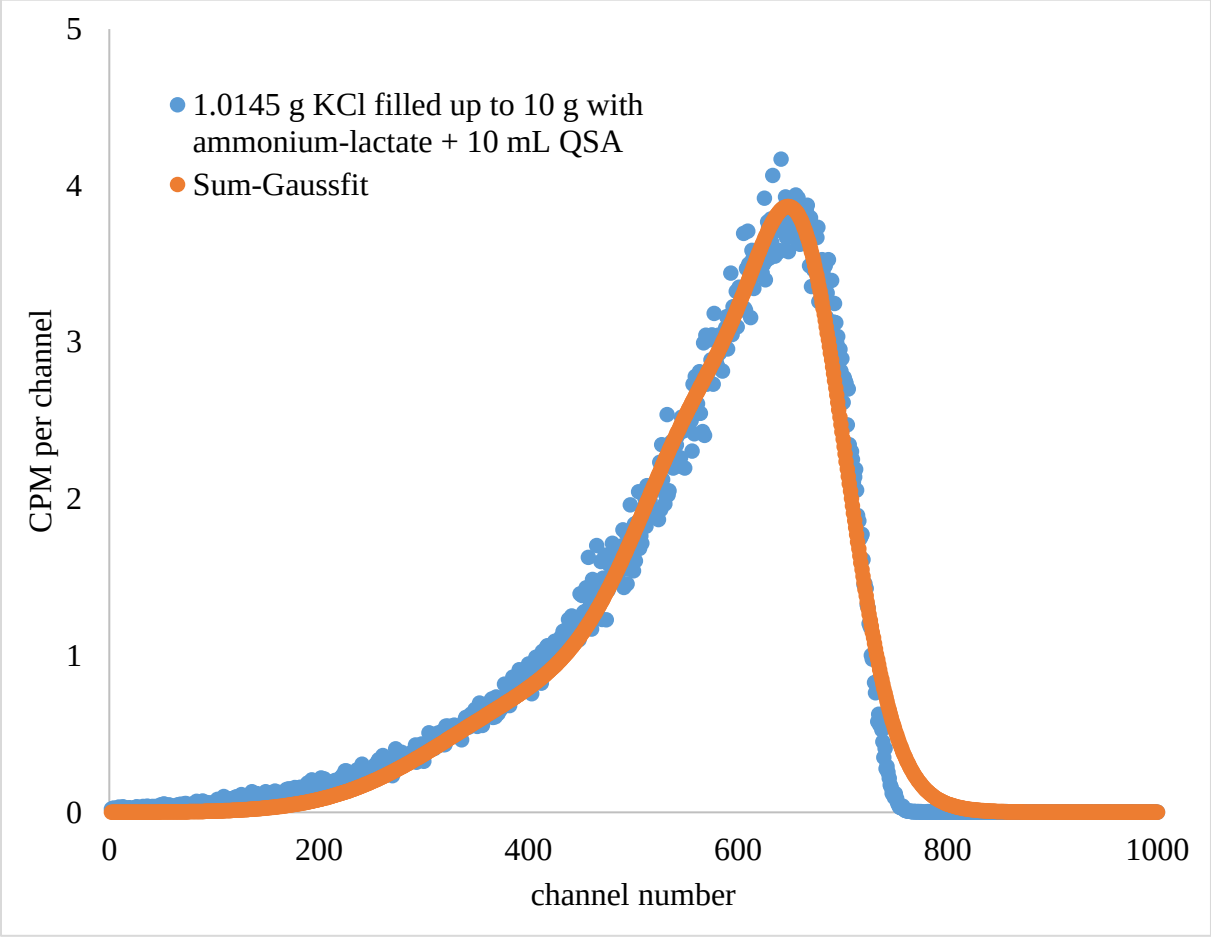

Figure 48: LSC spectrum of potassium-chloride, 1.0145 g KCl (equivalent to 16.09 Bq) filled up to 10 g with ammonium-lactate (eluent) + 10 mL QSA scintillation-cocktail, measurement time: 493.134 min, measured at the QUANTULUS 1220 in the control area with a sum Gaussfit for the approximation of the measured values

Unfortunately, this fit was also not universally transferable to other ^{40}K measurement data. The parameter Y_0, the count maximum, is strongly dependent on the content of ^{40}K in the sample and varies from sample to sample. The elution fraction samples had a significantly lower ^{40}K content than the pre-sample. This content could not be determined in advance to the LSC measurement, as this measurement was intended to be the content determination tool.

Therefore, Y_0 could not be reasonably defined for the samples and thus, the Gaussfit could not be applied.

To, at least qualitatively, determine in which samples ^{137}Cs was present, the fractions 33-59, which showed a signal above the background in the LSC measurements, were additionally measured with the gamma spectrometer GEM40 for 900 s per sample. This was possible because ^{40}K and ^{137}Cs are also indirect gamma-emitters, in addition to being beta-emitters. Because gamma spectrometry has a better energy resolution than LSC, a differentiation between a ^{137}Cs and a ^{40}K signal was possible with this measurement method. As the added ^{137}Cs tracer was not measured preemptively to the separation, it could not be used as a 100 % sample. But the added activity could be determined with the ^{137}Cs pre-measurement. The 500 mL kautex tracer container was measured as a whole in the gamma spectrometer GEM4 for 1,400 s, to achieve a count number of at least 10,000 in the relevant emission region. The measurement data was processed with a file specialized for the analysis of ^{137}Cs samples, taking into account the detector, the measurement geometry and the tracer mass. As result, the specific activity of 5.49 ± 0.075 Bq/g was obtained. The goal of the tracing was to add 50 Bq of ^{137}Cs to the ash sample. In reality 9.1066 g, equivalent to 49.98 Bq, tracer were added as 100 % sample.

The measured count rates for ^{137}Cs and ^{40}K could be considered qualitatively and from those values the elution region of ^{137}Cs was determined. As the distribution of the analyte and its content values relative to each other were relevant for the elution regions, and not the absolute activity values in each fraction, the measured data was sufficient for its determination. The resulting elution region of cesium was then compared to the cesium elution regions of earlier measurements, for which the established DOWEX by Serva was used.

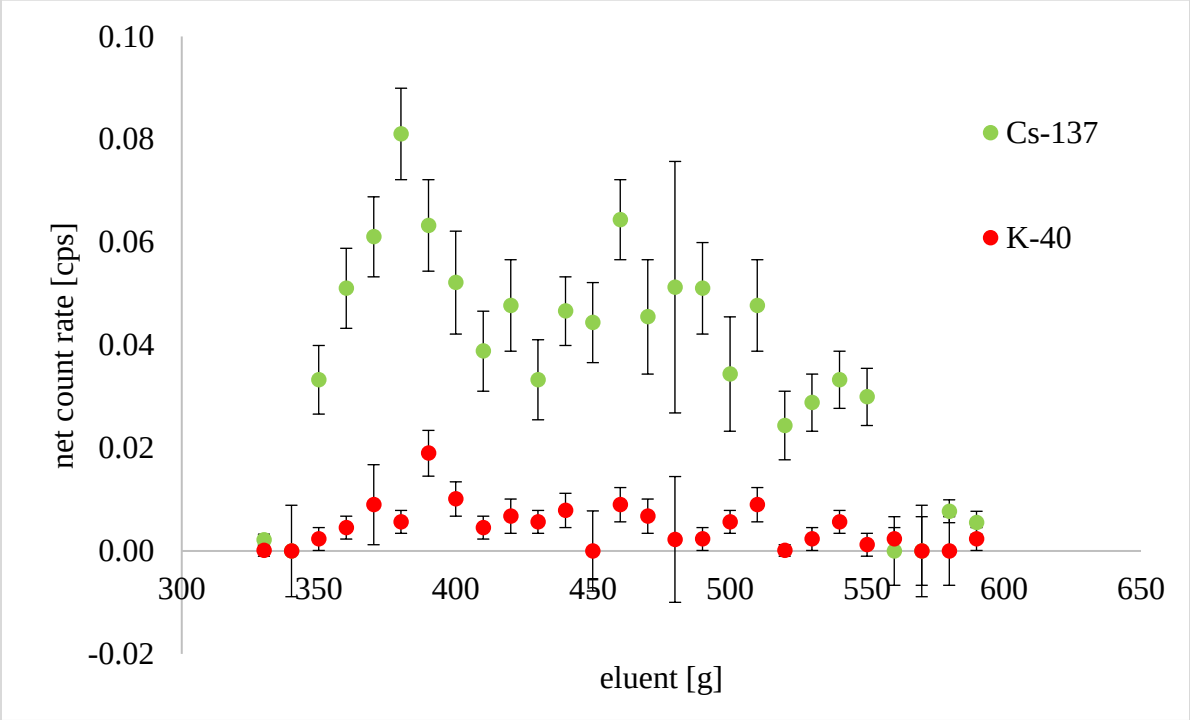

Figure 49: Elution curve of milk ash + 49.98 Bq ^{137}Cs, DOWEX by Alfa Aesar, fraction 33-59

Figure 49 shows that ^{137}Cs was significantly present in the elution region of 340 to 550 g eluent and showed net count rates of 0.0244 cps to 0.0811 cps. The values for ^{40}K were consistently

lower in this region of interest. This could be due to the significantly lower physical efficiency of this method compared to LSC with the QUANTULUS, especially as it varies strongly with the emission energy. The higher the emission energy, the lower the physical efficiency. And the emission energy of ^{40}K is significantly higher than for ^{137}Cs.

From this distribution data and the known activity of the added ^{137}Cs tracer the ^{137}Cs activity in each fraction could be calculated, if it was assumed that all of the added cesium was separated from the column and eluted just in this elution region. For this the net count rates shown in figure 49 were summed up and considered as 100 % count rate, corresponding to the added activity of 49.98 Bq ^{137}Cs. Then the count rates for the individual fractions were divided by this 100 % count rate value and multiplied with the 49.98 Bq to obtain the activities of each fraction. But as the region of interest is about the relative distribution of the analyte, the unit in which this distribution is presented is not relevant, as long as it is proportional to its quantity. So the count rates in figure 49 are completely sufficient to represent the distribution of ^{137}Cs during the Hot Column Chromatography and its elution region.

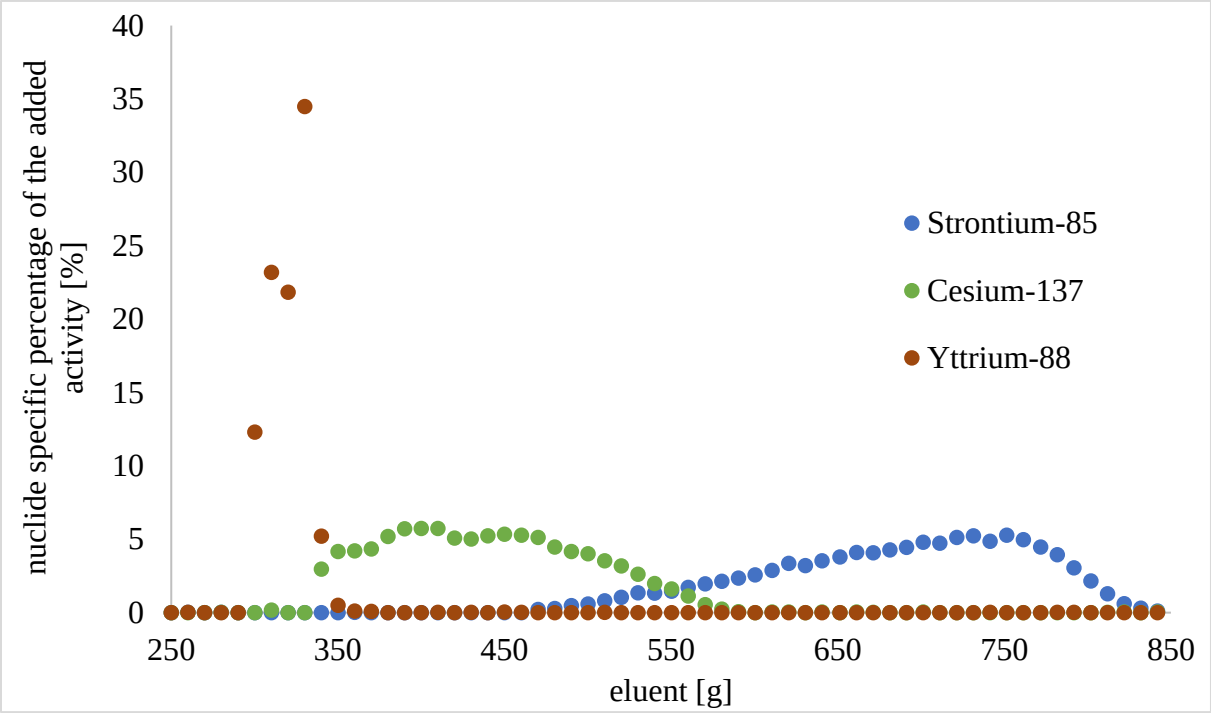

Figure 50: Elution curve milk ash + 7.530 g multi-nuclide tracer, DOWEX by Serva, fraction 25-84, elution region of Y, Sr, Cs

In comparison to this new elution curve, the elution region of ^{137}Cs, achieved with the established DOWEX by Serva, as shown in figure 50, is at 330-570 g eluent. The declining slope of the curve is additionally much flatter, as seen in figure 50. This shows that the elution region of cesium achieved with the DOWEX by Alfa Aesar is in the range of the cesium elution region achieved with the established DOWEX. Additionally, the new elution region is 30 g eluent narrower than the older one, which would cause a better separation between the interfering nuclide ^{137}Cs and the analytes ^{90}Y and ^{90}Sr.

5.3.3 Elution acceleration by eluent change to six molar hydrochloric acid

The Hot Column Chromatography separation with the new DOWEX® 50 WX8 (200-400 mesh) by Alfa Aesar resulted in the strontium elution region being shifted by 40 g to higher eluent volumes and being significantly broadened, compared to the elution region of strontium achieved with the DOWEX® 50 WX8 (200-400 mesh) by Serva. This makes longer elution times necessary. To maintain the efficiency of the separation method, an acceleration of the elution was wanted. This could be achieved through a change of the eluent from ammonium-lactate to 6 M hydrochloric acid, as 6 M hydrochloric acid is already used to regenerate the column and remove any remaining ions in a relatively short amount of time. The eluent change was planned to be performed as soon as the strontium elution fraction began and the other analytes and interfering substances were already removed from the column. With this set up, the elution curve could be optimized due to the good separation with ammonium lactate and the fast elution with 6 M hydrochloric acid.

As standard sample matrix, 10.00 g not contaminated milk ash, prepared from commercially available whole long-life milk by the brand Berchtesgadener Land, was used. It was solved in the usual 1:1 mixture of 6 M hydrochloric acid and 1.5 M lactic acid. Additionally, 2 mL stable strontium tracer, containing in total 100 mg Sr, was added. Potassium and calcium were naturally present in the sample matrix in significant amounts, according to the milk packaging 124 mg calcium per 100 mL. After the sample was solved and applied to the column, the Hot Column Chromatography was performed at the elution speed of 2.5 mL/min. Up until the fraction 620, ammonium-lactate at pH7 was used as eluent. During the elution of fraction 620, after the prepared sample solution and approximately 530 g of ammonium-lactate eluent have passed the column, the eluent was changed to 6 M hydrochloric acid.

During the elution 100 fractions à 10 ml were collected. For the ICP-OES measurement, the fraction samples were diluted 1:250. Per ICP-OES sample, 40 µL of the fractions were used and 2 mL concentrated nitric acid was added for pH adjusting. The samples were filled up to a volume of 10 mL with bid water.

For the ICP-OES measurement, the same calibration curve was used as the one calculated for the initial determination of the elution curve with the new DOWEX® 50 WX8 (200-400 mesh) by Alfa Aesar in section 5.3.1.

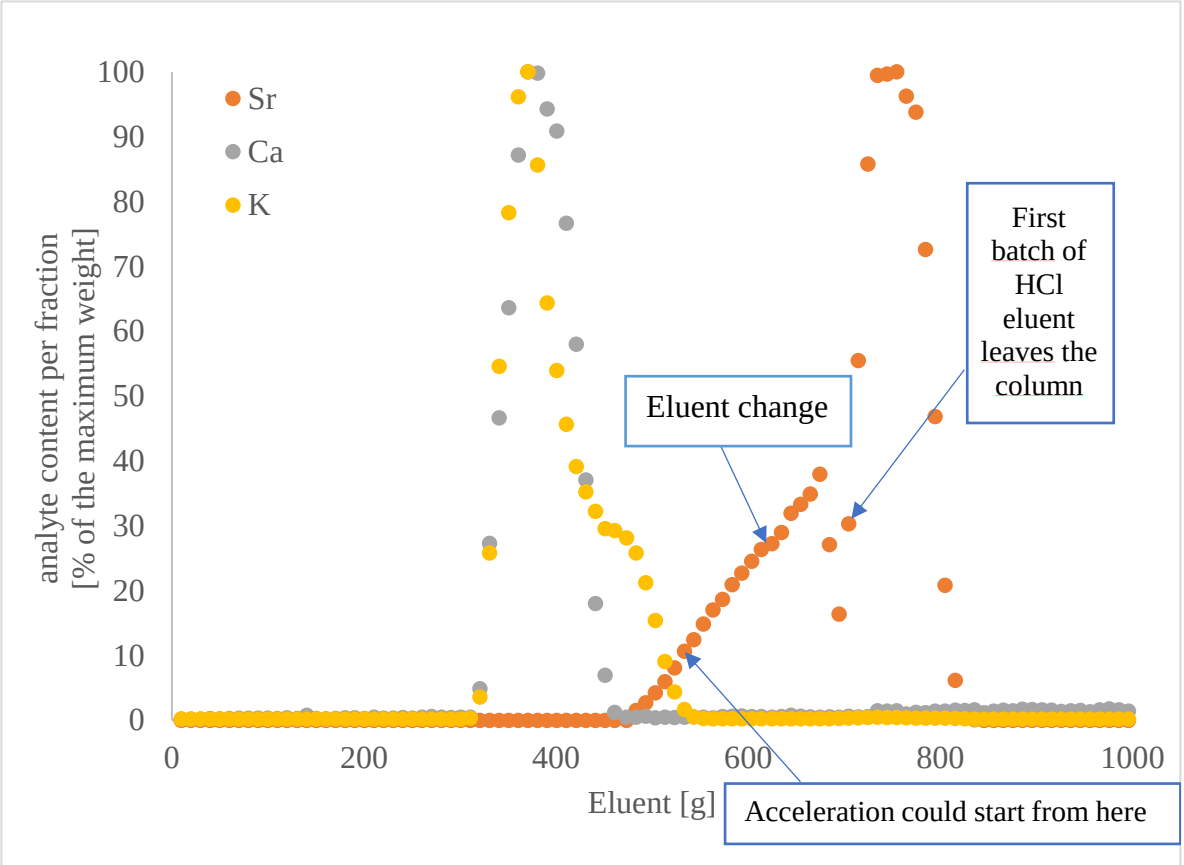

Figure 51: Relative elution curve for the determination of K, Ca and Sr in milk ash with the DOWEX® 50 WX8 (200-400 mesh) by Alfa Aesar and sample measurement with ICP-OES. effect of the eluent change from ammonium-lactate at pH7 to 6 molar hydrochloric acid on the elution curve of strontium

Figure 51 shows the effect of the eluent change on the elution curve of strontium. First, the concentration slope stayed constant, as the rest of the ammonium-lactate, that was still present in the column, was eluted. After five fractions, a strong decrease in the Sr content from the fraction 68 onwards could be observed, until it significantly increased again in fraction 70. This indicates that the decrease was due to a mixture of 6 molar hydrochloric acid and ammonium-lactate and fraction 70 was the first fraction with mainly hydrochloric acid as eluent. This new eluent accelerated the elution and increased the strontium content in this sample. After that, a steep elution “peak” could be observed, that ended with fraction 81, approximating the end of the elution region of strontium that was achieved with the established DOWEX® 50 WX8 (200-400 mesh) by Serva. So, the acceleration of the elution with the new batch of column material with hydrochloric acid as eluent was successful. This effect could be increased by implementing the eluent change sooner. It was initially planned to perform it after fraction 50, as soon as Sr was separated from the interfering elements, but ammonium-lactate was still present in the column reservoir and had to be removed from the column before an eluent change could be performed. With a sooner eluent change, an even faster strontium elution than for the established DOWEX could be achieved.

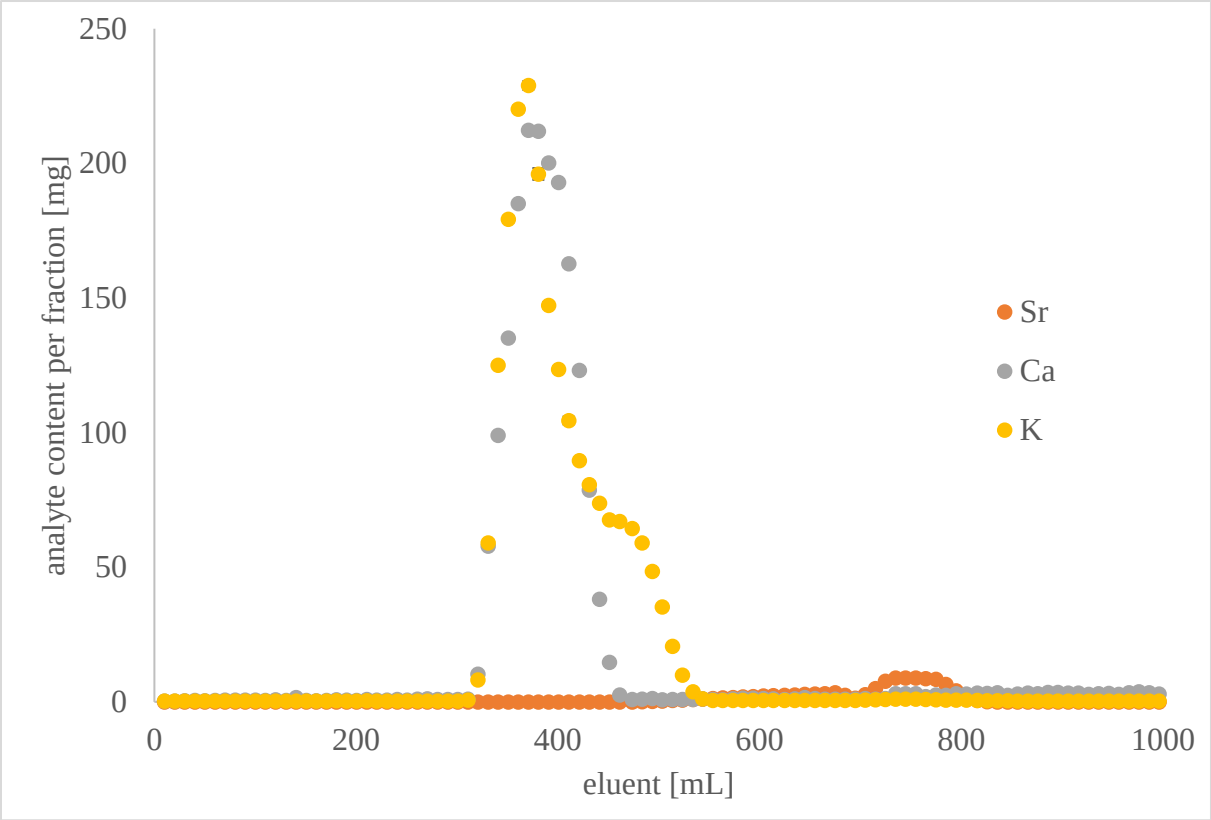

Figure 52: Absolute elution curve for the determination of K, Ca and Sr in milk ash with the DOWEX® 50 WX8 (200-400 mesh) by Alfa Aesar and sample measurement with ICP-OES. Effect of the eluent change from ammonium-lactate at pH7 to 6 molar hydrochloric acid on the elution curve of strontium

For comparison, figure 52 shows the absolute results of the distribution of the different analytes during the elution process and its acceleration. The interfering elements calcium and potassium were present in much higher concentrations in the sample matrix than the added strontium. The amount of strontium tracer represents the expected amounts of the analyte strontium, if it was present in a real sample. So, the strontium amount in a real milk sample, if present at all, would be significantly exceeded by the interfering elements potassium and calcium. Additionally, a significant potassium background was measured for all the fractions. This could be because of the use of glassware, which contains potassium, or because of the insufficient separation performance of the column for potassium.

5.3.4 Precipitation of $SrSO_4$ in ammonium-lactate-hydrochloric acid mixtures

As the elution region of strontium was broadened and shifted to higher volumes with the new DOWEX® 50 WX8 (200-400 mesh) by Alfa Aesar, an acceleration of the strontium elution was needed, to prevent this separation method from becoming even more laborious and time intensive than it already is. An acceleration of the strontium elution was made possible through an eluent change from ammonium-lactate at pH7 to 6 M hydrochloric acid.

After the separation with the Hot Column Chromatography, the strontium is precipitated as $SrSO_4$ (strontium sulfate) and separated through filtration as described in section 5.4.1.

As the eluent was changed from ammonium-lactate at pH7 to 6 M hydrochloric acid, it had to be made sure that this precipitation worked as well and as efficient in 6 molar hydrochloric acid as in ammonium-lactate at pH7 and in the mixtures of these eluents. The eluent change could only be implemented in routine analytics if it had no negative influence on the precipitation of $SrSO_4$. If this is the case is explored in the following section.

The steps of the precipitation experiment are based on the analysis steps of the sample after the separation, according to the analysis instruction [63]. First, the samples for the experiment were prepared from different mixing ratios of ammonium-lactate at pH7 and 6 M hydrochloric acid. Each sample had a total mass of 200 g. To each sample 1 mL of a 50 mg Sr/mL Sr-tracer was added, as it is usually added to each real sample before the analysis starts. The sample preparation is presented in table 30.

Table 30: Sample preparation for the precipitation experiment of Sr as $SrSO_4$ in different mixing ratios of ammonium-lactate at ph7 and 6 M hydrochloric acid

sample number	1	2	3	4	5
ratio ammonium-lactate: hydrochloric acid	100:0	75:25	50:50	25:75	0:100
ammonium-lactate [g]	200	150	100	50	0
hydrochloric acid [g]	0	50	100	150	200
total mass [g]	200				
added Sr-tracer	1 mL equivalent to 50 mg Sr				

Then concentrated sulfuric acid (97 %) was slowly added to each sample with a dropping funnel, while stirring and in an ice bath, to compensate for the produced heat. To complete the precipitation, the samples were placed in an ice cooled ultrasonic bath. After the precipitate was separated, it was filtered through a Satorius filter cubicle with a paper filter (Whatman 42) and washed with 10 mL sulphate containing water and 10 mL acetone (p.a.). The filtration did not work as well for higher concentrations of hydrochloric acid, probably due to the small pH. After the filtration, turbidity could still be observed in the filtrate and in some cases the filter was damaged during the filtration. The labelled filters with the precipitate were then placed in labelled and tared small porcelain bowls. In these bowls, the filters were incinerated at 600 °C±20 °C for 20 minutes in the muffle furnace. After the resulted ashes cooled down, they were weighed in an analytical balance. The results were then compared to the added Sr-mass and the resulting 100 % precipitation value, that would be achieved if all the added strontium were to be precipitated.

$$\text{added Sr mass: } m = 50\ mg\ Sr = 0.05\ g\ Sr \tag{5.9}$$

$$M(Sr) = 87.62\ \frac{g}{mol} \tag{5.10}$$

$$M = \frac{m}{n} \rightarrow n = \frac{m}{M} \tag{5.11}$$

$$n(Sr) = \frac{m(Sr)}{M(Sr)} = \frac{0.05\ g}{87.62\ \frac{g}{mol}} = 0.000570646\ mol \tag{5.12}$$

From the known mass of the added Sr m (5.9) through the tracer and the molar mass of strontium M (5.10) the added quantity of strontium n could be calculated with the basic equation 5.11. With the quantity of strontium known, the mass of the resulting 100 % $SrSO_4$ precipitate could be calculated with the equation 5.14.

$$M(SrSO_4) = 183.68\ \frac{g}{mol} \tag{5.13}$$

$$m(SrSO_4) = n(Sr) \cdot\ M(SrSO_4) =\ 0.000570646\ mol \cdot 183.68\ \frac{g}{mol} = 0.1048\ g \tag{5.14}$$

$$m(SrSO_4)_{100\,\%} = 0.1048\ g \tag{5.15}$$

With the 100 % precipitation result calculated as 0.1048 g $SrSO_4$ with equation 5.14, the precipitation results of the samples were directly compared to it and to each other, as seen in table 31. Additionally, they were presented as percentages of the 100 % value of 0.1048 g $SrSO_4$ in table 31.

Table 31: Precipitation results of Sr as $SrSO_4$ in different mixing ratios of ammonium-lactate at ph7 and 6 molar hydrochloric acid

sample number	1	2	3	4	5
ratio ammonium-lactate: hydrochloric acid	100:0	75:25	50:50	25:75	0:100
$SrSO_4$ precipitate [g]	0.0966 ± 0.001	0.1005 ± 0.001	0.1050 ± 0.001	0.0372 ± 0.001	0.0952 ± 0.001
Percentage of the 100 % value [%]	92.2 ± 2.2	95.9 ± 2.3	100.2 ± 2.4	35.5 ± 0.8	90.8 ± 2.2

The precipitation experiment showed comparably high precipitation yields for almost all samples. The sample 3, with a 50:50 mixture of ammonium-lactate and hydrochloric acid as medium, showed a result of over 100 %. This could be due to unprecise weighing or because of an uncomplete incineration of the filter. The filters used for the separation normally are burned completely during incineration and no ashes remain of them, leaving only analyte ashes behind. For this sample, and maybe also for the other samples, the burning of the filter might be incomplete. So, the results should be compared relatively to each other and not in absolute numbers. The results for sample 4, with a 25:75 mixture of ammonium-lactate and hydrochloric acid showed the most deviation from the 100 % sample, with a yield of only 35.5 %. This result

was interpreted as outliner, as it was the only sample with a yield this low and the yield increased with higher amounts of hydrochloric acid and higher amounts of ammonium-lactate.

All in all, the results of this experiment were interpreted as successful, as a relatively constant and good yield of the precipitation could be achieved for almost all mixtures of the eluents ammonium-lactate and hydrochloric acid.

5.3.5 Repetition: precipitation of $SrSO_4$ in eluent mixtures

Previously, it was tested whether an eluent change influenced the precipitation of $SrSO_4$ after the sample separation. It had to be made sure, that this precipitation worked as well and as efficient in 6 M hydrochloric acid as in ammonium-lactate at pH7 and in the mixtures of these eluents. The experiment resulted in good and stable yields for most of the mixtures of 6 molar hydrochloric acid with ammonium-lactate at pH7 as for the original eluent, except for one. The $SrSO_4$ precipitation yield for sample 4, with a 25:75 mixture of ammonium-lactate and hydrochloric acid, was only 35.50 %. This result was interpreted as outliner. But this mixture ratio is very representative for the eluent change, as in the resulting sample there would be a majority of 6 M hydrochloric acid and a rest of ammonium-lactate present. To make sure, that the poor precipitation result of this mixture was really an outliner and not a general problem for the precipitation, and therefore the eluent change, the experiment was repeated.

First, the samples for the experiment were prepared from different mixing ratios of ammonium-lactate at pH7 and 6 M hydrochloric acid, equivalent to the sample preparation in section 5.3.4, as presented in table 32.

Table 32: Sample preparation for the repetition of the precipitation experiment of Sr as $SrSO_4$ in different mixing ratios of ammonium-lactate at ph7 and 6 molar hydrochloric acid

sample number	1	2	3	4	5
ratio ammonium-lactate: hydrochloric acid	100:0	75:25	50:50	25:75	0:100
ammonium-lactate [g]	200	150	100	50	0
hydrochloric acid [g]	0	50	100	150	200
total mass [g]	200				
added Sr-tracer	1 mL equivalent to 50 mg Sr				

Then the Sr in the samples was precipitated as $SrSO_4$ by adding concentrated sulfuric acid, the precipitate filtered, the filters incinerated and the resulting ashes weighed as previously detailed in section 5.3.4. The filtration did not work as well for higher concentrations of hydrochloric acid, probably due to the small pH. After the filtration, turbidity could still be observed in the filtrate and in some cases the filter was damaged during the filtration. The results were then compared to the added Sr-mass and the resulting 100 % precipitation value of 0.1048 g $SrSO_4$, that would be achieved if all the added strontium were to be precipitated.

The precipitation results were compared to each other and to the 100 % value as seen in table 33.

Table 33: Precipitation results of Sr as $SrSO_4$ for the repetition of the precipitation experiment in different mixing ratios of ammonium-lactate at ph7 and 6 molar hydrochloric acid

sample number	1	2	3	4	5
ratio ammonium-lactate: hydrochloric acid	100:0	75:25	50:50	25:75	0:100
$SrSO_4$ precipitate [g]	0.1047 ± 0.001	0.1052 ± 0.001	0.1094 ± 0.001	0.0965 ± 0.001	0.0179 ± 0.001
percentage of the 100 % value [%]	99.9 ± 2.4	100.4 ± 2.4	104.4 ± 2.5	92.1 ± 2.2	17.1 ± 0.4

As for several samples a precipitation yield of over 100 % was achieved, unprecise weighing or an uncomplete incineration of the filter were suspected as possible causes. Because of this, the ashes were incinerated again over night in the muffle furnace at 600°C ± 20°C. The results after the additional incineration are shown in table 34.

Table 34: Precipitation results of Sr as $SrSO_4$ after a second incineration in different mixing ratios of ammonium-lactate at ph7 and 6 M hydrochloric acid

sample number	1	2	3	4	5
ratio ammonium-lactate: hydrochloric acid	100:0	75:25	50:50	25:75	0:100
$SrSO_4$ precipitate [g]	0.1038 ± 0.001	0.1051 ± 0.001	0.1129 ± 0.001	0.0949 ± 0.001	0.0168 ± 0.001
percentage of the 100% value [%]	99.0 ± 2.4	100.3 ± 2.4	107.7 ± 2.6	90.6 ± 2.2	16.0 ± 0.4

The results show that the additional incineration did not have a significant effect. Several samples still had a precipitation result of over 100 %. Even though the ash mass decreased for most samples after the incineration, it increased additionally for the sample with the highest precipitation yield, sample 3 with a 50:50 mixture of ammonium-lactate and hydrochloric acid as medium. This sample already had the highest yield in the first try of this experiment. Based on these results, the yields of over 100 % percent were interpreted to be caused by uncertainties in the weighing.

Like the first precipitation experiment, this precipitation experiment showed comparably high precipitation yields for almost all samples. Among them sample 4, with a 25:75 mixture of ammonium-lactate and hydrochloric acid as medium. It achieved only a low precipitation yield in the last experiment, which was the main reason for this experiment. But in this experiment, the outliner was sample 5, with hydrochloric acid as medium and a precipitation yield of only 16.0 %.

For both experiments, a sample with a high hydrochloric acid content achieved only a small $SrSO_4$ yield and these are the samples most comparable to the sample after the eluent change. The precipitation worked for all mixing ratios of the eluents, but the filtration of $SrSO_4$ was inefficient at higher concentrations of hydrochloric acid. This is maybe due to the very low pH of the medium, which caused damage in the filter and left turbidity, assumed to be $SrSO_4$, in the filtrate.

All in all, this meant that the eluent change worked in accelerating the elution but disrupted the filtration step of the process. Based on this, the eluent change to 6 molar hydrochloric acid was rejected as an elution acceleration strategy.

5.3.6 DOWEX® 50 WX8 (200-400 mesh) by Sigma Aldrich for the determination of K, Ca, Y and Sr in milk ash

In addition to the new DOWEX® 50 WX8 (200-400 mesh) by Alfa Aesar, the DOWEX material by the provider Sigma Aldrich was tested. As the DOWEX by Alfa Aesar broadened and shifted the elution region of strontium significantly and the tested eluent change could not be used for the acceleration of the strontium elution, due to problems with filtration, it was hoped that the DOWEX by Sigma Aldrich would lead to results more similar to the established DOWEX by Serva. This expectation was based on the fact, that the new column material was presented as exactly the same material that was used before.

The new DOWEX® 50 WX8 200-400 (H) resin by Sigma Aldrich was tested by determining the elution regions of yttrium, strontium, potassium and calcium with this DOWEX as column material.

As detection method, for the quantification of these elements in the different fractions, ICP-OES was used, as previously for the elution curve with the DOWEX by Alfa Aesar.

As standard sample matrix 10.01 g not contaminated milk ash, prepared from commercially available whole long-life milk by the brand Berchtesgadener Land, was used. It was solved in 80 mL of the usual 1:1 mixture of 6 molar hydrochloric acid and 1.5 M lactic acid. Additionally, 1 mL of the stable yttrium tracer, containing 10 mg Y, and 2 mL stable strontium tracer, containing in total 100 mg Sr, were added. Potassium and calcium were naturally present in the sample matrix in significant amounts, according to the milk packaging 124 mg calcium per 100 mL. After the sample was solved and applied to the column, the Hot Column Chromatography was performed at the elution speed of 2.5 mL/min. During this, 100 elution fractions à 10 mL were collected. For the ICP-OES measurement, the fraction samples were diluted 1:250. Per ICP-OES sample 40 µL of the fractions were used and 2 mL concentrated nitric acid was added for pH adjusting. The samples were filled up to a volume of 10 mL with bidistilled water.

For the ICP-OES measurement, the same calibration curve was used as the one calculated for the initial determination of the elution curve with the new DOWEX® 50 WX8 (200-400 mesh) by Alfa Aesar in section 5.3.1.

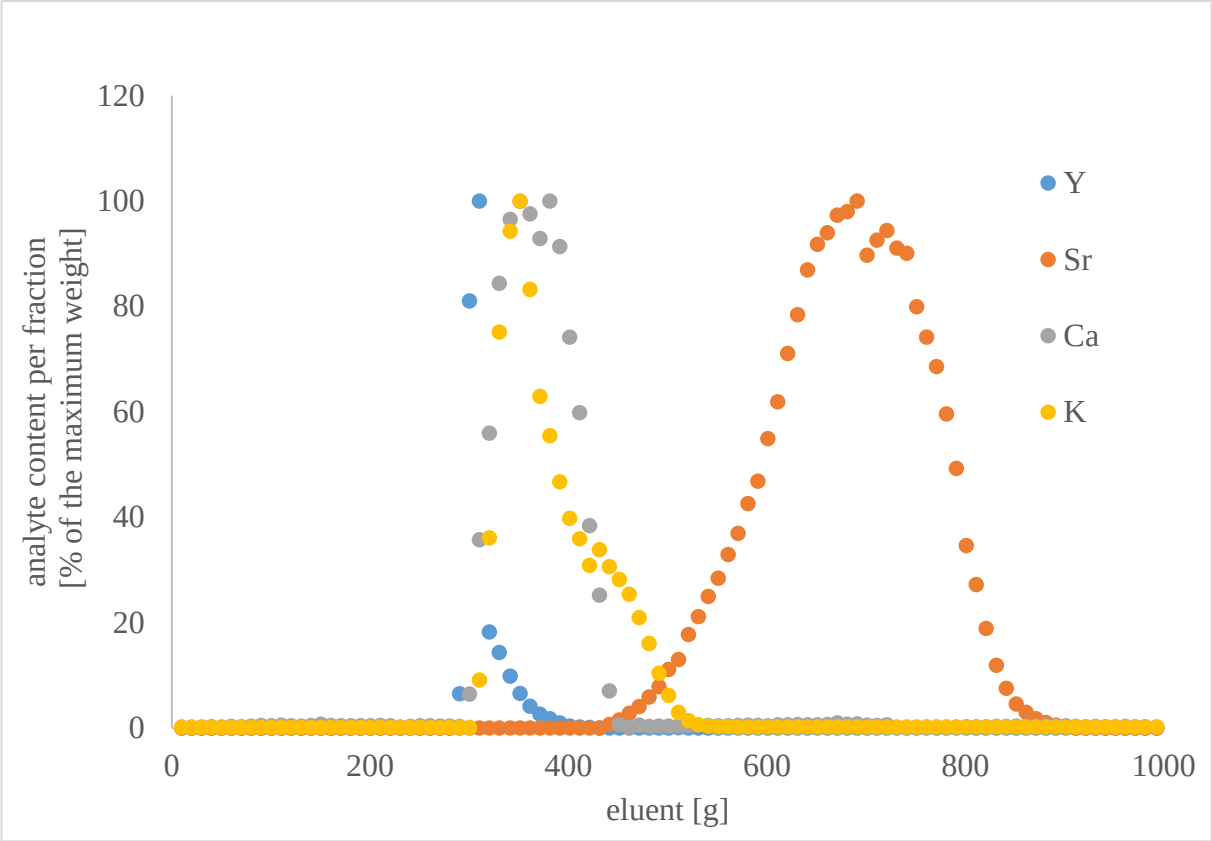

Figure 53: Relative elution curve for the determination of Y, K, Ca and Sr in milk ash with the DOWEX® 50 WX8 (200-400 mesh) by Sigma Aldrich and sample measurement with ICP-OES

The resulting elution curve for the for the determination of K, Ca, Y and Sr in milk ash with the DOWEX® 50 WX8 (200-400 mesh) by Sigma Aldrich and sample measurement with ICP-OES is shown in figure 53. This is the relative elution curve with the concentration maximum normed to 100 % and the rest of the concentrations presented relative to the maximum concentration of the analyte during the elution.

A very good separation between yttrium and strontium, a good separation between calcium and strontium and an acceptable separation between potassium and strontium were achieved. The separation between yttrium, calcium and potassium was only mediocre. But at least the relative content of potassium and calcium was quite small in the maximum range of yttrium. The reason for this could also be, that fraction 31, which is the fraction with the highest Y content, contained solid precipitate, that could not be resolved through heating after the sample cooled down. This precipitate is likely calcium, but could also contain potassium, that subsequently was not accounted for during the ICP-OES measurement.

Table 35: Elution regions and the concentration maxima of the analytes K, Ca, Y and Sr in milk ash recorded with the DOWEX® 50 WX8 (200-400 mesh) by Sigma Aldrich and sample measurement with ICP-OES

element	elution region [g]	concentration maximum [g]
yttrium	280-400	300-310
strontium	440-880	680-690
calcium	290-450	370-380
potassium	300-520	340-350

Table 35 shows the elution regions of the analytes and their concentration maxima for a direct comparison and numerical visualization of the overlap of their elution regions.

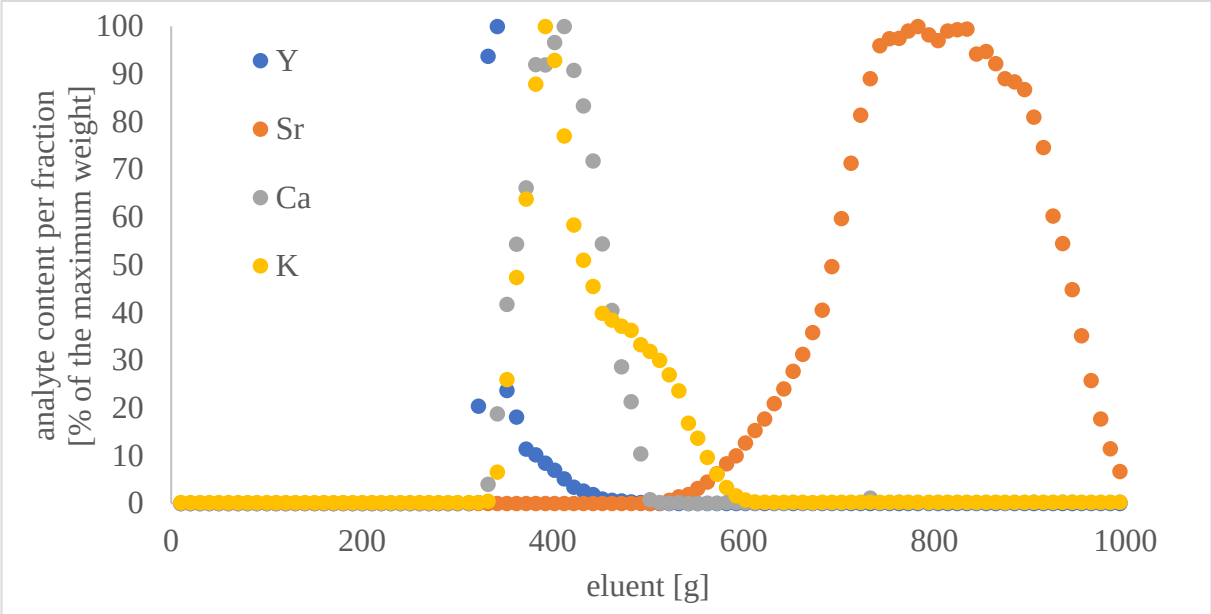

Figure 54: Relative elution curve for the determination of Y, K, Ca and Sr in milk ash with the DOWEX® 50 WX8 (200-400 mesh) by Alfa Aesar and sample measurement with ICP-OES

Table 36: Elution regions and the concentration maxima of the analytes K, Ca, Y and Sr in milk ash recorded with the DOWEX® 50 WX8 (200-400 mesh) by Sigma Aldrich in comparison with the DOWEX by Alfa Aesar

DOWEX provider	**Sigma Aldrich**		**Alfa Aesar**	
element	**elution region [g]**	**concentration maximum [g]**	**elution region [g]**	**concentration maximum [g]**
yttrium	280-400	300-310	310-480	330-340
strontium	440-880	680-690	510-1000	770-780
calcium	290-450	370-380	320-510	400-410
potassium	300-520	340-350	330-600	380-390

Figure 54 shows the elution curve for the determination of K, Ca, Y and Sr in milk ash with the DOWEX® 50 WX8 (200-400 mesh) by Alfa Aesar and sample measurement with ICP-OES for comparison. The elution curve achieved with the DOVEX by Alfa Aesar is quite similar to the one achieved with the DOWEX by Sigma Aldrich. Both show a narrow yttrium elution region with a strong overlap with the calcium and potassium elution regions, that are located between the elution curves of yttrium and strontium. In both cases, only a small overlap between the elution regions of calcium and strontium are noticeable. But the elution regions achieved with the DOWEX by Sigma Aldrich are all shifted to lower eluent volumes, compared to the elution regions achieved with the DOWEX by Alfa Aesar. The elution regions of yttrium, calcium and potassium start at 30 g less eluent than with the resin by Alfa Aesar and the strontium elution region is even shifted by 60 g eluent to smaller eluent volumes. Additionally,

the strontium elution region is by 50 g eluent narrower than with the Alfa Aesar resin. This Data, including the overlaps, differences and commonalities of the elution regions, is shown in table 36, which allows for a direct comparison between the elution regions with the DOWEX by Sigma Aldrich and the DOWEX by Alfa Aesar.

All in all, the separation quality with the Sigma Aldrich DOWEX is similar to the separation quality with the Alfa Aesar resin, but the analytes were eluted from the column at lower eluent volumes and a narrower strontium elution curve was achieved. This would make a faster Hot Column Chromatography separation possible than with Alfa Aesar.

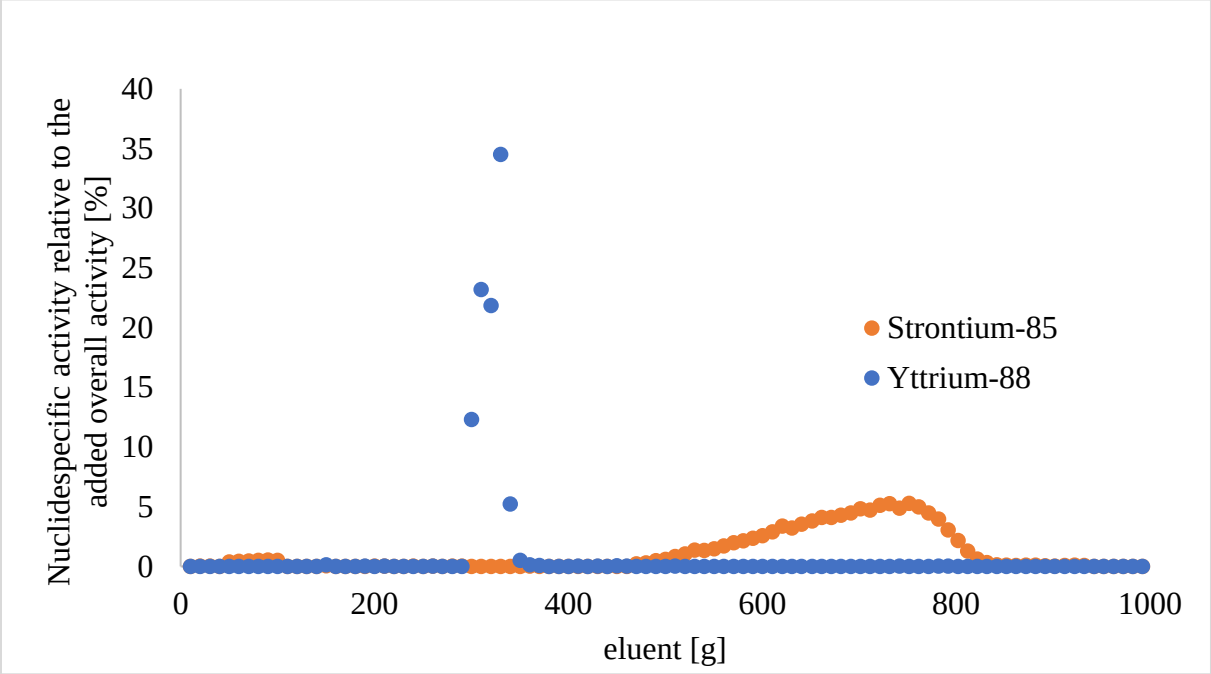

Figure 55: Elution regions of Y and Sr in milk as recorded with the established DOWEX® 50WX8 200-400 (H) resin by Serva

Figure 55 shows a recording of the elution regions of yttrium and strontium achieved with the established DOWEX® 50WX8 200-400 (H) resin by Serva, to compare these results with the new results with the DOWEX by Sigma Aldrich. The distribution was determined with a gamma active multi-nuclide tracer and the activities relative to the 100 % tracer were measured with gamma spectrometry (5.2.2.1). As the tracer did not contain calcium or potassium isotopes, their elution regions could not be determined with this method. Because of the different methods, the absolute quantities of analytes in the individual samples cannot be compared, but the distribution of the analytes, alias the elution regions, are comparable, as the Hot Chroma separations were performed in an almost identical way.

Table 37: Elution regions and the concentration maxima of the analytes Y and Sr in milk ash recorded with the DOWEX® 50 WX8 (200-400 mesh) by Sigma Aldrich in comparison with the established DOWEX by Serva

DOWEX provider	**Serva**		**Sigma Aldrich**	
element	**elution region [g]**	**maximum [g]**	**elution region [g]**	**maximum [g]**
yttrium	270-440	300-310	280-400	300-310
strontium	470-840	730-740	440-880	680-690

Figure 55 and table 37 show that the shift of the yttrium elution region to higher eluent volumes is quite small with the Sigma Aldrich resin, only about 10 g eluent, which is relatively negligible for the comparison with the old resin. The yttrium maxima are at the same eluent throughput. Additionally, the yttrium elution region was even narrower with the DOWEX by Sigma Aldrich. This makes the new material very comparable to the old one in regard to the yttrium separation, even preferrable, because of the narrower elution region. The strontium elution region was shifted to lower eluent volumes by 30 g eluent, but was broadened by 70 g eluent, with an end point of the elution 40 g eluent above the one in the separation with the DOWEX by Serva. This would make the separation of the strontium elution region more time consuming and increase the amount of necessary chemicals per sample with the new DOWEX by Sigma Aldrich, compared to the established DOEWX by Serva. But the results were still better and closer to the established DOWEX than the ones achieved with the resin by Alfa Aesar. This shows the variety in elution results for the product DOWEX® 50WX8 200-400 (H) by different providers.

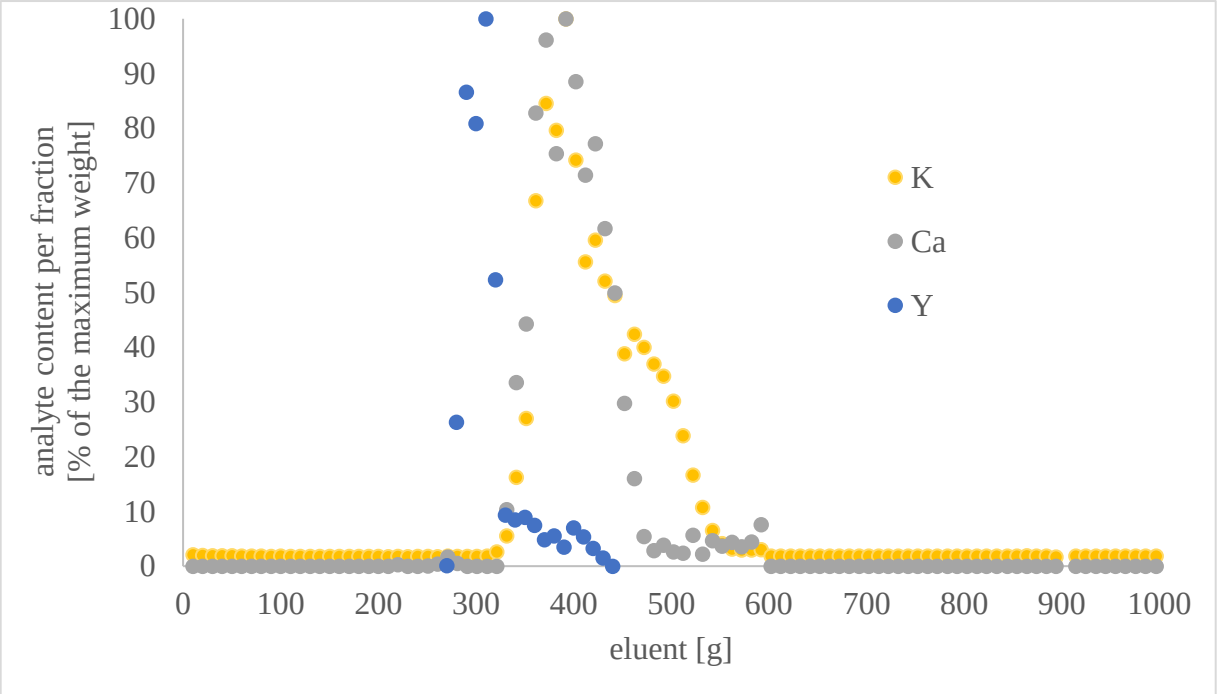

Figure 56: Elution regions of Y, Ca and K recorded with the established DOWEX® 50WX8 200-400 (H) resin by Serva

Figure 56 shows an older recording of the elution regions of yttrium, calcium and potassium, achieved with the established DOWEX® 50WX8 200-400 (H) resin by Serva, to compare these results with the new results with the Sigma Aldrich resin. These elution curves were also recorded with ICP-OES measurements using stable tracers.

The older elution curve is not as exact as the newer one. This is because, instead of professional standards, a self-made salt solution was used for the preparation of the ICP-OES calibration curve. Additionally, the yttrium curve was recorded separately from the calcium and potassium elution curves and there could be differences in the separations during the Hot Column Chromatography. Therefore, the edges of the elution regions for this older elution curves are less precise and tailing is present at their ends.

Table 38: Comparison between the DOWEX® 50 WX8 (200-400 mesh) by Serva and by Sigma Aldrich Elution regions and the concentration maxima of the analytes Y, Ca and K in milk ash

DOWEX provider	**Serva**		**Sigma Aldrich**	
element	**elution region [g]**	**maximum [g]**	**elution region [g]**	**maximum [g]**
yttrium	270-440	300-310	280-400	300-310
calcium	320-480	380-390	290-450	370-380
potassium	320-560	380-390	300-520	340-350

As is evident from table 38 and figure 56, the elution curves recorded with the DOWEX by Sigma Aldrich shift the elution regions slightly, compared to the older recording. The yttrium elution curve has its maximum at the same eluent volume as the elution curve recorded with the older DOWEX. But its beginning is slightly shifted to higher eluent volumes and the elution region is by 50 g eluent narrower than the one recorded with the Serva DOWEX. The maximum of the calcium elution curve is shifted by 10 g to lower eluent volumes compared to the maximum of the elution curve recorded with the older DOWEX. The elution region of calcium is in general shifted by 30 g eluent to lower eluent volumes but has the same breadth as the one recorded with the Serva DOWEX. The maximum of the potassium elution curve is shifted by 40 g to lower eluent volumes. The elution curve is in general shifted by 20 g to lower eluent volumes, compared to the potassium elution curve recorded with the Serva DOWEX. Additionally, the elution region was by 20 g eluent narrower than the one recorded with the Serva DOWEX. All in all, these changes of the elution regions meant a stronger overlap between the elution region of the analyte yttrium with the interfering elements calcium and potassium, than was the case for the older elution curves, which would affect the separation and analysis of yttrium negatively.

For comparison figure 57 shows the absolute results of the distribution of the different analytes during the elution process with the DOWEX by Sigma Aldrich. The interfering elements calcium and potassium were present in much higher concentrations in the sample matrix than the expected amounts of the analytes yttrium and strontium, if they were present. Additionally, a significant potassium background was measured for all fractions. This could be because of the use of glassware, which contains potassium, or because of the insufficient separation performance of the column for potassium.

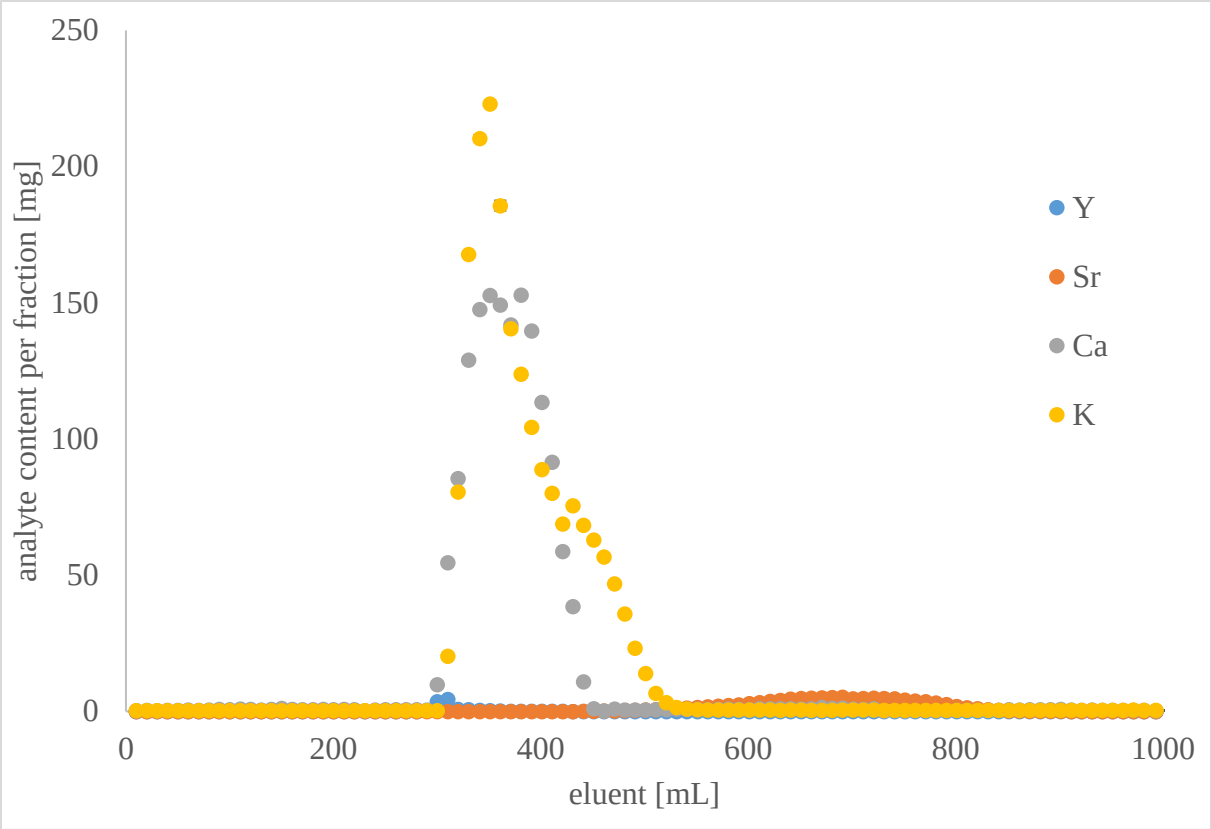

Figure 57: Absolute elution curve for the determination of Y, K, Ca and Sr in milk ash with the DOWEX® 50 WX8 (200-400 mesh) by Sigma Aldrich and sample measurement with ICP-OES

As a summary of the results, it was found that the column material by Sigma Aldrich led to a shift of the elution regions compared to the established DOWEX. The yttrium elution region was only shifted by 10 g to higher eluent volumes, but the strontium elution region was shifted by 30 g to lower eluent volumes and was significantly broadened. This would make longer elution times necessary, but still to a significantly lesser extent than was the case for the DOWEX by Alfa Aesar. Additionally, the changes of the elution regions meant a stronger overlap between the elution region of the analyte yttrium with the interfering elements calcium and potassium, which would affect the separation and analysis of yttrium negatively.

5.3.7 Effect of the eluent pH change to six on the separation quality of Y, Sr, K and Ca, with the DOWEX® 50 WX8 (200-400 mesh) by Alfa Aesar

The new DOWEX by Alfa Aesar broadened and shifted the elution region of strontium significantly and the tested eluent change could not be used for the acceleration of the strontium elution due to problems with filtration. Then the DOWEX by another provider, Sigma Aldrich, was tested in hopes of more favorable elution results more similar to the ones with the established DOWEX by Serva. But unfortunately, this DOWEX showed results more similar to the ones by Alfa Aesar and also led to a significant broadening of the strontium elution region.

A new approach was to test whether a pH change of the original eluent ammonium lactate would lead to a narrower strontium elution region, without sabotaging the separation. This idea was based on the previous experiment with the eluent change to the strongly acidic 6 M hydrochloric acid. The eluent change was successful in accelerating the strontium elution, but the low pH led to problems during the filtration. The plan was to first decrease the pH only slightly, to test if there would be an effect on the spectrum, without interfering with the filtration and, if necessary, decrease the pH stepwise. The new pH of the eluent ammonium-lactate for this experiment was pH6, lowered from the established pH7.

The new pH of the eluent was tested by determining the elution regions of yttrium, strontium, potassium and calcium with the DOWEX by Alfa Aesar as column material.

As detection method, for the quantification of these elements in the different fractions, ICP OES was used, as previously for the elution curve with the DOWEX by Alfa Aesar with ammonium-lactate at pH7.

As standard sample matrix 10.00 g not contaminated milk ash, prepared from commercially available whole long-life milk by the brand Berchtesgadener Land, was used. It was solved in 80 mL of the usual 1:1 mixture of 6 M hydrochloric acid and 1.5 M lactic acid. Additionally, 1 mL of the stable yttrium tracer, containing 10 mg Y, and 2 mL stable strontium tracer, containing in total 100 mg Sr, were added. Potassium and calcium were naturally present in the sample matrix in significant amounts, according to the milk packaging 124 mg calcium per 100 mL. After the sample was solved and applied to the column, the Hot Column Chromatography was performed at the elution speed of 2.5 mL/min. During this, 100 elution fractions à 10 mL were collected. For the ICP-OES measurement, fraction samples were diluted 1:250. Per ICP-OES sample, 40 µL of the fractions were used and 2 mL concentrated nitric acid was added for pH adjusting. The samples were filled up to a volume of 10 mL with bidisstilled water.

For the ICP-OES measurement, the same calibration curve was used as the one calculated for the initial determination of the elution curve with the new DOWEX® 50 WX8 (200-400 mesh) by Alfa Aesar in section 5.3.1.

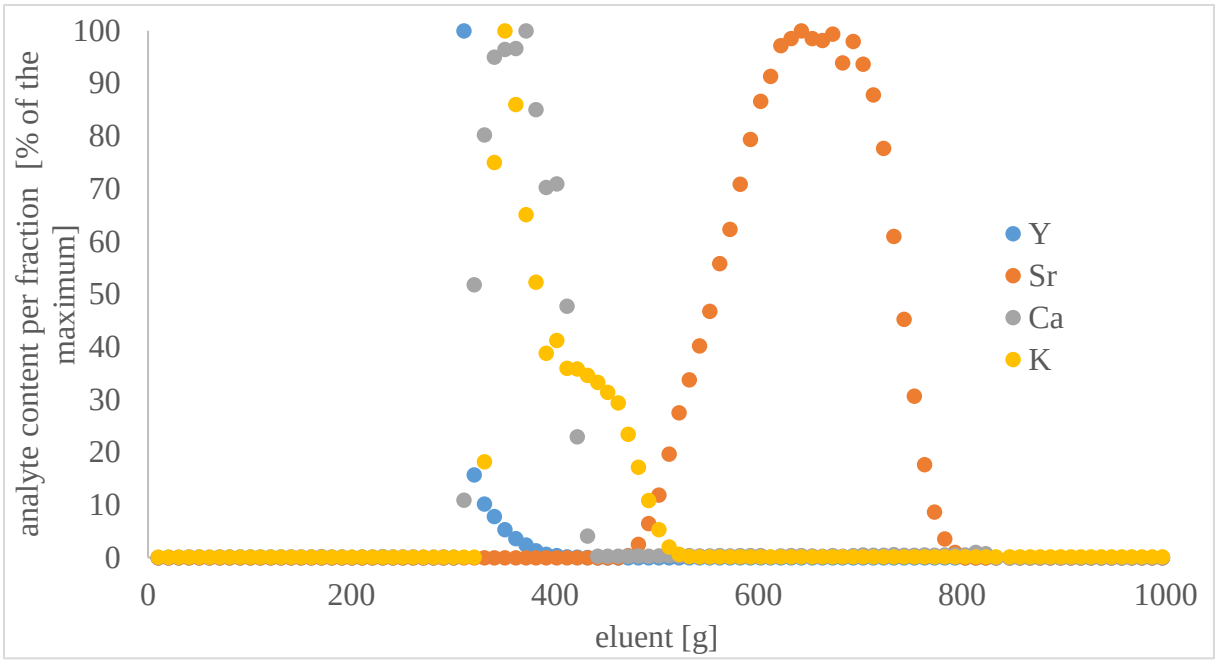

Figure 58: Relative elution curve for the determination of Y, K, Ca and Sr in milk ash with the DOWEX® 50 WX8 (200-400 mesh) by Alfa Aesar, eluent ammonium-lactate at pH6, and sample measurement with ICP-OES

The resulting elution curve for the for the determination of K, Ca, Y and Sr in milk ash with the DOWEX® 50 WX8 (200-400 mesh) by Alfa Aesar and the eluent ammonium-lactate at pH6 is shown in figure 58. The sample measurement was performed with ICP-OES. This is the relative elution curve with the concentration maximum normed to 100 % and the rest of the concentrations presented relative to the concentration maximum of the analyte during the elution.

A very good separation between yttrium and strontium, a good separation between calcium and strontium and an acceptable separation between potassium and strontium were achieved. The separation between yttrium, calcium and potassium was quite bad, the elution regions of the elements overlapped almost completely. But at least the relative content of potassium and calcium was quite small in the maximum range of yttrium. The reason for this could also be, that fraction 31, which is the fraction with the highest yttrium content, contained solid precipitate, that could not be resolved by heating after the sample cooled down. This precipitate is likely calcium, but could also contain potassium, that subsequently was not accounted for during the ICP-OES measurement.

Table 39: Elution regions and the concentration maxima of the analytes K, Ca, Y and Sr in milk ash recorded with the DOWEX® 50 WX8 (200-400 mesh) by Alfa Aesar, eluent ammonium-lactate at pH6, sample measurement with ICP-OES

element	elution region [g]	concentration maximum [g]
yttrium	300-410	300-310
strontium	470-790	630-640
calcium	300-440	360-370
potassium	320-520	340-350

Table 39 shows the elution regions of the analytes and their concentration maxima for a direct comparison and numerical visualization of the overlap of their elution regions.

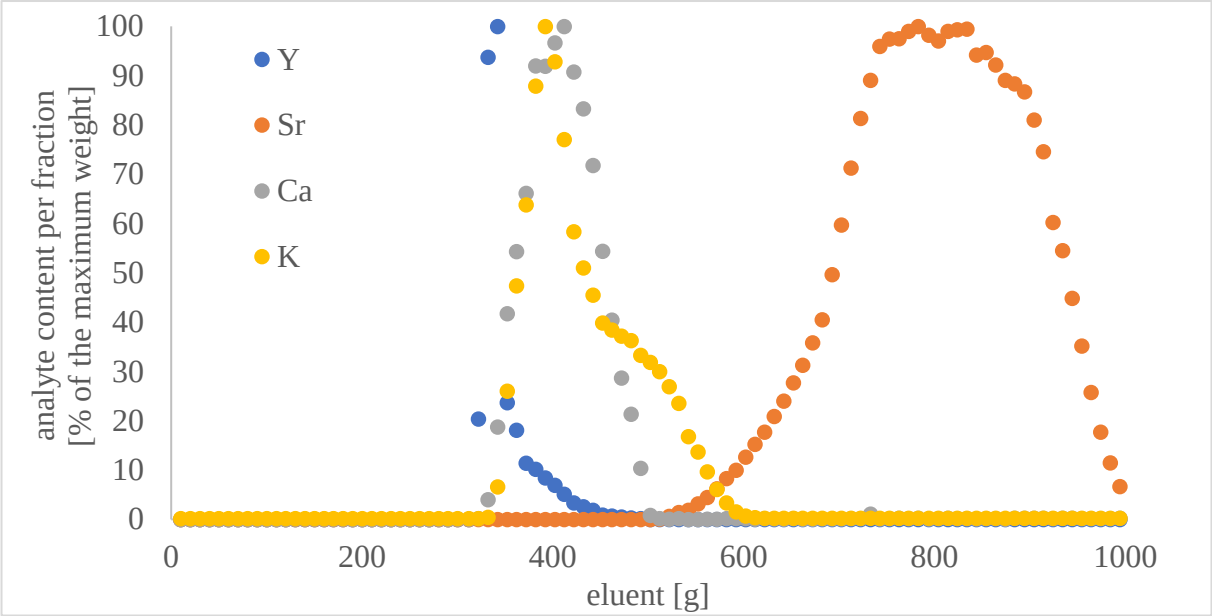

Figure 59: Relative elution curve for the determination of Y, K, Ca and Sr in milk ash with the DOWEX® 50 WX8 (200-400 mesh) by Alfa Aesar, eluent ammonium-lactate at pH7, and sample measurement with ICP-OES

Figure 59 shows the elution curve for the determination of K, Ca, Y and Sr in milk ash with the DOWEX® 50 WX8 (200-400 mesh) by Alfa Aesar and the eluent ammonium-lactate at pH7. The sample measurement was performed with ICP-OES. The general structure and positions of the elution regions between the elution curves with ammonium-lactate at pH 7 and at pH 6 are quite similar. The elution curve with ammonium-lactate at pH6 as eluent showed a stronger overlap between the elution regions of yttrium, calcium and potassium and more narrow elution curves for these elements, possibly through an elution acceleration due to a lower pH. The most significant difference between those two elution curves was the elution region of strontium, that was shifted by 40 g eluent to lower eluent volumes and was narrowed by 170 g eluent through lowering the eluent pH. With this, a comparable strontium elution region to the established DOWEX was achieved with a simple adjusting of the eluent pH. This solved the problem of a longer and more laborious separation with the new DOWEX and the pH change was planned to be incorporated into routine analytics.

Table 40: Comparison between eluent ammonium-lactate at pH6 and at pH7, elution regions and the concentration maxima of the analytes K, Ca, Y and Sr in milk ash recorded with the DOWEX® 50 WX8 (200-400 mesh) by Alfa Aesar, sample measurement with ICP-OES

eluent pH	**ammonium-lactate pH 6**		**ammonium-lactate pH 7**	
element	**elution region [g]**	**concentration maximum [g]**	**elution region [g]**	**concentration maximum [g]**
yttrium	300-410	300-310	310-480	330-340
strontium	470-790	630-640	510-1000	770-780
calcium	300-440	360-370	320-510	400-410
potassium	320-520	340-350	330-600	380-390

Table 40 shows the comparison of the elution regions for the separation of each analyte with ammonium-lactate at pH 6 and at the established pH 7.

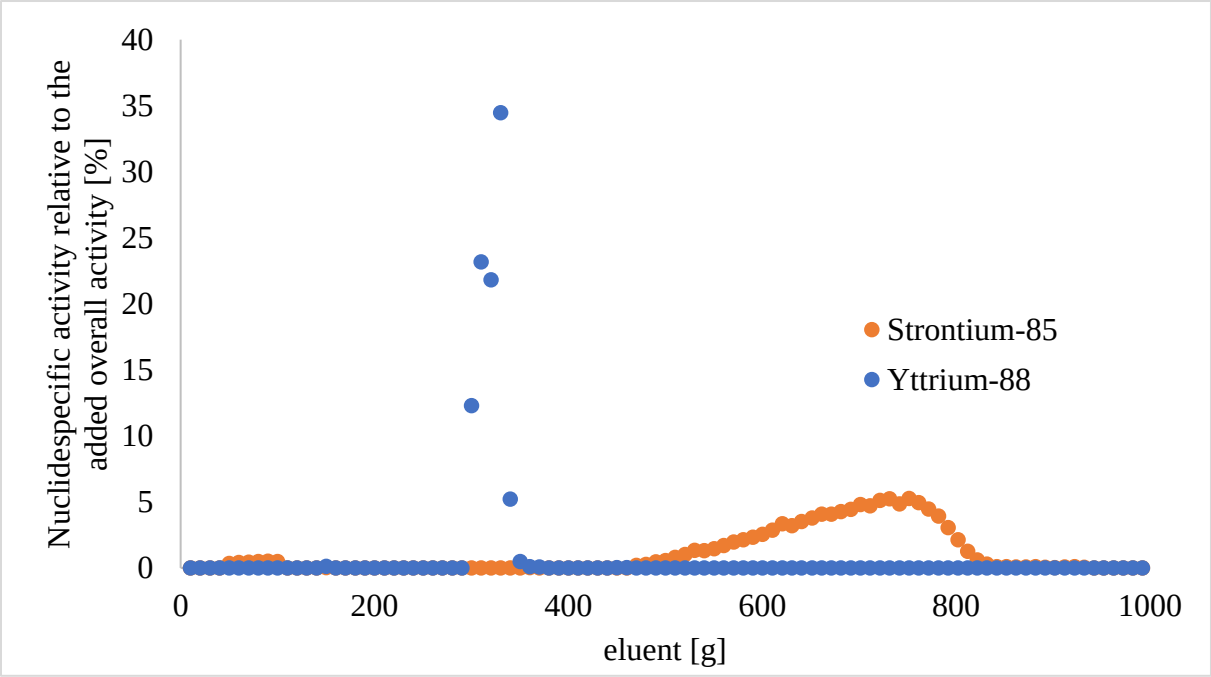

Figure 60: Elution regions of Y and Sr in milk as recorded with the established DOWEX® 50 WX8 200-400 (H) resin by Serva, eluent ammonium-lactate at pH7

Figure 60 shows a recording of the elution regions of yttrium and strontium achieved with the established DOWEX® 50 WX8 200-400 (H) resin by Serva to compare these results with the new results with the DOWEX by Alfa Aesar with the eluent ammonium-lactate at pH6. The distribution was determined with a gamma active multi-nuclide tracer and the activities relative to the 100 % tracer were measured with gamma spectrometry (5.2.2.1). As the tracer did not contain calcium or potassium isotopes, their elution region could not be determined with this method. Because of the different methods, the absolute quantities of analytes in the individual samples cannot be compared, but the distribution of the analytes, alias the elution regions, are comparable, as the Hot Chroma separations were performed in an almost identical way.

Table 41: Comparison of the results between the DOWEX® 50 WX8 (200-400 mesh) by Serva, eluent ammonium-lactate at pH7, and by Alfa Aesar, eluent ammonium-lactate at pH6, elution regions and the concentration maxima of the analytes Y and Sr in milk ash

DOWEX provider	**Serva ammonium-lactate pH7**		**Sigma Aldrich ammonium-lactate pH6**	
element	**elution region [g]**	**maximum [g]**	**elution region [g]**	**maximum [g]**
yttrium	270-440	300-310	300-410	300-310
strontium	470-840	730-740	470-790	630-640

Figure 60 and table 41 show the shift of the yttrium elution region by 30 g eluent to higher eluent volumes with the Alfa Aesar resin and ammonium-lactate at pH6 compared to the established separation system. The yttrium maxima are at the same eluent throughput and the yttrium elution regions have the same width. This makes the new material very comparable to the old one in regard of yttrium separation. The strontium elution region started at the same eluent throughput but was narrowed by 50 g eluent using ammonium-lactate at pH6 as eluent in combination with the DOWEX by Alfa Aesar. This makes the separation systems comparable and allows for the application of this new system for environmental monitoring. The only factors that would change is the DOWEX resin, as the older one is no longer available, and the

pH of the prepared ammonium-lactate solution. The rest of the separation parameters could be applied as usual for the established separation.

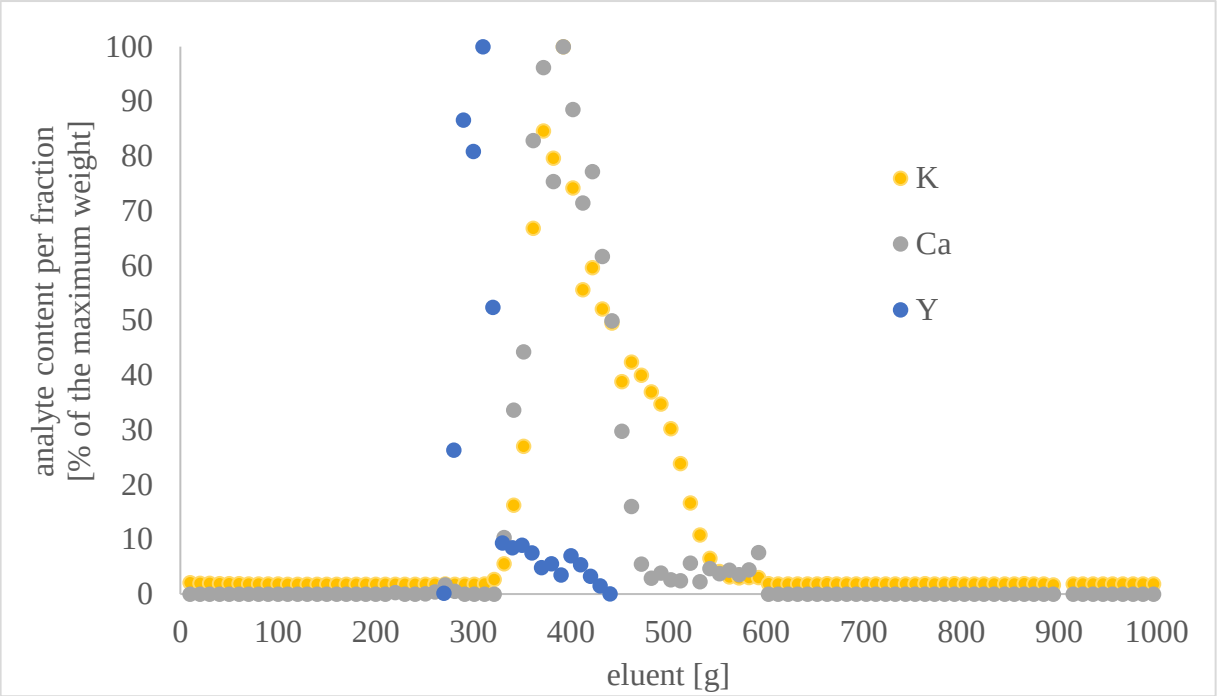

Figure 61: Elution regions of Y, Ca and K recorded with the established DOWEX® 50 WX8 200-400 (H) resin by Serva

Figure 61 shows an older recording of the elution regions of yttrium, calcium and potassium, achieved with the established DOWEX® 50 WX8 200-400 (H) resin by Serva, to compare these results with the new results with the Alfa Aesar resin with ammonium-lactate at pH6. These elution curves were also recorded with ICP-OES measurements using stable tracers.

The older elution curve is not as exact as the newer one. This is because, instead of a professional standard, a self-made salt solution was used for the preparation of the ICP-OES calibration curve. Additionally, the yttrium curve was recorded separately from the calcium and potassium elution curves and there could be differences in the separations during the Hot Column Chromatography. Therefore, the edges of the elution regions for this older elution curves are less precise and tailing is present at their ends.

Table 42: Comparison of the results between the DOWEX® 50 WX8 (200-400 mesh) by Serva, eluent ammonium-lactate at pH7, and by Alfa Aesar, eluent ammonium-lactate at pH6, elution regions and the concentration maxima of the analytes Y, Ca and K in milk ash

DOWEX provider	**Serva ammonium-lactate pH7**		**Alfa Aesar ammonium-lactate pH6**	
element	**elution region [g]**	**maximum [g]**	**elution region [g]**	**maximum [g]**
yttrium	270-440	300-310	300-410	300-310
calcium	320-480	380-390	300-440	360-370
potassium	320-560	380-390	320-520	340-350

As is evident from table 42 and figure 61, the elution curves recorded with the DOWEX by Alfa Aesar and ammonium-lactate at pH6 are narrower, compared to the older recording. The yttrium elution curve has its maximum at the same eluent volume as the elution curve recorded with the older DOWEX, but its beginning is shifted to higher eluent volumes and the elution region is by 60 g eluent narrower than the one recorded with the Serva DOWEX. The maximum

of the calcium elution curve is shifted by 20 g to lower eluent volumes compared to the maximum of the elution curve recorded with the older DOWEX. The elution region of calcium is narrowed by 40 g eluent with the new system. The maximum of the potassium elution curve is shifted by 40 g to lower eluent volumes compared to the elution curve recorded with the Serva DOWEX. All in all, these changes of the elution regions meant a stronger overlap between the elution region of the analyte yttrium with the interfering elements calcium and potassium, than was the case for the older elution curves, which would affect the separation and analysis of yttrium negatively.

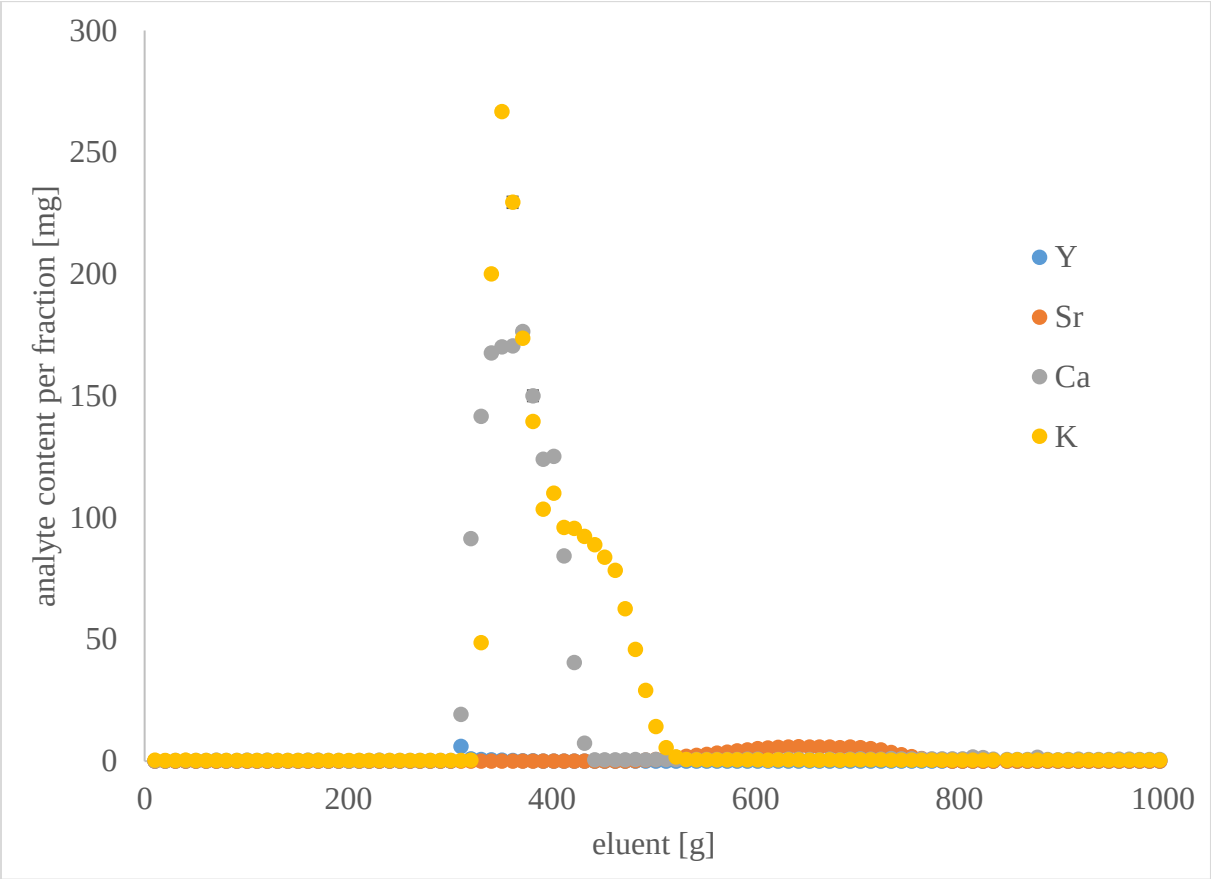

Figure 62: Absolute elution curve for the determination of Y, K, Ca and Sr in milk ash with the DOWEX® 50 WX8 (200-400 mesh) by Alfa Aesar, eluent ammonium-lactate at pH 6, and sample measurement with ICP-OES

For comparison, the figure 62 shows the absolute results for the distribution of the different analytes during the elution process with the DOWEX by Alfa Aesar and the eluent ammonium-lactate at pH6. The interfering elements calcium and potassium were present in much higher concentrations in the sample matrix than the expected amounts of the analytes yttrium and strontium, if they were present at all. Additionally, a significant potassium background was measured for all fractions. This could be because of the use of glassware, which contains potassium, or because of the insufficient separation performance of the column for potassium.

As a summary of the results, it was found that the change of the pH of ammonium-lactate from 7 to 6 lead to the significant acceleration of the strontium elution, that was hoped for. With this slight change, the Hot Column Chromatography could be performed as usual with the new column material. The downside to this is the worse separation of yttrium from potassium and calcium due to accelerated elution and narrower elution regions of these analytes and their resulting overlap.

5.3.8 Effect of the eluent pH change to six on the elution region of ^{137}Cs separated with the DOWEX® 50 WX8 (200-400 mesh) by Alfa Aesar

In the following section, the determination of the elution region of ^{137}Cs, a very important interfering nuclide, with the new DOWEX® 50WX8 (200-400 mesh) by Alfa Aesar and ammonium-lactate at pH6 is presented. As cesium is not suitable for the measurement with ICP-OES, its elution region was determined separately, with an active ^{137}Cs solution as tracer, via gamma spectrometry.

For this process 10 g of not contaminated milk ash was used as sample matrix and 161.77 Bq, equivalent to 30.03 g of ^{137}Cs tracer was added. This activity was chosen as a compromise of work safety and acceptable measurement times. Then a Hot Column Chromatography was performed with ammonium-lactate at pH 6 as eluent and 100 elution fractions à 10 mL were collected.

As the LSC measurement showed uncertain results for the last the determination of ^{137}Cs in elution fractions (5.3.2), the samples were directly measured with gamma spectrometry. This method did not require sample preparation.

The samples were measured at least half a workday. Most samples were measured for a whole workday or over-night. Some were measured over the weekend, to optimize the use of the measurement capacity of the detectors. All three gamma detectors in the control area, GEM3, GEM4 and GEM40 were used for these measurements, to achieve an efficient sample throughput. As this measurement system required a lot more measurement and labor time, not all fractions were measured. Based on the previous experiments, it was approximately known where the elution region of ^{137}Cs should be. Additionally, the elution region of ^{137}Cs is continuous and the fractions containing activity were the ones next to each other. In the elution region all the samples were measured. In the regions, where only background was suspected, approximately every second sample was measured, to make sure that no ^{137}Cs activity was missed.

For the data processing, the ROI of ^{137}Cs was marked in each measurement file. The net area and its error were noted and the count rate was calculated by dividing the net rate by the life time, the death time corrected measurement time.

As the samples were measured at different gamma spectrometers with different physical efficiencies, the measurement results of samples measured at different devices could not be directly compared to each other or expressed in relation to a previously measured 100 % value, as was done for the previous gamma measurements of elution curves (5.2.2). The activities of each measured fraction were calculated with the measured count rates and the physical efficiencies from the calibration for ^{137}Cs samples in a 20 mL LSC vial performed by Michael Hechtel in his scientific work [60]. A represents the radioactivity of the sample, R the measured count rate and η_{phys} the physical efficiency determined in the work of Michael Hechtel [60].

$$A = \frac{R}{\eta_{phys}} \tag{5.16}$$

The physical efficiencies depended on the emission energy, which in this experiment was constant, as ^{137}Cs was the only investigated nuclide, the detector, the measurement geometry, in this case the 20 mL LSC vial, and the sample volume in the LSC vial. The analyte, the

measurement geometry and the sample volume stayed the same for this experiment and only the detectors varied.

Table 43 presents the η_{phys} values, which were used for the measurements of ^{137}Cs in a 10 g sample in a 20 mL LSC vial for the different detectors.

Table 43: η_{phys} values used for the measurements of ^{137}Cs in a 10 g sample in a 20 mL LSC vial for the gamma-detectors GEM3, GEM4 and GEM40

Sample: ^{137}Cs in 10 g sample in 20 mL LSC vial	
Gamma detector	**η_{phys}**
GEM 3	0.0232
GEM 4	0.0216
GEM 40	0.0318

After the activity was calculated, a decay correction was performed, to ensure comparability between the samples. As they were measured over a longer period, more ^{137}Cs isotopes decayed in the samples that were measured later, before they could be detected. All samples were normed to the time of the measurement of the 100 % sample.

For the decay correction, the time differences between the measurement of the 100 % sample and measurement of each fraction sample were calculated. Form this the A/A_0 ratio, the activity of the nuclide in the sample at the measurement time divided by the hypothetical activity at the measurement time of the 100 % sample, was calculated with the equation 5.18. $t_{1/2}$ represents the half-life of the nuclide and Δt represents the time difference between the measurement of the respective fraction sample and the 100 % sample.

$$A = A_0 \cdot e^{-\frac{ln2}{t_{1/2}} \cdot \Delta t} \tag{5.17}$$

$$\frac{A}{A_0} = e^{-\frac{ln2}{t_{1/2}} \cdot \Delta t} \tag{5.18}$$

With this ratio, the relative activity values of the nuclides in the fractions, representing A, were multiplied to get the decay time corrected A_0 values. These values were visualized together with the eluent fraction in figure 63.

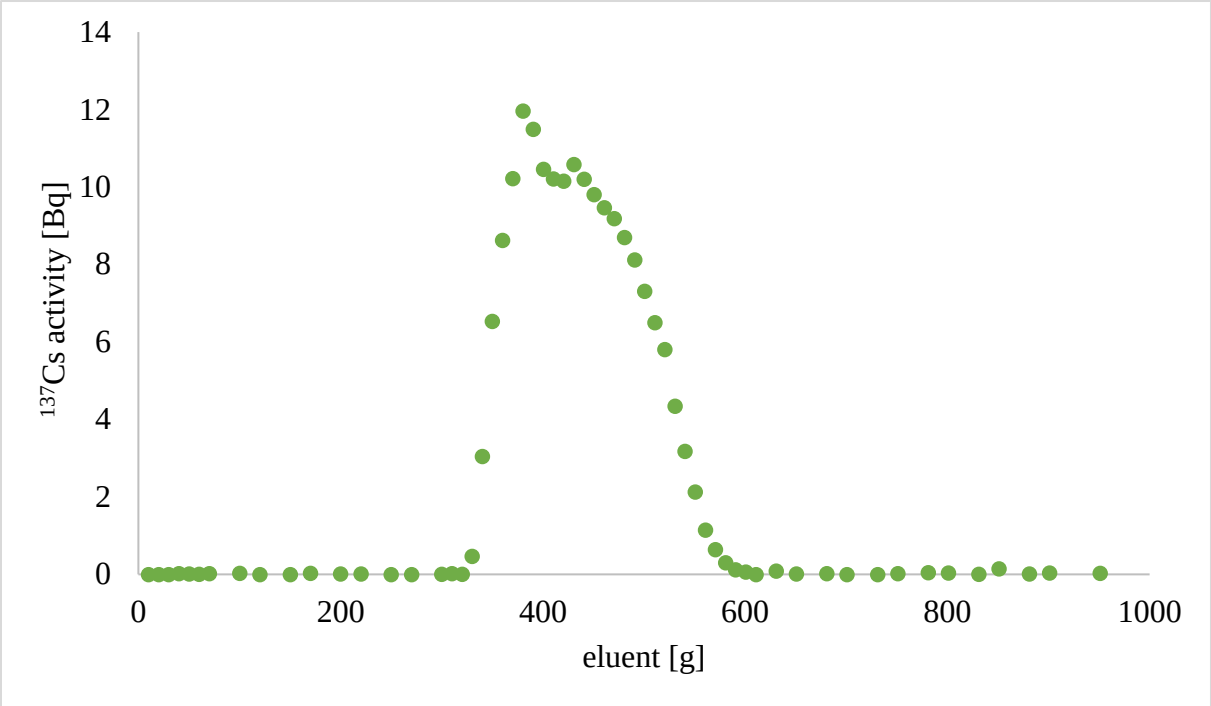

Figure 63: Absolute elution curve for the determination of ^{137}Cs in milk ash with the DOWEX® 50 WX8 (200-400 mesh) by Alfa Aesar, eluent ammonium-lactate at pH6, and sample measurement with gamma spectrometry

Figure 63 shows the progression of the ^{137}Cs elution during the Hot Column Chromatography with the DOWEX® 50 WX8 200-400 (H) by Alfa Aesar and the eluent ammonium-lactate at pH6. The elution region of ^{137}Cs was in this case between 310 and 600 g eluent. The activity maximum was 11.5 Bq in the elution fraction of 370-380 g eluent.

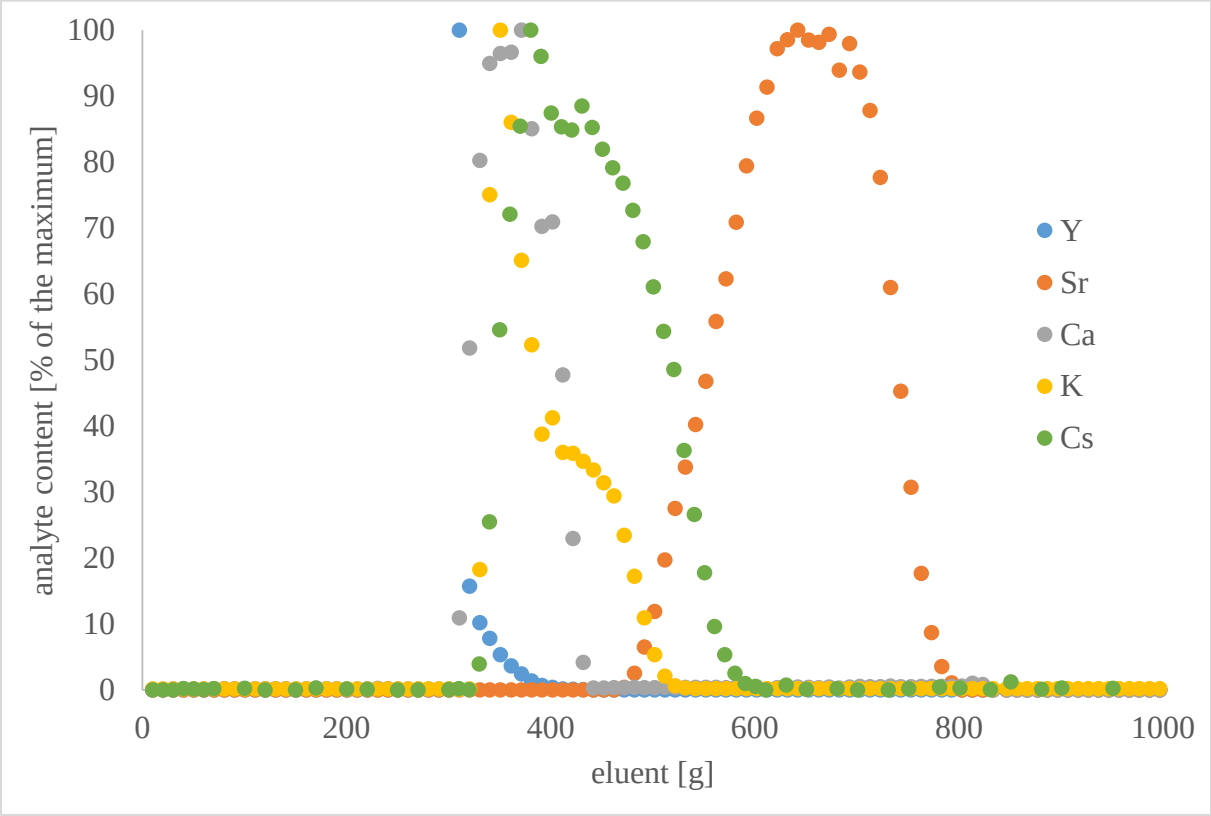

Figure 64: Relative elution curve for the determination of Y, K, Ca, Sr and Cs in milk ash with the DOWEX® 50 WX8 (200-400 mesh) by Alfa Aesar, eluent ammonium-lactate at pH6

Figure 64 presents the cesium elution region in relation to the elution regions of the other analytes: yttrium, calcium, potassium and strontium. To get a comparable elution curve, the activity values were all divided by the activity maximum and multiplied by 100 %. With this, a relative curve normed to the maximum was calculated, that was comparable to the elution curves of the other analytes. Figure 64 shows a strong overlap of the cesium elution region with the calcium and potassium elution regions and a partial overlap with the elution regions of the analytes yttrium and strontium. The overlap with the strontium elution curve is already known and accounted for during the routine analysis, separating the strontium fraction only after all cesium left the separation column. The overlap with the yttrium elution curve could be a problem during future yttrium separations. At least the cesium elution curve starts after the peak of the yttrium elution curve already left the column, so a partial separation could be possible, with only a small decrease of the yttrium yield.

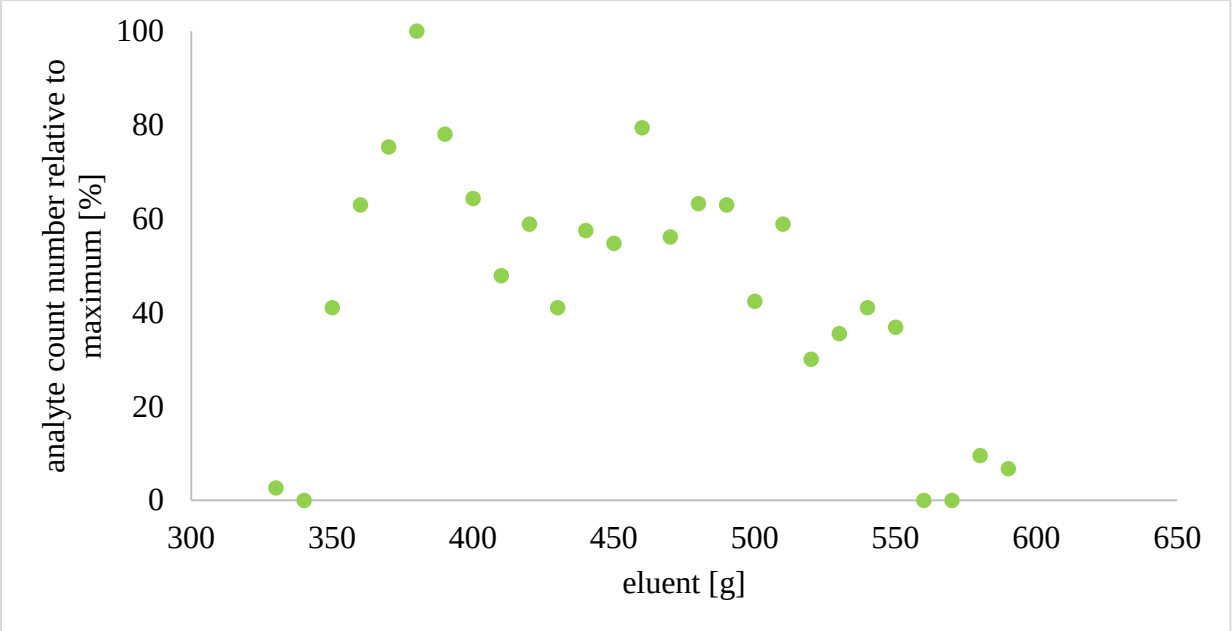

Figure 65: Elution curve of milk ash + 49.98 Bq ^{137}Cs, DOWEX by Alfa Aesar, fraction 33-59, eluent ammonium-lactate at pH7

Figure 65 shows the elution curve of ^{137}Cs detected with the Hot Column Chromatography with the DOWEX® 50 WX8 200-400 (H) by Alfa Aesar and the eluent ammonium-lactate at pH7. The curve shows the net counts of the presented fractions normed to the maximum value, which is presented at 100 %. Only the fractions, which showed significant signals during the LSC measurement, were measured with a gamma spectrometer. Therefore, the figure shows only a fraction of the elution process. A quantitative comparison between this elution curve and the elution curve for ^{137}Cs with the eluent at pH6 is not possible, as here the samples had a different measurement geometry. For the curve with the eluent at pH7, the samples were already mixed with LSC cocktail. But the relative values of the curve maximum and the elution region can be compared. The elution region of ^{137}Cs in this curve with ammonium-lactate at pH7 is 340 to 550 g eluent. Therefore, it is shifted by 30 g eluent to higher eluent throughput and is 80 g eluent narrower that the curve with ammonium-lactate at pH6, with an elution region for cesium at 310 to 600 g eluent. This means, the separation of cesium from the analytes yttrium and strontium worsens with a lower pH, due to the shift and broadening of the elution curve of cesium and the resulting stronger overlap with the analyte elution curves.

5.3.9 Effect of the eluent pH change to six on the separation quality of Y, Sr, K and Ca with the DOWEX® 50 WX8 (200-400 mesh) by Sigma Aldrich

As the acceleration of the strontium elution region with the pH change of the eluent ammonium-lactate from 7 to 6 was very successful for the DOWEX® 50 WX8 (200-400 mesh) by Alfa Aesar, it was tested whether the pH change would have a similar effect on the separation of strontium with the DOWEX by Sigma Aldrich.

The new pH of the eluent was tested by determining the elution regions of yttrium, strontium, potassium and calcium with the DOWEX by Sigma Aldrich as column material.

As detection method, for the quantification of these elements in the different fractions, ICP-OES was used, as previously for the elution curve with the DOWEX by Sigma Aldrich with ammonium-lactate at pH7.

As standard sample matrix, 10.00 g not contaminated milk ash, prepared from commercially available whole long-life milk by the brand Berchtesgadener Land, was used. It was solved in 80 mL of the usual 1:1 mixture of 6 M hydrochloric acid and 1.5 molar lactic acid. Additionally, 1 mL of the stable yttrium tracer, containing 10 mg Y, and 2 mL stable strontium tracer, containing in total 100 mg Sr, were added. Potassium and calcium were naturally present in the sample matrix in significant amounts, according to the milk packaging 124 mg calcium per 100 mL. After the sample was solved and applied to the column, the Hot Column Chromatography was performed at the elution speed of 2.5 mL/min. During this, 100 elution fractions à 10 ml were collected. For the ICP-OES measurement, fraction samples were diluted 1:250. Per ICP-OES sample, 40 µL of the fractions were used and 2 mL concentrated nitric acid was added for pH adjusting. The samples were filled up to a volume of 10 mL with bidistilled water.

For the ICP-OES measurement, the same calibration curve was used as the one calculated for the initial determination of the elution curve with the new DOWEX® 50 WX8 (200-400 mesh) by Alfa Aesar in section 5.3.1.

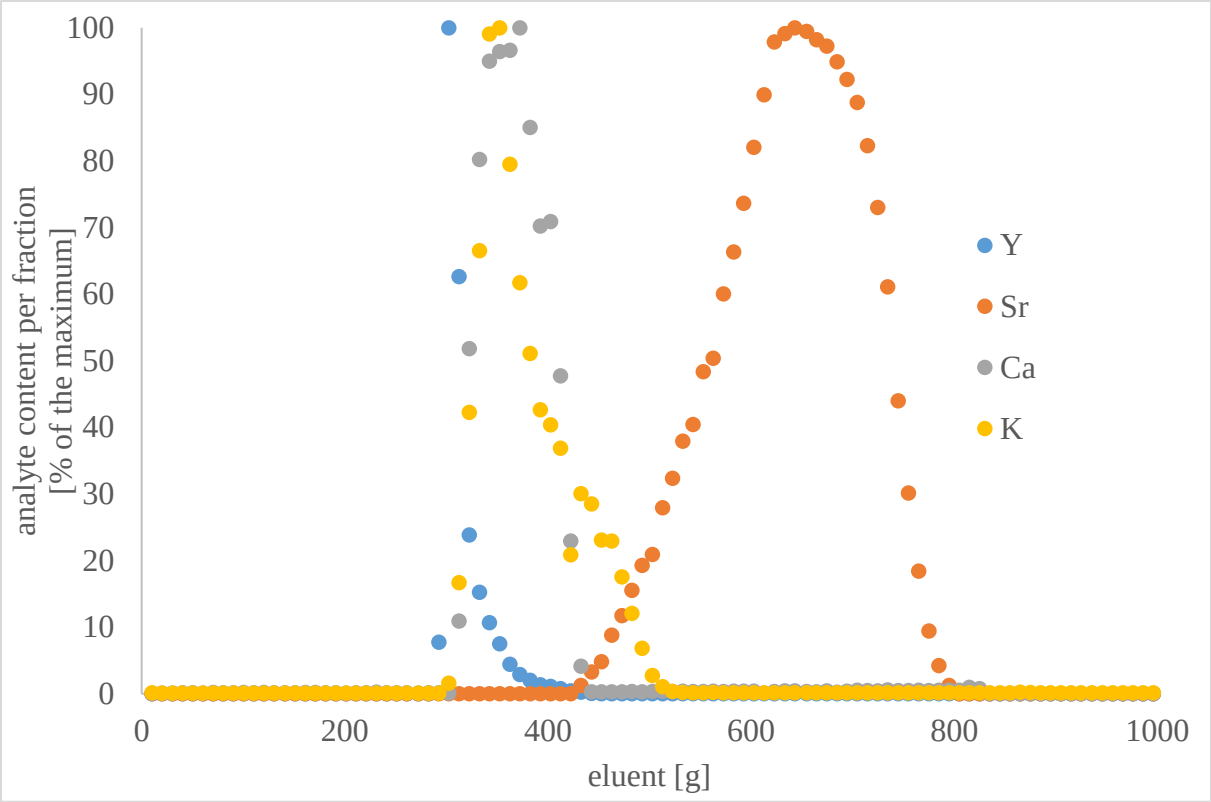

Figure 66: Relative elution curve for the determination of Y, K, Ca and Sr in milk ash with the DOWEX® 50 WX8 (200-400 mesh) by Sigma Aldrich, eluent ammonium-lactate at pH6, and sample measurement with ICP-OES

Figure 66 shows the resulting elution curves for the for the determination of K, Ca, Y and Sr in milk ash with the DOWEX® 50 WX8 (200-400 mesh) by Sigma Aldrich and the eluent ammonium-lactate at pH6. The sample measurement was performed with ICP-OES. This is the relative elution curve with the concentration maximum normed to 100 % and the rest of the concentrations presented relative to the concentration maximum of the of the analyte during the elution.

A very good separation between yttrium and strontium, a good separation between calcium and strontium and an acceptable separation between potassium and strontium were achieved. The separation between yttrium, calcium and potassium was quite bad, the elution regions of the elements overlapped almost completely. But at least the relative content of potassium and calcium was quite small in the maximum range of yttrium. The reason for this could also be, that fraction 30, which is the fraction with the highest yttrium content, contained solid precipitate, that could not be resolved through heating after the sample cooled down. This precipitate is likely calcium, but could also contain potassium, and subsequently was not accounted for during the ICP-OES measurement.

Table 44: Elution regions and the concentration maxima of the analytes K, Ca, Y and Sr in milk ash recorded with the DOWEX® 50 WX8 (200-400 mesh) by Sigma Aldrich, eluent ammonium-lactate at pH6, sample measurement with ICP-OES

element	elution region [g]	concentration maximum [g]
yttrium	280-420	290-300
strontium	430-790	630-640
calcium	280-440	360-370
potassium	300-510	340-350

Table 48 shows the elution regions of the analytes and their concentration maxima for a direct comparison and numerical visualization of the overlap of their elution regions.

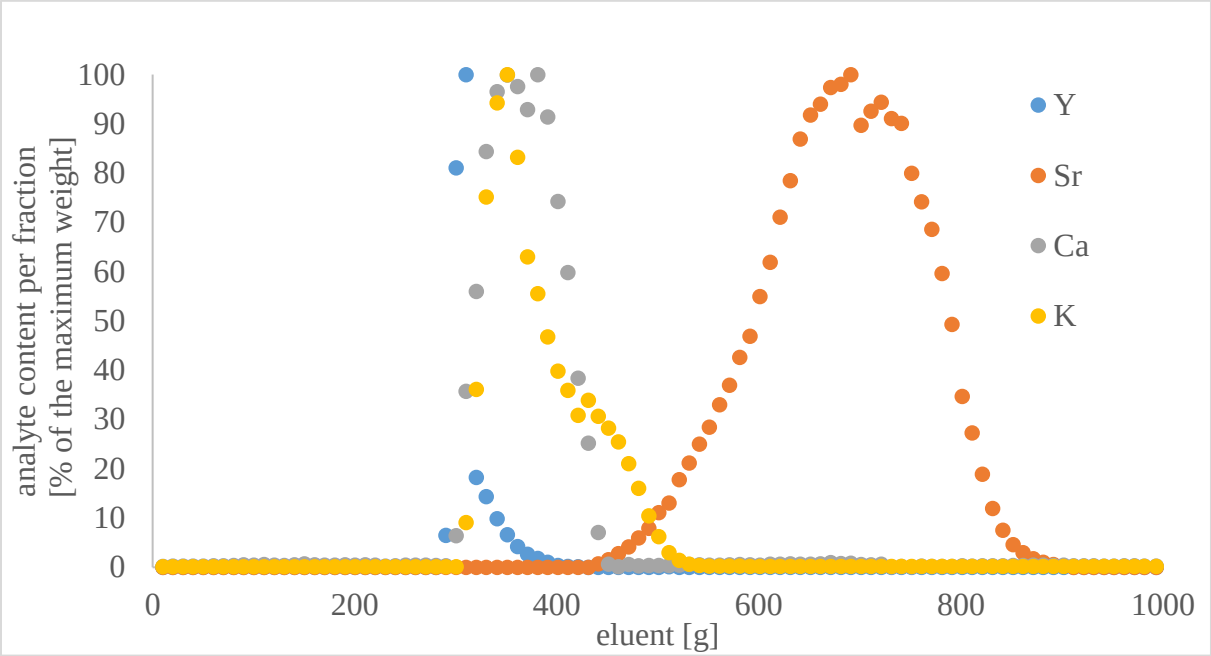

Figure 67: Relative elution curve for the determination of Y, K, Ca and Sr in milk ash with the DOWEX® 50 WX8 (200-400 mesh) by Sigma Aldrich, eluent ammonium-lactate at pH7, and sample measurement with ICP-OES

Figure 67 shows the elution curve for the determination of K, Ca, Y and Sr in milk ash with the DOWEX® 50 WX8 (200-400 mesh) by Sigma Aldrich and the eluent ammonium-lactate at pH7. The sample measurement was performed with ICP-OES. The general structure and positions of the elution regions between the elution curves with ammonium-lactate at pH 7 and at pH 6 are quite similar. The elution curve with ammonium-lactate at pH6 as eluent showed a similar overlap between the elution regions of yttrium, calcium and potassium and a similar width of the curves for these elements, as the elution curve at pH7. The most significant difference between those two elution curves was the elution region of strontium, that was narrowed by 100 g eluent through lowering the eluent pH. With this, a comparable strontium elution region to the established DOWEX was achieved with simple adjusting of the eluent pH. This solved the problem of a longer and more laborious separation with the new DOWEX and the pH change was planned to be incorporated into routine analytics.

Table 45 shows the comparison of the elution regions for the separation of each analyte with ammonium-lactate at pH 6 and at the established pH 7.

Table 45: Comparison between eluent ammonium-lactate at pH6 and at pH7, elution regions and the concentration maxima of the analytes K, Ca, Y and Sr in milk ash recorded with the DOWEX® 50 WX8 (200-400 mesh) by Sigma Aldrich, sample measurement with ICP-OES

eluent pH	**ammonium-lactate pH 6**		**ammonium-lactate pH 7**	
element	**elution region [g]**	**concentration maximum [g]**	**elution region [g]**	**concentration maximum [g]**
yttrium	280-420	290-300	290-400	300-310
strontium	430-790	630-640	430-890	680-690
calcium	280-440	360-370	290-450	370-380
potassium	300-510	340-350	300-520	340-350

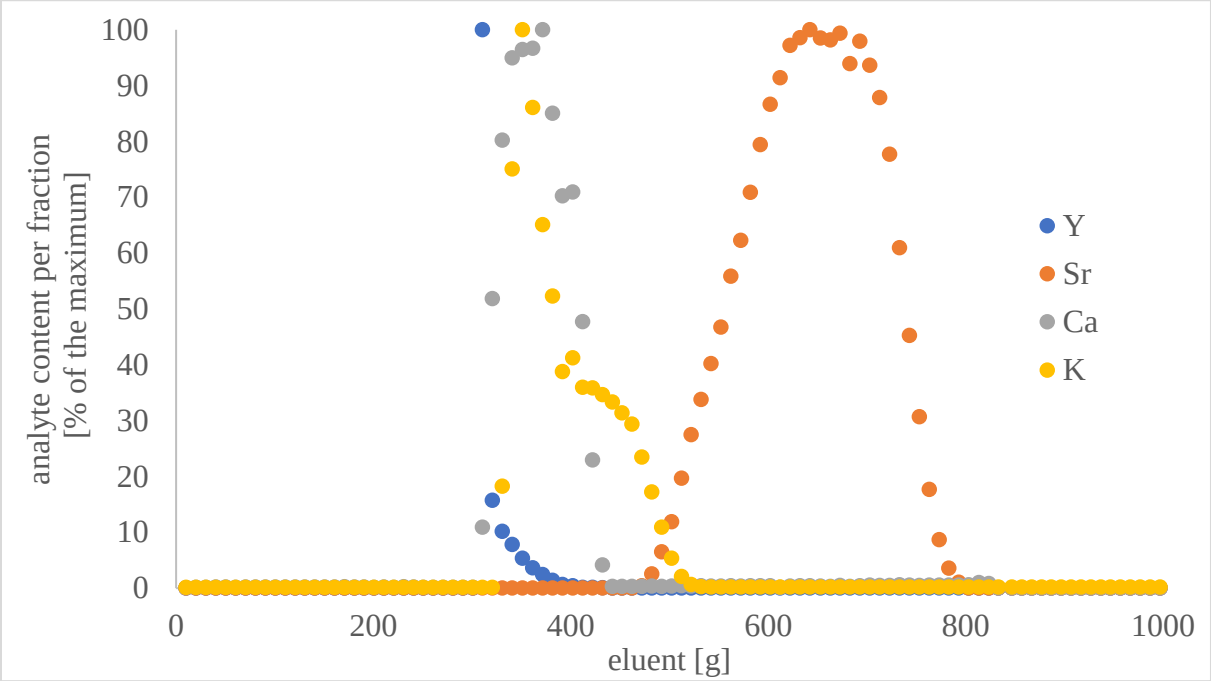

Figure 68: Relative elution curve for the determination of Y, K, Ca and Sr in milk ash with the DOWEX® 50 WX8 (200-400 mesh) by Alfa Aesar, eluent ammonium-lactate at pH6, and sample measurement with ICP-OES

Figure 68 shows the elution curve for the for the determination of K, Ca, Y and Sr in milk ash with the DOWEX® 50 WX8 (200-400 mesh) by Alfa Aesar and the eluent ammonium-lactate at pH6 for comparison with the one achieved with the DOWEX by Sigma Aldrich and ammonium-lactate at the same pH.

With both DOWEX providers, very good separations between yttrium and strontium, good separations between calcium and strontium and acceptable separations between potassium and strontium were achieved. The separations between yttrium, calcium and potassium were quite bad, the elution regions of these elements overlapped almost completely. The maxima of the elution curves were for both DOWEX providers approximately at the same eluent throughput. The elution regions were broader with the DOWEX by Sigma Aldrich with the beginning of the elution regions slightly shifted to lower eluent volumes.

Table 46: Comparison between the DOWEX by Alfa Aesar and Sigma Aldrich, elution regions and the concentration maxima of the analytes K, Ca, Y and Sr in milk, eluent ammonium-lactate at pH6, sample measurement with ICP-OES

DOWEX provider	**Alfa Aesar ammonium-lactate pH6**		**Sigma Aldrich ammonium-lactate pH 6**	
element	**elution region [g]**	**concentration maximum [g]**	**elution region [g]**	**concentration maximum [g]**
yttrium	300-410	300-310	280-420	290-300
strontium	470-790	630-640	430-790	630-640
calcium	300-440	360-370	280-440	360-370
potassium	320-520	340-350	300-510	340-350

Table 46 shows the elution regions of the analytes and their concentration maximum for a direct comparison between the DOWEX by the providers Sigma Aldrich and Alfa Aesar and numerical visualization of the overlap of their elution regions.

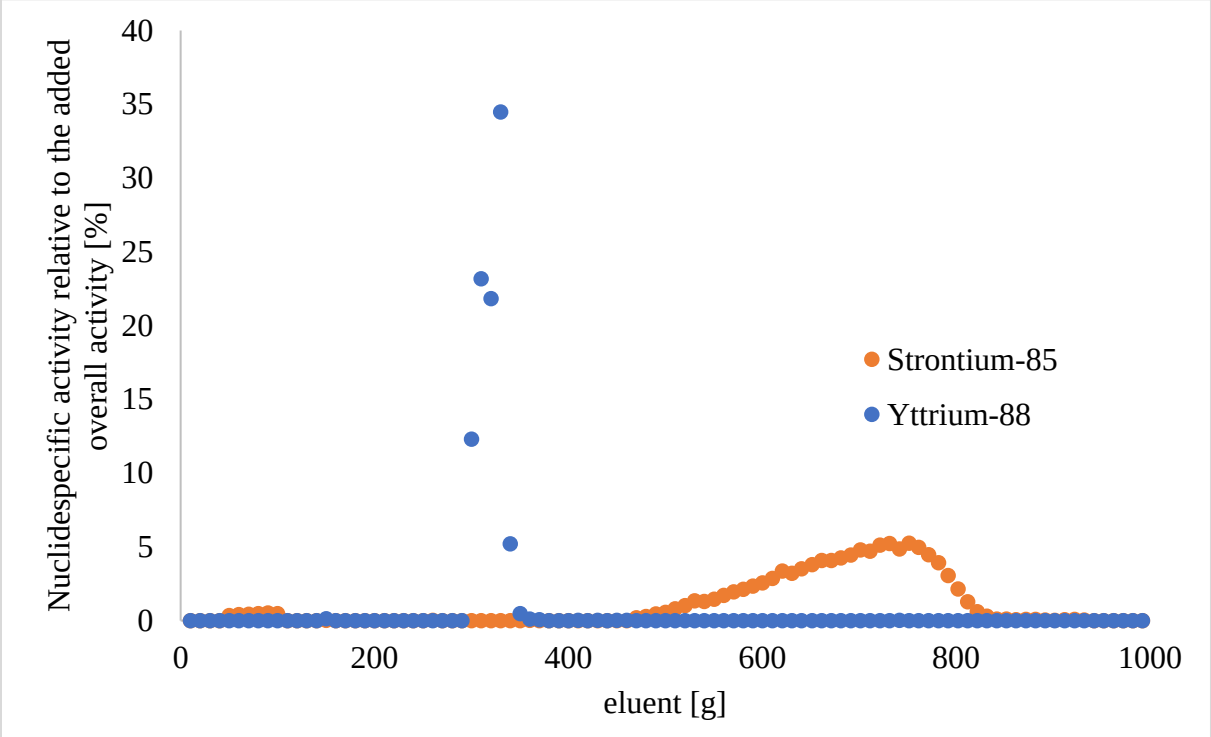

Figure 69: Elution regions of Y and Sr in milk as recorded with the established DOWEX® 50 WX8 200-400 (H) resin by Serva

Figure 69 shows a recording of the elution regions of yttrium and strontium achieved with the established DOWEX® 50 WX8 200-400 (H) resin by Serva, to compare these results with the new results with the DOWEX by Sigma Aldrich with the eluent ammonium-lactate at pH6. The distribution was determined with a gamma active multi-nuclide tracer and the activities relative to the 100 % tracer were measured with gamma spectrometry (5.2.2.1). As the tracer did not contain calcium or potassium isotopes, their elution region could not be determined with this method. Because of the different methods, the absolute quantities of analytes in the individual samples cannot be compared, but the distribution of the analytes, alias the elution regions, are comparable as the Hot Chroma separations were performed in an almost identical way.

Table 47: Comparison of the results between the DOWEX® 50 WX8 (200-400 mesh) by Serva, eluent ammonium-lactate at pH7, and by Sigma Aldrich, eluent ammonium-lactate at pH6, elution regions and the concentration maxima of the analytes Y and Sr in milk ash

DOWEX provider	**Serva ammonium-lactate pH7**		**Sigma Aldrich ammonium-lactate pH6**	
element	**elution region [g]**	**maximum [g]**	**elution region [g]**	**maximum [g]**
yttrium	270-440	300-310	280-420	290-300
strontium	470-840	730-740	430-790	630-640

Figure 69 and table 47 show the shift of the yttrium elution region by 20 g eluent to higher eluent volumes with the Sigma Aldrich resin and ammonium-lactate at pH6, compared to the establishes separation system. The yttrium maxima were almost at the same eluent throughput and the yttrium elution region of the newer system was by 30 g eluent narrower than with the older system. The strontium elution regions have almost the same width, with the newer one being slightly narrower. The strontium elution region with the DOWEX by Sigma Aldrich and ammonium-lactate at pH6 was shifted by about 40 g eluent to lower eluent throughput, compared to the established system with the DOWEX by Serva and ammonium-lactate at pH7. This would mean a faster strontium elution, but also a stronger overlap of its elution region with the cesium elution region.

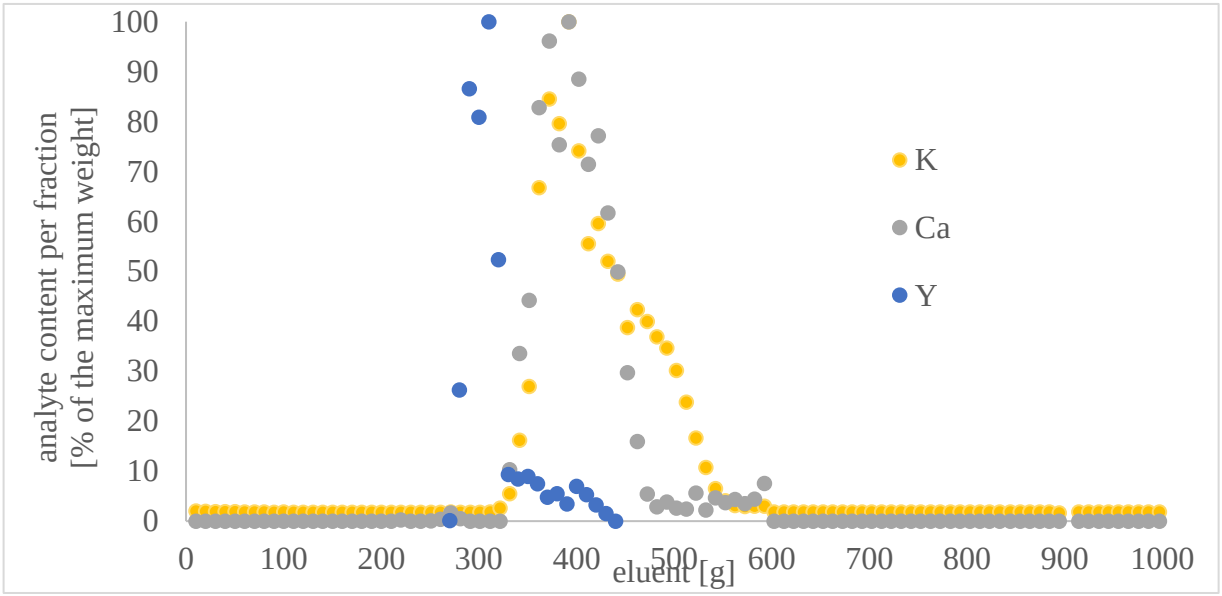

Figure 70: Elution regions of Y, Ca and K recorded with the established DOWEX® 50 WX8 200-400 (H) resin by Serva

Figure 70 shows an older recording of the elution regions of yttrium, calcium and potassium, achieved with the established DOWEX® 50 WX8 200-400 (H) resin by Serva, to compare these results with the new results with the Sigma Aldrich resin with ammonium-lactate at pH6. These elution curves were also recorded with ICP-OES measurements using stable tracers.

The older elution curve is not as exact as the newer one. This is because, instead of a professional standard, a self-made salt solution was used for the preparation of the ICP-OES calibration curve. Additionally, the yttrium curve was recorded separately from the calcium and potassium elution curves and there could be differences in the separations during the Hot Column Chromatography. Therefore, the edges of the elution regions for this older elution curves are less precise and tailing is present at their ends.

Table 48: Comparison of the results between the DOWEX® 50 WX8 (200-400 mesh) by Serva, eluent ammonium-lactate at pH7, and by Sigma Aldrich, eluent ammonium-lactate at pH6, elution regions and the concentration maxima of the analytes Y, Ca and K in milk ash

DOWEX provider	**Serva ammonium-lactate pH7**		**Sigma Aldrich ammonium-lactate pH6**	
element	**elution region [g]**	**maximum [g]**	**elution region [g]**	**maximum [g]**
yttrium	270-440	300-310	280-420	290-300
calcium	320-480	380-390	280-440	360-370
potassium	320-560	380-390	300-510	340-350

Table 48 and figure 70 show the elution curves recorded with the DOWEX by Sigma Aldrich and ammonium-lactate at pH6, compared to the older recording with the DOWEX by Serva and ammonium lactate at pH7. The yttrium elution curve had its maximum almost at the same eluent volume as the elution curve recorded with the older DOWEX, but its beginning was shifted to slightly higher eluent volumes and the elution region was by 30 g eluent narrower than the one recorded with the Serva DOWEX. The maximum of the calcium elution curve was shifted by 20 g to lower eluent volumes, compared to the maximum of the elution curve recorded with the older DOWEX. The elution region of calcium was the same width as the older one with the new system. The maximum of the potassium elution curve is shifted by 40 g to lower eluent volumes, compared to the elution curve recorded with the Serva DOWEX. All in all, these changes of the elution regions meant a stronger overlap between the elution region of the analyte yttrium with the interfering elements calcium and potassium, than was the case for the older elution curves, which would affect the separation and analysis of yttrium negatively.

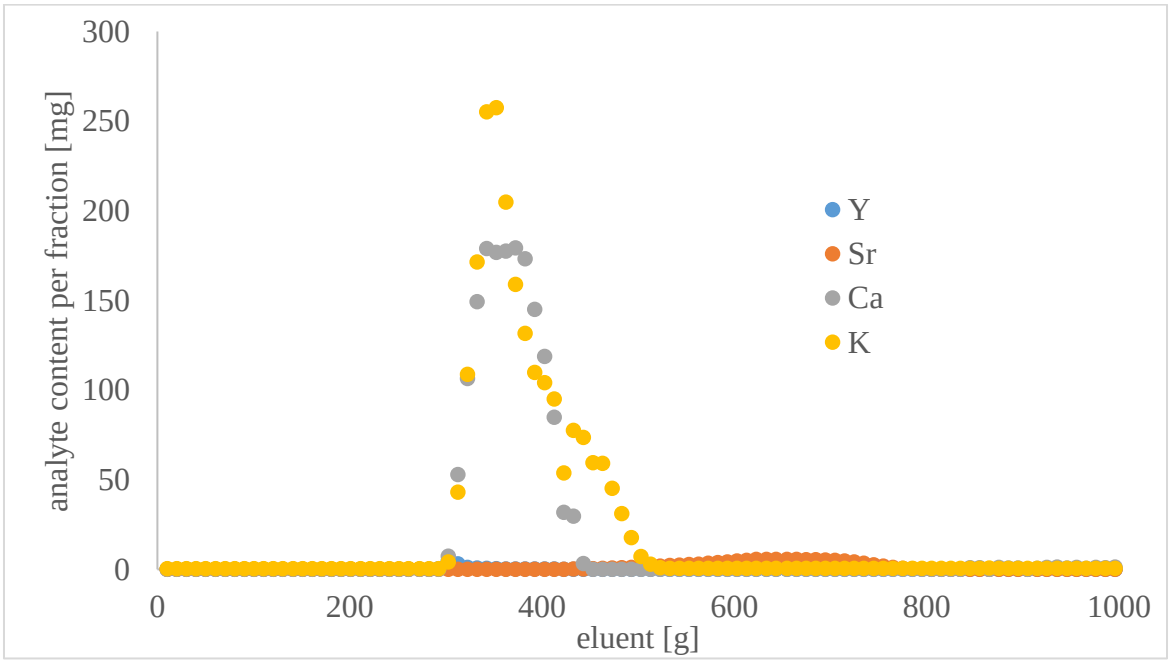

Figure 71: Absolute elution curve for the determination of Y, K, Ca and Sr in milk ash with the DOWEX® 50 WX8 (200-400 mesh) by Sigma Aldrich, eluent ammonium-lactate at pH6, and sample measurement with ICP-OES

For comparison, figure 71 shows the absolute results of the distribution of the different analytes during the elution process with the DOWEX by Sigma Aldrich and the eluent ammonium-lactate at pH6. The interfering elements calcium and potassium were present in much higher concentrations in the sample matrix as the expected amounts of the analytes yttrium and

strontium, if they were present at all. Additionally, a significant potassium background was measured for all fractions. This could be because of the use of glassware, which contains potassium, or because of the insufficient separation performance of the column for potassium.

As a summary of the results, it was found that the change of the pH of ammonium-lactate from 7 to 6 led to the significant acceleration of the strontium elution, that was hoped for. The downside to this was the worse separation of yttrium from potassium and calcium, due to accelerated elution and narrower elution regions of these analytes and the resulting overlap of their elution regions.

5.3.10 Precipitation of $SrSO_4$ in eluent at pH6 and pH7

An acceleration of the strontium elution, and therefore narrowing of the elution curve, was achieved through the pH change of the eluent ammonium-lactate from seven to six. This change was successful with the DOWEX® 50 WX8 (200-400 mesh) by both new providers, Alfa Aesar and Sigma Aldrich. As the pH of the eluent was changed from pH7 to pH6, it had to be made sure, that the precipitation of strontium as $SrSO_4$ (strontium sulphate), following the Hot Column Chromatography separation, worked as well and as efficient in ammonium-lactate at pH6, as in ammonium-lactate at pH7. The pH change could only be implemented in routine analytics if it had no negative influence on the precipitation of $SrSO_4$. Whether this is the case, is explored in the following section.

The steps of the precipitation experiment were based on the analysis steps after the separation, according to the analysis instruction [63] and as detailed in section 5.1.4. First, the samples for the experiment were prepared from ammonium-lactate at pH6 and pH7, 200 g each. Then to each sample 1 mL of a 50 mg Sr/mL strontium-tracer was added, as it is usually added to each real sample before the analysis starts. The sample preparation is presented in table 53.

Table 49: Sample preparation with ammonium-lactate at pH6 and pH7 for the precipitation experiment of strontium as $SrSO_4$

ammonium-lactate pH	pH6	pH7
ammonium-lactate mass [g]	200	
added Sr-tracer	1 mL equivalent to 50 mg Sr	

Then concentrated sulfuric acid (97 %) was slowly added to each sample with a dropping funnel, while stirring and in an ice bath, to compensate for the produced heat. The samples were placed in an ice cooled ultrasonic bath, to complete the precipitation. After the precipitate was settled, it was filtered through a Satorius filter cubicle with a paper filter (Whatman 42) and washed with 10 mL sulphate containing water and 10 mL acetone (p.a.). The labelled filters with the precipitate were then placed in labelled and tared small porcelain bowls. In these bowls, the filters were incinerated at 600°C ± 20°C for 20 minutes in the muffle furnace. After the resulted ashes cooled down, they were weighed with an analytical balance. The results were then compared to the 100 % precipitation value of 0.1048 g $SrSO_4$, which would be achieved if all the added strontium were to be precipitated. The resulting precipitation yields are shown in table 50.

Table 50: Results of the precipitation experiment of $SrSO_4$ in ammonium-lactate at pH6 and pH7

ammonium-lactate pH	pH6	pH7
$SrSO_4$ precipitate [g]	0.1074 ± 0.001	0.1049 ± 0.001
percentage of the 100 % value [%]	102.5 ± 2.5	100.1 ± 2.4

The experiment showed comparably high precipitation yields for both samples, indicating a complete precipitation. Both samples showed a result of over 100 %. This could be due to unprecise weighing, or because of an uncomplete incineration of the filter. The filters used for the separation normally are burned completely during incineration and no ashes remain of them,

leaving only analyte ashes behind. For these samples, the burning of the filter might be incomplete. So, the results should be compared relatively to each other and not in absolute numbers.

The deviation of the yield with ammonium-lactate at pH6 from the yield with the eluent at pH7 and from the 100 % yield is only 2.38 %. This is an acceptable deviation for an experimental step. All in all, the results of this experiment were interpreted as successful and the precipitation yields for $SrSO_4$ with ammonium-lactate at pH6 and pH7 as comparable. This makes a pH change of the eluent from 7 to 6 permissible for the elution acceleration.

5.3.11 Comparison of the Sr-yields for environmental monitoring between the established and the new column material with the adjusted eluent pH

The new DOWEX® 50 WX8 (200-400 mesh) by Alfa Aesar was previously extensively tested, regarding its abilities to separate the analytes yttrium and strontium from the confounding elements cesium, potassium and calcium. Finally, it was applied for the strontium analysis of real samples for the routine environmental monitoring. The analysis with the new DOWEX was performed according to the established instruction detailed in section 5.1. The strontium-yield was determined titrimetrically. The only adjustment for the new resin was the pH change of the eluent ammonium-lactate from pH7 to pH6. This change proved successful in counteracting the broadening and shift of the elution curve of strontium to higher eluent volumes, caused by the new DOWEX. Two Hot Chroma columns were filled with the new DOWEX® 50 WX8 (200-400 mesh) by Alfa Aesar and were used for the analyses. The strontium yields of the analyses performed with this new DOWEX by Alfa Aesar were recorded and compared to each other and earlier analyses of comparable samples with the established DOWEX by Serva. The results of these investigations and comparisons are presented in the following section.

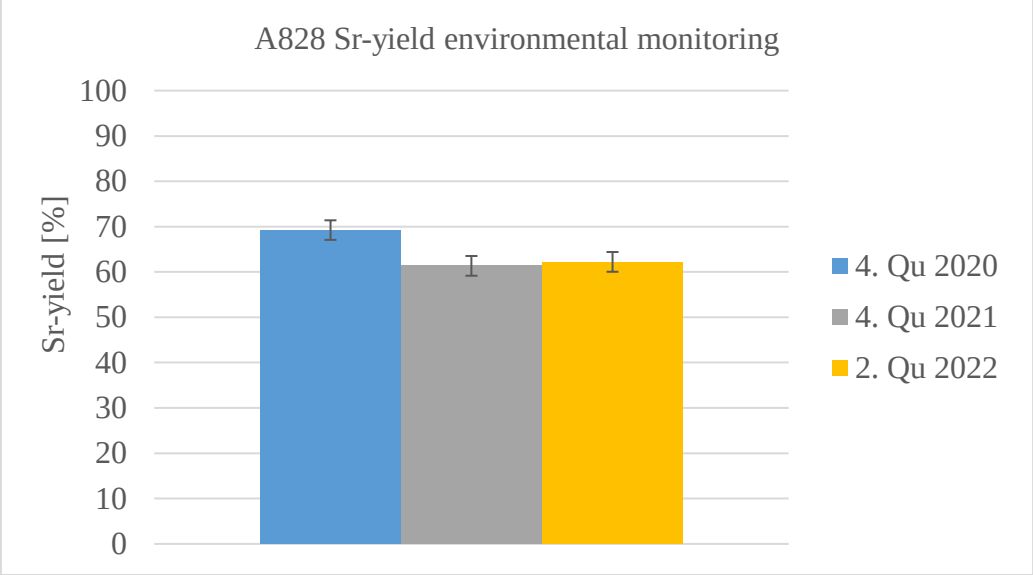

Figure 72: Sr yields for milk samples from the sampling point A828 for comparison

Table 51: Overview over the Sr-yield results for the milk samples from the sampling point A828 and the complications during the analyses

sample number	sample kind	quarter/ year	reference date	sampling place	Sr-yield [%]	challenges
#3002007	milk	2. Qu 2022	02.05.2022	A828	62 ± 2	Irregular color change of the indicator during yield determination
#3001971	milk	4. Qu 2021	25.10.2021	A828	61 ± 2	
#3001908	milk	2. Qu 2021	25.05.2021	A828	80 ± 2	Problems during yield determination: irregular color change of the indicator, no color change during titration, otherwise normal analysis, medium of other sample yields used as yield
#3001872	milk	4. Qu 2020	29.10.2020	A828	69 ± 2	

Figure 72 and table 51 show the measurement results for milk samples taken at different times at the sampling place A828, representing a farm located near a nuclear power plant. The milk sample number #3002007 was analyzed with the new DOWEX by Alfa Aesar and eluent at pH6. For this sample, a strontium-yield of 62 % was achieved under the new analysis conditions. There were problems with an irregular color change of the indicator before the titration for the yield determination could be performed. But regardless of this, the yield determination could be reliably performed by titration of the sample with 0.1 M $ZnSO_4$. The comparison to the Sr yields achieved for samples of the same kind and origin with the established DOWEX shows an acceptable deviation. Even though the sample number #3001908 from the second quarter of 2021 on the first glance seems to have a significantly better yield, it caused severe problems during the yield determination. This sample also caused an irregular color change of the indicator, before the titration for the yield determination could be performed. But compared to the new sample, no color change during the titration could be achieved. Because no other problems occurred during the analysis and it was performed as planned, the medium strontium-yield of all the other environmental monitoring samples from this time period was calculated and utilized as yield for the sample number #3001908. This process was acceptable for the environmental monitoring routine analysis. But because the strontium-yield for this sample is a constructed and not experimentally determined value, it is not suitable for this scientific comparison. Concluding from this, the most recent strontium analysis of milk from this farm with the new DOWEX by Alfa Aesar, performed by the same operator, was more successful than the analysis from the year before with the established DOWEX by Serva, as a more reliable strontium yield could be determined with the new DOWEX.

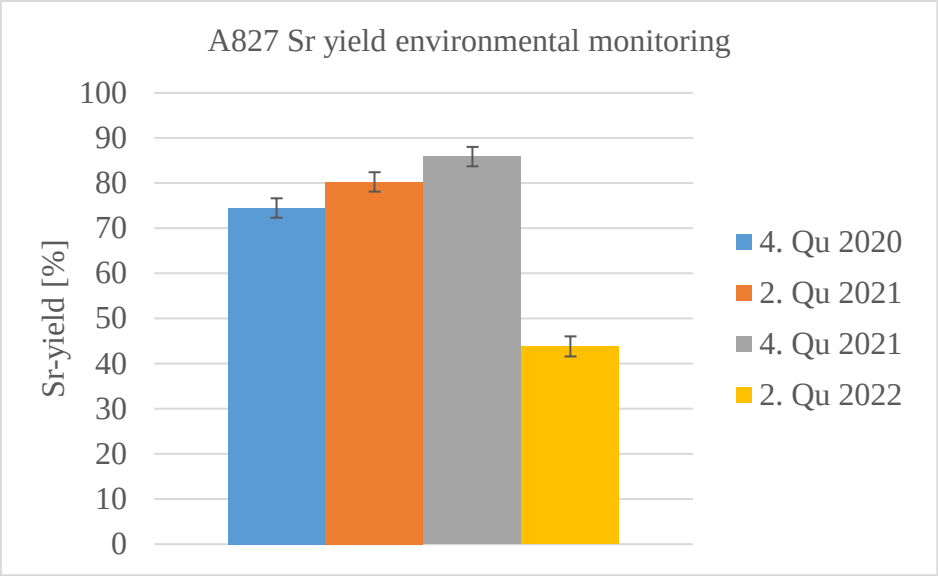

Figure 73: Sr yields for milk samples from the sampling point A827 for comparison

Table 52: Overview over the Sr-yield results for the milk samples from the sampling point A827 and the complications during the analyses

sample number	sample kind	quarter/ year	reference date	sampling place	Sr-yield [%]	challenges
#3002008	milk	2. Qu 2022	02.05.2022	A827	44 ± 2	Problems with scales Irregular color change of the indicator during yield determination
#3001972	milk	4. Qu 2021	27.10.2021	A827	86 ± 2	
#3001909	milk	2. Qu 2021	25.05.2021	A827	80 ± 2	Problems during yield determination: irregular color change of the indicator, no color change during titration, otherwise normal analysis, medium of other sample yields used as yield
#3001873	milk	4. Qu 2020	29.10.2020	A827	74 ± 2	

Figure 73 and table 52 show the measurement results for milk samples taken at different times at the sampling place A827, representing a farm located near a nuclear power plant. The milk sample number #3002008 was analyzed with the new DOWEX by Alfa Aesar and eluent at pH6. For this sample, a strontium-yield of 44 % was achieved under the new analysis conditions. There was a problem with an overload of the scales during the analysis, but it was successfully solved. There were additional problems with an irregular color change of the indicator before the titration for the yield determination could be performed. But regardless of this, the yield determination could be reliably performed by titration of the sample with 0.1 M $ZnSO_4$. The comparison to the Sr yields achieved for samples of the same kind and origin with the established DOWEX shows a significant yield loss for the most recent strontium analysis with the new DOWEX. But even though the Sr-yield was significantly smaller than for the

previous analyses, the yield was enough to achieve the necessary level of detection and ensure a reliable environmental monitoring of the area. Even though the sample number #3001909, from the second quarter of 2021, on the first glance seems to have a significantly better yield, it caused severe problems during the yield determination. This sample also caused an irregular color change of the indicator, before the titration for the yield determination could be performed. But compared to the new sample, no color change during the titration could be achieved. Because no other problems occurred during the analysis and it was performed as planned, the medium strontium-yield of all the other environmental monitoring samples from this time period was calculated and utilized as yield for the sample number #3001909. This process was acceptable for the environmental monitoring routine analysis. But because the Sr-yield for this sample is a constructed and not experimentally determined value, it is not suitable for this scientific comparison. Concluding from this, the most recent strontium analysis of milk from this farm with the new DOWEX by Alfa Aesar, performed by the same operator, was more successful than the analysis from the year before with the established DOWEX by Serva, as a more reliable Sr yield could be determined with the new DOWEX.

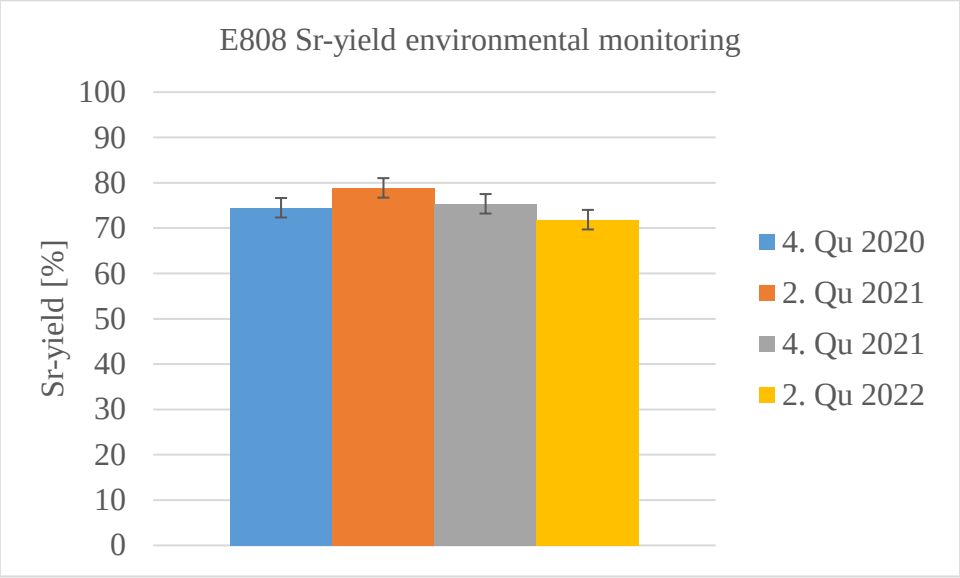

Figure 74: Sr yields for milk samples from the sampling point E808 for comparison

Table 53: Overview over the Sr-yield results for the milk samples from the sampling point E808 and the complications during the analyses

sample number	sample kind	quarter/ year	reference date	sampling place	Sr yield [%]	challenges
#4002131	milk	2. Qu 2022	10.05.2022	E808	72 ± 2	
#4002098	milk	4. Qu 2021	19.10.2021	E808	75 ± 2	
#4002020	milk	2. Qu 2021	18.05.2021	E808	79 ± 2	
#4001987	milk	4. Qu 2020	07.10.2020	E808	74 ± 2	

Figure 74 and table 53 show the measurement results for milk samples taken at different times at the sampling place E808, representing a farm located near a nuclear power plant. The milk sample number #4002131 was analyzed with the new DOWEX by Alfa Aesar and eluent at pH6. For this sample, a strontium-yield of 72 % was achieved under the new analysis conditions. The comparison to the strontium yields achieved for samples of the same kind and origin with the established DOWEX shows a slightly smaller yield for the most recent Sr analysis, but this deviation is still at an acceptable level.

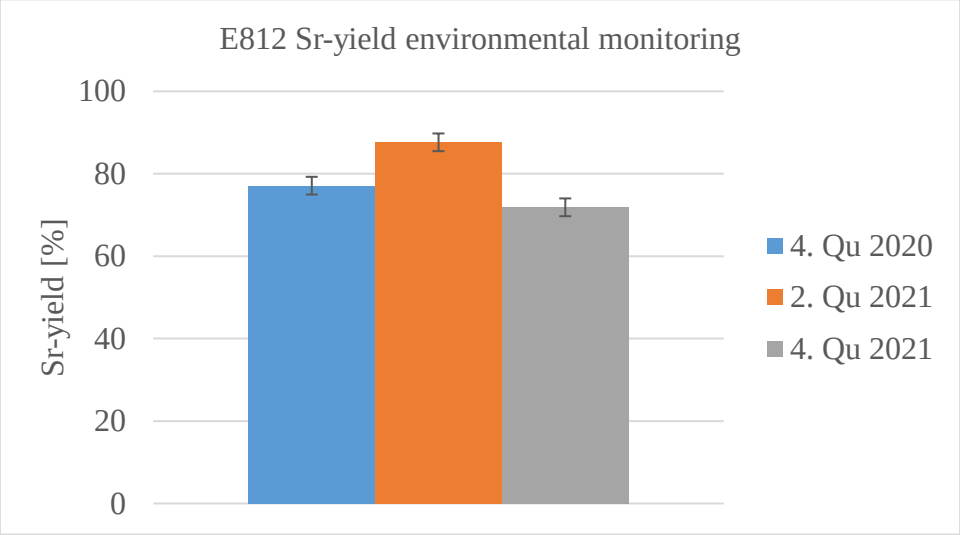

Figure 75: Sr yields for milk samples from the sampling point E812 for comparison

Table 54: Overview over the Sr-yield results for the milk samples from the sampling point E812 and the complications during the analyses

sample number	sample kind	quarter/ year	reference date	sampling place	Sr yield [%]	challenges
#4002132	milk	2. Qu 2022	10.05.2022	E812	50 ± 2	Extremely low yield determined (9.6 mL $ZnSO_4$ during titration needed, 10 mL $ZnSO_4 \equiv$ 0 % yield) otherwise normal analysis, yield of 50 % was assumed
#4002099	milk	4. Qu 2021	19.10.2021	E812	72 ± 2	
#4002021	milk	2. Qu 2021	18.05.2021	E812	88 ± 2	
#4001988	milk	4. Qu 2020	28.10.2020	E812	77 ± 2	

Figure 75 and table 54 show the measurement results for milk samples taken at different times at the sampling place E812, representing a farm located near a nuclear power plant. A reliable strontium yield for the milk sample number #4002132 could unfortunately not be determined with the new DOWEX by Alfa Aesar. The color change during the titration for the yield determination of Sr occurred only at 9.6 mL of added $ZnSO_4$. This would correspond to a yield of only 7 %. No other problems occurred during the analysis and it was performed as planned: turbidity was observed in the sample during the precipitation and a significant amount of precipitate was deposited on the filter after filtration. Because of this, it was assumed that the

separation was successful and the problem occurred during the yield determination. Therefore, the result of the yield determination was declared implausibly low. It was rejected and instead conservatively assumed as 50 %. This process was acceptable for the environmental monitoring routine analysis. But because the strontium-yield for this sample was a constructed and not experimentally determined value, it was not suitable for this scientific comparison. Therefore, the comparison of the Sr yield with the new DOWEX to the Sr yields achieved for samples of the same kind and origin with the established DOWEX was, in this case, not reasonable.

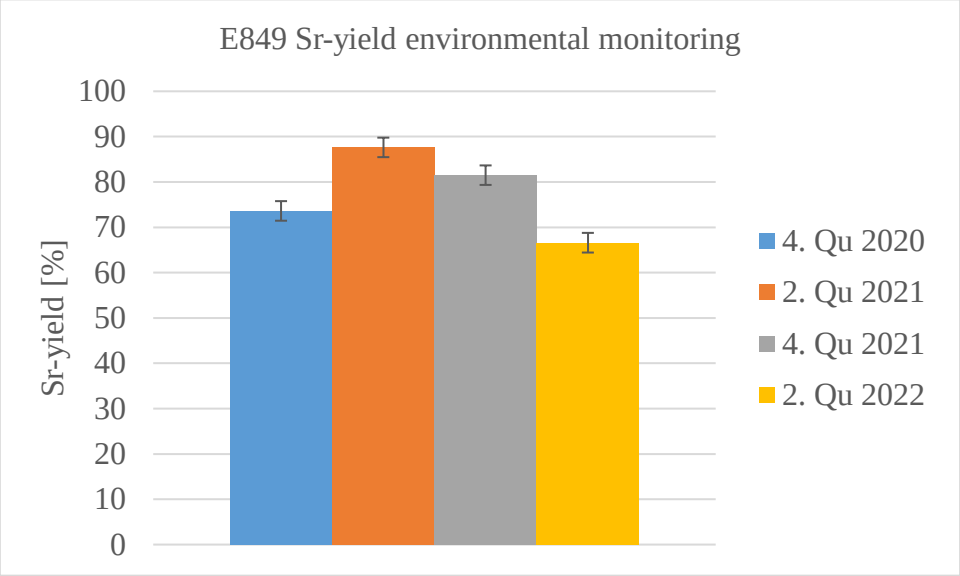

Figure 76: Sr yields for milk samples from the sampling point E849 for comparison

Table 55: Overview over the Sr-yield results for the milk samples from the sampling point E849 and the complications during the analyses

sample number	sample kind	quarter/ year	reference date	sampling place	Sr-yield [%]	challenges
#4002133	milk	2. Qu 2022	10.05.2022	E849	67 ± 2	challenges with scales
#4002100	milk	4. Qu 2021	19.10.2021	E849	82 ± 2	
#4002022	milk	2. Qu 2021	18.05.2021	E849	74 ± 2	
#4001989	milk	4. Qu 2020	28.10.2020	E849	74 ± 2	

Figure 76 and table 55 above show the measurement results for milk samples taken at different times at the sampling place E849, representing a farm located near a nuclear power plant. The milk sample number #4002133 was analyzed with the new DOWEX by Alfa Aesar and eluent at pH6. For this sample, a strontium-yield of 67 % was achieved under the new analysis conditions. There was a problem with an overload of the scales during the analysis, but it was successfully solved. The comparison to the strontium yields achieved for samples of the same kind and origin with the established DOWEX shows a significant yield loss for the most recent strontium analysis with the new DOWEX. But even though the strontium-yield was significantly smaller than for the previous analyses, the yield was enough to achieve the necessary level of detection and ensure reliable environmental monitoring of the area.

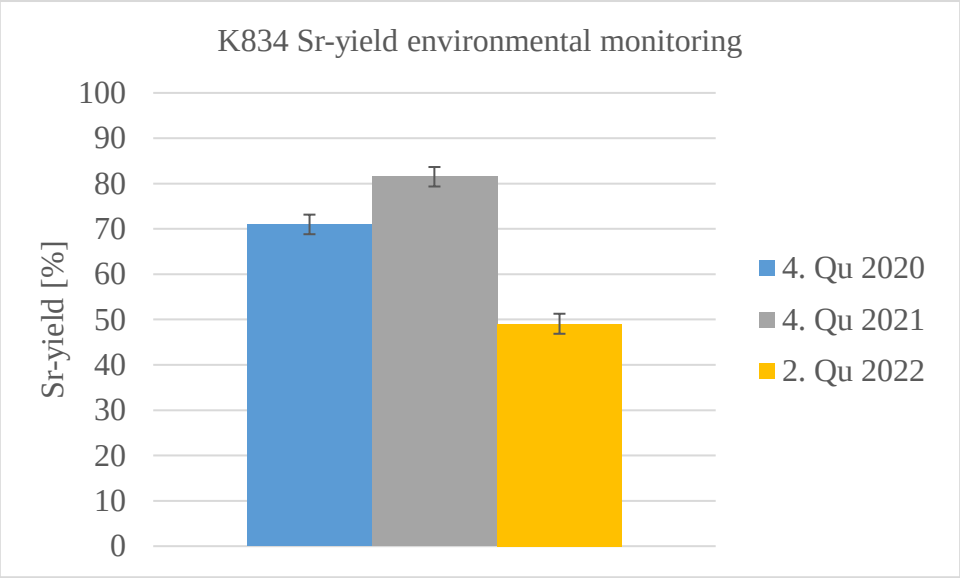

Figure77: Sr yields for milk samples from the sampling point K834 for comparison

Table 56: Overview over the Sr-yield results for the milk samples from the sampling point K834 and the complications during the analyses

sample number	sample kind	quarter/ year	reference date	sampling place	Sr-yield [%]	challenges
#5001084	milk	2. Qu 2022	04.05.2022	K834	49 ± 2	
#5001000	milk	4. Qu 2021	12.08.2021	K834	82 ± 2	
#5000954	milk	2. Qu 2021	16.06.2021	K834	80 ± 2	Extremely low yield determined (9.55 mL $ZnSO_4$ during titration needed, 10 mL $ZnSO_4 \equiv 0$ % yield), otherwise normal analysis, medium of other sample yields used as yield
#5000869	milk	4. Qu 2020	17.09.2020	K834	71 ± 2	

Figure 77 and table 56 show the measurement results for milk samples taken at different times at the sampling place K834, representing a farm located near a nuclear power plant. The milk sample number #5001084 was analyzed with the new DOWEX by Alfa Aesar and eluent at pH6. For this sample, a strontium-yield of 49 % was achieved under the new analysis conditions. The comparison to the strontium yields achieved for samples of the same kind and origin with the established DOWEX shows a significant yield loss for the most recent strontium analysis with the new DOWEX. But even though the strontium-yield was significantly smaller than for the previous analyses, the yield was enough to achieve the necessary level of detection and ensure reliable environmental monitoring of the area. Even though the sample number #5000954 from the second quarter of 2021 on the first glance seems to have a significantly better yield than the most recent sample, it caused severe problems during the yield determination. The color change during the titration for the yield determination of strontium occurred only at 9.55 mL of added $ZnSO_4$. This would correspond to a yield of only 8 %.

Because no other problems occurred during the analysis and it was performed as planned, the medium strontium-yield of all the other environmental monitoring samples from this time period was calculated and utilized as yield for the sample number #5000954. This process was acceptable for the environmental monitoring routine analysis. But because the strontium-yield for this sample was a constructed and not experimentally determined value, it was not suitable for this scientific comparison. Concluding from this, the most recent strontium analysis of milk from this farm with the new DOWEX by Alfa Aesar, performed by the same operator, was more successful than the analysis from the year before, with the established DOWEX by Serva, as a more reliable strontium yield could be determined with the new resin.

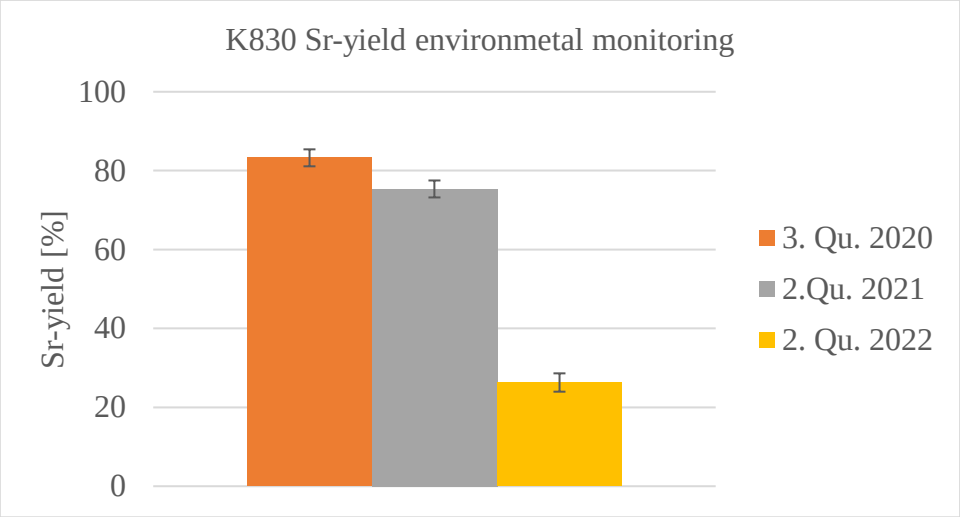

Figure 78: Sr yields for salad samples from the sampling point K830 for comparison

Table 57: Overview over the Sr-yield results for the salad samples from the sampling point K830 and the complications during the analyses

sample number	sample kind	quarter/ year	reference date	sampling place	Sr-yield [%]	challenges
#5001085	salad	2. Qu. 2022	04.05.2022	K830	26± 2	very low yield
#5000965	salad	2.Qu. 2021	16.06.2022	K830	75± 2	
#5000870	salad	3. Qu. 2020	17.09.2022	K830	83± 2	

Figure 78 and table 57 show the measurement results for salad samples taken at different times at the sampling place K830, representing a farm located near a nuclear power plant. The salad sample number #5001085 was analyzed with the new DOWEX by Alfa Aesar and eluent at pH6. For this sample, a strontium-yield of merely 26 % was achieved under the new analysis conditions. The comparison to the strontium yields achieved for samples of the same kind and origin with the established DOWEX shows a significant yield loss for the most recent strontium analysis with the new DOWEX. The analysis could not have been repeated, because all of the sample ash produced from the provided sample was used for the first try. Additionally, no other problems occurred during the analysis and it was performed as planned: turbidity of the sample was observed during the precipitation and a significant amount of precipitate was deposited on the filter after filtration. With some ascertainment of the data processing parameters and more realistic evaluations of the uncertainties, the yield was enough to achieve the necessary level of detection and ensure reliable environmental monitoring of the area.

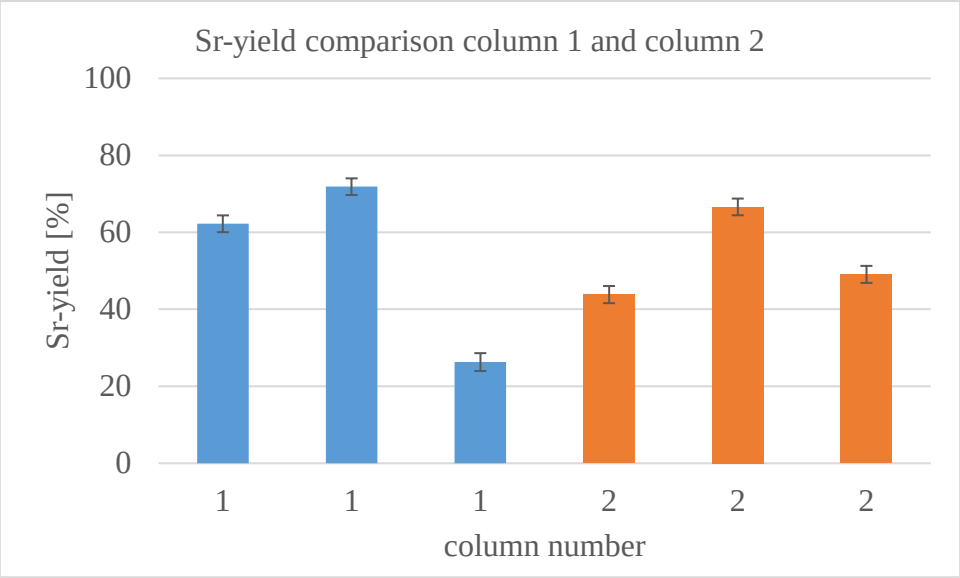

Figure 79: Sr-yield results achieved with column 1 and column 2 with the DOWEX resin by Alfa Aesar and the eluent ammonium-lactate at pH6

Table 58: Overview over the Sr-yield results for different samples from different sampling points achieved with column 1 and column 2 with the new separation system

nuclear power plant	sample number	sample kind	quarter/ year	reference date	column	Sr-yield [%]	sampling place
A	#3002007	milk	2. Qu 2022	02.05.2022	1	62.22 ± 2.18	A828
E	#4002131	milk	2. Qu 2022	10.05.2022	1	71.86 ± 2.16	E808
K	#5001085	salad	2. Qu 2022	04.05.2022	1	26.29 ± 2.32	K830
A	#3002008	milk	2. Qu 2022	02.05.2022	2	43.82 ± 2.23	A827
E	#4002133	milk	2. Qu 2022	10.05.2022	2	66.6 ± 2.17	E849
K	#5001084	milk	2. Qu 2022	04.05.2022	2	49.07 ± 2.21	K834

Figure 79 and table 58 show the comparison between the Sr-yield results between the two Hot Chroma columns, that were filled with the new DOWEX by Alfa Aesar and were used for the previous experiments. Column 1 was filled with 151.51 g DOWEX, column 2 with 151.50 g DOWEX. The columns have slightly different geometries, as they were custom built and not mass produced. Because of these different geometries, the fill levels were slightly different. The fill level of column 1 with the DOWEX was 20.2 cm, the fill level of column 2 with the DOWEX was 23.2 cm. As consequence of this and based on previous experiences with different fill levels in columns with the established DOWEX, different elution regions for strontium were chosen for the different columns. For column 1, the chosen elution region for strontium was 460 to 780 g eluent, as it is shorter and the strontium elution from the column should therefore start sooner. For column 2, the chosen elution region for strontium was 500 to 800 g eluent, as it is longer and the Sr elution from the column should therefore start later. The medium of the strontium-yields for the strontium analyses with column 1 was 53.5 %. The medium of the

strontium-yields for the strontium analyses with column 2 was 53.2 %. The values show no significant deviation from each other.

First it seemed that the strontium-yields of the strontium analyses performed with column 1 and the strontium elution region chosen for it were significantly higher. But for the strontium analysis of the salad sample #5001085, which was also performed with column 1, an especially low strontium-yield was obtained. This result pushed the medium Sr-yield for column 1 down, almost to the same value as achieved with column 2. Additionally, the milk sample #4002132, which caused problems during the yield determination, was also separated with column 1. Because the Sr-yield for this sample was a constructed one, as it could not be plausibly experimentally determined, it was not suitable for this scientific comparison and the calculation of a medium yield. With column 2 and the strontium-elution region chosen for it, more stable strontium-yields without strong fluctuations and outliners were achieved.

How good the performance of the two Hot Chroma columns is, compared to each other, will show in the future, as more analysis cycles are performed with them. It cannot be ruled out, that significant differences in strontium-yields will become noticeable, which did not show with this small sample size and the comparably high number of outliners.

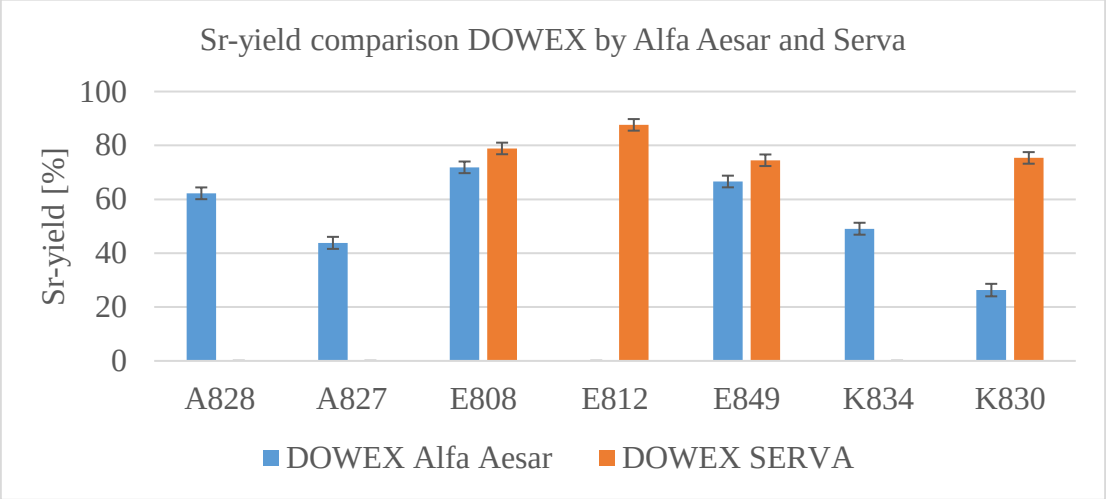

Figure 80: Sr-yields for the same sample kinds and sampling points, achieved with the DOWEX by Alfa Aesar and ammonium-lactate at pH6 and with the established DOWEX by Serva and ammonium-lactate at pH7.

Table 59: Overview over the Sr-yield results for the same sample kinds from the same sampling points achieved with the DOWEX by Alfa Aesar and ammonium-lactate at pH6 and with the established DOWEX by Serva and ammonium-lactate at pH7.

sampling place	Sr-yield 2022 with DOWEX by Alfa Aesar [%]	Sr-yield 2021 with DOWEX by Serva [%]	Constructed yield value due to problems during yield determination
A828	62 ± 2	0	80
A827	44 ± 2	0	80
E808	72 ± 2	79 ± 2	
E812	0	88 ± 2	50
E849	67 ± 2	74 ± 2	
K834	49 ± 2	0	80
K830	26 ± 2	75 ± 2	

Table 60: Medium yield results and number of outliners achieved with the DOWEX by Alfa Aesar and ammonium-lactate at pH6 and with the established DOWEX by Serva and ammonium-lactate at pH7

	Sr-yield 2022 with DOWEX by Alfa Aesar [%]	**Sr-yield 2021 with DOWEX by Serva [%]**
medium:	53	79
	1-2 outliers	3 outliers

Finally, the strontium-yields in environmental monitoring achieved in 2022 with the new DOWEX by Alfa Aesar and the eluent at pH6 were compared to the Sr-yields achieved with the established DOWEX by Serva in the previous year. For this, the strontium-yields for the same sample kinds from the same sampling places were compared. Both test series were performed one year apart from each other by the same operator.

As figure 80 and tables 59 and 60 show, only in three cases a direct comparison of the yield values was possible, as there were problems with the yield determination in both trial periods. Because of this, the exact value of the strontium-yield could not have been determined for several samples. Instead, a constructed value was used for the calculation of the results, in most cases the medium strontium-yield for all the samples in the same test period. This process was acceptable for the environmental monitoring routine analysis. But because the strontium-yields for these samples were constructed and not experimentally determined values, they were not suitable for this scientific comparison.

But this also shows that problems with the titrimetric yield determination are not new and were already an obstacle with the established DOWEX. Therefore, the yield determination problems are not caused by the new DOWEX by Alfa Aesar but can be traced back to a general error rate of the titrimetric yield determination and the lacking experience of the operator. An indicator for this is that the number of problems with yield determination was reduced in the current trial period.

The average strontium-yield for the strontium-separation with the established DOWEX by Serva in 2021 was 79 % with three outliners, for which constructed yield values were used. The average Sr-yield for the strontium-separation with the new DOWEX by Alfa Aesar and the eluent at pH6 in 2022 was 53 % with one to two outliners, for one of which a constructed yield value was used. The strontium yields significantly decreased with the new DOWEX. But even these lower yields were enough, to achieve the necessary level of detection and ensure reliable environmental monitoring of the area.

5.3.12 Application of the new column material with the adjusted eluent pH for the age determination of ivory via ^{90}Sr detection

The Hot Column Chromatography separation method is routinely applied for the separation of ^{90}Sr in the context of the age determination of ivory. This is done, to be able to distinguish legal antique ivory from new illegal ivory. So, the new DOWEX® 50 WX8 (200-400 mesh) by Alfa Aesar with the adapted separation conditions had to be tested for this application. This was done, to ensure that no problems would occur with real ivory samples, that were not previously noticed and solved for the milk ash samples of the preliminary investigations and the samples for environmental monitoring.

The analysis with the new DOWEX was performed according to the established instruction for the determination of the specific activity of ^{90}Sr in raw ivory [66, 68]. The process is in most work steps identical to the determination of $^{89/90}$Sr in environmental samples, which was detailed in section 5.1.

Before the determination of the ^{90}Sr content of the ivory sample takes place, its ^{14}C content is determined, which is also part of the age determination of ivory. After the ^{14}C determination, the remaining burned ivory is filled in a tared small quartz bowl, weighed and grinded into a powder. Then 60 to 80 mL of 65 % concentrated nitric acid (HNO_3) are added to the ash, so that it is coated. The exact volume depends on the amount of ivory ash present. The sample nitric acid mix is then heated in the sand bath until the liquid is completely evaporated and the sample is dry. During this process, bright orange nitro gases are emitted from the sample. This step is used to bind organic sample constituents and remove them via the formation of said nitro gases [66].

In the next step, that sample is incinerated overnight in the muffle furnace again at 650°C ± 20°C and cooled down to room temperature. After that, 60 to 80 mL of 32 % concentrated hydrochloric acid (HCl) are added to coat the ash. The sample hydrochloric acid mix is heated in the sand bath until the liquid is completely evaporated and the sample is dry. During this process, intense gas emission occurs and the sample and hydrochloric acid take on a yellow color. This step is used to remove remaining nitrates, which would disturb the column material [66].

Finally, the sample is incinerated one last time overnight in a muffle furnace at 650°C±20°C. After the sample has cooled down, the quartz bowl is weighed again. The remaining, now white, ash is removed from the quartz bowl, grinded in a mortar and weighed [66].

As soon as the ivory ash is prepared, its calcium content is determined. As calcium is such an important interfering element in the Hot Column Chromatography, the analysis method is optimized for the calcium load of 3 ± 0.5 g of calcium in the sample. Based on this value, the amount of sample used for the analysis is chosen, with the standard being 10 g of sample ash, or all the sample ash, if 10 g cannot be provided. If not enough calcium is present in the amount of sample, that is available, ashed $Ca_5(PO_4)_3OH$ is added as a calcium source [66].

The determination of the calcium content is performed with the Spectroquant® calcium cell test by Merck KGaA [65]. This method is based on the reaction of calcium ions in neutral solution with phthalein purple. Through this reaction, a violet dye is formed, that is then determined photometrically. As the measuring range of this test is 10-250 mg/L Ca, because it

is mostly intended for water samples, the sample ashes have first to be solved and then diluted. (0.100 ± 0.001) g of sample ashes are solved in 7 mL of a 1:1 mixture of 6 M hydrochloric acid and 1.5 molar lactic acid, while heating and stirring. Then the pH of the solution is adjusted to the value of 3 to 9 with hydroxide pallets, as is required in the instruction for the calcium test. After the solution cools down, it is completely transferred into a 100 mL volumetric flask, filled up to 100 mL with bidistilled water and thoroughly mixed. One mL of this solution is retrieved with an Eppendorf pipette and again diluted 1:10 in a 10 mL volumetric flask. Then, one mL of this solution is filled in a reaction cell from the calcium cell test kit, that is already filled with a kit liquid. One mL of the reagent Ca-1K solution is added and the reagents mixed. The solution turns violet after mixing. The reaction cell is left for exactly 3 minutes of reaction time and then 0.5 mL of the yellow reagent Ca-2K is added. After the sample is mixed, it is measured in the Spectroquant® photometer with the suitable settings program for a calcium measurement. Each sample is measured at least seven times [65,66].

The following scheme shows the process for calculating the calcium content of the sample ashes from the result measured with the photometer.

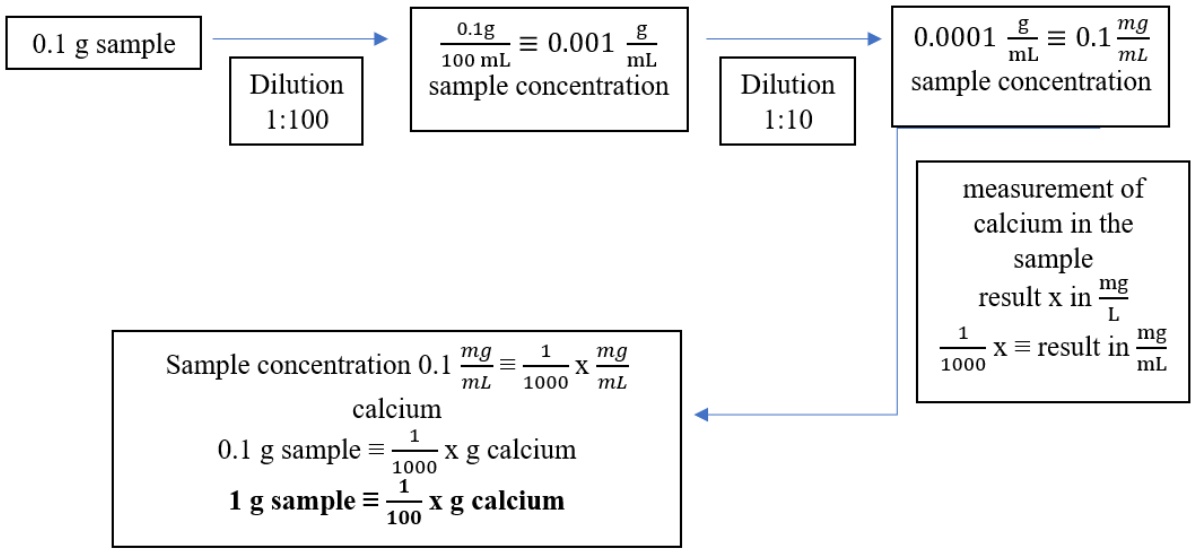

Finally, 1 g sample ≡ $\frac{1}{100}$ x g calcium with x being the measurement result, shown by the photometer. The calculation of the error for the calcium content determination is shown in equation 5.19:

$$\Delta m_{Ca} = t \cdot \frac{s}{\sqrt{N}} \text{ [66]} \qquad (5.19)$$

In this equation, Δm_{Ca} represents the uncertainty of the calculated Ca mass. t represents the table value of the Student distribution (t-distribution), with an α value of 0.05 and therefore a level of confidence of 95 %. S is the standard deviation of the measured values and N is the number of measurements [66].

According to the calculated calcium content of the sample ash, enough ivory ash is used, to correspond to 3 g ± 0.5 g of calcium. If not enough sample is available to achieve 3 g of calcium, ashed $Ca_5(PO_4)_3OH$ is added as calcium source. 6.5 g ashed $Ca_5(PO_4)_3OH$ corresponds to 3 g calcium [66].

In most cases, the separation of ^{90}Sr with the Hot Column Chromatography is combined with the thorium analysis. In this case, 5 mL of a ^{229}Th-tracer (Ac-227 (5_Ac227) tracer 0.0279 Bq/mL in 7.2 M HNO_3, 23.06.96 containing ^{229}Th) is added beforehand and a thorium fraction is separated with the column, additionally to the strontium fraction. 5 mL of the Th-tracer are added with an Eppendorf pipette into a 250 mL beaker and the liquid is evaporated in a sand bath. The residue is solved in a small amount of hydrochloric acid and dried again in the sand bath two times, to clean the tracer. Then the ivory sample and the necessary amount of ashed $Ca_5(PO_4)_3OH$ are added to the beaker in addition to a stable Sr-tracer solution containing 50 mg Sr. As solvent 80 mL of a 1:1 mix of 6 M hydrochloric acid and 1.5 M lactic acid are added. The mixture is heated, while stirring, until the ash is completely dissolved. The sample is centrifuged if some ash remains unsolved. The sample solution is applied to the column and run in at the velocity of 2.5 mL per minute. The velocity is controlled with a scale, measuring how much eluent has left the column, and a stopwatch, measuring how much time has passed [68].

As eluent, 800 mL 1.5 molar ammonium-lactate solution is used, normally at pH7, but with the DOWEX by Alfa Aesar the eluent is at pH6. A constant velocity of 2.5 mL/min is important for the reproducibility of this process and a good separation. This has to be controlled and eventually adapted manually. The thorium in the sample is separated in the elution fraction of 210 to 340 g eluent, that passed the column, without counting the sample inlet. The region of 480 to 800 g eluent contains the ^{90}Sr fraction without ^{137}Cs. These elution regions are separated for further analysis [68].

After the separation, the ^{90}Sr fraction is concentrated to a volume of about 200 mL by evaporation in the sand bath. After cooling down, the strontium is precipitated as $SrSO_4$ (strontium sulphate). This is done by slowly adding 60 mL concentrated sulfuric acid (97 %), while stirring and in an ice bath, to compensate for the produced heat. The precipitation is completed over night in the laboratory refrigerator. Then the precipitate is filtered through a Satorius filter cubicle with a paper filter (Whatman 42) and washed with 10 mL sulphate containing water and 10 mL acetone (p.a.) [68].

The sample is measured in the low level β counter Berthold in the beta mode for 1,000 min, after a waiting time of at least 14 days. This time is necessary for the radioactive equilibrium between ^{90}Y and ^{90}Sr to establish. The increased ^{90}Y content enables higher count rates and therefore a lower level of detection for the measurement. The labelled filter is placed in a round little steel tray with a diameter of 55 mm and measured as described in the Berthold section. After the measurement, the filter is incinerated at 600°C ± 20°C for 30 minutes in the muffle furnace in a weighed porcelain bowl. After the resulted ashes are cooled, they are weighed in an analytical balance [68].

From this weight, the chemical yield of the strontium separation can be calculated, as the filter is completely burned and only the filtered $SrSO_4$ remains. As 50 mg Strontium were added as tracer in the beginning, this equates to 0.00057 mol, as the molecular weight of strontium is 87.62 g/mol. For $SrSO_4$ 0.00057 mol equates to 0.1048 g, as its molecular weight is 183.68 g/mol. If the measured weight of the filtered $SrSO_4$ is divided by 0.1048 g and multiplied by 100 %, the strontium yield in % is obtained, as shown in equation 5.20, with y being the measured $SrSO_4$ ash weight in g.

$$\eta_{chem} = \frac{y}{0.1048g} \cdot 100\% \tag{5.20}$$

$$\Delta\eta_{chem} = \eta_{chem} \cdot \sqrt{\left(\frac{\Delta y}{y}\right)^2 + \left(\frac{\Delta m_{sr}}{m_{sr}}\right)^2} \quad (5.21)$$

The uncertainty of the chemical yield can be calculated with the chemical yield η_{chem}, the measured $SrSO_4$ ash weight y, its uncertainty Δy, the mass of the strontium in the added tracer m_{Sr} and its uncertainty Δm_{Sr}, as shown in equation 5.21.

The resulting values from the ivory analyses performed with the new column material by Alfa Aesar and with the eluent ammonium-lactate at pH6 are the strontium-yields of the analyses. For the determined ages of the ivory, no target values were known and they therefore could not be used for the quality control of this analysis.

The resulting strontium-yields for the ivory age determinations performed with the DOWEX by Alfa Aesar and the eluent at pH6 are presented in the table below.

Table 61: Sr-yields of the ivory age determinations with the DOWEX by Alfa Aesar and ammonium-lactate at pH6 as eluent

Sample number	#8000322	#8000323	#8000324	#8000325	#8000326	#8000327
$SrSO_4$ precipitate [g]	0.0684 ± 0.001	0.0593 ± 0.001	0.0747 ± 0.001	0.0703 ± 0.001	0.0719 ± 0.001	0.0656 ± 0.001
Percentage of the 100 % value [%]	65.3 ± 1.5	56.6 ± 1.3	71.3 ± 1.7	67.1 ± 1.6	68.61 ± 1.6	62.6 ± 1.4

Table 61 shows the strontium yields of the ivory age determination. The yields are all significantly over 50 % and could be determined reliably without outliners. They were enough to achieve the necessary level of detection and provide reliable age determination of the ivory samples, as far as the method allows for it. The yield determination was performed with the gravimetric method instead of the titrimetric method, that is usually used in environmental monitoring. This method showed to be more robust. The results also indicate that the problems during the yield determination for the environmental monitoring samples were due to problems with the titrimetric method and not necessarily the analysis itself.

For comparison, table 62 shows the Sr-yields of ivory age determinations performed with the established Serva DOWEX and eluent at pH7 by the same operator.

Table 62: Sr-yields of the ivory age determinations with the DOWEX by Serva and ammonium-lactate at pH7 as eluent

Sample number	#8000304	#8000308	#8000311	#8000312
$SrSO_4$ precipitate [g]	0.0764 ± 0.001	0.0923 ± 0.001	0.0967 ± 0.001	0.0967 ± 0.001
Percentage of the 100 % value [%]	72.9 ± 1.7	88.1 ± 2.1	92.3 ± 2.2	92.27 ± 2.2

The values of table 62 show higher yields than with the new DOEWX by Alfa Aesar, a trend similar to the one present for the environmental samples. This indicates that the newly implemented measurement system is good enough to reach the necessary levels of detection and provide satisfactory results, but that the results are still worse than with the old DOWEX. But as the DOWEX by Serva is no longer available, the new system has to be implemented and potentially further optimized, for example concerning the elution region used for the separation of strontium.

Table 63: Comparison of the results with the DOWEX by Alfa Aesar for ivory age determination with its results for environmental monitoring and the results with the DOWEX by Serva for ivory age determination

	ivory samples DOWEX by Alfa Aesar	ivory samples DOWEX by Serva	environmental monitoring samples DOWEX by Alfa Aesar
average Sr-yield [%]	65.24	86.38	53.31
standard deviation of the Sr-yield [%]	4.71	7.97	15.48
outliners	0	0	1 - 2

Table 63 helps to evaluate the quality of the results achieved during the tests for reals samples with the new DOWEX by Alfa Aesar. It shows that with the established DOWEX by Serva, significantly higher yields were achieved than with the DOWEX by Alfa Aesar. But with the newer DOWEX, more constant results were achieved, that were still in an acceptable scale. In both cases no outliners were detected. For the analyses of environmental samples with the DOWEX by Alfa Aesar, the results were all in all worse, with more outliners, lower yields and a stronger variation in the results. But as for these samples the titrimetric yield determination process, which was more prone to errors, was used, these results could be traced back to problems with the yield determination.

5.3.13 Validation of the new column material in a ring analysis

Ring analyses are a tool to ensure the quality of different analysis types and the laboratories that offer them. For such analyses, samples are prepared by independent institutions or laboratories with a known content and distribution of typical analytes in typical sample matrices. These samples are sent to different participating laboratories, which analyse them with their methods and report back the analysis results. Those results are then evaluated and compared by the independent institution or laboratory with the target values and the results of the other laboratories. The participants then receive feedback about the quality of their results (and maybe a certificate stating said quality). Such ring analyses are used for the accreditation and re-accreditation of laboratories, for a constant quality control of the established analysis methods and for the validation of new methods. This was done in the ring analysis, described in the following section, for the new DOWEX® 50WX8 200-400 (H) resin by Alfa Aesar and the pH change of the eluent ammonium-lactate to 6.

The URA/ ZRN laboratory yearly participates in the ring analysis for different radionuclides, among them ^{90}Sr, in a milk matrix by MRI (Max Rubner-Institut, Bundesforschungsinstitut für Ernährung und Lebensmittel, control center for soil, vegetation, feed and food of plant-and animal-based origin). Two samples were provided, #1003151 and #1003153. These samples were used to validate the new DOWEX® 50 WX8 200-400 (H) resin by Alfa Aesar and the pH change of the eluent ammonium-lactate to 6. Both samples were divided in half and were analyzed in both active columns filled with the new DOWEX, column 1 and 2, as described in section 5.3.11 and used for environmental monitoring. This was done to validate both columns, to be able to compare the results, as well as having a backup analysis in case of disturbances. Sample #1003151 was analyzed by the author and its yield determined gravimetrically. Sample #1003153 was analyzed by an experienced laboratory technician and its yield determined titrimetrically. In total, four analyses for this ring experiment were performed.

The ring analysis samples were prepared and analysed according to the description in section 5.1. The only significant difference was the new DOWEX by Alfa Aesar and the pH of the eluent ammonium-lactate at 6.

First the samples were prepared. A significantly lower sample volume was accessible than is normally used for environmental monitoring, but the necessary levels of detection could still be achieved, due to the higher activity of the ring analysis samples. For the analysis of sample #1003151, 993.83 g milk were used in total. For the analysis of sample #1003153 only 613.75 g milk were used in total. The samples were incinerated to ash according to the description in section 5.1.1 and the analysis instruction [63].

Before the separation, the pH of the column was adjusted by conditioning with 250 mL of 1.5 molar lactic acid. After the separation, the column was regenerated with 500 mL of 6 M hydrochloric acid [10, 52, 63].

Due to the small volume of the provided milk sample, only 7.46 g of milk ash were produced for sample #1003151 and only 4.43 g of milk ash were produced for sample #1003153. As the samples were analysed in two columns, the ash, that could be removed from the quartz bowls, was additionally divided by two. For sample #1003151 2.93 g milk ash per analysis were used. For sample #1003153 1.85 g milk ash were used for analysis 3 (column 1) and 1.55 g milk ash were used for analysis 4 (column 2). As the analysis is optimized for 10 g milk ash, the samples

were filled up to 10 g with not contaminated milk ash, prepared from commercially available whole long-life milk by the brand Berchtesgadener Land or remaining milk ash from environmental monitoring, which was confirmed to be not radioactively contaminated.

A stable strontium-tracer containing 50 mg Sr and 80 mL of a 1:1 mix of 6 M hydrochloric acid and 1.5 molar lactic acid were added to the ash samples. The mixture was heated while stirring, until the ash was almost completely dissolved. Then the samples were centrifuged. The supernatant was applied to the columns and run in at the velocity of 2.5 mL per minute. The velocity was controlled with a scale, measuring how much eluent has left the column, and a stopwatch, measuring how much time has passed [10, 52, 63].

As eluent, 800 mL of 1.5 M ammonium-lactate solution at pH 6 was used. A constant flow velocity of 2.5 mL/min was controlled and ensured. The elution region of ^{90}Sr without ^{137}Cs depended on the column geometry, that varied slightly between the columns, as they were handmade in the university intern glass blower workshop. For column 1, the elution region was 460-780 g eluent without the sample inlet. For column 2, the elution region was 480-800 g eluent, or respectively 500-800 g eluent, without the sample inlet. This data is based on previous experiments and long-term experience with the columns [10, 52, 63].

Table 64: Analysis parameters for the four different ring analysis experiments

analysis	analysis 1	analysis 2	analysis 3	analysis 4
ring analysis sample	#1003151	#1003151	#1003153	#1003153
milk ash sample [g]	2.93 ± 0.01	2.93 ± 0.01	1.85 ± 0.01	1.55 ± 0.01
column	1	2	1	2
Sr elution region [g eluent]	460-780	500-800	460-780	480-800
analysis by	author	author	experienced laboratory technician	experienced laboratory technician
Sr yield determination	gravimetrically	gravimetrically	titrimetrically	titrimetrically

Table 64 shows an overview of the analysis parameters and clarifies the differences between the four ring analyses performed for the validation.

After the separation, the ^{90}Sr fractions were precipitated as $SrSO_4$ and the precipitate filtered, as detailed in section 5.1.4. The filters were labelled on the rim, placed in a round little steel tray with a diameter of 55 mm and fixed with adhesive tape [10, 52, 63].

All four ring analysis samples were measured two times, with a time difference of one week in-between, in the low level β counter Berthold, as described in the according section. The two measurements were necessary to distinguish the measurement results of ^{90}Sr from the measurement results of ^{89}Sr.

The filter with the $SrSO_4$ precipitate of analysis 1 was stuck in the Berthold measurement device during its first measurement, due to curving of the filter because of its suboptimal fixation in the steel tray. The device was opened, deconstructed and decontaminated, removing and collecting all the remains of the sample filter. These collected sample remains were fixed especially thoroughly in the steel tray for the second measurement in the Berthold.

For analysis 1 and 2 of the ring analysis sample #1003151, the strontium yield determination was performed gravimetrically. The filters were incinerated at 600°C ± 20°C for 30 minutes in the muffle furnace in a weighed porcelain bowl. After that, the resulting ashes were weighed in an analytical balance. From this weight, the chemical yields of the strontium separations could be calculated, as the filters were completely burned and only the filtered $SrSO_4$ remained. As 50 mg strontium were added as tracer in the beginning, this equates to 0.00057 mol, as the molecular weight of strontium is 87.62 g/mol. For $SrSO_4$, 0.00057 mol equates to 0.1048 g, as its molecular weight is 183.68 g/mol. If the measured weight of the filtered $SrSO_4$ is divided by 0.1048 g and multiplied by 100 %, the strontium yield in % is obtained [10, 52, 63].

For analysis 3 and 4 of the ring analysis sample #1003153, the strontium yield determination was performed titrimetrically. The filters with the precipitate were placed each in a 150 mL beaker and 10 mL 0.1 M EDTA solution was added. Then 4 mL concentrated ammonia was added for pH adjusting and the precipitate was solved through light heating of the sample. After that, 1 mL ammonium-chloride was added, and it was checked whether the pH of the solutions was above pH10. If this were not the case, it could be adjusted with concentrated ammonia. Then a little bit of the pH indicator Eriochrome black T was added. The solutions were titrated with 0.1 molar zinc sulphate solution until their color changed from bule to violet. The added EDTA complexes the strontium ions in the solution. The remaining EDTA reacts with the added zinc sulphate solution. As soon as all EDTA molecules have complexed either Sr or Zn, the color changes when a surplus of zinc sulphate solution is added. The chemical yields were calculated from the volume of zinc sulphate ($ZnSO_4$) solution needed for the color change. The less was needed, the more EDTA has already reacted with strontium, the more strontium was present in the solution and the higher was the chemical yield [64].

$$\eta_{chem} = (V(EDTA) - V(ZnSO_4)_{used}) \cdot \frac{8.763\ \frac{mg}{mL}}{m(Sr-tracer)} \cdot 100\ \% \tag{5.22}$$

Equation 5.22 shows the calculation of the chemical yield for the titrimetric method. V(EDTA) is the added volume of the 0.1 molar EDTA solution, which is 10 mL. $V(ZnSO_4)_{used}$ is the volume of $ZnSO_4$ needed for the color change and m(Sr-tracer) is the mass of strontium added in the beginning of the analysis, which is 50 mg [64].

Table 65: Analysis results for the four different ring analysis experiments

analysis	analysis 1	analysis 2	analysis 3	analysis 4
ring analysis sample	#1003151	#1003151	#1003153	#1003153
Sr-yield [%]	68.99 ± 1.6	57.54 ± 1.3	70.98 ± 1.00	68.35 ± 0.97
^{90}Sr best activity estimate [Bq/L]	1.11	2.23	2.38	2.32
^{90}Sr confidence interval [Bq/L]	1.02-1.20	2.05-2.42	2.18-2.58	2.12-2.51
^{90}Sr decision threshold [Bq/L]	0.0162	0.0191	0.0248	0.0307
^{90}Sr limit of detection [Bq/L]	0.0327	0.0388	0.0503	0.0621
^{89}Sr best activity estimate [Bq/L]	6.68	3.74	3.46	4.02
^{89}Sr confidence interval [Bq/L]	5.79-7.56	3.24-4.24	2.93-4.00	3.39-4.64
^{89}Sr decision threshold [Bq/L]	0.0140	0.0166	0.0223	0.0275
^{89}Sr limit of detection [Bq/L]	0.0282	0.0337	0.0450	0.0557

Table 65 shows the results of the ring analyses performed for the validation of the new DOWEX® 50 WX8 200-400 (H) resin by Alfa Aesar and the pH change of the eluent ammonium-lactate to 6. It includes the strontium yield for each separation and the best activity estimate, the confidence interval for this estimate, the decision threshold and the limit of detection for ^{89}Sr and ^{90}Sr for each separation.

Between analysis 1 and analysis 2, there was a significant discrepancy, even though the same sample #1003151 was analysed. The strontium yields were both acceptable. But the best activity estimate for ^{90}Sr for analysis 1 was only about half the value of analysis 2 and at the same time its ^{89}Sr best activity estimate was about double the value of analysis 2. This was most likely due to the sample of analysis 1 being stuck in the Berthold device, which disturbed the first measurement and consequently the analysis results. Nevertheless, the decision thresholds and limits of detection were comparable for both analyte nuclides for both analyses. As analysis 2 was performed without turbulences, its results were considered more reliable.

The results for the ring analysis sample #1003153 showed a lot more consistency. The strontium yields for the separations 3 and 4 were comparable. This was also the case for the best activity estimate, the confidence interval for this estimate, the decision threshold and the limit of detection for ^{89}Sr and ^{90}Sr for both separations. As the same sample was analysed, this was a quality sign of the analysis. As analysis 3 and 4 were performed without incidents, these results were considered reliable. One thing, that stood out for these results was that the decision thresholds and the limits of detection were significantly higher than for analysis 1 and 2. Another interesting observation was that the best estimated values for the activities of ^{89}Sr and

^{90}Sr for analysis 2 were very similar to the ones of analyses 3 and 4. This may be a hint that the ^{89}Sr and ^{90}Sr activities were originally the same for the samples #1003151 and #1003153 and the values for analysis 1 were only skewed due to the disruption during the measurement. All in all, the comparable results of analyses 3 and 4 show that the new column material is suitable for the separation of ^{89}Sr and ^{90}Sr and their subsequent detection.

The official results of the ring analysis, that would confirm or reject these results, were at the time of writing not yet announced.

5.4 Determination of ^{90}Sr via its daughter nuclide ^{90}Y and the separation of yttrium with the Hot Column Chromatography

In the following section, the focus is shifted from the analyte ^{90}Sr to its daughter nuclide ^{90}Y. The two nuclides are in radioactive equilibrium with each other and the ^{90}Sr activity can also be determined by the analysis of ^{90}Y in the sample, as they have an activity ratio of 1:1. Elution curves of yttrium were recorded and the separation of yttrium from the interfering nuclides and elements evaluated. The advantages of the ^{90}Y analysis compared to ^{90}Sr are its narrow elution range, the faster elution and the better separation from cesium. The final goal was a direct Cherenkov measurement of the yttrium fraction without post treatment. As ^{90}Y has a half-life of only about 64 hours, the measurement had to be performed immediately after the separation. But an advantage of this short half-life is the easier waste management of ^{90}Y, as it decays so fast, and the possibility to directly measure the background of the sample, after the ^{90}Y analyte has decayed.

This new analysis approach is very promising in reducing the time and costs necessary and making the analysis more suitable for immediate action, in case of a nuclear emergency.

5.4.1 Hot Column Chromatography for the determination of the elution region of yttrium in milk ash

A first hint of the elution region of yttrium in a Hot Column Chromatography separation was found in the work of Stefanie Schmied [10, 52]. It was approximately at 300-400 g eluent, a lot faster than the strontium elution. From the elution curves it was also evident, that the elution region of yttrium was quite narrow, which would make the separation of the complete yttrium fraction in a small sample volume possible. This was the motivation to determine the yttrium elution region more precisely, as well as its overlap with interfering elements, to investigate if a separation and subsequent detection of ^{90}Y to determine ^{90}Sr in the sample would be possible. The following steps were performed to determine if this separation would be reliable, reproducible and lead to an acceptably low level of detection.

A stable yttrium-tracer was added to the sample for the determination of the yttrium elution region. This could be done because different isotopes of the same element behave chemically similar, and therefore their ions eluate at the same retention time in the Hot Column Chromatography. As detection method, for the quantification of yttrium in the different fractions, ICP-OES was used.

As standard sample matrix 10.03 g not contaminated milk ash, prepared from commercially available whole long-life milk by the brand Berchtesgadener Land, was used. The ash was solved in the usual 1:1 mixture of 6 M hydrochloric acid and 1.5 molar lactic acid. Additionally, 1 mL of the stable yttrium tracer, containing 10 mg yttrium, was added. As column material for this separation, the established DOWEX by Serva was used. The Hot Column Chromatography was performed at 87°C and at the elution speed of 2.5 mL/min. Ammonium-lactate at pH 7 was used as eluent. During the elution 114 elution fractions were collected. Fractions 1-25, from 0 g eluent to 250 g eluent were 10 g eluent each, starting from the sample inlet into the column. Fractions 26-55, in which most of the added yttrium was expected, were 5 g eluent each, to

achieve a better resolution of the yttrium elution region. This section spanned 250 to 400 g eluent throughput. Fraction 56-113, from 400 to 980 g eluent, were also 10 g eluent each, as yttrium was not expected in this elution region. The samples were measured nonetheless, to make sure that no yttrium was present in these elution regions. The last fraction 114 contained only 1.6 g eluent, as the eluent added to the column ran out.

Fraction 37 contained a white precipitate after cooling down to room temperature. Fractions 38 to 55 turned completely into a white wax-like solid after cooling down. This was due to the high calcium content of the samples, which caused precipitation at room temperature.

5.4.2 ICP-OES measurement of the yttrium elution region in milk ash

For the ICP-OES measurement of the yttrium content in the fraction samples, they were diluted 1:1,000. Per ICP-OES sample 10 µL of the fractions were used and 2 mL concentrated nitric acid was added for pH adjusting. The samples were filled up to a volume of 10 mL with bidistilled water. This dilution was selected, because the ICP-OES is optimized for lower concentrations and ideally narrow concentration ranges.

A calibration curve had to be calculated and prepared for yttrium, to be able to sensibly measure the analyte content in the samples. For this, the expected concentration range in the elution curve had to be estimated and adjusted to the applied dilution. The calibration curve was optimized to encompass as large of a concentration range as possible and sensible, as is seen in table 66. The aim was, to be able to quantify the concentration maximum of the elution curve and at the same time to still be able to detect 1 % of the concentration maximum in the different fractions. The expected concentration maximum was 10 mg Y/ 5 mL eluent, if all the added yttrium were in one fraction, corresponding to 2000 µg Y/ mL eluent. The lower end of the estimation was 0.1 mg Y/ 10 mL eluent, for one percent of the added yttrium in one fraction, corresponding to 10 µg Y/mL. Respecting the dilution factor, the expected concentration range was 0.01-2 µg Y/ mL eluent. Based on these estimations and calculations, the following calibration setup was developed, as shown in table 66.

Table 66: Calibration data for the measurement of the Y-elution fractions with ICP-OES for the determination of the Y elution curve.

sample	c(Y) [µg/g]	c(Y) [µg/kg]	added Y-standard solution [mL]	added Y-standard solution [µL]
C0	0	0	0	0
C1	0.01	10	0.01	10
C2	0.05	50	0.05	50
C3	0.1	100	0.1	100
C4	0.5	500	0.5	500
C5	1	1,000	1	1,000
C6	2	2,000	2	2,000

The calibration standards were prepared the same way as the samples. The only difference was that instead of a constant amount of sample, a varying amount of the Multi-Element Calibration

Standard 2 by Perkin Elmer Pure Plus was added (see table 66), which contains 10 µg/g yttrium, among other elements. Then 2 mL concentrated nitric acid was added for pH adjusting and the calibration samples were filled up to a volume of 10 mL with bidistilled water.

With the calibration curve, a direct connection between the signal at the emission wavelength typical for yttrium and the yttrium concentration could be determined. This connection was then used by the measurement software for the quantification of the yttrium content in the fraction samples. The results were put out in the unit [µg/kg].

After the calibration, the 5 mL fractions 26-55, in which most of the added yttrium was expected, were measured. A direct sample preparation for the ICP-OES measurement with the fraction samples 38-55 was not possible, as they were completely solid at room temperature. They had to be heated in a water bath first, to solve the solid. Then these fractions were sampled while they were still warm. Additionally, the 10 mL fractions 11-25 and 56-75 were prepared for the ICP-OES measurement and were measured, as they were adjacent to the expected elution region of Yttrium.

After the measurement, the data was processed and visualized (see figure 81). The yttrium content in the fractions was presented as percentage of the added 10 mg yttrium tracer, that represented 100%.

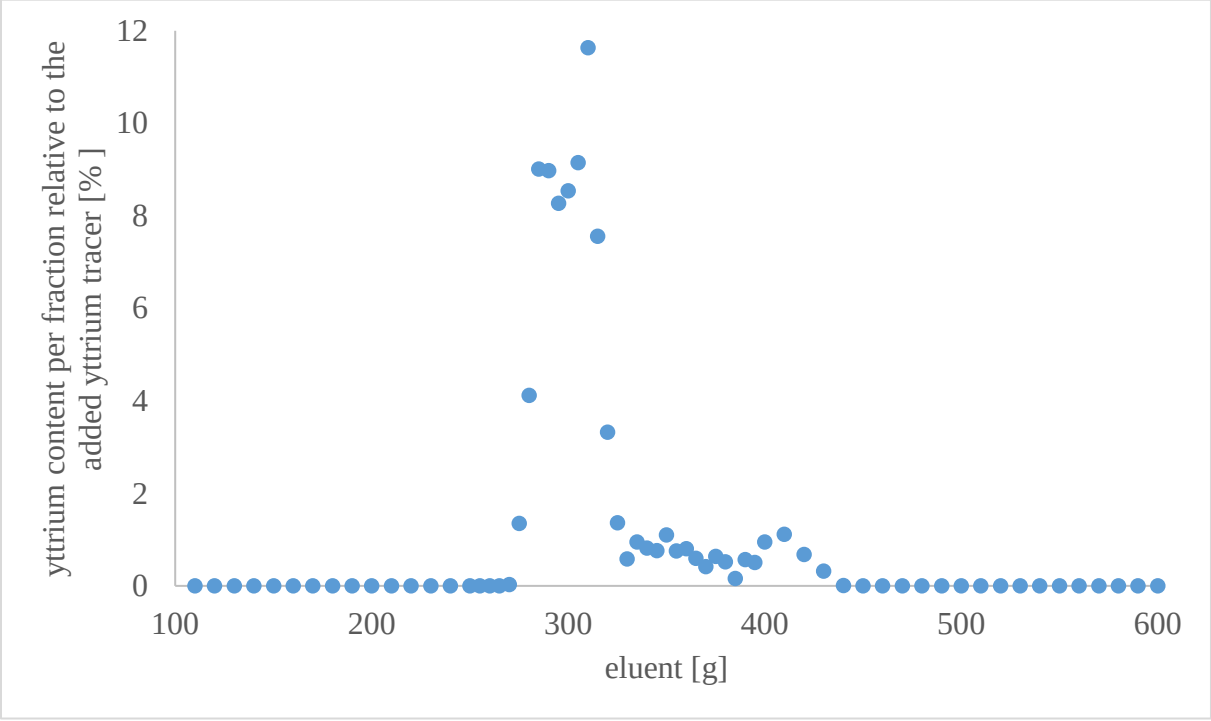

Figure 81: Relative Y elution curve, achieved with the DOWEX by Serva, eluent ammonium-lactate at pH 7, measurement with ICP-OES

Figure 81 shows the detected yttrium distribution during the elution. The narrow main elution region of yttrium between 270 and 330 g eluent throughput is noticeable. The complete yttrium elution region was between 270 and 440 g eluent, showing a peak tailing between 330 and 440 g eluent. The maximum of the yttrium elution region was between 305 and 310 g eluent throughput at 11.63 % of the added yttrium tracer. A recovery rate of 85.48 % could be achieved for yttrium in this experiment.

All in all, the general elution region of yttrium and its narrowness, that were expected based on the results of Stefanie Schmied [10, 52] were confirmed. The elution region of yttrium was additionally determined more precisely, as well as the recovery rate of the analyte. This data formed the basis for further experiments regarding the analysis of ^{90}Sr based on the detection of ^{90}Y.

5.4.3 Hot Column Chromatography for the determination of potassium and calcium as interfering substances in milk ash

Calcium and potassium are two of the most relevant interfering substances in the ^{90}Y analysis. They have the potential to disturb the Hot Column Chromatography separation of ^{90}Y or the subsequent determination of its activity in the sample.

The high calcium amount in many food and environmental samples can lead to precipitation during the Hot Chroma separation. This could result in clogging of the column, disrupting the whole analysis, coprecipitation of the analytes and the change of the physical state of the sample. In this case, the samples taken in the elution region of calcium turned into a waxlike while solid after cooling down from the operational temperature of 87°C to room temperature. This could lead to significantly lower physical yields during the Cherenkov measurement, as the measurement is optimized for clear, liquid and homogeneous aqueous solutions. As previous measurements showed precipitation and solidification in elution fractions in or near the elution range of yttrium, it could be expected that there was an overlap between the elution regions of yttrium and calcium or that they were at least quite close to each other. As this could be a problem in the implementation of a ^{90}Y analysis, the elution region of calcium had to be determined.

Since potassium is also present in milk ash and contains the naturally occurring radioisotope ^{40}K, which makes up 0.012 % (120 ppm) of the total amount of potassium found in nature, this is another element that could interfere during the analysis. This makes ^{40}K a practically ubiquitous β-emitting nuclide, present in relatively high amounts, as seen in figure 82.

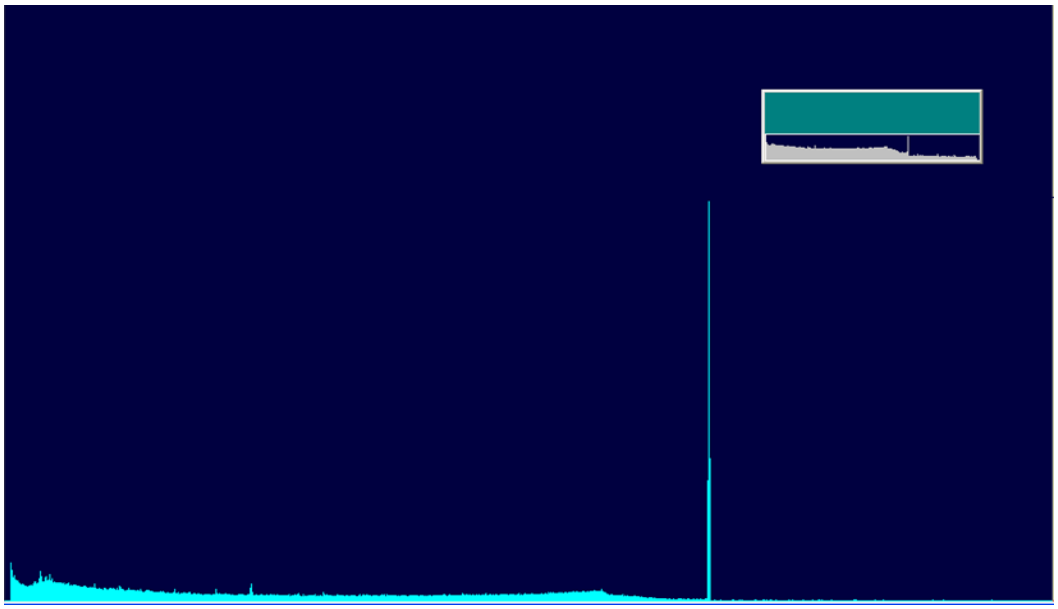

Figure 82: Gamma spectrum of not radioactively contaminated milk with a significant ^{40}K peak

Because ^{90}Y is also a β-emitter, the background radiation of ^{40}K could lead to a false positive ^{90}Y signal. This renders the reliable separation of ^{40}K from the yttrium elution region, or a dependable ^{40}K background, crucial. Stefanie Schmied [52] described an elution range of potassium between 50 and 350 g eluent, not including the sample inlet. This suggests a probable overlap of the elution regions of potassium and yttrium. As this could be a problem in the implementation of a ^{90}Y analysis, the elution region of potassium had to be determined.

As standard sample matrix 10.00 g not contaminated milk ash, prepared from commercially available whole long-life milk by the brand Berchtesgadener Land, was used. It was solved in the usual 1:1 mixture of 6 M hydrochloric acid and 1.5 molar lactic acid. No tracer was added, as potassium and calcium naturally occurred in significant amounts in the milk ash sample, according to the milk packaging 124 mg calcium per 100 mL. As column material for this separation, the established DOWEX by Serva was used. The Hot Column Chromatography was performed at the elution speed of 2.5 mL/min. Ammonium-lactate at pH 7 was used as eluent. During the elution 100 fractions à 10 ml were collected, including the sample inlet. As detection method for the quantification of potassium and calcium in the different fractions, ICP-OES was used.

5.4.4 ICP-OES measurement of potassium and calcium in milk ash

For the ICP-OES measurement, the fraction samples were diluted 1:2000. Per ICP-OES sample, 5 µL of the fractions were used and 2 mL concentrated nitric acid was added for pH adjusting. The samples were filled up to a volume of 10 mL with bidistilled water. This dilution was selected, because the ICP-OES is optimized for lower concentrations and ideally narrow concentration ranges. Additionally, the concentrations of potassium and calcium in a milk sample were significantly higher than the potential yttrium content in them.

A calibration curve had to be calculated and prepared for potassium and calcium, to be able to sensibly measure the analyte content in the samples. One calibration curve was prepared for both analytes. For this, the expected concentration range in the elution curve had to be estimated and corrected for the applied dilution. The calibration curve was optimized to encompass as large of a concentration range as possible and sensible, as is seen in table 67. The aim was to be able to quantify the concentration maximum of the elution curve and at the same time to still be able to detect 1 % of the concentration maximum in the different fractions. The expected concentration maximum in the fractions was 200 g Ca or K/ L eluent, if all the analyte from the sample were in one fraction, corresponding to approximately 5 mol Ca or K /L eluent. The lower end of the estimation was 1 g Ca or K/ L eluent, for 0.5 percent of the present potassium or calcium in one fraction, corresponding to approximately 25 mmol Ca or K /L. Divided by 2000, the sample dilution, the expected concentration range was 0.0125 mmol/L-2.5 mmol/L potassium or calcium. For this experiment no potassium or calcium standard has yet been acquired. So, it was planned to provide these elements for the calibration curve in form of the salts K_2SO_4 and $CaCl_2$, which could be found in the laboratory. But as the concentrations of the calibration curve were too low, to weigh in such small amounts of salts with an acceptable error, a concentrated standard solution had to be prepared, which was diluted to prepare the different calibration solutions. For the concentration of the standard solution 5 mmol/L of each K and Ca was chosen. For 100 mL of the standard solution, 0.0435 g K_2SO_4 and 0.0555 g $CaCl_2$ were weighed in a 100 mL volumetric flask and filled up to 100 mL with bidistilled water. Based on

these estimations and calculations the following calibration setup was developed, as presented in table 67.

Table 67: Calibration data for the measurement of the Ca and K-elution fractions with ICP-OES for the determination of the Ca and K elution curves

sample	**c [mmol/L]**	**c [mol/ 10 mL]**	**m K_2SO_4 [mg]**	**m $CaCl_2$ [mg]**	**added standard solution [mL]**	**c [µg/kg]**
C0	0	0	0	0	0	0
C1	0.01	0.0000001	0.00871	0.0111	0.02	400
C2	0.05	0.0000005	0.0436	0.0555	0.1	2,000
C3	0.1	0.000001	0.0871	0.111	0.2	4,000
C4	0.5	0.000005	0.436	0.555	1	20,000
C5	1	0.00001	0.871	1.11	2	40,000
C6	2	0.00002	1.74	2.22	4	80,000
C7	2.5	0.000025	2.18	2.77	5	100,000

Table 67 shows the concentration range, in which the calibration should be provided, as well as the theoretical mass of the salts, necessary to obtain the concentration, that was provided through adding the self-made standard. As the output data of the device is sometimes in µg/kg, the concentration values in mM/L were also converted into this unit.

The calibration standards were prepared the same way as the samples. The only difference was that instead of a constant amount of sample, a varying amount of the self-made Ca and K standard was added (see table 67), which contained 5 mM/L of each K and Ca. Then 2 mL concentrated nitric acid was added for pH adjusting and the calibration samples were filled up to a volume of 10 mL with bidistilled water.

The calibration curve was determined by measuring the calibration solutions. With the calibration curve, a direct connection between the signal at the emission wavelengths, typical for calcium and potassium and their concentration could be determined. This connection was then used by the measurement software for the quantification of the calcium and potassium content in the fraction samples. The results were put out in the unit [µmol/L].

After the calibration, all 100 fraction samples diluted 1:2,000 were measured. The samples that solidified at room temperature were melted through heating in a water bath before the sample preparation for the ICP-OES measurement. After the measurement, the data was processed and visualized.

Figure 83 shows the recording of the elution regions of yttrium, calcium and potassium, achieved with the established DOWEX® 50 WX8 200-400 (H) resin by Serva. The yttrium elution curve was recorded separately and is presented here for comparison. This is the relative elution curve, with the concentration maximum normed to 100 % and the rest of the concentrations presented relative to the maximum of the concentration of the analyte during the elution.

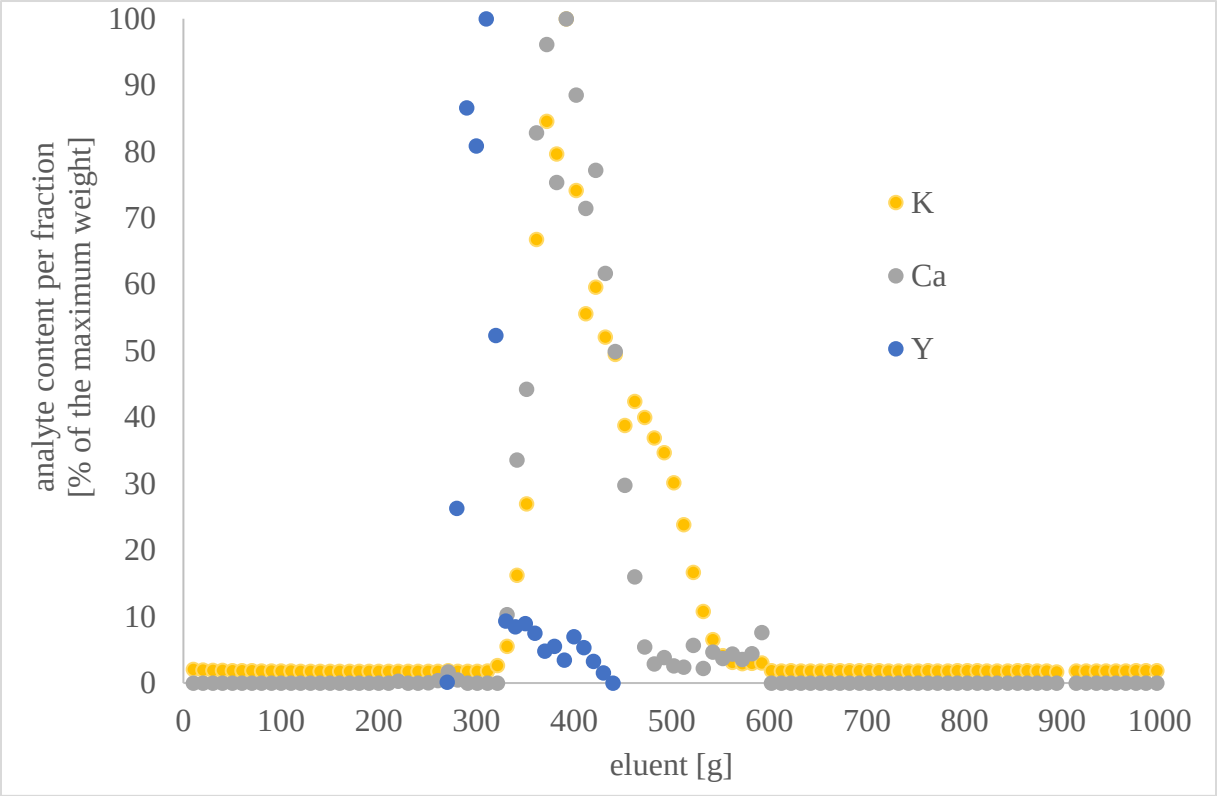

Figure 83: Relative Y, K and Ca elution curves, achieved with the DOWEX by Serva, eluent ammonium-lactate at pH 7, measurement with ICP-OES

A significant tailing of the elution curve was present for all three analytes. This may be due to the calibration with a self-made salt solution standard and an multielement standard, instead of standards specific for these analytes. This calibration makes the curve not as exact as the newer ones. A mediocre separation between the elution regions of the main analyte yttrium and the interfering elements potassium and calcium was achieved. There was no overlap between the elution maxima and main elution regions of yttrium and the interfering elements, but the tailing component of the yttrium elution region overlapped with the elution regions of calcium and potassium. An almost complete overlap of the potassium and calcium elution regions is evident. All in all, this shows that a separation of the majority of the yttrium fraction from calcium and potassium would be possible without severe yield losses. But the elution regions of the analytes are very close to each other and a slight shift of them could cause a more significant overlap.

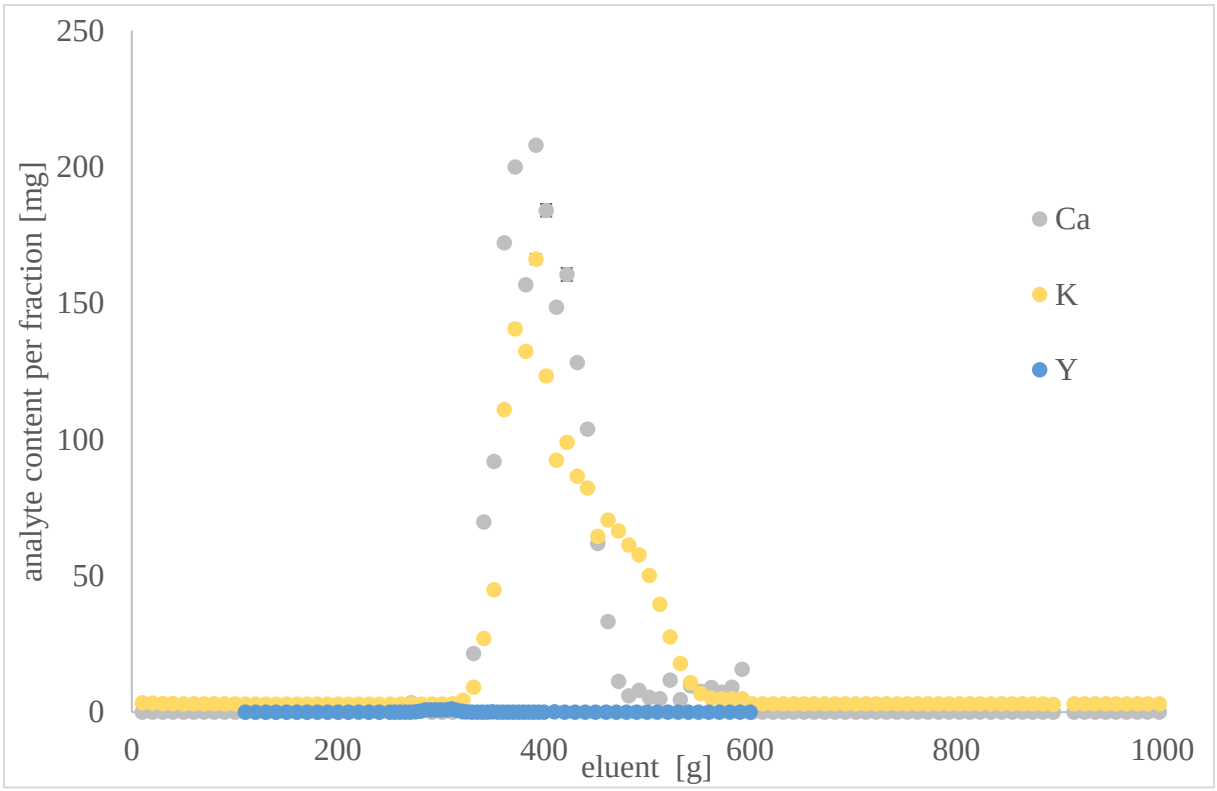

Figure 84: Absolute Y, K and Ca elution curves, achieved with the DOWEX by Serva, eluent ammonium-lactate at pH 7, measurement with ICP-OES

For comparison, figure 84 shows the absolute results of the distribution of the different analytes during the elution process. The interfering elements calcium and potassium were present in much higher concentrations in the sample matrix than the expected amounts of the analyte yttrium, if it were present at all. Additionally, a significant potassium background was measured for all fractions. This could be because of the use of glassware, which contains potassium, or because of the insufficient separation performance of the column for potassium.

Additionally, the fractions 27-32 of the calcium and potassium separation were measured again, with a lower dilution of just 1:4, as they represented the yttrium-elution fraction. This was done to determine the potassium background in the yttrium elution range more precisely. The results of these measurements are visualized below in figure 85.

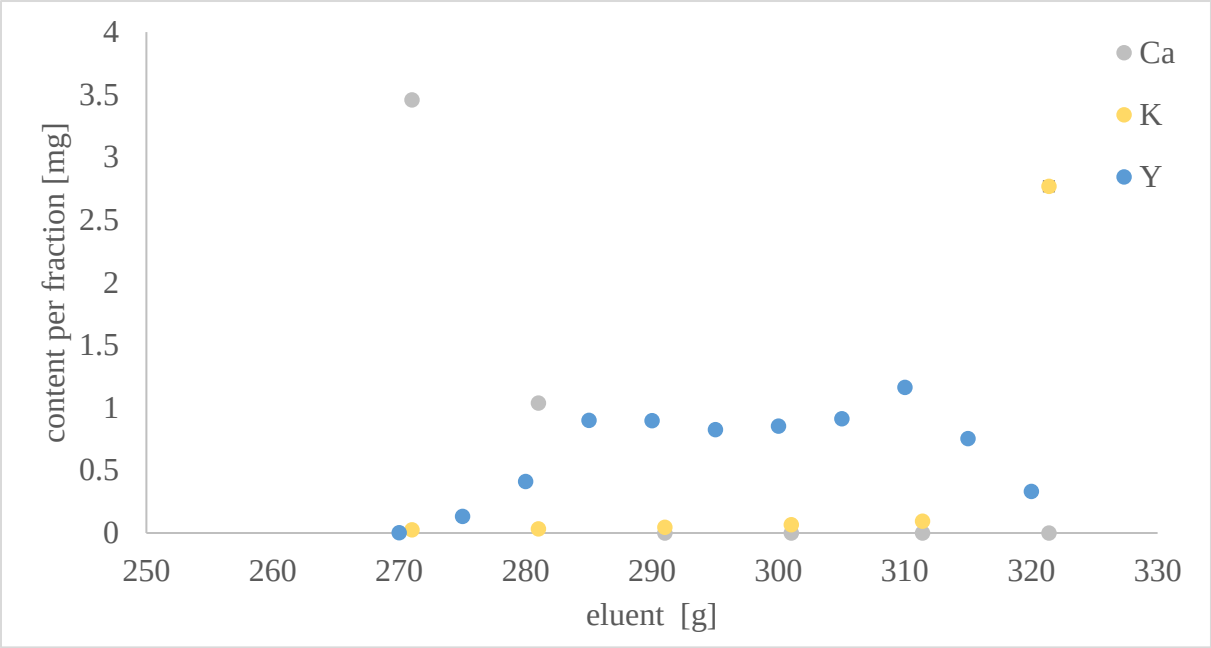

Figure 85: Close-up of the K and Ca content in the Y elution region, achieved with the DOWEX by Serva, eluent ammonium-lactate at pH 7, measurement with ICP-OES

Figure 85 shows the recording of the concentrations of potassium and calcium in the elution region of yttrium, achieved with the established DOWEX® 50 WX8 200-400 (H) resin by Serva. The yttrium elution curve was recorded separately and is presented here for comparison. It is shown how there was an overlap at the edges of the elution region of yttrium. At lower eluent volumes with calcium, which then decreases to a background signal. At higher eluent volumes with potassium, with its signal increasing after the maximum of the yttrium elution region. As shown in the previous figures, there is no overlap at the yttrium elution maximum, at which a sample for analysis would be taken. But the elution regions are dangerously close to each other, and small shifts could lead to a significantly stronger overlap.

5.4.5 Slower elution for a better separation between the elution regions of Y, K and Ca

After the previous pretests to approximately determine the elution regions of yttrium, calcium and potassium, if separated with the Hot Column Chromatography following the analysis instruction, a complete chromatogram with of these analytes and additionally strontium was recorded. This time in one separation, so differences in the elution process would be accounted for. For this, the elution was performed with the new DOWEX® 50 WX8 200-400 (H) resin by Alfa Aesar and the eluent ammonium-lactate at pH6, as established in chapter 5.3.

As standard sample matrix, 10.00 g not contaminated milk ash, prepared from commercially available whole long-life milk by the brand Berchtesgadener Land, was used. It was solved in the usual 1:1 mixture of 6 M hydrochloric acid and 1.5 M lactic acid. Additionally, 1 mL of the stable yttrium tracer, containing 10 mg Y, and 2 mL stable strontium tracer, containing in total 100 mg Sr, were added. Potassium and calcium were naturally present in the sample matrix in significant amounts, according to the milk packaging 124 mg calcium per 100 mL. After the sample was solved and applied to the column, the Hot Column Chromatography was performed at the elution speed of 2.5 mL/min. During this, 100 elution fractions à 10 mL were collected. As detection method, for the quantification of these elements in the different fractions, ICP OES was used. For the measurement, the fraction samples were diluted 1:250. Per ICP-OES sample 40 µL of the fractions were used and 2 mL concentrated nitric acid was added for pH adjusting. The samples were filled up to a volume of 10 mL with bidistilled water.

To be able to sensibly measure the analyte content in the samples, a calibration curve had to be calculated and prepared for all analytes. For this, the expected concentration range in the elution curve had to be estimated and divided by 250, the selected dilution, as the ICP-OES is optimized for lower concentrations and ideally narrow concentration ranges. For calcium and potassium, the basis for the calibration concentrations was the information from the milk packaging and previous measurements. For yttrium, the added tracer concentration and the distribution of yttrium during the elution, known from previous experiments, were used to estimate an optimal concentration range. For strontium, the tracer volume was increased, because it was known from previous experiments, that its elution region was wide. This means the strontium was distributed over more individual fractions, which contained smaller concentrations. So, to be able to reliably measure strontium in those fractions, the concentration had to be increased.

Table 68: Calibration for the measurement of yttrium, strontium, potassium and calcium in the elution fractions with ICP-OES

sample	c(Y) [µg/kg]	c(Sr) [µg/kg]	c(K) [µg/kg]	c(Ca) [µg/kg]
C0	0	0	0	0
C1	10	20	400	400
C2	50	200	2,000	2,000
C3	100	500	4,000	4,000
C4	500	1,000	20,000	20,000
C5	1,000	1,500	40,000	40,000
C6	2,000	2,000	80,000	80,000
C7	0	3,000	100,000	100,000

Finally, the concentrations in the calibration curve were optimized to encompass as large of a concentration range as possible and sensible, as is seen in the table 68. The aim was to be able to quantify the concentration maximum of the elution curve and at the same time to still be able to detect 1 % of the concentration maximum in the different fractions. Another aim was to be able to prepare one set of calibration solutions for all the analytes and samples. As analyte sources for the preparation of the calibration, the ICP standards by Bernd Kraft were used, which had a standard concentration of 1 g/L and in some cases were prediluted to obtain volumes, that were easier to handle with Eppendorf pipettes.

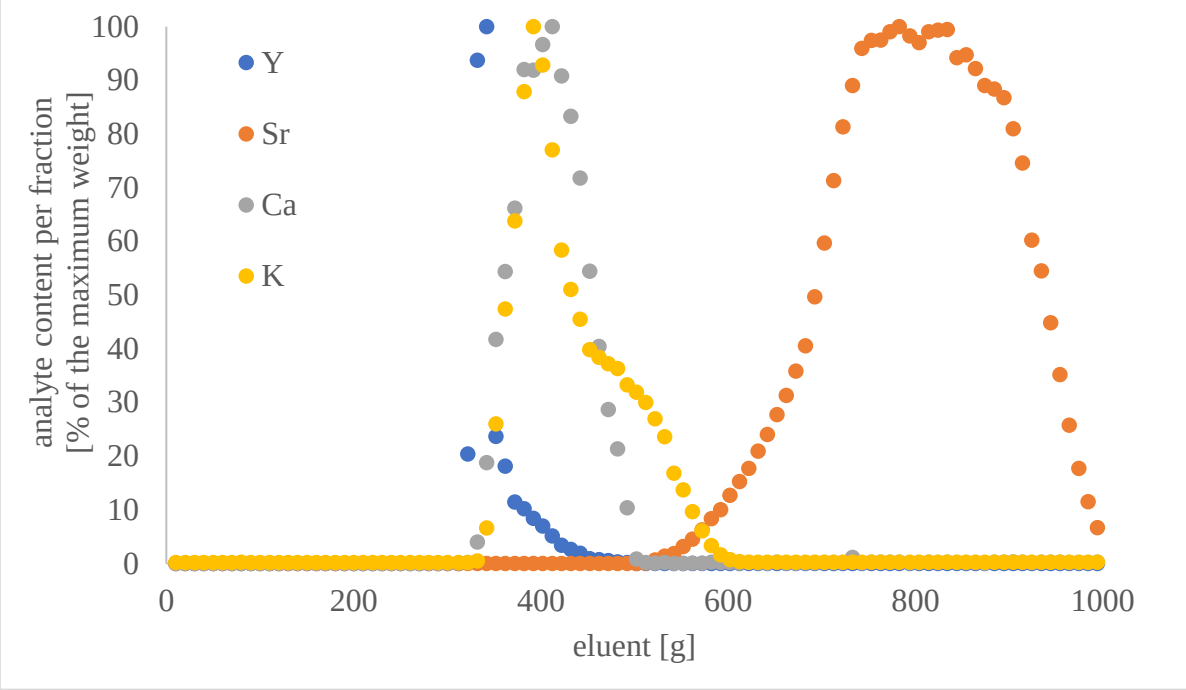

Figure 86: Relative Y, K, Ca and Sr elution curves, achieved with the DOWEX by Alfa Aesar, eluent ammonium-lactate at pH6, measurement with ICP-OES

The resulting elution curve for the determination of K, Ca, Y and Sr in milk ash with the DOWEX® 50 WX8 (200-400 mesh) by Alfa Aesar and sample measurement with ICP-OES is shown in figure 86. This is the relative elution curve, with the concentration maximum normed to 100 % and the rest of the concentrations presented relative to the concentration maximum of the analyte during the elution.

A very good separation between yttrium and strontium, a good separation between calcium and strontium and an acceptable separation between potassium and strontium were achieved. The separation between yttrium, calcium and potassium was only mediocre. But at least the relative content of potassium and calcium was quite small in the maximum range of yttrium. The reason for this could also be, that fraction 34, which was the fraction with the highest yttrium content, contained solid precipitate, that could not be solved through heating after the sample cooled down. This precipitate was likely calcium, but could also contain potassium, and subsequently was not accounted for during the ICP-OES measurement. All in all, this more recent elution curve shows no significant tailing of the elution regions, compared to the previously recorded ones. But a stronger overlap between the yttrium elution region and the elution regions of calcium and potassium occurred, the possibility of which was previously speculated about.

Next it was tested, if a slower elution speed would lead to a better separation between yttrium, potassium and calcium in the Hot Column Chromatography. To test this, the elution was performed with the new DOWEX® 50 WX8 200-400 (H) resin by Alfa Aesar and the eluent ammonium-lactate at pH6, as established in chapter 5.3. The elution speed was reduced in the elution region of the analytes, 200-500 g eluent throughput including the sample inlet, to 1.5 g/min. Additionally, to gain more precise elution regions, the fraction volume was reduced to 5 g eluent per fraction for the fractions 26-45, corresponding to the eluent throughput of 250-350 g eluent.

As standard sample matrix 10.00 g not contaminated milk ash, prepared from commercially available whole long-life milk by the brand Berchtesgadener Land, was used. It was solved in the usual 1:1 mixture of 6 molar hydrochloric acid and 1.5 molar lactic acid. Additionally, 1 mL of the stable yttrium tracer, containing 10 mg Y, and 2 mL stable strontium tracer, containing in total 100 mg Sr, were added. Potassium and calcium were naturally present in the sample matrix in significant amounts, according to the milk packaging 124 mg calcium per 100 mL. After the sample was solved and applied to the column, the Hot Column Chromatography was performed at the elution speed of 2.5 g/min until fraction 26, corresponding to 250 g eluent throughput, at which point it was reduced to 1.5 g/min. During this, 60 elution fractions, 20 à 5 g and 40 à 10 g were collected. As detection method, for the quantification of these elements in the different fractions, ICP OES was used. For the measurement, the fraction samples were diluted 1:250. Per ICP-OES sample, 40 µL of the fractions were used and 2 mL concentrated nitric acid was added for pH adjusting. The samples were filled up to a volume of 10 mL with bidistilled water.

For the ICP-OES measurement, the same calibration curve was used as the one calculated for the initial determination of the elution curve with the new DOWEX® 50 WX8 (200-400 mesh) by Alfa Aesar, as seen in table 68.

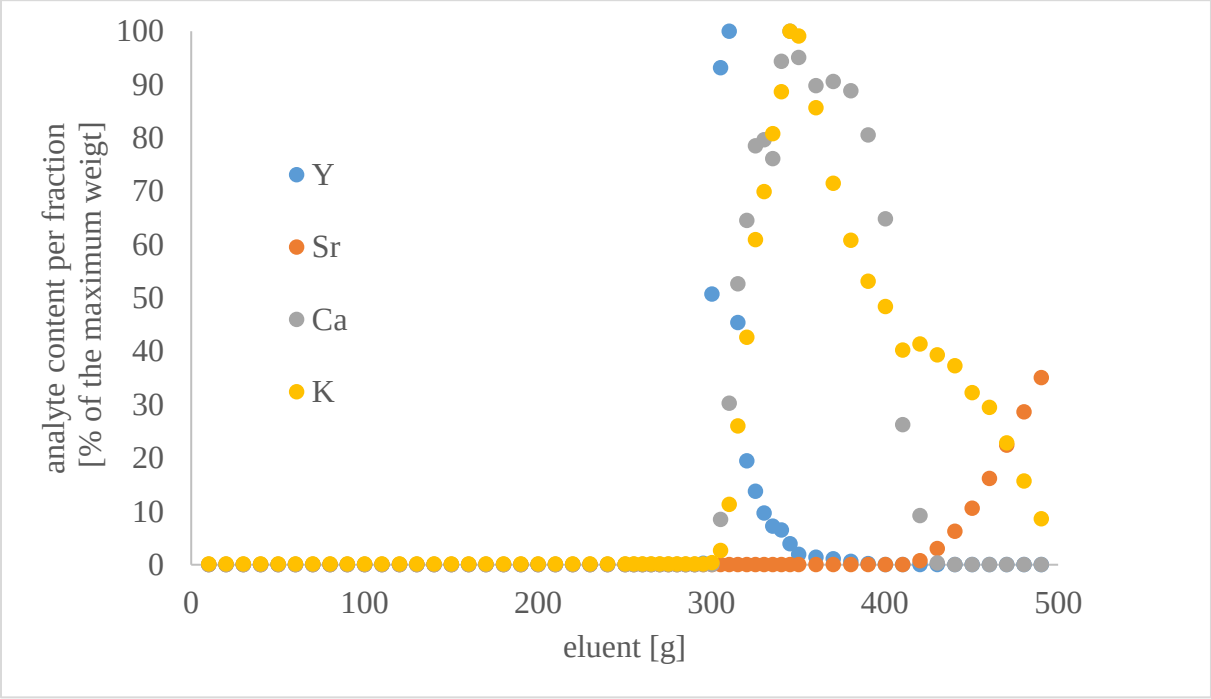

Figure 87: Relative Y, K, Ca and Sr elution curves, slowed down elution to 1.5 g/min between 200 and 500 g eluent, achieved with the DOWEX by Alfa Aesar, eluent ammonium-lactate at pH6, measurement with ICP-OES

The resulting elution curve for the determination of K, Ca, Y and Sr in milk ash with the DOWEX® 50 WX8 (200-400 mesh) by Alfa Aesar, a decreased elution speed in the elution region between 250 and 500 g eluent and sample measurement with ICP-OES is shown in figure 87. The fractions 26-45 contained only 5 g eluent. The rest of the fractions contained 10 g eluent. The eluent ammonium-lactate had the pH6. This is the relative elution curve, with the concentration maximum normed to 100 % and the rest of the concentrations presented relative to the concentration maximum of the analyte during the elution. The fractions 36-50, corresponding to 300-400 g eluent throughput, solidified after cooling down to room temperature to a white, wax like substance, due to their high calcium content. The fractions 36-38 could not be completely melted, even after heating in the water bath. The fractions 36 and 37 showed a significant yellow coloring.

With the slowed down elution, a very good separation between yttrium and strontium, a good separation between calcium and strontium and an acceptable separation between potassium and strontium were achieved. The separation between yttrium, calcium and potassium was only mediocre. But at least the relative content of potassium and calcium was quite small in the maximum range of yttrium. All in all, the results were very comparable to the ones achieved at the consistent elution speed of 2.5 g/min. The slowing down of the elution did not have a significant effect on the separation.

Table 69: Comparison between the elution results for the analytes Y, Ca, K and Sr with an elution at standard speed and a slowed down elution, achieved with the DOWEX by Alfa Aesar, eluent ammonium-lactate at pH6, measurement with ICP-OES

element	**elution region [g] elution at 2.5 g/min**	**concentration maximum [g] elution at 2.5 g/min**	**elution region [g] elution slowed down**	**concentration maximum [g] elution slowed down**
yttrium	310-480	330-340	295-390	305-310
strontium	510-1000	770-780	410->500	
calcium	320-510	400-410	295- > 500	345-350
potassium	330-600	380-390	330-600	340-345

Table 69 shows the overall shift of the elution regions to lower eluent volumes, in case of a slowed down elution. But the overlap between the elution regions did not decrease with a slower elution. It even increased, leading to a worse separation than with a higher and constant elution speed. Therefore, the slowing down of the elution would not be implemented in routine analytics.

5.4.6 Determination of the optimal sampling region for the ion chromatographic separation of yttrium for the determination of ^{90}Sr via ^{90}Y

The next step in the method development process for the quantification of ^{90}Sr in samples via its daughter nuclide ^{90}Y, was to determine the optimal sampling region for ^{90}Y. The aim was to achieve the highest yttrium yield and its best separation from the interfering elements possible.

The elution region of yttrium was previously determined in standard conditions as 290-330 g eluent throughput, including the sample inlet. The elution was performed with the new DOWEX® 50 WX8 200-400 (H) resin by Alfa Aesar and the eluent ammonium-lactate at pH6, as established in chapter 5.3.

The aim for the analysis of ^{90}Sr via its daughter nuclide ^{90}Y is to directly measure the yttrium-fraction with a Cherenkov measurement in the QUANTULUS. The volume of the measured fraction cannot exceed 20 mL, as this is the volume of the LSC-vials used for the measurement. The device is constructed and the measurement is standardized for this volume and geometry. Therefore, an optimal 20 mL sampling fraction in the narrow, but still significantly wider yttrium-elution region had to be determined.

For this, the following potential sampling fractions were considered:

290-310 g 295-315 g 300-320 g 305-325 g 310-330 g

The elution for the determination of the Y, K and Ca content of each potential sampling fraction was performed with the new DOWEX® 50 WX8 200-400 (H) resin by Alfa Aesar and the eluent ammonium-lactate at pH6, as established in chapter 5.3.

As standard sample matrix, 10.0 g not contaminated milk ash, prepared from commercially available whole long-life milk by the brand Berchtesgadener Land or remaining milk ash from environmental monitoring, which was confirmed to be not radioactively contaminated, was used. It was solved in 80 mL of the usual 1:1 mixture of 6 M hydrochloric acid and 1.5 M lactic acid. Additionally, 1 mL of the stable yttrium tracer, containing 10 mg Y was added. Potassium and calcium were naturally present in the sample matrix in significant amounts, according to the milk packaging 124 mg calcium per 100 mL. Then the sample was solved and applied to the column. The remaining ash residue was not washed or solved after that, to ensure a constant solvent volume for all fraction analyses. The Hot Column Chromatography was performed at the elution speed of 2.5 mL/min. The chosen 20 g fraction was separated and the determination of the Y, Ca and K content was performed via ICP-OES. For the measurement, the sampling fractions were diluted 1:250. Per ICP-OES sample, 40 µL of the fractions were used and 2 mL concentrated nitric acid was added for pH adjusting. The samples were filled up to a volume of 10 mL with bidistilled water.

For the ICP-OES measurement, the same calibration curve was used, as the one calculated for the initial determination of the elution curve with the new DOWEX® 50 WX8 (200-400 mesh) by Alfa Aesar, as presented in section 5.3.1.

The first sampling fraction of 290 to 310 g eluent throughput, including the sample inlet, contained neither yttrium nor calcium or potassium in measurable amounts. The reported values of the ICP-OES measurement program were <-503.9 µg/kg for Ca, <-219.3 µg/kg for K and <- 2.169 µg/kg for Y. Negative values occur due the calculations based on the calibration and

were corrected to zero. This sampling fraction was naturally deemed unsuitable for the yttrium sampling, as it did not contain any.

The sample inlet was 105.4 g. The measured sampling region encompassed 20 g eluent between 290 and 300 g eluent throughput, including the sample inlet. The yttrium yield was 0.00 % in this sampling fraction. The sampling fraction was clear, liquid and colorless.

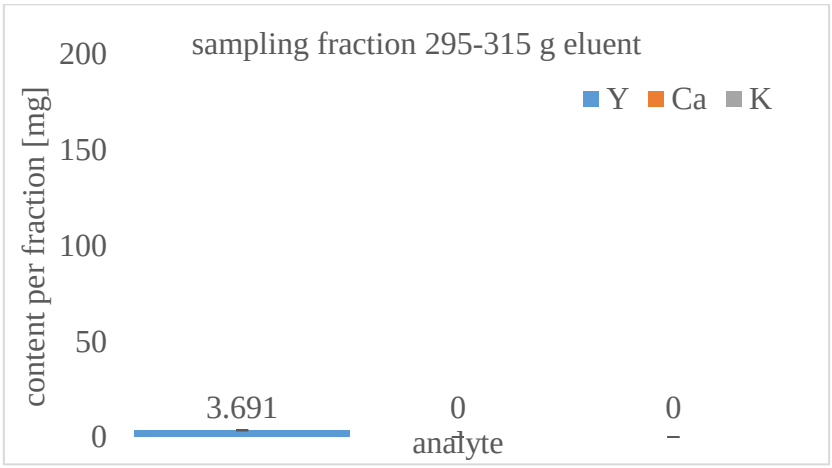

Figure 88: Y, Ca and K content in the sampling fraction of 295-315 g eluent, 100 % Y ≡10 mg

Figure 88 represents the Y, Ca and K content in the sampling fraction of 295 to 315 g eluent throughput, including the sample inlet. As is evident from the figure, this sampling fraction only contained yttrium and did not contain calcium or potassium in measurable amounts. The reported values of the ICP-OES measurement program were <-275.3 µg/kg for Ca and <-248.6 µg/kg for K. Of course, negative concentrations do not make sense. These values were determined though a calculation, based on the calibration, and were corrected to zero. As a complete separation of yttrium from the interfering elements was achieved in this sampling fraction, it was considered as a potential yttrium sampling region for the ^{90}Sr analysis via ^{90}Y.

The sample inlet was 103.7 g. The measured sampling region encompassed 20.1 g eluent between 295.2 g and 305.3 g eluent throughput, including the sample inlet. The yttrium yield was 36.91 % in this sampling fraction. The sampling fraction was clear, liquid and colorless.

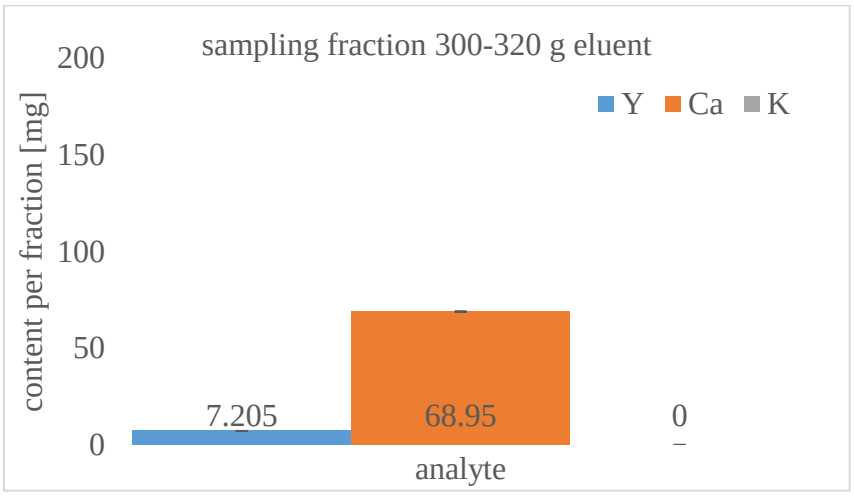

Figure 89: Y, Ca and K content in the sampling fraction of 300-320 g eluent 100 % Y ≡10 mg

Figure 89 represents the Y, Ca and K content in the sampling fraction of 300 to 320 g eluent throughput, including the sample inlet. As is evident from the figure, this sampling fraction contained yttrium and calcium, but did not contain potassium in measurable amounts. The reported value of the ICP-OES measurement program for potassium was <-250.1 µg/kg. Of course, negative concentrations do not make sense. The value was determined though a calculation, based on the calibration, and was corrected to zero. As a complete separation of yttrium from the interfering element potassium was achieved in this sampling fraction, as well as a relatively high yttrium yield, it was considered as potential yttrium sampling region for the ^{90}Sr analysis via ^{90}Y.

The sample inlet was 100.8 g. The measured sampling region encompassed 20.0 g eluent between 300 and 320 g eluent throughput, including the sample inlet. The yttrium yield was 72.05 % in this sampling fraction. It was slightly yellow and crystals formed in the fraction, after cooling down to room temperature. After heating in a water bath, the crystals could not be solved completely.

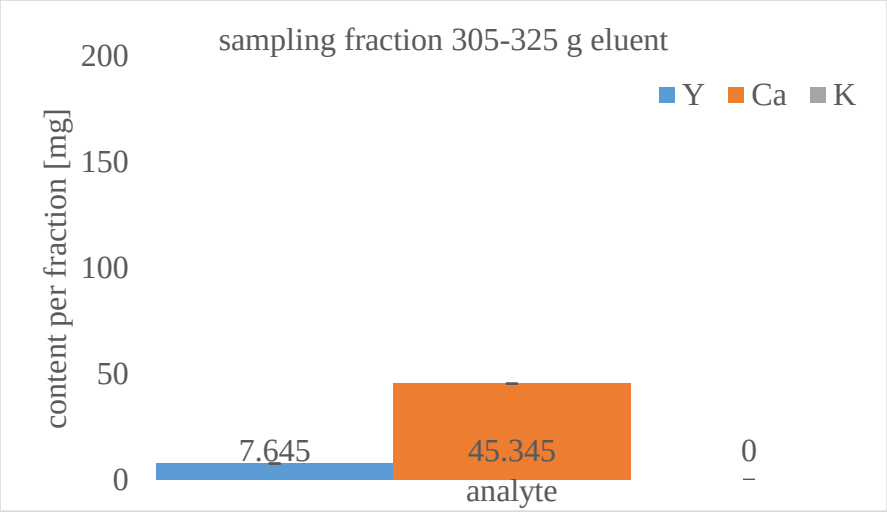

Figure 90: Y, Ca and K content in the sampling fraction of 305-325 g eluent 100 % Y ≡10 mg

Figure 90 represents the Y, Ca and K content in the sampling fraction of 305 to 325 g eluent throughput, including the sample inlet. As is evident from the figure, this sampling fraction contained yttrium and calcium, but did not contain potassium in measurable amounts. The reported value of the ICP-OES measurement program for potassium was <-250.5 µg/kg. Of course, negative concentrations do not make sense. The value was determined though a calculation, based on the calibration, and was corrected to zero. As a complete separation of yttrium from the interfering element potassium was achieved in this sampling fraction, as well as the highest yttrium yield of all sampling fractions, it was considered as potential yttrium sampling region for the ^{90}Sr analysis via ^{90}Y. All in all, the results for this sampling fraction were very similar to the previous one, with the only significant difference being the higher yttrium yield of this sampling fraction, which makes it preferable to the previous one.

The sample inlet was 102.0 g. The measured sampling region encompassed 20.0 g eluent between 305 and 325 g eluent throughput, including the sample inlet. The yttrium yield was 76.45 % in this sampling fraction. It was slightly yellow and crystals formed in the fraction, after cooling down to room temperature. After heating in a water bath, the crystals could not be solved completely.

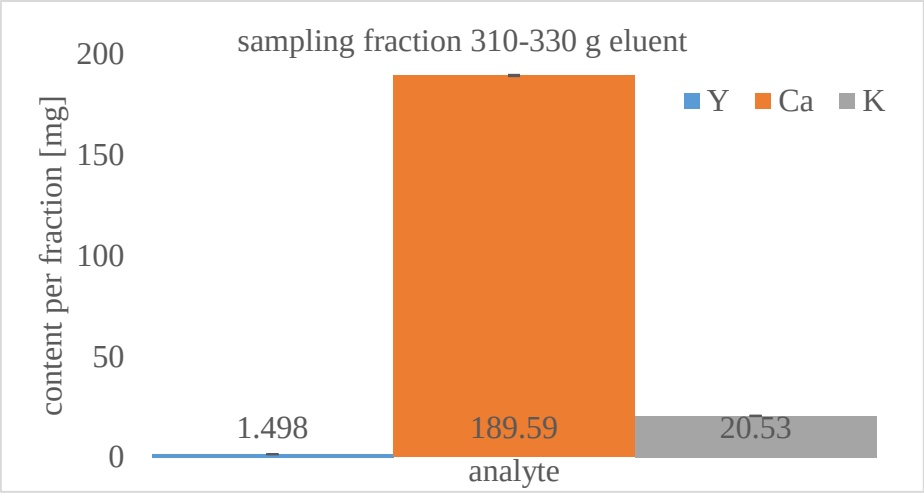

Figure 91: Y, Ca and K content in the sampling fraction of 310-330 g eluent, 100 % Y ≡10 mg

Figure 91 represents the Y, Ca and K content in the sampling fraction of 310 to 330 g eluent throughput, including the sample inlet. As is evident from the figure, this sampling fraction contained calcium, potassium and only a small amount of yttrium. It was deemed unsuitable for the yttrium sampling, as it contained the second to least amount of yttrium and no separation from the interfering elements calcium and potassium was achieved.

The sample inlet was 94.4 g. The measured sampling region encompassed 20.0 g eluent between 310 and 330 g eluent throughput, including the sample inlet. The yttrium yield was 14.98 % in this sampling fraction. It has turned into a white, wax-like solid upon cooling down to room temperature. The solid sample could be solved almost completely by heating in a water bath.

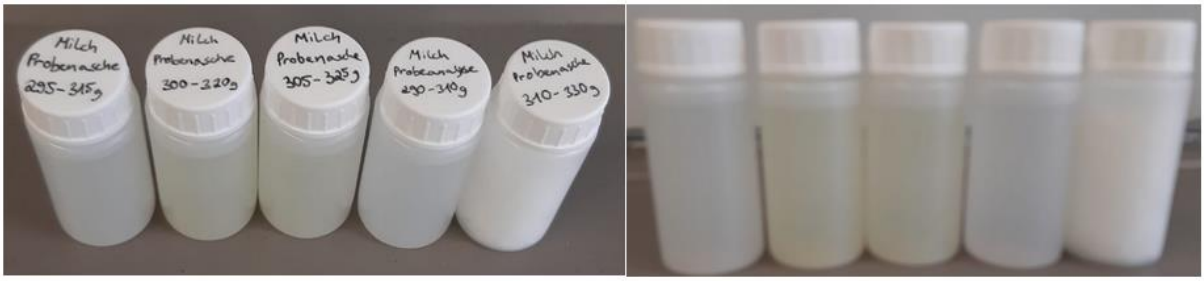

Figure 92: The five different potential sampling regions for Y and their condition after cooling down to room temperature

The textures and colors of the different sampling regions are visualized in figure 92. The sampling fractions of 290-310 g eluent and 295-315 g eluent were clear, colorless and liquid. The sampling fractions 300-320 g eluent and 305-325 eluent were slightly yellow and showed crystal formation after cooling down to room temperature. The sampling fraction 310-330 g eluent solidified into a white wax-like texture after cooling down to room temperature.

Table 70: Determination of the optimal sampling region of Y for the analysis of ^{90}Sr via ^{90}Y, summary of the results

elution region [g eluent]	Y-content per fraction [mg]	Y-yield [%]	Ca-content per fraction [mg]	K-content per fraction [mg]	texture and color of the sample
290-310	0 ± 0.000064	0	0 ± 0.051	0 ± 0.019	clear, liquid, colorless
295-315	3.7 ± 0.012	36	0 ± 0.0079	0 ± 0.0034	clear, liquid, colorless
300-320	7.2 ± 0.026	72	69 ± 0.21	0 ± 0.0024	slightly yellow, crystal formation
305-325	7.6 ± 0.016	76	45 ± 0.11	0 ± 0.0018	slightly yellow, crystal formation
310-330	1.5 ± 0.0040	14	190 ± 0.33	21 ± 0.15	white, soloid, wax-like

The results of the determination of the optimal sampling region are summarized in table 70. The collected data showed that the sampling regions of 295-315 g eluent and 305-325 g eluent, including the sample inlet, were the most suitable for the yttrium sampling.

In the sampling region of 295-315 g eluent only a comparably low yttrium yield of 36.91 % was achieved, but the interfering elements potassium and calcium were completely removed. Additionally, the sample was clear and liquid and stayed in this state after cooling down to room temperature. Those are optimal conditions for the Cherenkov measurement and would lead to a relatively high SQP(E) value, and therefore to a high physical yield.

In the sampling region of 305-325 g eluent, the highest yttrium yield of 76.45 % was achieved. Additionally, potassium and therefore the main interfering nuclide ^{40}K was completely separated from the sample. The downside of this sampling region was the significant calcium amount in the sample. This led to a yellow coloring and crystal formation, as soon as the sample cooled down to room temperature. This would lower the SQP(E) value of the Cherenkov measurement and subsequently the physical yield.

Which one of these sampling regions is chosen depends on whether the maximal yttrium yield or the best separation from interfering elements and the best sample conditions are prioritized.

The other sampling regions were, for various reasons, not or less suitable for the sampling of yttrium. The sampling region of 290-310 g eluent did not contain yttrium at all. The sampling region of 310-330 g eluent contained the second to least yttrium yield of 14.98 % and contained potassium, as the only sampling region. Additionally, it contained the highest amount of calcium, which caused the sample to solidify into a white, wax-like solid after cooling down to room temperature. This would lead to a very small physical yield during the Cherenkov measurement. The sampling region of 300-320 g eluent was similar to the sampling region of 295-315 g eluent but had a lower yttrium yield and at the same time a higher calcium content. This sampling region would theoretically be suitable for the yttrium sampling but was outperformed in every aspect by the sampling region of 295-315 g eluent.

5.4.7 Complete analysis for the determination of ^{90}Sr via ^{90}Y

After the preparational experiments described in the previous sections were performed, the focus of this work could be investigated. The complete analysis of ^{90}Sr via its daughter nuclide ^{90}Y could be tested and optimized, using the previously obtained knowledge.

Before the complete analysis could be performed, the parameters for the Cherenkov measurement in the QUANTULUS, which was not part of the previous experiments, had to be determined. The main parameters in question were which ^{90}Sr tracer would be used, the added activity of the ^{90}Sr tracer and the measurement time of the samples.

As ^{90}Sr tracer, the laboratory intern prepared ^{90}Sr solution from the 2.12.2004, with an activity of 20000 Bq/1001.6 g, or 19.24 Bq/g, at that time, was chosen. The current activity was determined with equation 5.23:

$$A = A_0 \cdot e^{\left(-\frac{\ln(2)}{t_{1/2}} \cdot \Delta t\right)} \tag{5.23}$$

A represents the current activity, A_0 the activity at the time of the tracer preparation (19.24 Bq/g), $t_{1/2}$ is the half- life of the nuclide ^{90}Sr (28.5 years) and Δt is the time difference between the tracer preparation and the current point in time. As current activity of the tracer at the time of the experiments, 12.9 Bq/g was calculated.

To confirm this calculation, a LSC measurement of the tracer was performed. For this, 0.2290 g of the ^{90}Sr tracer were weighed in a 20 mL LSC vial and filled up to 5 g with bidistilled water. 15 mL of the QSA scintillation cocktail were added. The sample was mixed and a LSC measurement of it was performed in the QUANTULUS. The aim was to reach at least 10,000 counts for a good differentiation between peak and background. The added activity was 2.58 Bq of ^{90}Sr and additionally 2.58 Bq of ^{90}Y, as they were in radioactive equilibrium and the activity of the daughter nuclide ^{90}Y was the same as the activity of the mother nuclide ^{90}Sr in the tracer solution. The physical yield of the LSC measurement of ^{90}Sr was assumed to be 95 %. From this information, the potential count rate R could be calculated.

$$R = A \cdot \eta_{phys} \tag{5.24}$$

$$R = (2.58 + 2.58)\ Bq \cdot 0.95 = 4.902\ cps \tag{5.25}$$

As the count rate R is the number of counts per time, the count rate and the aimed for number of counts N could be used to determine the necessary measurement time t.

$$R = \frac{N}{t} \tag{5.26}$$

$$t_m = \frac{N}{R} = \frac{10000}{4.902} \approx 2040\ s \approx 34\ min \tag{5.27}$$

As necessary measurement time, 34 minutes were determined. To make sure the 10,000 counts were reached, the sample was measured for 100 min.

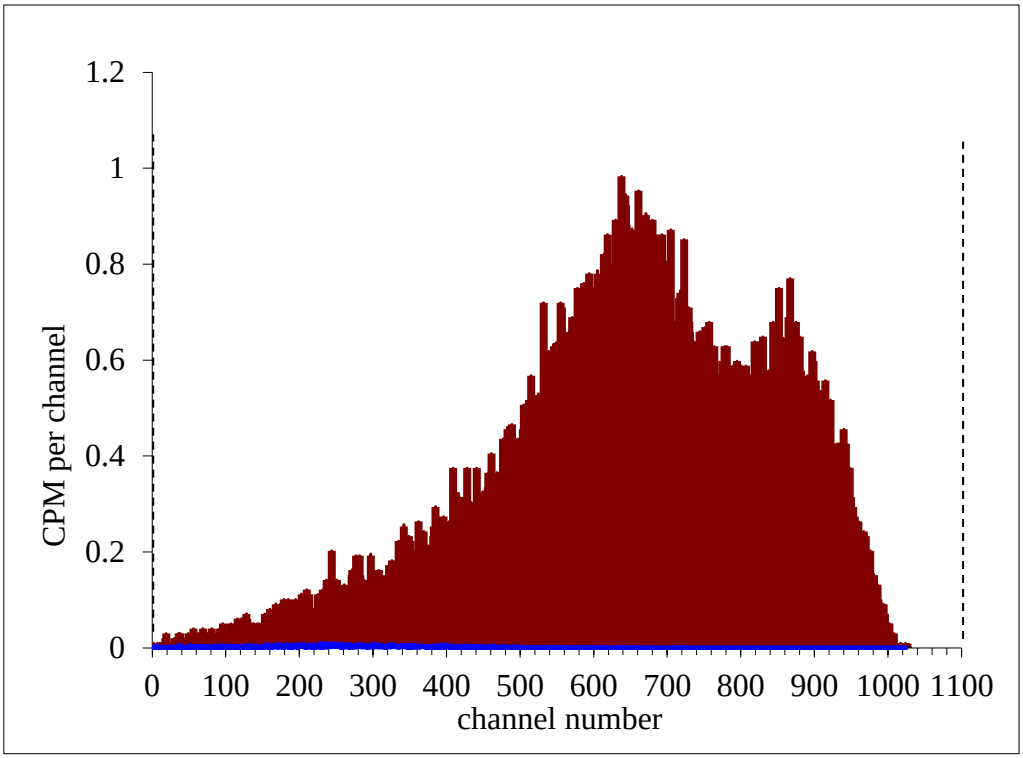

Figure 93: LSC spectrum of 0.2 g ^{90}Sr tracer filled up to 5 g with water + 15 mL QSA scintillation cocktail (red) t_m: 98.390 min with a Cherenkov measurement of 20 mL water as background (blue), QUANTULUS 1220 KB

Figure 93 shows the LSC spectrum of the 0.2 g ^{90}Sr tracer sample described above. The y-axis shows the counts per minute per channel, representing the number of decays. The x-axis shows the channels, corresponding to the decay energy. The red graph represents the sample signal. The blue graph represents the background signal, measured separately. The peak in the channels 400 to 800 represents the decays of ^{90}Sr, the peak in the channels 700-1,000 represents the decays of its daughter nuclide ^{90}Y, which is also the target of the complete analysis. All in all, 31,930 decay counts were detected, assigned to the practically complete measured energy span between the channels 2 and 1,024. From this the physical efficiency for the measurement could be calculated.

$$R = A \cdot \eta_{phys} \cdot \eta_{chem} \tag{5.28}$$

$$\eta_{phys} = \frac{R}{A} \tag{5.29}$$

As this was a direct measurement without chemical preparation η_{chem} equals 1. The count rate R could be calculated by dividing the number of counts N (31,930 decay counts) through the measurement time in seconds (5,918 s), resulting in 5.40. The added combined ^{90}Sr and ^{90}Y activity was 2.58 Bq times two (5.16 Bq). The resulting physical yield was 105 %, 10 percent points higher than the assumed physical yield. The physical yield being higher than 100 % was likely due to background radiation, that did not stem from the sample and increased the number of counts slightly. Another source for this deviation could be a rest-uncertainty of the activity of the tracer. All in all, the variation from the inserted values was only small and it can be assumed, that the calculated current activity of the tracer was correct with an acceptable rest deviation.

Then the physical yield of the Cherenkov measurement of ^{90}Sr had to be determined. It differs from the LSC physical yield from the previous measurement, as the Cherenkov measurement is performed with simply an aqueous solution of the analyte, without the signal enhancing LSC cocktail. Additionally, the Cherenkov measurement does not show an energy resolution and is only applicable for nuclides with high emission energies. For the measurement 20.0290 g of the ^{90}Sr tracer were filled in a LSC vial and measured in the QUANTULUS for 100 minutes.

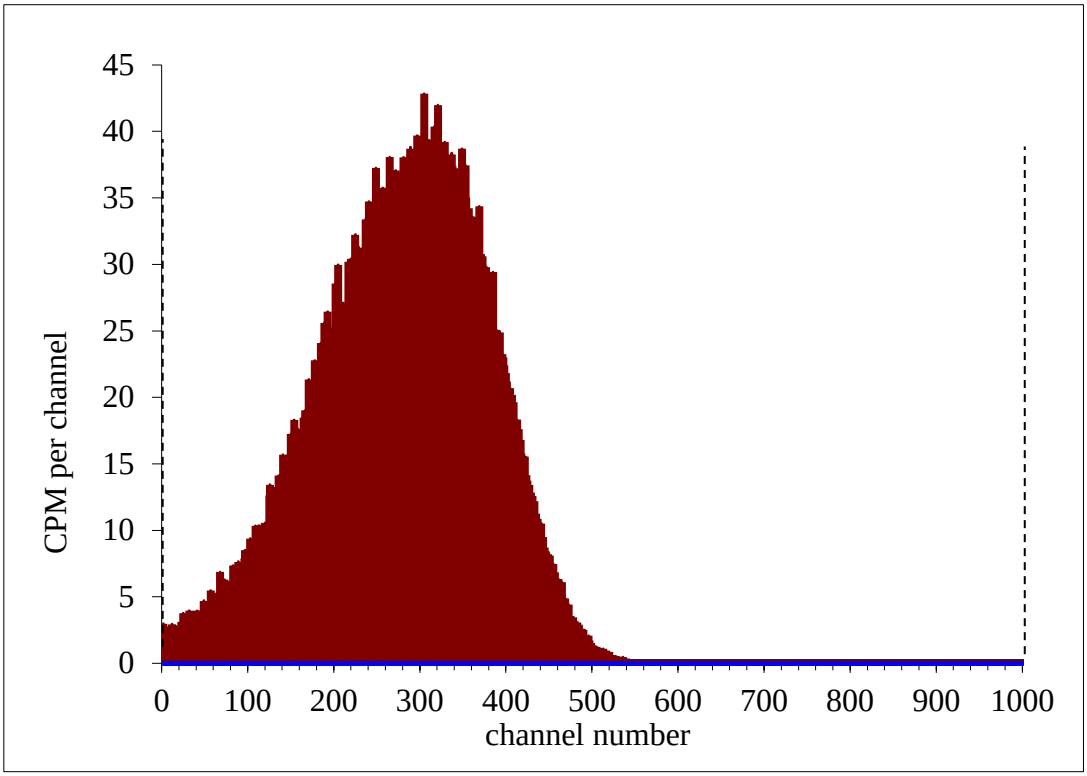

Figure 94: Cherenkov spectrum of 20.2090 g ^{90}Sr tracer (red) in radioactive equilibrium with ^{90}Y, t_m: 98.390 min with a Cherenkov measurement of 20 mL water as background (blue), QUANTULUS 1220 KB

Figure 94 shows the Cherenkov spectrum of the 20 g ^{90}Sr tracer sample described above. The y-axis shows the counts per minute per channel, representing the number of decays. The x-axis shows the channels, corresponding to the decay energy. The red graph represents the sample signal. The blue graph represents the background signal measured separately. All in all, 919150 decay counts were detected, assigned to the measured energy span between the channels 5 and 550, in which the signals mainly occurred. It is evident from the spectrum, that the energies detected with the Cherenkov measurement are significantly smaller than for the previous LSC measurement. From this measurement results, the physical efficiency could be calculated.

$$R = A \cdot \eta_{phys} \cdot \eta_{chem} \tag{5.28}$$

$$\eta_{phys} = \frac{R}{A} \tag{5.29}$$

As this was a direct measurement without chemical preparation η_{chem} equals 1. The count rate R could be calculated by dividing the number of counts N (919,150 decay counts) through the measurement time in seconds (5903 s), resulting in 155.70. The added combined ^{90}Sr and ^{90}Y activity was 12.9 Bq/g times two (25.08 Bq/g) times 20 g, resulting in 516 Bq. The calculated physical yield was 30.17 %, significantly lower than for the LSC measurement.

With this value, the necessary measurement time for the samples of the complete analysis was calculated, to achieve at least 20,000 counts. First the count rate was calculated.

$$R = A \cdot \eta_{phys} \cdot \eta_{chem} \tag{5.28}$$

The planned tracer activity for the analysis, 12.9 Bq, corresponding to 1 g tracer, was inserted for the activity A. The calculated physical yield of 0.3017 was inserted for η_{phys}. And the highest chemical yield achieved in a sampling region, 0.75 was inserted for η_{chem} for approximation. The resulting hypothetical count rate would be 5.805 cps. Dividing the aimed for 20,000 counts by this value, a measurement time of about 57 min is calculated. To make sure, that the count minimum was really achieved, the ^{90}Y samples of the complete analysis were measured for 2 hours each.

Additionally, a new background for the Cherenkov measurement was recorded. For this 20.0 g bidistilled water were weighed in a LSC vial and measured for 1,000 minutes in the QUANTULUS. The long measurement time was necessary to detect anything at all, due to the extremely small background signal and the very good isolation and background correction of the QUANTULUS device.

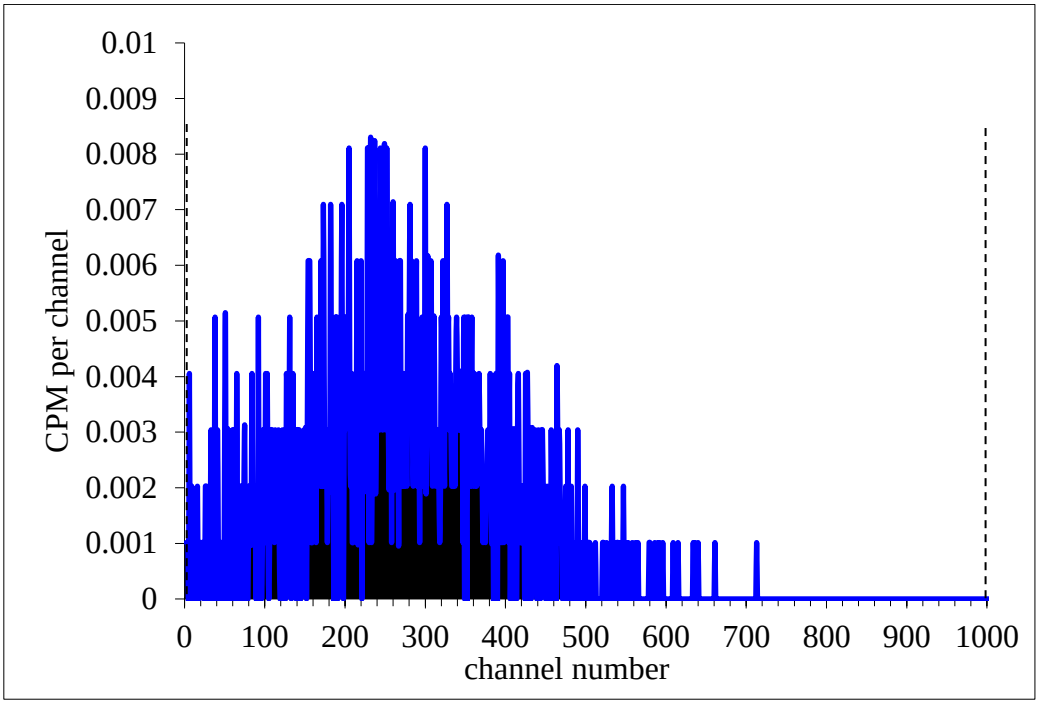

Figure 95: Cherenkov measurement of 20 mL water as background (blue), QUANTULUS 1220 KB, t_m:986.427 min

Figure 95 shows the Cherenkov spectrum of 20 g inactive water. The y-axis shows the counts per minute per channel, representing the number of decays. The x-axis shows the channels, corresponding to the decay energy. As is evident from the scale of the y-axis, the activity of the sample is very small. All in all, only 1,392 decay counts were detected, assigned to the measured energy span between the channels 1 and 1,000, representing the whole energy span, during this long measurement time. This corresponds to a count rate of 0.02 Bq.

In addition to that, a ^{40}K background was recorded, as the nuclide is also β-active and could increase the potential background, if not separated properly. For this, 2.0 g KCl were weighed in a LSC vial and filled up to 20 g with bidistilled water. The sample was shaken until the salt was solved and measured for 100 minutes in the QUANTULUS.

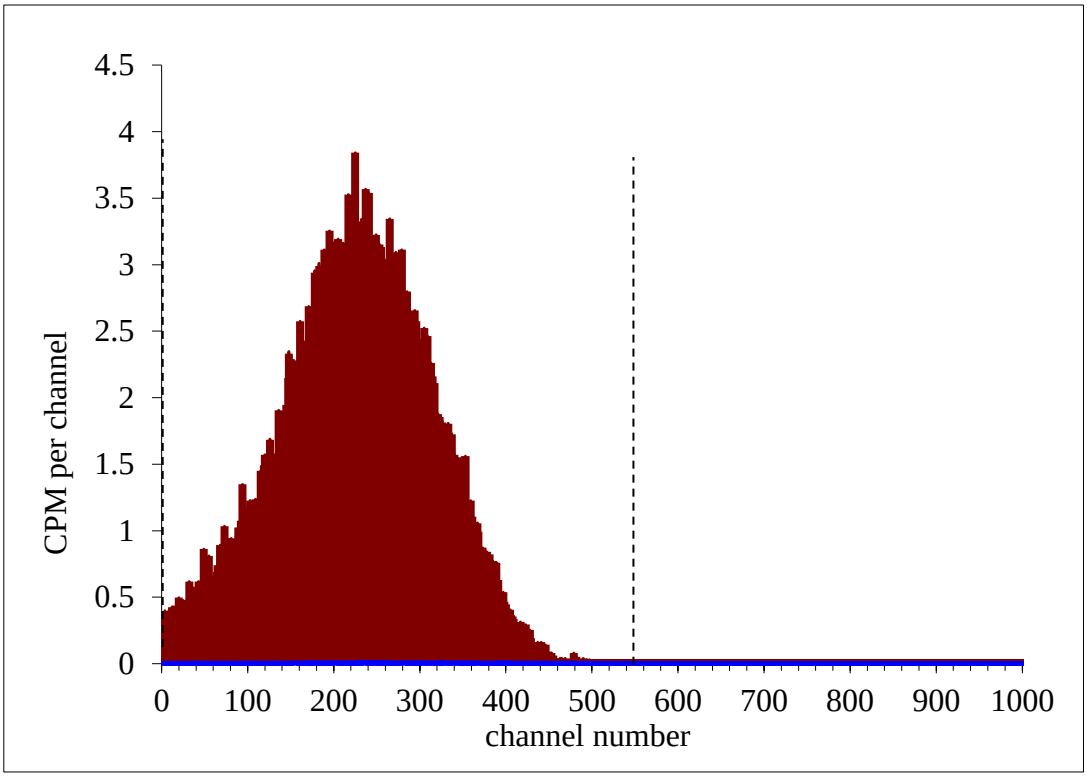

Figure 96: Cherenkov spectrum of 2.0 g KCl filled up to 20 g with bidistilled water (red) t_m: 98.633 min with a Cherenkov measurement of 20 mL water as background (blue), QUANTULUS 1220 KB

Figure 96 shows the Cherenkov spectrum of the 2 g KCl sample described above. The y-axis shows the counts per minute per channel, representing the number of decays. The x-axis shows the channels, corresponding to the decay energy. The red graph represents the sample signal. The blue graph represents the background signal, measured separately. All in all, 67,116 decay counts were detected, assigned to the measured energy span between the channels 2 and 550, in which the signals mainly occurred. From this measurement results, the physical efficiency for a ^{40}K measurement could be calculated.

$$R = A \cdot \eta_{phys} \cdot \eta_{chem} \tag{5.28}$$

$$\eta_{phys} = \frac{R}{A} \tag{5.29}$$

As this was a direct measurement without chemical preparation, η_{chem} equals 1. The count rate R could be calculated by dividing the number of counts N (67,116 decay counts) through the measurement time in seconds (5,918 s), resulting in 11.34 cps. The added ^{40}K activity was 31.72 Bq/g, as the activity per gram KCl is 15.86 Bq [25] and 2 g of KCl were used for the measurement. The calculated physical yield was 35.75 %, slightly higher than for ^{90}Sr.

As sample matrix for the complete analysis experiments, a mixture of milk ash from remaining environmental monitoring samples, that were already confirmed to not be radioactive, and milk ash prepared from whole long-life milk by the brand Berchtesgadener Land was used. This not contaminated milk ash matrix was, previous to its use, measured gamma-spectrometrically in the detectors GEM4 and GEM40 to determine its ^{40}K content. The measurement geometry was 115.00 g in a 500 mL Kautex with a filling height of about 3 cm.

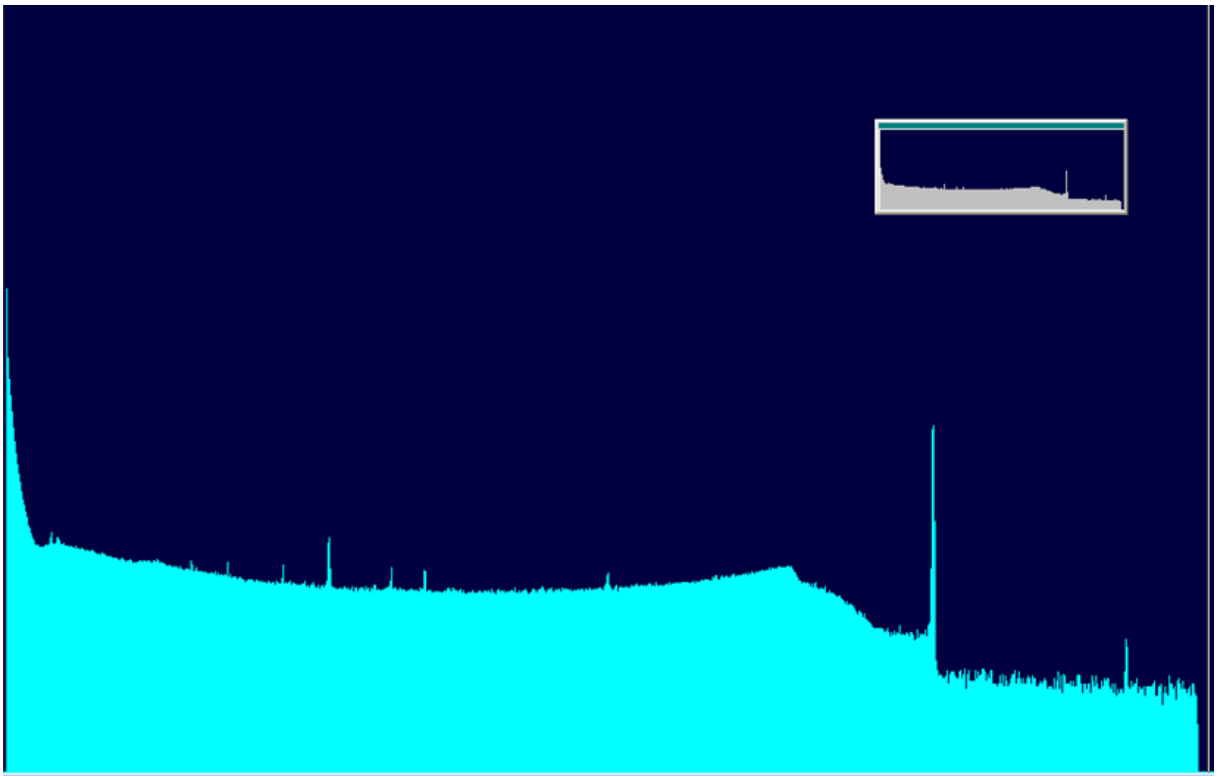

Figure 97: Gamma spectrum of not radioactively contaminated mixed milk with a significant ^{40}K peak, 115.00 g in a 500 mL Kautex with a filling height of about 3 cm, GEM40, Live time: 265,352.78 s, logarithmic y-axis presentation

Table 71: Measurement results of a not radioactively contaminated mixed milk sample, 115.00 g in a 500 mL Kautex with a filling height of about 3 cm, GEM40

Live time [s]	**Real time [s]**			
265,352.78	265,518.72			
Nuclide	**ROI [keV]**	**Net Area**	**Uncertainty Net Area**	**Count Rate [cps]**
K-40 main peak	1,450.22-1,469.08	202,732	484	0.764
annihilation peak	506.66-514.56	7,935	204	0.030
irrelevant	1,762.27-1,767.40	327	26	0.001
	293.20-297.15	807	110	0.003
	350.16-353.65	1,028	89	0.004
	437.13-440.85	1,047	87	0.004
	607.36-611.08	927	83	0.003
	659.69-662.95	802	72	0.003
	946.30-952.35	1,355	138	0.005

The milk sample was first measured in the GEM40 gamma-detector for 265,352.78 seconds (Live time). The results of the measurement are presented in figure 97 and table 71. As expected, a significant ^{40}K peak was found in the milk sample matrix, due to its high potassium content. Additionally, a significantly smaller annihilation peak was found in the gamma spectrum, that was also likely caused by ^{40}K. Some further peaks were found, but they were so small, that they basically morphed with the measured background and were not further considered.

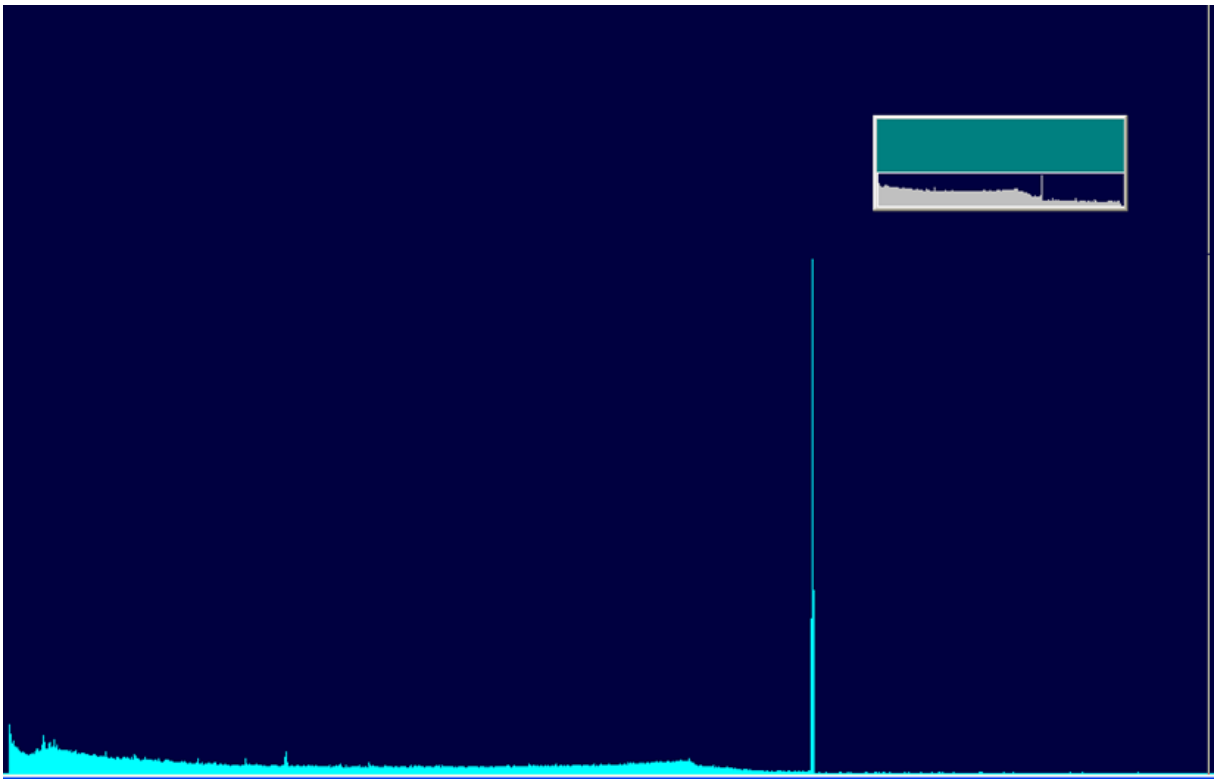

Figure 98: Gamma spectrum of not radioactively contaminated mixed milk with a significant ^{40}K peak, 115.00 g in a 500 mL Kautex with a filling height of about 3 cm, GEM4, Live time: 62998.56 s, automatic presentation

Table 72: Measurement results of a not radioactively contaminated mixed milk sample, 115.00 g in a 500 mL Kautex with a filling height of about 3 cm, GEM4

Live time [s]	**Real time [s]**			
62,998.56	63,010.38			
Nuclide	**ROI [keV]**	**Net Area**	**Error Net Area**	**Count Rate [cps]**
K-40	1,456.34-1,464.64	29,532	174	0.469
annihilation peak	506.16-515.24	1,188	87	0.019
irrelevat	435.93-440.46	286	43	0.005
	606.31-611.38	186	41	0.003
	658.40-664.27	258	49	0.004

The milk sample was then measured in the GEM4 gamma-detector for 62,998.56 seconds (Live time). This was done because for the GEM4 a suitable calibration for this measurement geometry was accessible, to determine the physical yield. The results of the measurement are presented in figure 98 and table 72. As for the GEM40 measurement, a significant ^{40}K peak was found in the milk sample matrix, due to its high potassium content. Additionally, a significantly smaller annihilation peak was found in the gamma spectrum, that was also likely caused by ^{40}K. Some further peaks were found, even less than for the GEM40 measurement, but they were also so small, that they basically morphed with the measured background and were not further considered.

After the pre-experiments, the complete analyses were performed, incorporating the results of the former experiments. The complete analyses were performed for the following sampling regions, including the sample inlet: 305-325 g eluent and 295-315 g eluent. These were deemed the optimal sampling regions, depending on the prioritization of separation quality or yield. Additionally, the medium sampling region of 300-320 g eluent was tested. The tests should show how well the analysis would work under real conditions and which sampling region would prove to provide the best results, regarding separation and ^{90}Y yield.

The complete analyses of ^{90}Sr via ^{90}Y were performed with the new DOWEX ®50 WX8 200-400 (H) resin by Alfa Aesar and the eluent ammonium-lactate at pH6, as established in chapter 5.3.

As standard sample matrix, 10.0 g not contaminated milk ash, prepared from commercially available whole long-life milk by the brand Berchtesgadener Land or remaining milk ash from environmental monitoring, which was confirmed to be not radioactively contaminated, was used. It was solved in 80 mL of the usual 1:1 mixture of 6 M hydrochloric acid and 1.5 molar lactic acid. 1 mL of the stable yttrium tracer, containing 10 mg Y, was added, as well as 1 g of the ^{90}Sr tracer (2.12.2004 20,000 Bq ^{90}Sr /1,001.6 g). Potassium and calcium were naturally present in the sample matrix in significant amounts, according to the milk packaging 124 mg calcium per 100 mL milk. Then the sample was solved and applied to the column. The remaining ash residue was not washed or solved after that, to ensure a constant solvent volume for all fraction analyses. The Hot Column Chromatography separations were performed at the elution speed of 2.5 mL/min.

The chosen 20 g fractions were separated and their ^{90}Y activities were immediately determined via a Cherenkov measurement in the QUANTULUS for 120 minutes. After minimum two weeks, which corresponds to approximately five half-lives of ^{90}Y and in which ^{90}Y decayed practically completely, another Cherenkov measurement of 120 minutes was performed in the QUANTULUS, to determine the background activity. It would stem mostly from not completely separated ^{40}K.

The chemical yield of the yttrium separation was determined via an ICP-OES measurement of the stable yttrium in the sample after ^{90}Y completely decayed. For this measurement, the same calibration curve was used, as the one calculated for the initial determination of the elution curve with the new DOWEX® 50 WX8 (200-400 mesh) by Alfa Aesar, as detailed in 5.3.1.

Table 73: Results of the complete analyses in the sampling fractions 305-325 g eluent, 295-315 g eluent and 300-320 g eluent

Analysis	Analysis 1	Analysis 2	Analysis 3	Analysis 4	Analysis 5	Analysis 6	Analysis 7
sampling region	305-325 g eluent			295-315 g eluent		300-320 g eluent	
^{90}Y separation time	03.11.22 13:42	09.11.22 14:10	10.11.22 12:26	14.11.22 12:47	15.11.22 13:01	17.11.22 12:52	24.11.22 12:11
measurement end	3.11.22 16:55	10.11.22 1:34	10.11.22 15:47	14.11.22 16:04	15.11.22 15:28	17.11.22 15.12	24.11.22 14:32
texture and color of the sample	slightly yellow, clear, liquid crystal forma-tion after some time	White, wax like solid	slightly yellow, clear, liquid crystal forma-tion after some time	slightly yellow, clear, liquid residue forma-tion	clear, liquid, color-less, no solid	slightly yellow, clear, liquid flakes forma-tion after some time	slightly yellow, clear, liquid flakes forma-tion after some time
sample inlet [g]	105.4	100.0	103.8	103.7	105.2	104.1	107.0
added ^{90}Sr tracer [g]	1.07	1.01	1.06	1.02	1.00	1.01	1.04
SQP(E) value	448.37	371.41	357.82	362.82	380.89	367.30	364.96
Activity [Bq]	16.29	4.53	13.09	12.58	0.77	13.78	13.62
background activity (^{40}K)	0.42	0.37	0.38	0.20	0.11	0.34	0.18
Y-yield [%]	57.7	22.25	74.55	36.68	2.68	46.14	6.68

Table 73 shows an overview of the results of the performed complete analyses. They were performed at least two times for each of the chosen sampling fractions: 305-325 g eluent, 295-315 g eluent and 300-320 g eluent. Those sampling fractions were chosen because in the pre-experiments, the sampling fraction 305-325 g eluent showed the best yttrium yield and a good separation from potassium. The sampling fraction 295-315 g eluent showed a complete separation from potassium and calcium and the sampling fraction 300-320 g eluent in between showed similar results to the sampling fraction 305-325 g eluent, but with a slightly lower yttrium yield and a slightly higher calcium content.

Almost all complete analysis fractions were measured directly after the separation for 120 minutes. The only exception was analysis 2 (305-325 g eluent), which was measured half a day later, because other measurements were already queued up in the device. Most samples were clear and liquid after separation. All of them, except for analysis 2 (305-325 g eluent) and analysis 5 (295-315 g eluent) showed a slightly yellow coloring. The only sample that stayed completely liquid even after some time was analysis 5 (295-315 g eluent). In all the other samples, crystals or residue formed a while after they cooled down to room temperature. The sample of analysis 2 (305-325 g eluent) became completely white and wax like after a while. For all analyses the sample inlet mass was approximately the same with the lowest mass being 100.0 g and the highest being 107.0 g. For all analyses approximately 1 g of the ^{90}Sr tracer was used, the highest added amount being 1.07 g tracer. The SQP(E) value was in the same range between 357.82 and 380.89 for most samples, even though they had different coloring and solid

formation. The only outlier was analysis 1 (305-325 g eluent) with the highest SQP(E) value 448.37. This showed that the condition of the sample did not influence the quality of the measurement significantly. For the measured activity results, there were two outliers. The obvious one being analysis 2 (305-325 g eluent), with a significantly lower measured activity of 4.53 Bq. There were several potential reasons for this: the late measurement or the solidification of the sample. This indicated a shift of the elution region, possibly caused by the separation of the DOWEX resin in the column, which made stirring necessary. The stirring could have partially disrupted the separation and shifted the elution region, so that the maximum was no longer in the separated fraction. Because of this low measured activity, a third analysis was performed for the sampling region of 305-325 g eluent. Another sample with a very low detected activity of 0.77 Bq was analysis 5 (295-315 g eluent). The low activity could also have been caused by a shift of the elution, so that the elution region of yttrium was almost completely missed. This was indicated by the continuously liquid and colorless condition of the sample. For the other samples, the measured activity was quite stable. The highest activity was measured for the sample of analysis 1 (305-325 g eluent) with 16.29 Bq. For the other samples, the activity was between 12.58 Bq and 13.78 Bq, approximating the value of the added ^{90}Y activity. The background for all samples, measured after two weeks, was quite low and in the same scale between 0.11 and 0.42 Bq.

The yttrium yields of the added stable yttrium corresponded approximately to the measured activities. In analyses with higher activities, the yield was also higher, and in analyses with lower activities, the yield was also lower. The only exception was analysis 7 that had a similar activity to the other samples but a significantly lower yttrium yield. It is also noticeable that the yttrium yield varied significantly more, even among the analyses that were not deemed outliers, than the activity, that was quite stable among most analyses. This could be due to the conditions of the samples. When their activity was measured for the first time, they were mostly still liquid. When the yttrium yield was determined, most of the samples contained solid, except for the sample of analysis 5. The solid could not be completely solved, even after heating in a water bath for a longer time. The solid could contain a varying amount of yttrium for the different samples and as it was not part of the measurement of the samples, it could have distorted the yield results and led to the observable fluctuation among the different analyses.

All in all, the experiment showed the most stable results for the medium sampling region of 300-320 g eluent, event tough it was not a favorite during the pretests. Due to its position in the middle between the other two sampling regions, it was less affected by slight shifts of the elution and in both cases the maximum of the yttrium elution could be separated.

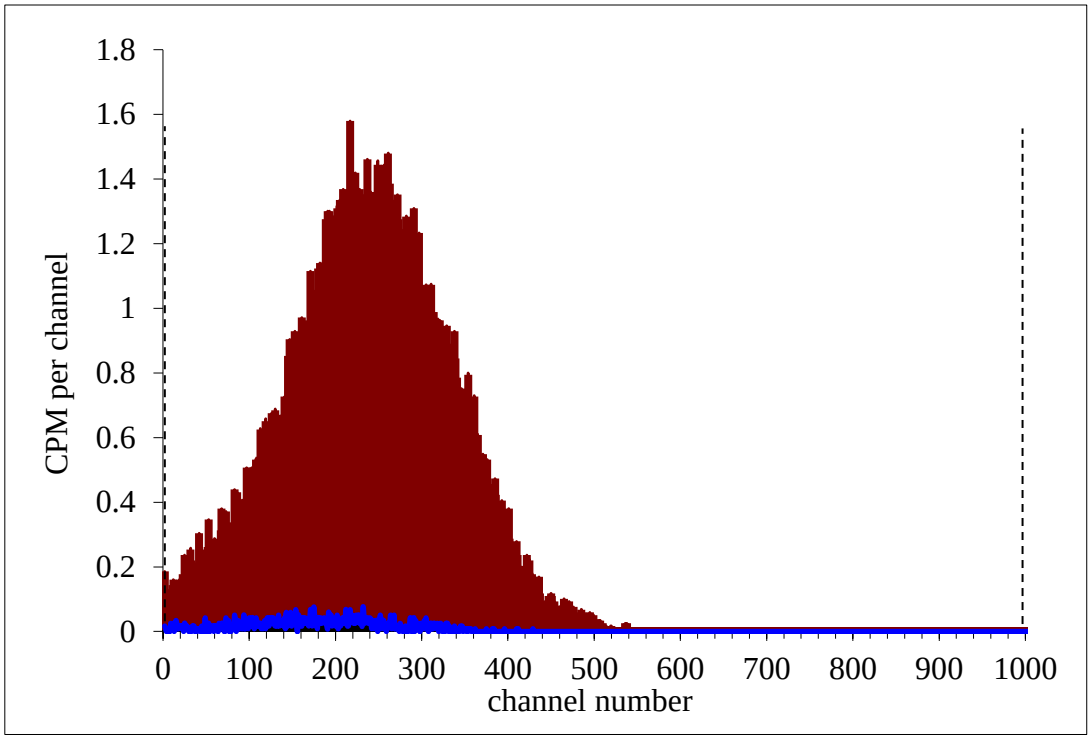

Figure 99: Cherenkov spectrum of the complete analysis 1, sampling fraction 305-325 g eluent (red) t_m: 98.390 min repeated measurement after two weeks as background (blue), QUANTULUS 1220 KB

Figure 99 shows the Cherenkov spectrum of the analysis 1 sample, with the sampling region of 305-325 g eluent. The y-axis shows the counts per minute per channel, representing the number of decays. The x-axis shows the channels, corresponding to the decay energy. The red graph represents the sample signal. The blue graph represents the background signal measured two weeks after the separation and after the ^{90}Y has mostly decayed. The sample contained 1.07 g ^{90}Sr tracer and its inlet was 105.4 g. After the separation and cooling down to room temperature and even to the measurement temperature in the QUANTULUS, the sample stayed clear and liquid, but was slightly yellow. After some time, crystallization started in the sample, but that was after the measurement. The sample was measured directly after the separation and had a quite good SQP(E) value of 448.37 for a Cherenkov measurement. All in all, 34,907 decay counts were detected assigned to the measured energy span between the channels 2 and 560, in which the signals mainly occurred. These counts corresponded to the count rate of 4.9 cps and therefore 16.29 Bq. The value is higher than the added ^{90}Y activity of 13.8 Bq. The measured background after two weeks was 0.42 Bq, so even when it is subtracted, the value is still approximately 2 Bq higher than the added activity. This can be because of some uncertainty during the calculation of the activity of the tracer, of the original tracer information or of the weighing of the tracer for the analysis. Despite this, it can be said that practically the whole ^{90}Y activity was separated in this sample. The yield of the stable yttrium in the sample was 57.7 %. But this value could be distorted due to sample solidification.

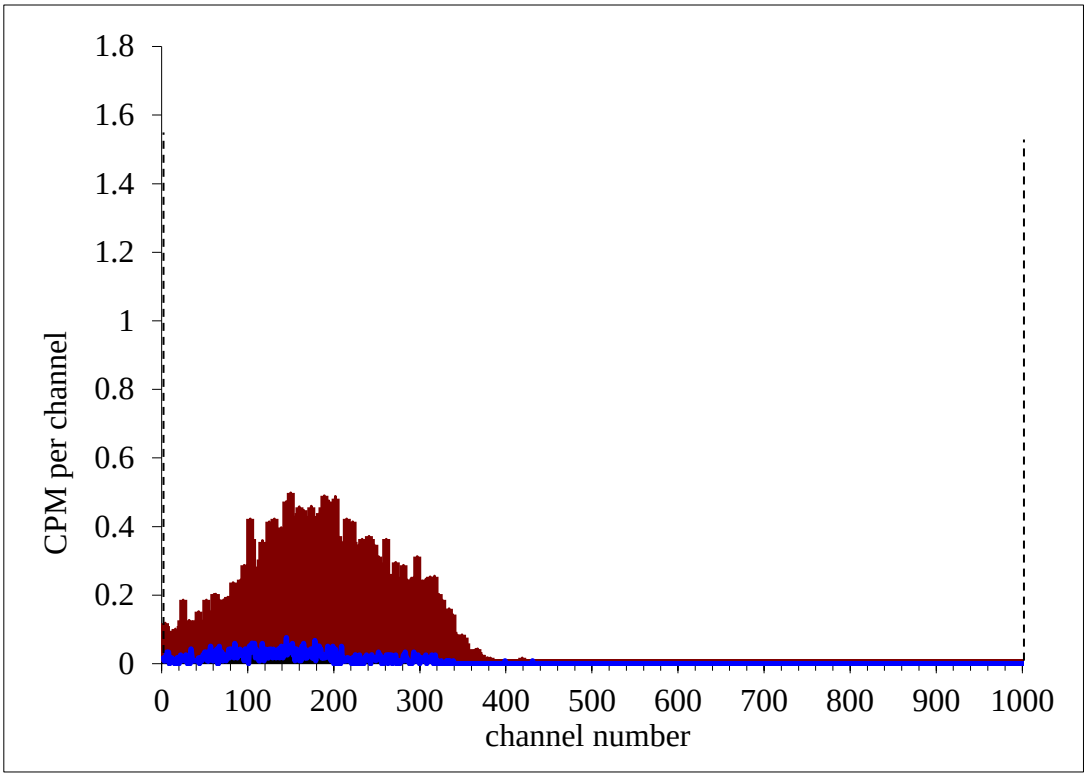

Figure 100: Cherenkov spectrum of the complete analysis 2, sampling fraction 305-325 g eluent (red) t_m: 98.390 min repeated measurement after two weeks as background (blue), QUANTULUS 1220 KB

Figure 100 shows the Cherenkov spectrum of the analysis 2 sample, with the sampling region of 305-325 g eluent. The y-axis shows the counts per minute per channel, representing the number of decays. The x-axis shows the channels, corresponding to the decay energy. The red graph represents the sample signal. The blue graph represents the background signal measured two weeks after the separation and after the ^{90}Y has mostly decayed. The sample contained 1.01 g ^{90}Sr tracer and its inlet was 100.0 g. Sometime after the separation and cooling down to room temperature, or rather to the measurement temperature in the QUANTULUS, the sample turned into a white, wax like solid. During the analysis several problems occurred. First there was a separation of the DOWEX in the column, which caused a gap in the column material. Because of this gap, the elution was halted. It had to be closed through stirring the upper layer of the column material. But as the sample was already in the column at that time, this caused a disturbance in the sample distribution in the column. This could have caused the elution shift that led to the separated sample fraction solidification. Another problem was that the sample could not be immediately measured after its separation, as another measurement was already in progress at the QUANTULUS at this time. This caused a measurement delay of 8 hours. The SQP(E) value of the measurement was 371.41, which was surprisingly comparable to the other samples. All in all, 9,704 decay counts were detected assigned to the measured energy span between the channels 2 and 560, in which the signals mainly occurred. These counts corresponded to the count rate of 1.4 cps and therefore 4.53 Bq. The measured background after two weeks was 0.37 Bq. The yield of the stable yttrium in the sample was 22.25 %. But this value could be distorted due to sample solidification.

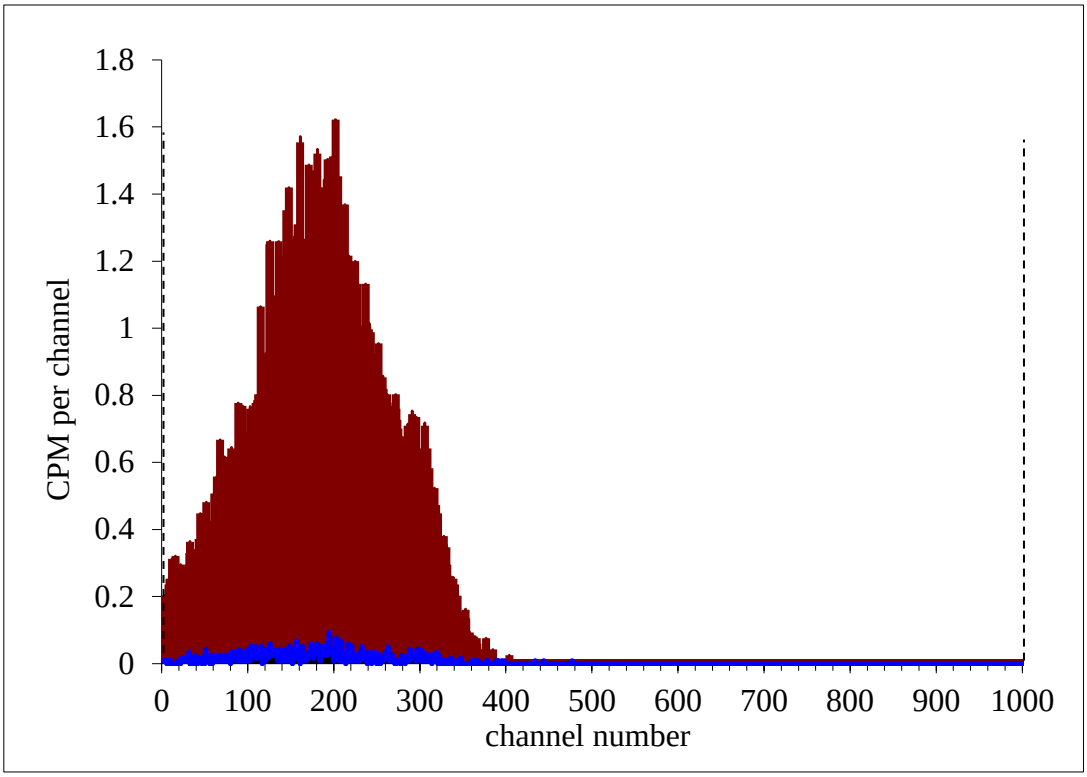

Figure 101: Cherenkov spectrum of the complete analysis 3, sampling fraction 305-325 g eluent (red) t_m: 98.390 min repeated measurement after two weeks as background (blue), QUANTULUS 1220 KB

Figure 101 shows the Cherenkov spectrum of the analysis 3 sample, with the sampling region of 305-325 g eluent. The y-axis shows the counts per minute per channel, representing the number of decays. The x-axis shows the channels, corresponding to the decay energy. The red graph represents the sample signal. The blue graph represents the background signal measured two weeks after the separation and after the ^{90}Y has mostly decayed. The sample contained 1.06 g ^{90}Sr tracer and its inlet was 103.8 g. After the separation and cooling down to room temperature and even to the measurement temperature in the QUANTULUS, the sample stayed clear and liquid, but was slightly yellow. After some time, crystallization started in the sample, but that was after the measurement. The sample was measured directly after the separation and had a SQP(E) value of 357.82, comparable to the other measurements. All in all, 28,050 decay counts were detected assigned to the measured energy span between the channels 2 and 560, in which the signals mainly occurred. These counts corresponded to the count rate of 3.95 cps and therefore 13.09 Bq, slightly lower than the added ^{90}Y activity of 13.67 Bq. The measured background after two weeks was 0.38 Bq. It can be said, that practically the whole ^{90}Y activity was separated in this sample. The yield of the stable yttrium in the sample was 74.55 %. But this value could be distorted due to sample solidification.

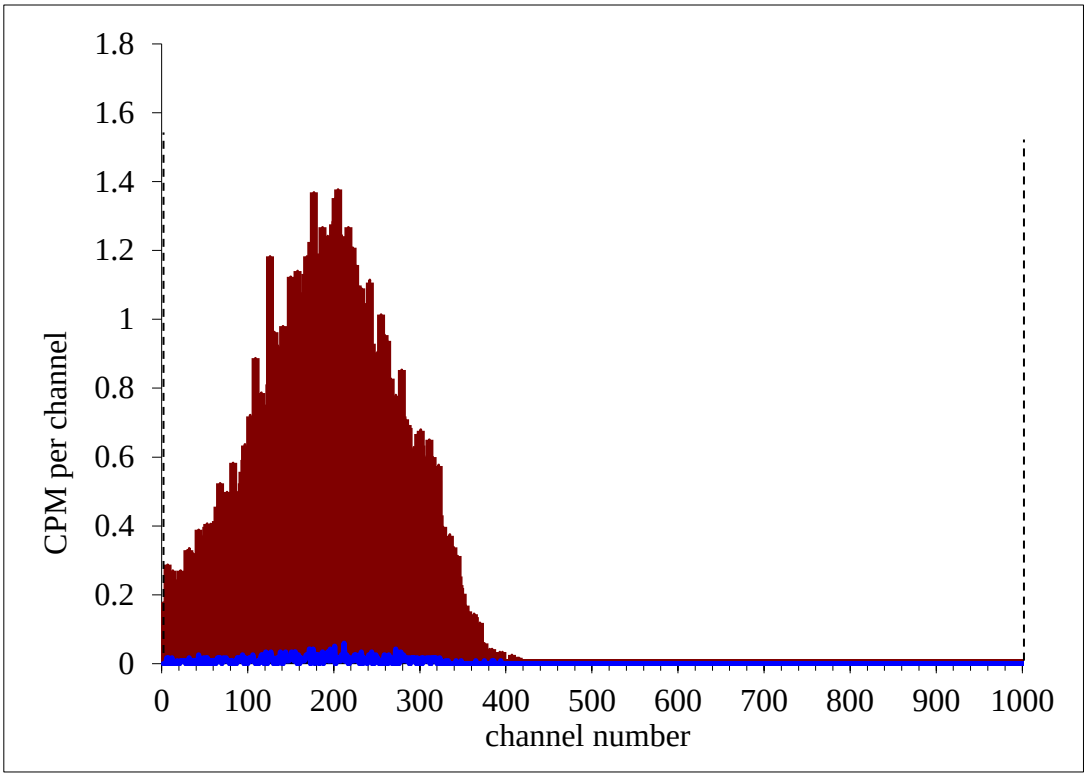

Figure 102: Cherenkov spectrum of the complete analysis 4, sampling fraction 295-315 g eluent (red) t_m: 98.390 min repeated measurement after two weeks as background (blue), QUANTULUS 1220 KB

Figure 102 shows the Cherenkov spectrum of the analysis 4 sample, with the sampling region of 295-315 g eluent. The y-axis shows the counts per minute per channel, representing the number of decays. The x-axis shows the channels, corresponding to the decay energy. The red graph represents the sample signal. The blue graph represents the background signal measured two weeks after the separation and after the ^{90}Y has mostly decayed. The sample contained 1.02 g ^{90}Sr tracer and its inlet was 103.7 g. After the separation and cooling down to room temperature and even to the measurement temperature in the QUANTULUS, the sample stayed clear and liquid, but was slightly yellow. After some time, residue formation started in the sample, but that was after the measurement. The sample was measured directly after the separation and had a SQP(E) value of 362.82, comparable to the other measurements. All in all, 26,950 decay counts were detected assigned to the measured energy span between the channels 2 and 560, in which the signals mainly occurred. These counts corresponded to the count rate of 3.79 cps and therefore 12.58 Bq, slightly lower than the added ^{90}Y activity of 13.16 Bq. The measured background after two weeks was 0.20 Bq. It can be said, that practically the whole ^{90}Y activity was separated in this sample. The yield of the stable yttrium in the sample was 36.68 %. But this value could be distorted due to sample solidification.

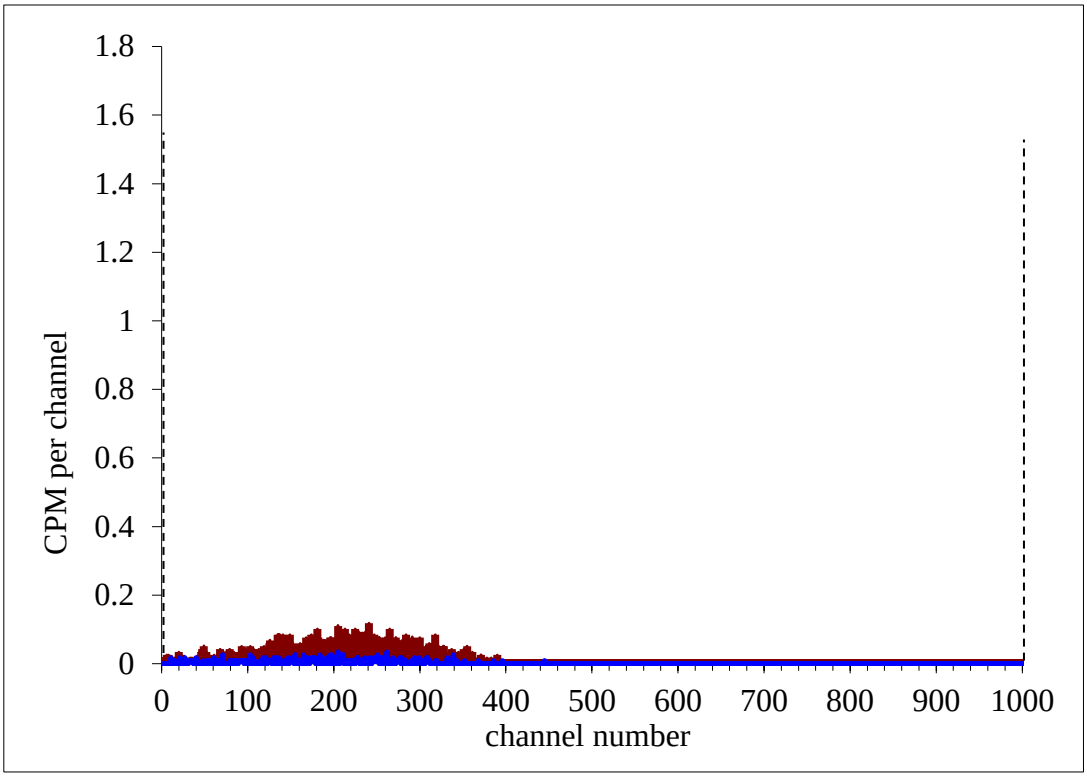

Figure 103: Cherenkov spectrum of the complete analysis 5, sampling fraction 295-315 g eluent (red) t_m: 98.390 min repeated measurement after two weeks as background (blue), QUANTULUS 1220 KB

Figure 103 shows the Cherenkov spectrum of the analysis 5 sample, with the sampling region of 295-315 g eluent. The y-axis shows the counts per minute per channel, representing the number of decays. The x-axis shows the channels, corresponding to the decay energy. The red graph represents the sample signal. The blue graph represents the background signal measured two weeks after the separation and after the ^{90}Y has mostly decayed. The sample contained 1.00 g ^{90}Sr tracer and its inlet was 105.2 g. The sample stayed clear, completely liquid without solid formation and colorless even long after the measurement. This already indicated a shift of the elution, that caused the sampling fraction to hardly contain any ^{90}Y. The sample was measured directly after the separation and had a SQP(E) value of 380.89, which was comparable to the other samples. All in all, 1,647 decay counts were detected, assigned to the measured energy span between the channels 2 and 560, in which the signals mainly occurred. These counts corresponded to the count rate of 0.23 cps and therefore 0.77 Bq. The measured background after two weeks was 0.11 Bq. This showed that hardly any ^{90}Y was present in the sample. The yield of the stable yttrium in the sample was only 2.68 %, which supports this finding.

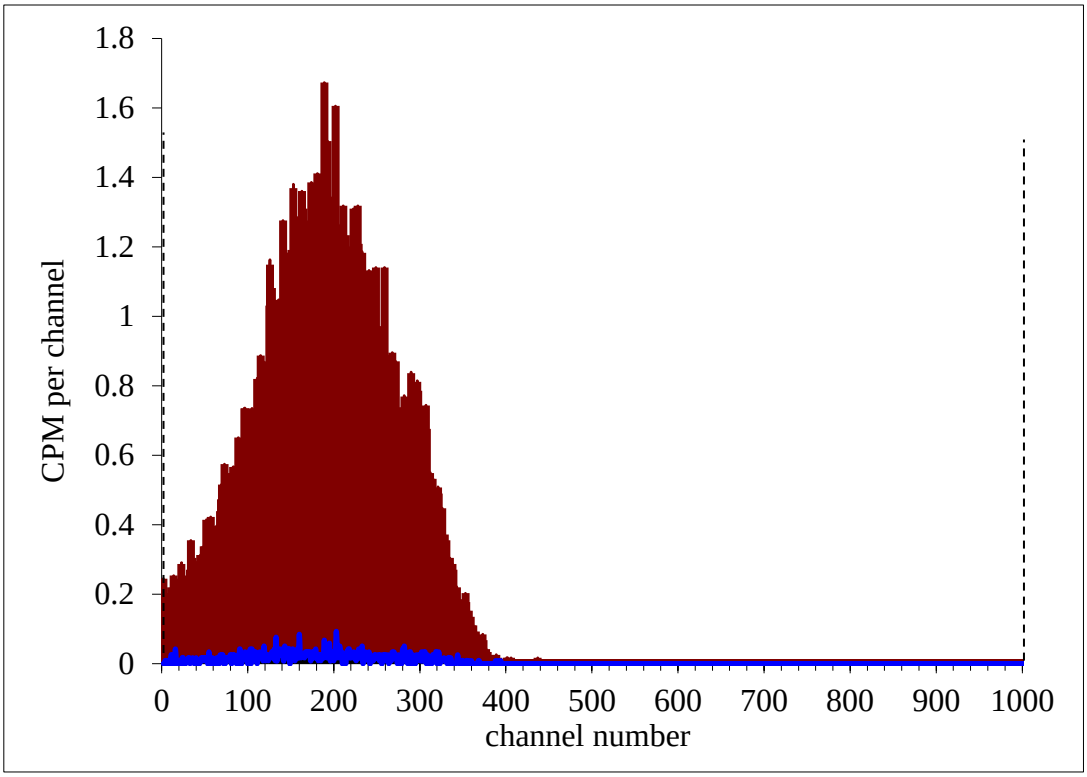

Figure 104: Cherenkov spectrum of the complete analysis 6, sampling fraction 300-320 g eluent (red) t_m: 98.390 min repeated measurement after two weeks as background (blue), QUANTULUS 1220 KB

Figure 104 shows the Cherenkov spectrum of the analysis 6 sample, with the sampling region of 300-320 g eluent. The y-axis shows the counts per minute per channel, representing the number of decays. The x-axis shows the channels, corresponding to the decay energy. The red graph represents the sample signal. The blue graph represents the background signal measured two weeks after the separation and after the ^{90}Y has mostly decayed. The sample contained 1.01 g ^{90}Sr tracer and its inlet was 104.1 g. After the separation and cooling down to room temperature and even to the measurement temperature in the QUANTULUS, the sample stayed clear and liquid, but was slightly yellow. After some time, flacking started in the sample, but that was after the measurement. The sample was measured directly after the separation and had a SQP(E) value of 367.30, comparable to the other measurements. All in all, 29,519 decay counts were detected, assigned to the measured energy span between the channels 2 and 560, in which the signals mainly occurred. These counts corresponded to the count rate of 4.16 cps and therefore 13.78 Bq. The value is higher than the added ^{90}Y activity of 13.03 Bq. The measured background after two weeks was 0.34 Bq, so even when it is subtracted, the value is still approximately 0.4 Bq higher than the added activity. This can be because of some uncertainty during the measurement, during the calculation of the activity of the tracer, of the original tracer information or of the weighing of the tracer for the analysis. Despite this, it can be said that practically the whole ^{90}Y activity was separated in this sample. The yield of the stable yttrium in the sample was 46.14 %. But this value could be distorted due to sample solidification.

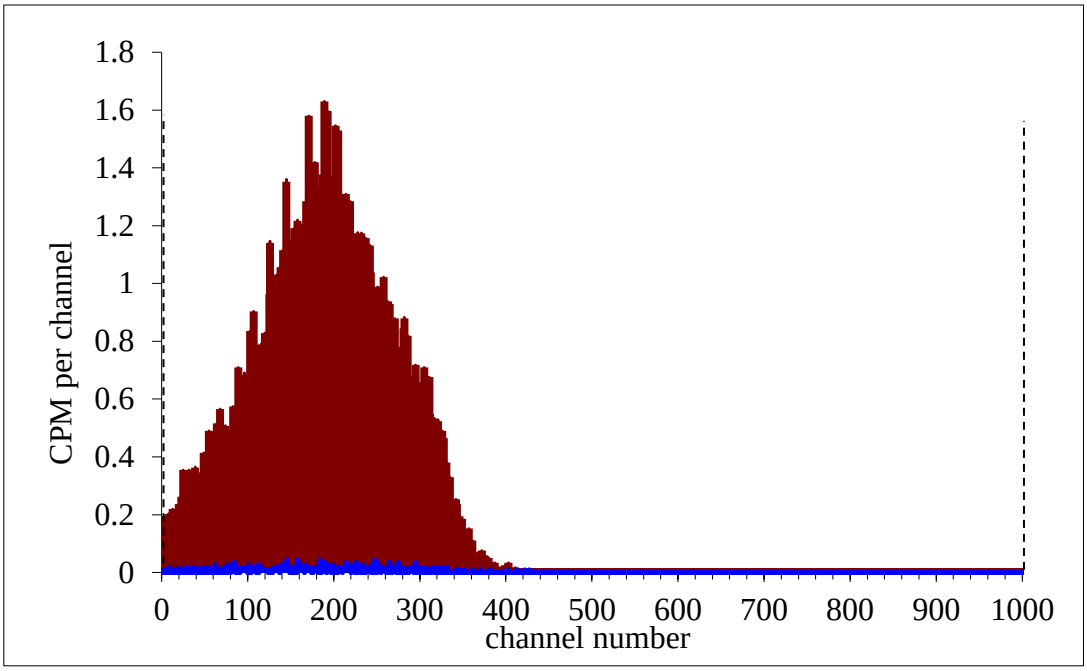

Figure 105: Cherenkov spectrum of the complete analysis 7, sampling fraction 300-320 g eluent (red) t_m: 98.390 min repeated measurement after two weeks as background (blue), QUANTULUS 1220 KB

Figure 105 shows the Cherenkov spectrum of the analysis 7 sample, with the sampling region of 300-320 g eluent. The y-axis shows the counts per minute per channel, representing the number of decays. The x-axis shows the channels, corresponding to the decay energy. The red graph represents the sample signal. The blue graph represents the background signal measured two weeks after the separation and after the ^{90}Y has mostly decayed. The sample contained 1.04 g ^{90}Sr tracer and its inlet was 107.0 g. After the separation and cooling down to room temperature and even to the measurement temperature in the QUANTULUS, the sample stayed clear and liquid, but was slightly yellow. After some time, flacking started in the sample, but that was after the measurement. The sample was measured directly after the separation and had a SQP(E) value of 364.96, comparable to the other measurements. All in all, 29,190 decay counts were detected assigned to the measured energy span between the channels 2 and 560, in which the signals mainly occurred. These counts corresponded to the count rate of 4.11 cps and therefore 13.62 Bq. The value is higher than the added ^{90}Y activity of 13.42 Bq. The measured background after two weeks was 0.18 Bq, so when it is subtracted, the value approximately is the same as the added activity. So, it can be said, that practically the whole ^{90}Y activity was separated in this sample. The yield of the stable yttrium in the sample was 6.68 %. But this value could be distorted due to sample solidification.

Table: 74: Additional results of the yttrium yield determination with ICP-OES

analysis	Y-content per fraction[mg]	Ca-content per fraction [mg]	K-content per fraction [mg]	Sr-content per fraction [mg]
1	5.77 ± 0.031	60.47 ± 0.39	0 ± 0.00096	0 ± 0.000047
2	2.23 ± 0.0086	245.34 ± 0.33	22.82 ± 0.12	0 ± 0.000021
3	7.46 ± 0.029	74.12 ± 0.11	0 ± 0.0038	0 ± 0.000019
4	3.67 ± 0.019	10.03 ± 0.052	0 ± 0.0032	0 ± 0.000016
5	0.27 ± 0.00090	0 ± 0.011	0 ± 0.0028	0 ± 0.000011
6	4.61 ± 0.027	17.13 ± 0.068	0 ± 0.0027	0 ± 0.000011
7	0.67 ± 0.0025	0.41 ± 0.011	0 ± 0.0016	0 ± 0.000018

The yttrium yield determination, including the measurement of the Y, Ca, K and Sr content was performed via ICP-OES. For the measurement, the sampling fractions were diluted 1:250. Per ICP-OES sample, 40 µL of the fractions were used and 2 mL concentrated nitric acid was added for pH adjusting. The samples were filled up to a volume of 10 mL with bidistilled water. The yttrium yields were already presented and discussed. Table 74 shows the additional information obtained from these measurements. It shows that a complete separation of strontium from all samples was achieved. The potassium separation was also complete for almost all samples, except for the sample of analysis 2. So, the measured background in the samples was not caused by ^{40}K. In almost all samples calcium was present. It was not or barely present in the samples of the analyses 5 and 7 and present in a low concentration in the samples of the analyses 4 and 6. It was present in a medium to high concentration in the samples of the analyses 1-3 with the sampling region of 305-325 g eluent. This shows that this sampling region has a worse separation from calcium than the others. The outliner analysis 2 contains the most calcium and was the only one that contained potassium. When the yttrium yield was determined, most of the samples contained solid, except for the sample of analysis 5. The solid could not be completely solved, even after heating in a water bath for a longer time. The solid is likely a calcium precipitate but could also contain yttrium and potassium co-precipitate. It could contain a varying amount of these elements for the different samples and as it was not part of the measurement of the samples, it could have distorted the results. This should be kept in mind when interpreting these result values.

In summary it can be said about the detection of ^{90}Sr via its daughter nuclide ^{90}Y, that the big advantage of this method is its significantly shorter active analysis time for a single sample. The previous analysis took 1.5 workdays, not including the measurement time and sample preparation. With this measurement, the analysis of one sample can be performed in half a workday. Additionally, the measurement time is reduced from an over-night measurement to a two-hour measurement. Due to the faster elution, also less chemicals are needed for this analysis concept, because the elution is only performed until 320 g eluent, including the sample inlet. Another advantage is the energy efficiency of this method, as the column has to be heated to 87°C for only 0.75 of a workday instead of two workdays and over-night between them.

The disadvantage of this method is that the measurement has to take place immediately after the separation, as ^{90}Y has only a half-life of 64 hours and a measurement delay could cause significant yield loss, as was shown with analysis 2. This also makes a simultaneous analysis of several samples, as is usual in this laboratory, difficult. The author routinely performed two separations in two different columns at once. The laboratory technicians performed four at once with the established method. A way of performing several separations at once would be to do it with a delay of two hours between the separations, so that the second separation would be finished at the same time as the measurement of the first sample. This would also enable two separations in a normal workday, but not more, as the columns had afterwards to be regenerated with 500 mL of 6 M hydrochloric acid, the throughput of which also takes at least 2 hours. At the moment, the time delayed analysis of two samples simultaneously is just an idea and it would have to be tested if it can be realized into praxis. If it would work, three analyses could be performed during the same time as previously four. Another disadvantage is that at least two weeks after the measurement must pass before the background and yttrium yield of the sample can be determined.

5.5 Preseparation of potential interfering substances

The previously recorded elution curves showed that in almost all separation cases the elution regions of potassium and calcium overlapped with the elution region of yttrium. Even in the cases, in which a complete separation was possible, the elution regions were really close to each other and small variations in the elution, which are a normal aspect of this analysis method, could lead to an overlap of the elution regions of the analyte and the interfering substances.

The aim of the following section was to find a fast and easy way to pre-separate potassium and calcium from yttrium to prevent the overlap of the elution regions of yttrium, calcium and potassium in the Hot Column Chromatography separation. If found, this method could be performed before the Hot Colum Chromatography as a purification step. The focus in the search of such a method was mostly on potassium, as ^{40}K is present in a significant amount in all potassium matrices and causes a background signal, as β-emitting nuclide, which would make additional measurements necessary and extend the analysis time.

5.5.1 Hydroxide-precipitation of Y

One method that was tested for the pre-separation of yttrium from the interfering substances was the yttrium hydroxide Scavenger-precipitation found in the instruction "Meßanleitungen für die Überwachung der Radioaktivität in der Umwelt und zur Erfassung radioaktiver Emissionen aus Kerntechnischen Anlagen" [69].

For this, the pH of the yttrium solution had to be adjusted to 9 with concentrated ammonia while stirring and heating. Then the solution had to be stirred for another five minutes and after that left to cool down. Finally, the yttrium hydroxide precipitate had to be separated through centrifugation and filtration. These steps had to be repeated for a quantitative separation.

After the Scevenger precipitation, it was planned to perform an yttrium oxalate precipitation. For this, the yttrium hydroxide precipitate had to be solved in 3 M hydrochloric acid. The solvent would then be diluted to approximately 20 mL and 1 mL saturated oxalic acid (90-100 g/L) would be added to the solution. Then the pH of the solution had to be adjusted to 2-3 with ammonia for a quantitative precipitation of yttrium oxalate. The precipitate would then again be separated through centrifugation and filtration.

As this method was tried, a problem occurred right at the beginning of the experiment. To 65 g of the eluent ammonium-lactate at pH7 1 mL yttrium-tracer, corresponding to 10 mg Y, was added. This was used as the model Y-fraction after the Hot Chroma separation. But the adjusting of the pH of the sample to 9 with ammonia, while stirring and heating, did not result in yttrium hydroxide precipitation. The experiment was performed four times, but the precipitation occurred not once. Even after adjusting the pH to 10. Then it was tried to reduce the solvent volume to 10 mL by heating the samples in the sand bath. But this only resulted in a viscous residue, that did not correspond to the expected precipitate.

The experiment was repeated another time with four samples, this time it was tried to reduce the solvent volume to 10 mL before adjusting the pH. But ammonium-lactate precipitated as a white gel again. The precipitate was dried completely, and it was tried to remove the matrix, as

it is done according to the instruction for the analysis of actinoids [70]. Small volumes of nitric acid and hydrogen peroxide were added, and the samples heated in the sand bath, until they were dry again. This step was repeated until the remaining precipitate was almost white with some leftover brownish coloring. It was very time intensive and required a lot of chemicals. Then it was tried to solve the remaining precipitate in 0.3 mL of concentrated sulfuric acid while heating, but it could not be solved. Instead, the precipitate turned white and white gases were emitted from the samples. Then the remaining sulfuric acid in the samples was evaporated and it was tried to solve the sample again in a mixture of nitric acid and hydrogen peroxide while heating. As this also did not work, this method was given up as a potential fast way to separate yttrium from potassium and calcium.

5.5.2 Ion-chromatographic separation of Y from K and Ca with CHELEX 100 column material

One possible pre-separation method would be another ion-chromatographic separation of the analyte yttrium with CHELEX 100 as column material. The method was developed by Wolfgang König in his dissertation "Entwicklung und Anwendung einer Analysen-und Messmethode für Fe55 als wichtiges Nuklid des Rückbaus stillgelegter Kernkraftwerke" [71] and described in the analysis instruction for ^{55}Fe [72]. As is evident from the title, the analysis was not developed for the main analyte of this work ^{90}Y, but for ^{55}Fe. But as the iron in this instruction is separated as three valent ion Fe^{3+} and the method is based on ion-chromatography, it was hoped that it could also be used to separate the three valent Y^{3+} ion from K^{+} and Ca^{+2}.

In the original analysis, iron is separated from the sample matrix by forming an anionic complex in the highly acidic medium, in which the iron is present as three valent ions, which bind strongly to the highly basic column material. At the same time ions as Na^{+}, K^{+}, $Ca^{2+}$and Mg^{2+} can pass the column without retention. So, the iron is concentrated in the column material until it is eluted with a higher concentrated acid. This method showed to be selective, quite fast, robust and sensitive for iron and it was hoped that if would be possible to achieve the same results for yttrium.

For the experimental separation of yttrium with the CHELEX 100 column material, the sample solution was prepared as usually. As standard sample matrix 10 g not contaminated milk ash, prepared from commercially available whole long-life milk by the brand Berchtesgadener Land, was used. It was solved in 80 mL of the usual 1:1 mixture of 6 M hydrochloric acid and 1.5 molar lactic acid, while stirring and heating. Additionally, 1 mL of the stable yttrium tracer, containing 10 mg Y, was added. Potassium and calcium were naturally present in the sample matrix in significant amounts, according to the milk packaging 124 mg calcium per 100 mL. Then the sample was centrifuged to separate the sample solution from the unsolved ash remains. As the separation of yttrium from the interfering substances was controlled via ICP-OES measurements, samples for these measurements were taken at each relevant separation step. And so, a sample for ICP-OES measurement was taken from this initial sample solution. After that, the steps of the ^{55}Fe analysis instruction [72] were followed. The temperature had to be below 75°C, to prevent damage of the column material, so the sample had to slightly cool down. Then the pH had to be adjusted to 1.6-1.9, for which ammonia was used. For the column, 22.0 g CHELEX 100 was suspended in 10 mL 1 M hydrochloric acid and left to well for 15 to 30 minutes. Then the suspension was filled in a chromatography column made from glass with a

diameter of 2 cm and a frit with the pore size GO. The excess liquid was released from the column. Then the prepared sample was applied to the column and eluted at a speed of 2-5 mL/min into the column material. The liquid, that left the column after this step, was sampled for an ICP-OES measurement as “eluate first”. Then the column was washed three times with 25 mL 0.025 M hydrochloric acid at a time. After every washing step, the liquid leaving the column was sampled for an ICP-OES measurement as washing step 1-3. Then, hopefully, the yttrium was eluted from the column with two times 40 mL of 1 molar hydrochloric acid. The liquid that left the column after this step was sampled for an ICP-OES measurement as “eluate final”. If the separation worked, this would be the fraction that would be applied to the Hot Column Chromatography for further separation.

For the ICP-OES measurement, the fraction samples were diluted 1:250. Per ICP-OES sample 40 µL of the fractions were used and 2 mL concentrated nitric acid was added for pH adjusting. The samples were then filled up to a volume of 10 mL with bidistilled water.

For the ICP-OES measurement, the same calibration curve was used, as the one calculated for the initial determination of the elution curve with the new DOWEX® 50 WX8 (200-400 mesh) by Alfa Aesar, as detailed in section 5.3.1.

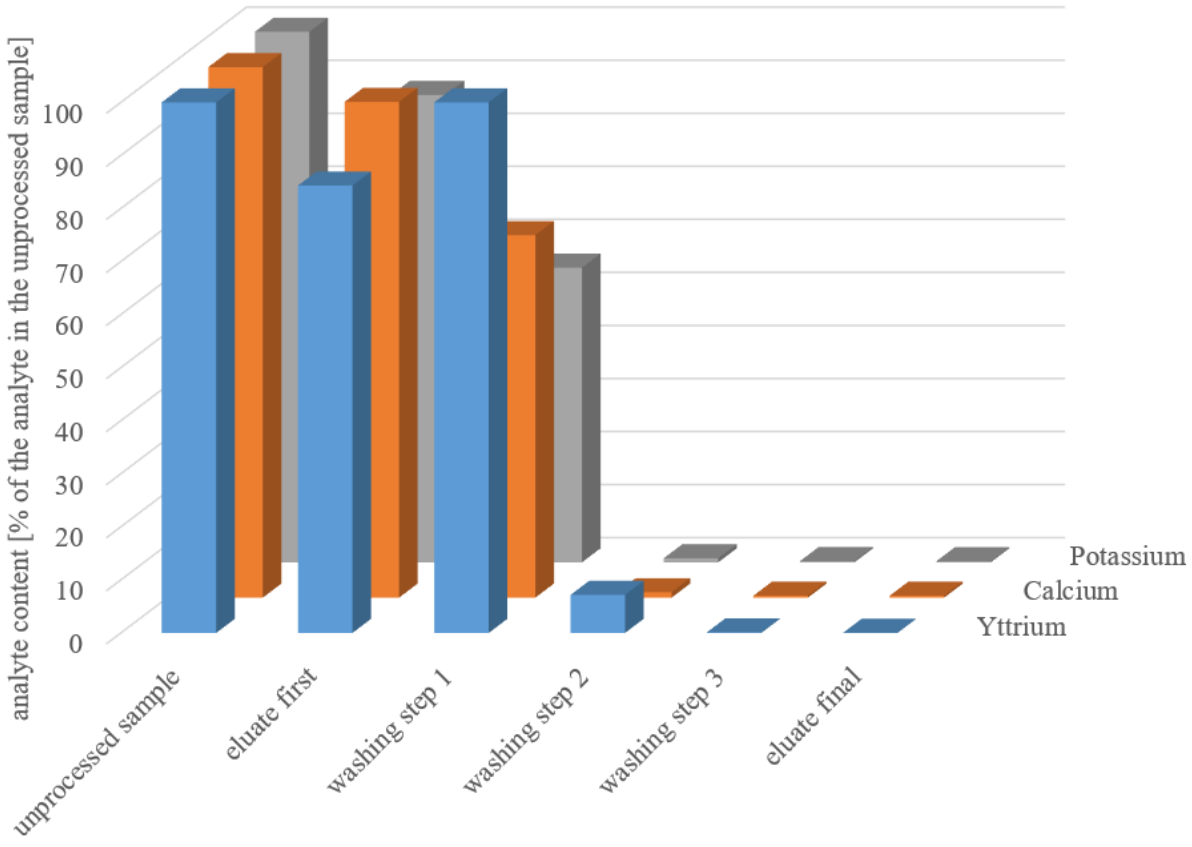

Figure 106: Results of the pre-separation of yttrium from potassium and calcium with the CHELEX 100 resin, analyte content after every elution step for comparison

Figure 106 shows the separation results for the pre-separation of yttrium from potassium and calcium with CHELEX 100. As can be seen in the graphic, the pre-separation did not work. Most of the analyte, as well as the interfering substances, passed the column during the sample inlet and were almost completely washed from the column by the second washing step. The yttrium concentration increased in the solution after the first washing step, compared to the

sample inlet, and had the highest relative concentration in the solution after the second washing step. But these differences were not enough to call this tried pre-separation successful. The retention of yttrium ions in the column was not significantly stronger than the retention of calcium and potassium ions.

5.5.3 Repetition: ion-chromatographic separation with CHELEX 100 column material with adjusted sample solvent

One possible reason for the failure of the first try to separate yttrium from potassium and calcium with the CHELEX 100 column material may be the wrong sample medium. The sample in the previous section was prepared as usual in a mixture of 6 M hydrochloric acid and 1.5 M lactic acid. But the sample in the ^{55}F analysis instruction was solved in 1 M hydrochloric acid [72]. Maybe there were unfortunate interactions with the lactic acid or the high concentration of hydrochloric acid, that caused the bad separation. So, in the next experiment, the separation with CHELEX 100 was performed exactly as the previous time, but this time the sample ash was solved in 80 mL 1 M hydrochloric acid.

As standard sample matrix 10.00 g not contaminated milk ash, prepared from commercially available whole long-life milk by the brand Berchtesgadener Land, was used. It was solved in 80 mL of 1 M hydrochloric acid. Additionally, 1 mL of the stable yttrium tracer, containing 10 mg Y, was added. Potassium and calcium were naturally present in the sample matrix in significant amounts, according to the milk packaging 124 mg calcium per 100 mL. Then the sample was centrifuged to separate the sample solution from the unsolved ash remains. The rest of the analysis was performed as described in section 5.5.2, based on the ^{55}Fe analysis instruction [72].

For the ICP-OES measurement, the fraction samples were diluted 1:250. Per ICP-OES sample 40 µL of the fractions were used and 2 mL concentrated nitric acid was added for pH adjusting. The samples were filled up to a volume of 10 mL with bidistilled water. For a first overview, only “eluate first”, “eluate final” and the sample itself were measured.

For the ICP-OES measurement, the same calibration curve was used as the one calculated for the initial determination of the elution curve with the new DOWEX® 50 WX8 (200-400 mesh) by Alfa Aesar, as detailed in section 5.3.1.

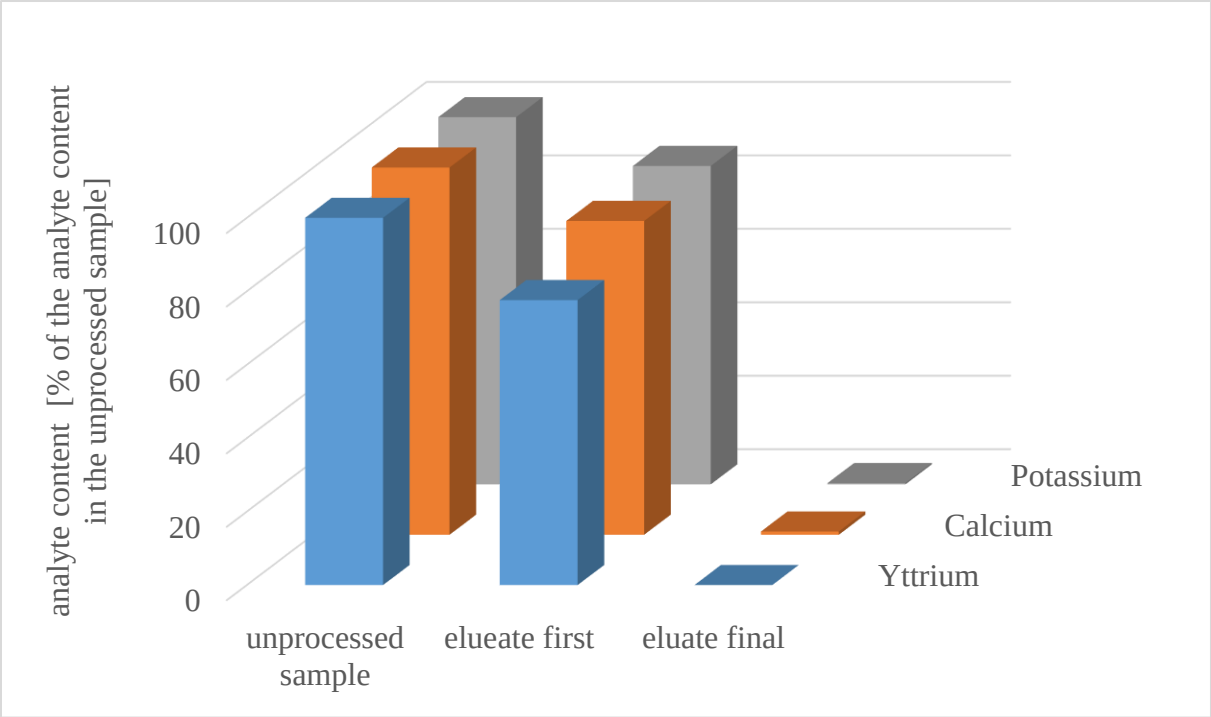

Figure 107: Results of the repetition of the pre-separation of yttrium from potassium and calcium with the CHELEX 100 resin and 1 M hydrochloric acid as solvent, analyte content after every elution step for comparison

Figure 107 shows the separation results for the pre-separation of yttrium from potassium and calcium with CHELEX 100, with the sample solved in 1 M hydrochloric acid. As for the first try, no retention of yttrium in the column is visible. It passes the column, its remains washed away, without significant interactions with the column material. So, the change of the sample solvent did not influence the separation quality of this experiment and the pre-separation of yttrium from potassium and calcium failed another time.

The separation has many variables, among them the pH or the eluent, that could be varied to achieve better results. But these variations were not further investigated in this work.

6 Conclusion

In this work it was tested whether different sample types had significantly different calcium contents, which would make a variation in sample mass necessary, depending on which sample type is analyzed. The tested sample types were milk, sugar beets, salad, corn, spelt, barley and wheat. All of them in ash form. The experiments showed that even though there were variations in the calcium-content, it was in the same range for all sample types. Therefore, the same standard sample mass of 10 g could be used for the analysis, regardless of the sample type. Then it was tested whether varying sample types would influence the elution regions of different elements in the Hot Colum Chromatography separation. The focus was especially on the analytes yttrium and strontium and the interfering nuclide ^{137}Cs. This elution curves were detected with milk, wheat, salad and corn ash as samples. The experiments showed that the elution curves for the different sample types looked very similar and were comparable. There were variations between the elution curves, which in turn were sometimes more and sometimes less pronounced. This could be taken into consideration for future analyses. But the elution region of yttrium was always quite narrow, did not vary much and in most cases only a verry small overlap with the elution region of cesium was present. The salad sample was the only one that showed a significant overlap between the elution regions of yttrium and cesium. Also, the overlap between the elution regions of strontium and cesium was a lot more significant for milk than for the other samples. This indicates that a complete separation of the strontium elution region could be possible for these samples, increasing the yield of the analysis.

The column material for the Hot Column Chromatography, the DOWEX® 50 WX8 (200-400 mesh) by the provider Serva was no longer available. A product under the same name was ordered from another provider, Alfa Aesar. Before applying it to real samples, it was tested and characterized by determining the elution regions of the analytes yttrium and strontium and the interfering elements calcium, potassium and the interfering nuclide ^{137}Cs with it. Contrary to the expectations, the results with the new column material by Alfa Aesar varied significantly from the results with the established DOWEX by Serva. The new column material led to a shift of the elution regions to higher eluent volumes. The yttrium elution region was only shifted by 10 mL to higher eluent volumes, but the strontium elution region was shifted by whole 40 mL to higher eluent volumes and was significantly broadened. This would make significantly longer elution times for the strontium analysis necessary. Further experiments had to be performed to find a way to accelerate the strontium elution. Apart from that, a very good separation between yttrium and strontium, a good separation between calcium and strontium and an acceptable separation between potassium and strontium were achieved. The separation between yttrium, calcium and potassium was only mediocre. But at least the relative content of potassium and calcium was quite small in the maximum range of yttrium. The elution region of cesium was in the range of the cesium elution region achieved with the established DOEWX. Additionally, the new elution region was 30 mL narrower than the older one, which would cause a better separation between the interfering nuclide ^{137}Cs and the analytes ^{90}Y and ^{90}Sr.

After the DOWEX® 50 WX8 (200-400 mesh) by Alfa Aesar, the product under the same name by another provider, Sigma Aldrich, was tested, in hopes it would provide more similar results to the established DOWEX by Serva. The separation quality of the analytes yttrium and strontium from the interfering elements calcium and potassium achieved with the Sigma Aldrich DOWEX was similar to the one with the column material by Alfa Aesar. Both show a

narrow yttrium elution region with a strong overlap with the calcium and potassium elution regions, that are located between the elution curves of yttrium and strontium. In both cases only a small overlap between the elution regions of calcium and strontium were noticeable. But the analytes were eluted from the column at lower eluent volumes and a narrower strontium elution curve was achieved with the DOWEX by Sigma Aldrich. But the strontium-elution region was still significantly broader than with the column material by Serva. So, the change of DOWEX® 50 WX8 (200-400 mesh) provider could not solve this problem.

Another approach to accelerate the elution of strontium was to change the eluate. It was changed from ammonium-lactate at pH7 to 6 M hydrochloric acid, the substance used to recondition the column and remove remaining analyte ions from it, as soon as the strontium fraction was separated from the interfering elements. For this experiment, the DOWEX® 50 WX8 (200-400 mesh) by Alfa Aesar was used. The resulting strontium-elution region from this experiment had approximately the same end point as the elution region achieved with the established DOWEX® 50 WX8 (200-400 mesh) by Serva. The broadening of the elution region of strontium could therefore be counteracted with the eluent change after the separation from the interfering elements. The acceleration was successful.

After the separation of the strontium-fraction, the strontium is precipitated as $SrSO_4$ from it. As the eluent was changed, it had to be tested whether the precipitation would work in pure 6 M hydrochloric acid or in mixtures of it with ammonium-lactate as well as in pure ammonium-lactate. The precipitation experiment was performed two times for different mixing ratios of hydrochloric acid and ammonium-lactate as media. For both experiments, a sample with a high hydrochloric acid content achieved only a small $SrSO_4$ yield, and these are the samples most comparable to the sample after the eluent change. One time it was the sample with pure hydrochloric acid as medium and the other time the sample with a mixture of 75 % hydrochloric acid and 25 % ammonium-lactate as medium. The precipitation worked for all mixing ratios of the eluents, but the following filtration of $SrSO_4$ was inefficient at higher concentrations of hydrochloric acid. This was maybe due to the very low pH of the medium, which caused damages in the filter and left turbidity, assumed to be $SrSO_4$, in the filtrate. All in all, this meant that the eluent change worked in accelerating the elution but disrupted the filtration step of the process. Based on this, the eluent change to 6 molar hydrochloric acid was rejected as an elution acceleration strategy

Another approach to accelerate the elution of strontium was to make the pH of the eluent ammonium-lactate slightly more acidic. For the experiment, the DOWEX® 50 WX8 (200-400 mesh) by Alfa Aesar was used and the pH of the eluent was reduced to 6, form the established pH7. As a result, it was found that the change of the pH lead to the significant acceleration of the strontium elution, that was hoped for. With this slight change, the Hot Column Chromatography could be performed as usual with the new column material. The downside to this was the worse separation of yttrium from potassium and calcium, due to accelerated elution and narrower elution regions of these analytes and the resulting overlap of their elution regions. This experiment was repeated with the DOWEX® 50 WX8 (200-400 mesh) by Sigma Aldrich. The results were reproducible for this column material by the other provider and the same conclusions were made as for the DOWEX® 50 WX8 (200-400 mesh) by Alfa Aesar.

After this result, it had to be tested whether the pH-change of the eluent would have negative effects on the precipitation of strontium as $SrSO_4$ after its separation. The precipitation was tested in ammonium-lactate at pH 6, compared to ammonium-lactate at pH 7. The experiment

showed comparably high precipitation yields for both samples, indicating a complete precipitation. The deviation of the yield with ammonium-lactate at pH 6 from the yield with the eluent at pH 7 and from the 100 % yield was only 2.38 %. This was an acceptable deviation for an experimental step. The results of this experiment were interpreted as successful, and the precipitation yields for $SrSO_4$ with ammonium-lactate at pH 6 and 7 as comparable. This made a pH change of the eluent from 7 to 6 for the elution acceleration permissible.

The results obtained from the previous experiments were tested on real food samples for environmental monitoring and compared to the results achieved with the established DOWEX by Serva. For these experiments the DOWEX by Alfa Aesar and ammonium-lactate at pH6 were used. The average strontium yield for the strontium separation with the established DOWEX by Serva in 2021 was 79.09 % with three outliners, for which constructed yield values were used. The average strontium yield for the strontium separation with the new DOWEX by Alfa Aesar and the eluent at pH6 in 2022 was 53.31 % with one to two outliners, for one of which a constructed yield value was used. The strontium yields were significantly lower with the new DOWEX, fewer outliners were present. The yields were also enough to achieve the necessary level of detection and ensure reliable environmental monitoring of the area.

In addition to this, the new DOWEX by Alfa Aesar in combination with ammonium-lactate at pH6 was applied for the age determination of ivory samples. These results were also compared to former results achieved with the DOWEX by Sreva. The results showed that with the established DOWEX by Serva, significantly higher yields than with the DOWEX by Alfa Aesar were achieved. But the newer DOWEX delivered more constant results, that were still in an acceptable scale. In both cases no outliners were detected.

Another way to test the novel system was to participate with it in a ring experiment. The comparable results of the analyses for the same sample showed that the new column material is suitable for the separation of ^{89}Sr and ^{90}Sr and their subsequent detection. The official results of the ring analysis, that would confirm or reject these results, were at the time of writing not yet announced.

The focus of this work was the determination of ^{90}Sr via its daughter nuclide ^{90}Y. For this, yttrium had to be separated with the Hot Column Chromatography, instead of strontium. First, the elution region of yttrium in a milk sample was determined as very narrow and at significantly lower eluent throughput than for strontium with an elution region 270-330 g eluent, including sample inlet, and a maximum at 300-310 g eluent. Then the elution regions of the interfering elements potassium and calcium were determined. Complete peak separation was achieved between the elution maxima and main elution regions of yttrium and the interfering elements, but the tailing component of the yttrium elution region overlapped with the elution regions of calcium and potassium. An almost complete overlap of the potassium and calcium elution regions was evident. This showed that a separation of most of the yttrium fraction from calcium and potassium would be possible without severe yield losses. But the elution regions of the analytes were very close to each other and a slight shift of them could cause a significant overlap.

To counteract this overlap, it was tested to slow down the elution speed in the elution region of yttrium, calcium and potassium to 1.5 g/min, instead of the established 2.5 g/min. For this experiment the DOWEX by Alfa Aesar and ammonium-lactate at pH6 were used. The resulting chromatogram showed that the overlap between the elution regions increased with a slower

elution, leading to a worse separation than with a higher and constant elution speed. Therefore, the slowing down of the elution was not implemented in routine analytics.

The plan for the yttrium analysis was to separate a 20 mL yttrium fraction of the elution, that has the highest yttrium yield and the best separation from calcium and potassium as possible and measure it directly in the QUANTULUS via a Cherenkov measurement. As the elution region of yttrium was broader than 20 mL, an optimal sampling region for this had to be found. For these experiments the DOWEX by Alfa Aesar and ammonium-lactate at pH6 were used. The collected data showed that the sampling regions of 295-315 g eluent and 305-325 g eluent, including sample inlet, were the most suitable for the yttrium sampling. In the sampling region of 295-315 g eluent only a comparably low yttrium yield of 36.91 % was achieved, but the interfering elements potassium and calcium were completely removed. Additionally, the sample was clear and liquid and stayed in this state after cooling down to room temperature. Those were optimal conditions for the Cherenkov measurement and would lead to a relatively high SQP(E) value and therefore to a high physical yield. In the sampling region of 305-325 g eluent the highest yttrium yield of 76.45 % was achieved. Additionally, potassium and therefore the main interfering nuclide ^{40}K was completely separated from the sample. The downside of this sampling region was the significant calcium amount in the sample. This led to a yellow coloring and crystal formation as soon as the sample cooled down to room temperature. This would lower the SQP(E) value of the Cherenkov measurement and subsequently the physical yield. The sampling region of 300-320 g eluent was similar to the sampling region of 305-325 g eluent but had a lower yttrium yield and at the same time a higher calcium content. This sampling region would theoretically be suitable for the yttrium sampling but was outperformed in every aspect by the sampling region of 305-325 g eluent. Other sampling regions were not suitable due to a complete lack of yttrium content or the lack of a separation between yttrium and the interfering elements.

After the optimal sampling regions were determined, the complete analysis experiments of ^{90}Y were performed in the sampling regions of 295-315 g eluent, 300-320 g eluent and 305-325 g eluent based on the data from pre-experiments. As tracer, an active ^{90}Sr one was used. The complete analyses were performed including the Cherenkov measurements directly after the Hot Chroma separation. Apart from two outliners, due to an elution shift, approximately the complete ^{90}Y activity could be separated in the other sampling fractions. All samples showed a low and relatively consistent background lower than 0.5 Bq. The yttrium yield was quite inconsistent due to sample solidification but corresponded in most cases to the activity. Almost all samples showed a yellow coloring and solidification after some time. Even though the samples were in different conditions, almost all of them had a comparable SQP(E) value, representing the quality of the measurement. All in all, the experiment showed the most stable results for the medium sampling region of 300-320 g eluent, event tough it did not seem favorable in pretests. Due to its position in the middle between the other two sampling regions, it was less affected by slight shifts of the elution and in all cases the maximum of the yttrium elution could be separated in this sampling region.

As the elution regions of calcium and potassium were quite close to the elution region of yttrium, an overlap could not be excluded. Therefore, several potential quick separation techniques of yttrium from calcium and especially potassium were tried. It was hoped that these could be implemented as additional separations, either before or after the Hot Column Chromatography. But, unfortunately, neither of the tried methods were successful.

7 Outlook

In this work the foundation for the detection of ^{90}Sr via its daughter nuclide ^{90}Y was laid by investigating the possibility of the application of this method. But until it can be used for the detection of ^{90}Sr in real samples, further experiments and investigations are necessary, that exceed the volume of this work. Some suggestions for said investigations are presented below.

One of them would be to test this analysis system on different columns, as the elution regions vary slightly from column to column, due to small differences in the geometries. Before it is applied on real samples, it has to be optimized for each column respectively, as the elution region of yttrium is so narrow, that even small changes in the elution can have severe effects on the analysis.

Another question, that has to be answered, is how robust and reproducible this method is, due to the narrow elution region of yttrium. This leads to its susceptibility to variations in the elution process. One way to counteract this, would be to separate a larger volume than 20 mL, encompassing the whole elution region of yttrium. This would make this method less susceptible to elution variations. Then the volume would be reduced back to 20 mL, for example by heating. The downside of this could be a worse separation from calcium and potassium, as their elution regions were quite close to the one of yttrium. Additionally, the time that is needed to reduce the sample volume could have an adversary effect on the yttrium yield, as ^{90}Y has a half-life of only 64 hours.

Overall, the time sensitivity of the ^{90}Y yield requires further investigation. If a time delay of the measurements would deliver acceptable limits of detection, a parallel analysis of up to four samples, as it is practiced now with the ^{90}Sr analysis, would be possible. This would enable a similar analysis efficiency, while reducing the time and labor intensity and the electricity and chemicals used.

If the time delay would have a too strong effect on the measurement results, an alternative to increase the sample throughput would be the performance of two separations at once, with a time delay of two hours between the separations. This would also enable two separations in a normal workday, but not more, as the columns had afterwards to be regenerated with 500 mL of 6 M hydrochloric acid, the throughput of which also takes at least 2 hours. But at this moment, the time delayed analysis of two samples simultaneously is just an idea and it would have to be tested, if it can be realized into praxis.

Another experiment worth trying would be to perform the ^{90}Y analysis with ammonium-lactate at pH7, as strontium does not have to be separated in this analysis and therefore its elution does not have to be accelerated. Pervious experiments showed a better separation between yttrium and calcium and potassium at pH7, due to the slower elution and it is worth trying, if the effect is significant enough to make a difference in the measurement results.

When the method is sufficiently optimized, it can be tested in a ring-analysis, before it is applied to real samples. During this stage, its long-term performance can be surveilled.

Additional to the determination of ^{90}Sr via ^{90}Y, the Sr analysis with a new DOWEX material was investigated and optimized. Even though the yields achieved with the new DOWEX by Alfa Aesar were acceptable and sufficient levels of detection were reached, the results were nevertheless worse than with the established DOWEX. One task would be, to find out what is

the exact reason for this and to modify the separation regions for strontium accordingly, to achieve better yields with the new column material. Another recommendation would be, to switch the yield determination from the titrimetric method back to the gravimetric one, as it is less prone to error than the former one.

Another part of this work dealt with the comparison of the elution results between different sample types. One of the results was, that the overlap between the strontium and the cesium elution regions is strongest for milk and not as pronounced for other sample types. If this is investigated further, this information could be used to broaden the sampling region of strontium and increase the analysis yield.

8 References

[1] Wissenschaftliche Dienste des Deutschen Bundestages, CO2-Bilanzen verschiedener Energieträger im Vergleich, Zur Klimafreundlichkeit von fossilen Energien, Kernenergie und erneuerbaren Energien, elaboration, 04.04.2007

[2] O. Becker, A. Y. Indradiningrat, on behalf of BUND, Atomstrom 2018: Sicher, sauber, alles im Griff? Aktuelle Probleme und Gefahren bei deutschen Atomkraftwerken, study, april 2018

[3] http://www.environmental-studies.de/Radioecology/Radiocesium/Cs_E1/cs_e1.html (28.11.2022)

[4] https://www.bge.de/de/abfaelle/ (28.11.2022)

[5] https://www.bundesregierung.de/breg-de/suche/bundesregierung-beschliesst-ausstieg-aus-der-kernkraft-bis-2022-457246 (28.11.2022)

[6] https://www.zeit.de/wirtschaft/2022-11/atomausstieg-bundesrat-aufschub-weiterbetrieb?utm_referrer=https%3A%2F%2Fwww.ecosia.org%2F (28.11.2022)

[7] https://www.tagesschau.de/inland/innenpolitik/suche-nach-atommuell-endlager-101.html (28.11.2022)

[8] https://www.br.de/nachrichten/deutschland-welt/zeitungsbericht-endlager-fuer-atommuell-steht-fruehestens-2046,TMtoUmB (28.11.2022)

[9] https://www.wissen.de/welche-reichweite-und-welches-schadenausmass-haben-atombomben (28.11.2022)

[10] S. A. K. Schmied, Entwicklung und Validierung einer Analysenmethode zur Bestimmung von ^{90}Sr im Rahmen der Datierung von Elfenbein mittels der Radionuklide ^{14}C, ^{90}Sr und $^{228/232}$Th, dissertation, january 2012

[11] G. M. Milton, W.E. Grummit, Ion Exchange Methods for the Quantitative Separation of the Alkaline Earths, and their Application to the Determination of Sr-90 in Milk Ash, Canadian Journal of Chemistry 35 (1957) 541

[12] National Institute of Standards and Technology, CODATA Task Group on Fundamental Constants, 04.07.2019

[13] Harvard Natural Sciences Lecture Demonstrations: α, β, γ Penetration and Shielding, 20.02.2020

[14] V. Martini, Entwicklung und Validierung einer Analysenmethode zur Bestimmung von ^{210}Pb, ^{228}Ra und ^{238}U in Trinkwasser mittels Cerenkov-Counting, master thesis, august 2013

[15] H. Krieger, Grundlagen der Strahlungsphysik und des Strahlenschutzes, 2 edition

[16] BG RCI, Informationsschreiben, 2.04.2015

[17] R. Schupfner, Am URA-Lab verfügbare Themen für Masterarbeiten und ein Promotionsprojekt, exposé, 20.01.2020

[18] https://www.nndc.bnl.gov/nudat3/ (28.11.2022)

[19] https://www-nds.iaea.org/sgnucdat/c3.htm (01.02.2023)

[20] M. Eisenbud, Environmental Radioactivity

[21] M. Chinol, D. J. Hnatowich, Generator-produced yttrium-90 for radioimmunotherapy, Journal of Nuclear Medicine, 28 (9): 1465–70, september 1987

[22] PNNL, PNNL: Isotope Sciences Program - Yttrium-90 Production, february 2012

[23] Berkeley Lab, Y-90 Handling Precautions, 15 January 2018

[24] Bundesamt für Strahlenschutz, Welche Radionuklide kommen in Nahrungsmitteln vor?, 19. 08 2014

[25] R. Schupfner, Versuch 6: Kernspektrometrie α, β, γ−Strahler, laboratory course experiment instruction

[26] C. Michael Lederer, Jack M. Hollander, Isadore Perlman, Table of isotopes, John Wiley & Sons, New York, 1967

[27] H. Leutz, G. Schulz, H. Wenninger, The decay of potassium-40, Zeitschrift für Physik, DOI 10.1007/BF01387190, 1965

[28] A. Ažman, A. Moljk, J. Pahor, Electron capture in potassium 40, Zeitschrift für Physik A, DOI 10.1007/BF01379914, 1968

[29] W. Sahm, A. Schwenk, 39K, 40K and 41K Nuclear Magnetic Resonance Studies, Zeitschrift für Naturforschung A, DOI 10.1515/zna-1974-1208, 2014

[30] The Lund/LBNL Nuclear Data Search, Table of radioactive isotopes, K-40

[31] M. M. Bé, V. Chisté, C. Dulieu, E. Browne, C. Baglin, V. Chechev, K. B. Lee, Table of Radionuclides, monograph, vol. 3–A= 3 to 244 BIPM, 5, 2006

[32] D. Delacroix, J. P. Guerre, P. Leblanc, C. Hickman, Radionuclide and Radiation Protection Handbook, Nuclear Technology Publishing, ISBN 978-1870965873, 2002

[33] R. L. Bunting, Nuclear Data Sheets for A=137, Nuclear Data Sheets 15. 335, 1975

[34] WWF Deutschland, 43 Jahre CITES – Erfolge und Misserfolge: https://www.wwf.de/fileadmin/fm-wwf/Publikationen-PDF/WWF-Positionspapier-CITES-Erfolge-Misserfolge.pdf, (26.03.2020), 2016

[35] J. Anderson, Colorado Journal of International Environmental Law and Policy 2001, https://heinonline.org/HOL/P?h=hein.journals/colenvlp12&i=479.

[36] CITES, Appendices I, II and III: accessible under https://cites.org/eng/app/appendices.php: (07.08.2020)

[37] M. J. Brunnermeier, Entwicklung und Validierung einer Methode zur Bestimmung des Todeszeitpunkts von Elefanten durch Bestimmung von 14C und 228Th/232Th in Elfenbein, dissertation, 2012

[38] S. Ziegler, V. Reifenstein, B. Simon, Auf den Zahn gefühlt - Handel und Kunst mit Elfenbein, 2008

[39] T. Siegert, Age determination of ivory via two-point-method of suitable radionuclides and the application of EPR, master thesis, december 2020

[40] A. Schmidberger, Development and application of an analytical strategy for the determination of 232Th and 228Th in ivory based on the combined use of inductively coupled plasma mass spectrometry and α-spectrometry, dissertation, april 2019

[41] S. A. K. Schmied, M. J. Brunnermeier, R. Schupfner, O. S. Wolfbeis, Dating ivory by determination of 14C, 90Sr and 228/232Th, Forensic science international, 221, 5., 2012

[42] Q. Hua, M. Barbetti, A.Z Rakowski, Atmospheric Radiocarbon for the Period 1950-2010, Radiocarbon 55 (2013) 2059-2072, 2013

[43] M. Auerhammer, Erstellung des Isotopenprofils für $^{14}C/C$ für aktuelle Proben von Elefantenelfenbein, bachelor thesis, 2015

[44] A. Wieberneit, Elfenbeindatierung durch ^{14}C Analyse, bachelor thesis, june 2018

[45] A. Schmidberger, B. Durner, D. Gehrmeyer, R. Schupfner, Development and application of a method for ivory dating by analyzing radioisotopes to distinguish legal from illegal ivory, FSI Forensic Science International, FSI 9363, 2018

[46] F. Schmidt, Elfenbeindatierung mittels ^{90}Sr Analyse, bachelor thesis, june 2018

[47] R. Schupfner, Altersbestimmung von Elfenbein durch Erstellung des Isotopenprofils 14C/C, 90Sr/Ca und 228Th/232Th, analysis instruction, URA/ZRN, institute for analytical chemistry, University of Regensburg

[48] M. Otto, Analytische Chemie, 2 edition, WILEY-VCH, Weinheim, 2004

[49] https://www.crawfordscientific.com/chromatography-blog/post/van-deemter-equation-the-lockdown-guide (27.02.2023)

[50] J.Weiss, Ion Chromatography, 2 edition, VCH, Weinheim, 1995

[51] M. Otto, Analytische Chemie, 3 edition, WILEY-VCH, Weinheim, 2006

[52] S. A. K. Schmied, Optimierung und Validierung einer Analysenmethode zur Bestimmung von Sr-89 und Sr-90 in ausgewählten Materialien mit hohem Calciumgehalt, diploma thesis, september 2008

[53] https://dow-answer.custhelp.com/app/answers/dtail/a_id/6921/~/dow-ion-exchange-resins (10.09.12)

[54] SPECTRO AMETEK materials analysis division, SPECTROBLUE FMX36, model FMX 36 of the type 76004563, operating manual

[55] ICP-OES instruction, developed by the operating staff

[56] R. Nicoletti, M. Oberladstätter, F. König, Messtechnik und Instrumentierung in der Nuklearmedizin: Eine Einführung, facultas.wuv Universitätsverlag, 2010

[57] G. F. Knoll, Radiation Detection and Measurement, 4. edition Wiley, New York, 2010

[58] G. Gilmore, Practical Gamma-ray Spectrometry, Wiley, Chichester, 2008

[59] W. R. Leo, Techniques for Nuclear and Particle Physics Experiments: A How-to Approach, Springer, New York, 1994

[60] M. Hechtel, Bilanzierung der Freisetzung von Cs-137 bei der Verbrennung von Pilzen, diploma thesis, march 2022

[61] Perkin Elmer, 1220 QUANTULUS Ultra Low Level Liquid Scintillation Spectrometer description specifications, operation manual

[62] BERTHOLD GmbH Co. KG, PC-gesteuerter 10 Kanal α-β-Messplatz LB 770Win-PC, operating manual

[63] S. A. K. Schmied, Analysevorschrift zur Bestimmung der spezifischen Aktivität von ^{90}Sr in Umgebungsüberwachungsproben, analysis instruction, URA/ ZRN, institute for analytical chemistry, University of Regensburg

[64] Analysenvorschrift zur Bestimmung von 90Sr und 89Sr nach Aufreinigung durch mehrmaliges Umfällen, analysis instruction, URA/ ZRN, institute for analytical chemistry, University of Regensburg

[65] Merck KGaA, Spectroquant® calcium cell test 1.00858.0001, analysis instruction

[66] S. A. K. Schmied, Arbeitsvorschrift für die Bestimmung der spezifischen Aktivität von Sr-90 in Elfenbein zur Feststellung, ob Elfenbein vor oder nach 1947 gewonnen wurde, analysis instruction, URA/ZRN, institute for analytical chemistry, University of Regensburg, 2009

[67] Das Deutsche Institut für Normung e.V. (DIN), DIN ISO 11929-1 norm, Determination of the characteristic limits (decision threshold, detection limit and limits of the coverage interval) for measurements of ionizing radiation - Fundamentals and application - Part 1: Elementary applications (ISO 11929-1:2019), march 2020

[68] Analysevorschrift für die Bestimmung der spezifischen Aktivität von ^{90}Sr in Rohelfenbein, analysis instruction, URA/ ZRN, institute for analytical chemistry, University of Regensburg

[69] Published in the name of the minister for environment, nature protection and reactor safety (Bundesminister für Umwelt, Naturschutz und Reaktorsicherheit), Meßanleitungen für die Überwachung der Radioaktivität in der Umwelt und zur Erfassung radioaktiver Emissionen aus Kerntechnischen Anlagen, volume 2, control center E-K,

[70] H. Gammel updated, Analysevorschrift Trennung Aktinoiden, analysis instruction, URA/ ZRN, institute for analytical chemistry, University of Regensburg, 2018

[71] W. König, Entwicklung und Anwendung einer Analysen-und Messmethode für Fe55 als wichtiges Nuklid des Rückbaus stillgelegter Kernkraftwerke, dissertation, 1996

[72] S. A. K. Schmied, Arbeitsvorschrift zur Bestimmung von Fe-55, analysis instruction, URA/ ZRN institute for analytical chemistry, University of Regensburg, 2009

[73] Bundesamt für Justiz, Strahlenschutzverordnung, Verordnung zum Schutz vor der schädlichen Wirkung ionisierender Strahlung, 29.11.2018

9 Appendix

9.1 Work in a control-area

The work with higher active materials, whose radioactivity significantly exceeds the environmental radioactivity, is only permitted in the control area. The entry is forbidden for unauthorized persons. Work safety regulations are based on European and national law.

Before a person can enter the control area, the following conditions have to be fulfilled. They must receive an adequate instruction in radiation protection before their first entry (Article 63 Paragraph 1 StrlSchV) [73], which is repeated yearly for the staff working regularly in the control area. They should have a permit to work in the control area, have sufficient knowledge of their task in the control area and basic knowledge of radiation protection (Article 55 Paragraph 1 Number 1) [73]. Pregnant or breastfeeding people are not allowed to enter the control area, due to higher risk (Article 55 Paragraphs 2, 3 and 69 StrlSchV) [73]. In the case that the person worked in another control area before, the category of the professional radiation exposure must be checked (Article 71 StrlSchV) [73]. If it is necessary, medical supervision of the activity in the control area must be provided. In the case of students, additional technical supervision in the control area is necessary. To enter the control area, one has to wear long bottoms and closed and flat shoes for safety reasons.

If those conditions are fulfilled, the person can enter the control area. This happens through a sluice, where one tests for radioactive contamination. This happens to make sure, that no one enters the control area already radioactively contaminated. In most cases, a contamination can be ruled out. First one's hands are washed and disinfected. Then one walks over an adhesive foil to remove dirt and little stones from one's shoes. Also, all jewelry is removed from one's hands. This is done for the protection of the very sensitive detector foil in the Hand-foot-clothing monitor used for the measurement. Then one can enter the device by putting one's feet completely to the front of each foot slot and one's hands in the slots for the hands and presses them together. After that one waits for 10 seconds, while the device completes the measurement, and tries to move as little as possible, as this could disrupt the measurement. After ten seconds, in most cases, the notification "not contaminated" pops up.

The following figure shows the Hand-foot-clothing monitor in the sluice, with slots for hands and feet. In the bottom area, the adhesive foil can be seen. On the right the entry book, electrical and film-dosimeters are seen on a table. In the background, an instruction is seen, to remove jewelry from one's hands and dirt from one's shoes.

Figure 108: Hand-foot clothing monitor in the sluice

After the contamination control, the entry is documented in the entry book. There one's name, the date and time of entry, the room in which one will be active, the reason for the entry, the confirmation of the contamination control and finally the current value of one's electrical dosimeter are entered. This information is necessary to maintain an overview over who entered the control area over a longer time period, in case of a contamination or missing radiators. But it is also important in the short term, as in case of an emergency it is directly evident who is in the control area and has to be evacuated.

Everyone, who enters the control area, must at least wear an electrical dosimeter. They show if one is exposed to ionizing radiation and are always readable. The electrical dosimeter measures the body dose and is worn at a representative position on the upper part of the torso. In the presence of radiation, the shown µSv value increases. In case of a strong increase, it starts to beep. The electrical dosimeter also beeps if it`s battery is low, so the sound is not automatically a sign for danger. A small increase of 1 µSv per workday is normal and safe. It is due to environmental radiation. The electrical dosimeters are the reason why mobile phones are only permitted in the control area if they are in flight mode or switched off. The dosimeters cannot differentiate between the radiation of a mobile phone and the ionizing radiation of a radio nuclide. This could lead to an overestimation of the radiation exposure and lead to a false alarm. The values of the electrical dosimeters are weekly documented and set back to zero.

The regular staff of the control area additionally wear a semiconductor dosimeter. The additional measurement with a different detection principle increases the work safety. The semiconductor dosimeters provide the evidence, that the dose limits per calendar year are not exceeded. They are not readable and have to be evaluated monthly by an independent measurement site.

Figure 109: Electrical dosimeter (on the right) and semiconductor dosimeter (on the left)

After these safety precautions are fulfilled, the control area can be entered. Depending on the work performed in the control area, additional safety gear may be necessary, like a laboratory coat, safety goggles, gloves or respiratory protection. The regular safety rules for the work in a laboratory also apply in the control area. Additionally, the windows cannot be opened, to prevent the contamination of outside air. A ventilation system is installed in the control area, to provide enough influx of fresh air. The wastewater is collected in a decay system and samples are measured regularly. The control area may only be entered or left through the sluice, except in case of an emergency, in which the additional emergency exits may be used. The stay in the control area has to be as temporally limited as possible and only used for tasks, that cannot be performed elsewhere. When working with radioactive materials, one has to prioritize handling only the smallest sensible amount of activity and, if possible, replace the radioactive material with a stable isotope. When handling radioactive samples, one has to keep the contact times as short as possible, keep as much distance as possible and use lead or plexiglass shielding if possible. There are no trash cans in the control area, to prevent the accumulation of uncharacterized radioactive trash. The trash produced during the stay is measured before leaving and taken out of the control area, in case of no contamination, or documented and stored safely, after informing the supervisor for radiation protection, in case of a significant contamination.

After the work in the control area, one leaves as one has come in through the sluice. First the hands must be washed and disinfected. Then the jewelry must be removed from the hands and the shoe soles must be cleaned on the adhesive foil. Then one can enter the Hand-Foot-Clothing monitor again. One proceeds the measurement as described before, when entering the control area. In most cases, the notification “not contaminated” pops up. In the very rare case that the pop-up states “contaminated” one has to stay calm and try to decontaminate one’s hands by washing them thoroughly again and one’s shoes by walking some more on the adhesive foil. If after that the measurement result is still “contaminated”, one must call the supervisor for radiation protection and follow their orders. Until they arrive, it is important to stay calm and not leave the sluice.

The trash that was produced during the stay has to be collected and taken with one into the sluice. It is measured with a contamination monitor, a handheld device containing a thin detector foil like the Hand-foot-clothing monitor and based on the same principle. First, the background is measured by pressing the middle button. The results are noted and the contamination monitor is placed on the trash and the measurement is started again. Normally, the results for the trash are in the same magnitude as the background and the trash can be

disposed of as normal household waste. But before it can be removed from the control area, it has to be entered in the entry book. There, the consecutive number, the date and time of the removal, the kind of item, the background values for α and β/ γ radiation, the measured values for α and β/ γ and the evaluation of the finding are entered and confirmed with the signature of the operator. This process is performed with all items, that are removed from the control area.

Figure 110: Contamination monitor a) from the front and b) from the back

The figure above shows a contamination monitor. In part a) it is shown from the front with the typical background activity values on the display. 0.0 Ips of α activity and 13.5 Ips for βγ activity. Part b) shows the backside of the contamination monitor with its sensitive, both for radiation detection and damage, sensor foil.

Finally, one enters the remaining information of one's stay in the entry book: the time of leaving the control area, the confirmation of the contamination control after the stay and the current µSv value of one's electrical dosimeter after the stay. Then one puts back one's dosimeters and can leave the control area, taking one's trash along.

9.2 Illustration directory

9.3 List of Tables

Erklärung

Ich habe die vorliegende Arbeit selbstständig verfasst, keine anderen als die angegebenen Quellen und Hilfsmittel benutzt und bisher keiner anderen Prüfungsbehörde vorgelegt. Von den in § 27 Abs. 5 vorgesehenen Rechtsfolgen habe ich Kenntnis genommen.

Regensburg, den 27.03.2023

Alina Scheklaukov